bulletin 35

technical report

fib
CEB-FIP

Retrofitting of concrete structures by externally bonded FRPs

with emphasis on seismic applications

Retrofitting of concrete structures by externally bonded FRPs

with emphasis on seismic applications

Course material prepared by
the authors of the 2005 *fib* short courses
held in Istanbul and Ankara

April 2006

Subject to priorities defined by the Steering Committee and the Presidium, the results of ***fib***'s work in Commissions and Task Groups are published in a continuously numbered series of technical publications called 'Bulletins'. The following categories are used:

category	minimum approval procedure required prior to publication
Technical Report	approved by a Task Group and the Chairpersons of the Commission
State-of-Art Report	approved by a Commission
Manual or Guide (to good practice)	approved by the Steering Committee of ***fib*** or its Publication Board
Recommendation	approved by the Council of ***fib***
Model Code	approved by the General Assembly of ***fib***

Any publication not having met the above requirements will be clearly identified as preliminary draft.

This Bulletin N° 35 was approved as an ***fib*** Technical Report by Working Group 2, *Short courses*, of Special Activity Group 2, *Dissemination of knowledge.*

Members of Working Group 2, *Short courses*, of Special Activity Group 2, *Dissemination of knowledge*:

György L. Balázs (Convener, Budapest Univ. of Technology and Economics, Hungary)
Brian Cox (Tsala-VSL, South Africa), Michael Fardis (Univ. of Patras, Greece), Jim Forbes (Hyder Consulting, Australia), James Jirsa (Univ. of Texas, USA), Vijaz Kumar (Uttar Pradesh State Bridge Corp. Ltd., India), Giorgio Monti (Univ. "La Sapienza" di Roma, Italy), Yoshio Ozaka (Tohoku-Gakuin Univ., Japan), Lidia Shehata (Univ. Fed. Rio de Janeiro, Brazil), Enzo Siviero (Italy), Joost Walraven (Delft Univ. of Technology, The Netherlands)

Full address details of Task Group members may be found in the ***fib*** Directory or through the online services on ***fib's*** website, www.fib-international.org.

Cover photos, clockwise from top left:
- Failure of a column due to inadequate detailing of transverse bars (see Figure 14, page 134)
- Test setup for two-storey specimen subjected to reversed cyclic lateral loading (see Figure 13, page 184)
- FRP column wrapping (photo courtesy of Heinz Meier, SIKA)

First published in 2006 by the International Federation for Structural Concrete (*fib*)
Post address: Case Postale 88, CH-1015 Lausanne, Switzerland
Street address: Federal Institute of Technology Lausanne - EPFL, Section Génie Civil
Tel +41 21 693 2747, Fax +41 21 693 6245, E-mail fib@epfl.ch, web www.fib-international.org

ISSN 1562-3610
ISBN 2-88394-075-4

Printed by Sprint-Digital-Druck, Stuttgart

Preface

In most countries of the world, the building stock is ageing and needs continuous maintenance or repair. Moreover, the majority of existing constructions are substandard and deficient in the light of our current knowledge and current design codes. The direct and indirect costs of demolition and reconstruction of structurally deficient constructions are prohibitive for most individual owners, as well as for the national or regional economy. Moreover, it is unacceptable for the society and for the environment, as it represents a large and unnecessary waste of natural resources and energy. Therefore, structural retrofitting is becoming more and more important and receives considerable emphasis throughout the world.

The problem of structural deficiency of existing constructions is especially acute in seismic regions, as, even there, seismic design of structures is relatively recent. In these regions the major part of the seismic threat to human life and property comes from old buildings. Concrete buildings constructed in the past without a proper seismic design pose a serious public safety problem. Casualties from earthquakes in Europe during the 20^{th} century reached about 128000 in Italy, 110000 in Turkey, 71000 in the former Soviet Union, 2600 in Romania, 2500 in former Yugoslavia and 1300 in Greece. In countries with modern seismic standards in force, most of the casualties in recent earthquakes are due to substandard concrete buildings. It is characteristic that in Kobe (1995), where the death toll approached 6300, only 6.5% of the buildings built after the last revision of the seismic design (in 1981) collapsed or suffered heavy damage. By contrast, 16% of the pre-1981 buildings collapsed or were heavily damaged.

Recent earthquakes have exacted very heavy tolls from developed countries with modern seismic standards in force. The Kobe (1995) event caused a property loss of 80 billion Euro (55 billion in buildings alone). Economic losses in the Loma Prieta (1989) earthquake in California were less, but those of the Northridge (1994) earthquake approached 80 billion Euro. The European experience is fortunately less impressive. In Greece, the annual property loss due to earthquakes is over 200 million Euro, with the worst recent event, that of Athens (1999), causing a direct loss of over 2 billion Euro, representing the replacement cost of about 6500 buildings that collapsed or were demolished and the repair cost of 50000 to 60000 buildings. Property loss in the Irpinia (1980) earthquake exceeded 40 billion Euro. Losses in the Armenia (1988), Montenegro (1979) and Bucharest (1977) earthquakes were 16.5 billion, 2.1 billion and 0.75 billion Euro respectively. Most importantly, the 1999 Kocaeli (Izmit) and Duzce earthquakes in Turkey caused the collapse of about 70000 buildings and a direct economic loss to constructed facilities of over 20 billion Euro.

Development and standardisation of simple, cost-effective structural retrofitting solutions, that can fulfill the requirements for public safety with least disruption of occupancy, will enhance public safety and improve quality of life at costs that both the owners and the national economy can bear. It will reduce the annual cost of strengthening of existing buildings, estimated to be around 30 billion Euro in the European Union alone. Retrofitting with externally bonded advanced composites (Fibre Reinforced Polymers - FRPs), to which the present Bulletin is devoted, is cleaner and easier to apply than conventional retrofitting techniques (notably jackets of cast-in-situ concrete or shotcrete), disrupts less the occupancy and operation of the facility, does not generate debris or waste, reduces health and accident hazards at the construction site and noise or air pollution there and in the surroundings. Therefore, application of externally bonded Fibre Reinforced Polymers (FRPs) are rapidly becoming the technique of choice for structural retrofitting.

The International Federation for Structural Concrete (fédération internationale du béton, *fib*), and its parent organisation, CEB, before, have placed considerable emphasis on assessment and retrofitting of existing concrete structures, with special emphasis on externally bonded Fibre Reinforced Polymers. In the broader, non-seismic field, *fib* has published in 2001 bulletin 14: “Externally bonded FRP reinforcement for RC structures” and in 2002 bulletin 17: “Management, maintenance and strengthening of concrete structures”. More recently, in 2003, *fib* produced bulletin 24: “Seismic assessment and retrofit of reinforced concrete buildings”, which has been a source document for the European standard: EN 1998-3:2005 “Eurocode 8: Design of structures for earthquake resistance – Part 3: Assessment and retrofitting of buildings”. Earlier, in 1998, CEB produced Bulletin 243: “Strategies for testing and assessment of concrete structures – Guidance Report”, in 1989 Bulletin

192: “Diagnosis and assessment of concrete structures – State-of-the-art Report” and as early as in 1983, Bulletin 162: “Assessment of concrete structures and design procedures for upgrading (Redesign)”, which has been a source document for ENV 1998-1-4:1996, i.e. the pre-standard version of Eurocode 8 on “Strengthening and repair of buildings”. CEB has also published in 1996 Bulletin 232: “Fastenings for seismic retrofitting – State-of-the-art Report on design and application”, another source document for international standardisation in seismic retrofitting.

fib organizes short courses worldwide on advanced knowledge of structural concrete in general, or on specific topics. The courses are organized by *fib* and are given by internationally recognized experts in *fib*, often supplemented with local experts active in *fib*. They are based on the knowledge accumulated in the ten Commissions and almost fifty Task Groups in *fib*. The courses are part of the programme of dissemination of knowledge.

The *fib* expert groups are responsible for the development of the technical/scientific programme of the course and for the contacts to the local organizers. Background assistance is provided by the Special Activity Group 2 “Dissemination of knowledge”. Courses are given in English and supported by course documents. All participants receive a Course Certificate.

To date, *fib* courses have been held as follows:

2003 in Athens, Greece, and in Chennai, India;

2004 in New-Delhi, India;

2005 in Ankara and Istanbul, Turkey.

The course in Ankara (June 24/25) and Istanbul (June 27/28) on “Retrofitting of Concrete Structures through Externally Bonded FRP, with emphasis on Seismic Applications” has drawn for expertise both from outside Turkey and from the large pool of local experts on this subject. Along with a State-of-the-Art coverage of the subject matter, it gave the opportunity to present essentially for the first time to an international audiance the relevant provisions in three recent (2004-5) standardisation milestones:

- EN 1998-3:2005 “Eurocode 8: Design of structures for earthquake resistance – Part 3: Assessment and retrofitting of buildings”, published in June 2005 by CEN as the first European standard for assessment and retrofitting of existing structures;
- The 2005 Draft of the Turkish seismic design code, produced in 2005 by the Ministry of Public Works and Settlement, in Ankara;
- Regulatory document CNR-DT 200/04, issued by the National Research Council (CNR) of Italy: “Instructions for Design, Execution and Control of Strengthening Interventions by Means of Fibre-Reinforced Composites” (2004).

In November 2005, *fib* decided to publish course material of high quality that is of interest to the majority of its subsribing members, within the series of *fib* bulletins in the category “Technical Reports”. The material of the Ankara/Istanbul 2005 course will inaugurate this new kind of bulletins. It is hoped that this endeavour will spread the valuable contents of the course material outside the Turkish Structural Concrete community and will contribute further to the reinforcement of the ties between this community and *fib*.

Budapest and Patras, January 2006

György L. Balázs
Convener, Working Group “Short courses”

Michael N. Fardis
Coordinator, experts group,
Ankara/Istanbul course

Contents

General concepts and design aspects – Materials and techniques

Thanasis C. Triantafillou
University of Patras, Greece

1 Introduction

This chapter provides general information on advanced composite materials used in concrete strengthening, on systems and techniques (including some quite recent ones) for their application and on some issues regarding the fields of application of composites as strengthening/retrofitting materials of concrete structures. Some of the material presented herein has been taken from *fib* (2001).

The issue of upgrading the existing civil engineering infrastructure has been one of great importance in recent years. Deterioration of bridge decks, beams, girders and columns, buildings, parking structures and others may be attributed to ageing, environmentally induced degradation, poor initial design and/or construction, lack of maintenance, and to accidental events such as earthquakes. The infrastructure's increasing decay is frequently combined with the need for upgrading so that structures can meet more stringent design requirements (e.g. increased traffic volumes in bridges exceeding the initial design loads), and hence the aspect of civil engineering infrastructure renewal has received considerable attention over the past few years throughout the world. At the same time, seismic retrofit has become at least equally important, especially in areas of high seismic risk.

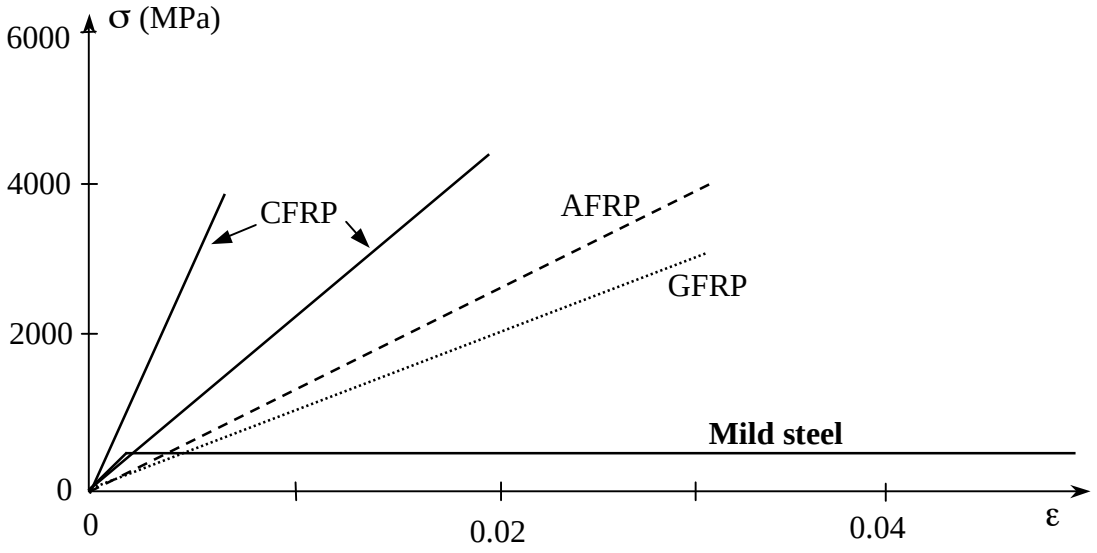

Fig. 1:Uniaxial tension stress-strain diagrams for different unidirectional FRPs and steel. CFRP = carbon FRP, AFRP = aramid FRP, GFRP = glass FRP.

Recent developments related to materials, methods and techniques for structural strengthening have been enormous. One of today's state-of-the-art techniques is based on the use of fibre reinforced polymer (FRP) composites, which are currently viewed by structural engineers as "new" and highly promising materials in the construction industry. Moreover, recent developments have focused on the combination of continuous fibre-based textiles with mortars (instead of resins, as in the case of FRP), leading to the development of the so-called

textile-reinforced mortars (TRM). Both FRP and TRM materials may be given the term "continuous fibre composites" or "advanced composites" or simply "composites". For comparison with steel, typical stress-strain diagrams for unidirectional composites under short-term monotonic loading are given in Figure 1.

Composite materials for strengthening of civil engineering structures are available today mainly in the form of: (a) thin unidirectional *strips* (with thickness in the order of 1 mm) made by pultrusion; flexible *sheets* or *fabrics* or *textiles* made of fibres in one, two or more directions.

The reasons why composites are increasingly used as strengthening materials of reinforced concrete elements may be summarised as follows: immunity to corrosion; low weight (about ¼ of steel), resulting in easier application in confined space, elimination of the need for scaffolding and reduction in labour costs; very high tensile strength (both static and long-term, for certain types of fibres); stiffness which may be tailored to the design requirements; large deformation capacity; and practically unlimited availability of sizes, geometry and dimensions. Composites suffer from certain disadvantages too, which are not to be neglected by engineers: contrary to steel, which behaves in an elastoplastic manner, composites in general are linear elastic to failure (although the latter occurs at large strains) without any yielding or plastic deformation, leading to reduced (but typically sufficient) deformability at ultimate. Additionally, the cost of materials on a weight basis is several times higher than that for steel (but when cost comparisons are made on a strength basis, they become less unfavourable). Moreover, some fibre materials, e.g. carbon and aramid, have incompatible thermal expansion coefficients with concrete. Finally, the exposure of FRPs to high temperatures (e.g. in case of fire) may cause premature degradation and collapse (some epoxy resins start softening at about 45-70 ^{o}C); this is not the case with TRMs, which contain inorganic (cement-based) binders instead of resins. Hence composite materials should not be thought of as a blind replacement of steel (or other materials) in structural intervention applications. Instead, the advantages offered by them should be evaluated against potential drawbacks, and final decisions regarding their use should be based on consideration of several factors, including not only mechanical performance aspects, but also constructibility and long-term durability.

2 Materials

2.1 General

The selection of materials for different strengthening systems is a critical process. Every system is unique in the sense that the fibres and the binder components are designed to work together. This implies that a binder for one strengthening system will not automatically work properly for another. Furthermore, a binder for the fibres will not necessarily provide a good bond to concrete. Hence, only systems that have been tested extensively on reinforced concrete structures shall be used in strengthening with composites.

Today there are several types of composite material strengthening systems, which are summarised below:

- Wet lay-up systems
- Systems based on prefabricated elements
- Special systems, e.g. automated wrapping, prestressing, near-surface mounted bars, mechanically attached laminates, etc.

These systems correspond to several manufacturers and suppliers, and are based on different configurations, types of fibres, adhesives, etc. Also, the suitability of each system depends on the type of structure that shall be strengthened. For example, prefabricated strips

are generally best suited for plane and straight surfaces, whereas sheets or fabrics are more flexible and can be used to plane as well as to convex surfaces. Near-surface mounted bars can be preferable if the bond conditions between composites and concrete should be improved and/or if the externally applied reinforcement should be better protected. Automated wrapping can be an option in cases when many columns need to be strengthened at the same site.

Practical execution and application conditions, for example cleanness and temperature, are very important in achieving a good bond. A dirty surface will never provide a good bond and hence premature failure of the strengthening system will occur. Moreover, typical adhesives undergo a chemical process during hardening that needs a temperature above 10 °C to start. If the temperature drops, the hardening process delays.

In the following sections the three main components, namely adhesives, matrices and fibres of a composite material strengthening system will be discussed briefly.

2.2 Adhesives

The purpose of the adhesive is to provide a shear load path between the concrete surface and the composite material, so that full composite action may develop. The science of adhesion is a multidisciplinary one, demanding a consideration of concepts from such topics as surface chemistry, polymer chemistry, rheology, stress analysis and fracture mechanics. It is not our aim to cover this field in any detail. It is rather to emphasise that key information about adhesives relevant to their use needs to be provided by the manufacturer of the strengthening system.

The most common type of structural adhesives is epoxy, which is the result of mixing an epoxy resin (polymer) with a hardener. Other types of adhesives may be based on inorganic materials (mainly cement-based), discussed later. Depending on the application demands, the adhesive may contain fillers, softening inclusions, toughening additives and others. The successful application of an adhesive system requires the preparation of an adequate specification, which must include such provisions as adherent materials, mixing/application temperatures and techniques, curing temperatures, surface preparation techniques, thermal expansion, creep properties, abrasion and chemical resistance.

When using **epoxy** adhesives there are two different time concepts that need to be taken into consideration. The first is the *pot life* and the second is the *open time*. Pot life represents the time one can work with the adhesive after mixing the resin and the hardener before it starts to harden in the mixture vessel; for an epoxy adhesive, it may vary between a few seconds up to several years. Open time is the time that one can have at his/her disposal after the adhesive has been applied to the adherents and before they are joined together. Another important parameter to consider is the *glass transition temperature*, T_g. Most synthetic adhesives are based on polymeric materials, and as such they exhibit properties that are characteristic for polymers. Polymers change from relatively hard, elastic, glass-like to relatively rubbery materials at a certain temperature. This temperature level is defined as glass transition temperature, and is different for different polymers.

Epoxy adhesives have several advantages over other polymers as adhesive agents for civil engineering use, namely (Hollaway and Leeming 1999): High surface activity and good wetting properties for a variety of substrates; relatively long open time; high cured cohesive strength, so that failure may be dictated by adherent strength; may be toughened by the inclusion of dispersed rubbery phase; lack of by-products from curing reaction minimises shrinkage and allows the bonding of large areas with only contact pressure; low shrinkage compared with polyesters, acrylics and vinyl types; low creep and superior strength retention under sustained load; can be made thixotropic for application to vertical surfaces; ability to

accommodate irregular or thick bond lines.

Typical properties for cold cured epoxy adhesives used in civil engineering applications are given in Table 1 (Mays and Hutchinson 1992). For the sake of comparison, the same table provides information for concrete and mild steel too.

Alternative materials to epoxies may be of the **inorganic binder** type. These materials are based on cement in combination with other binders (e.g. fly ash, silica fume, metakaolin), additives (e.g. polymers) and fine aggregates. In this case the adhesive also plays the role of the matrix in the composite material, hence it must be designed such that compatibility with the fibres (textiles) will be maximized. General requirements for inorganic binders are high shear (that is tensile) strength, suitable consistency, low shrinkage and creep and good workability.

Property (at 20 °C)	Cold-curing epoxy adhesive	Concrete	Mild steel
Density (kg/m^3)	1100 – 1700	2350	7800
Young´s modulus (GPa)	0.5 - 20	20 - 50	205
Shear modulus (GPa)	0.2 – 8	8 - 21	80
Poisson´s ratio	0.3 – 0.4	0.2	0.3
Tensile strength (MPa)	9 - 30	1 - 4	200 - 600
Shear strength (MPa)	10 - 30	2 - 5	200 - 600
Compressive strength (MPa)	55 - 110	25 - 150	200 - 600
Tensile strain at break (%)	0.5-5	0.015	25
Approximate fracture energy (Jm^{-2})	200-1000	100	10^5-10^6
Coefficient of thermal expansion (10^{-6}/°C)	25 - 100	11 - 13	10 - 15
Water absorption: 7 days - 25 °C (% w/w)	0.1-3	5	0
Glass transition temperature (°C)	45 - 80	---	---

Table 1: Comparison of typical properties for epoxy adhesives, concrete and steel (Täljsten 1994).

2.3 Matrices

The matrix for a structural composite material is typically a polymer, of thermosetting type or of thermoplastic type, with the first being the most common one. Alternatively, the matrix can be based on inorganic materials. The function of the matrix is to protect the fibres against abrasion or environmental corrosion, to bind the fibres together and to distribute the load. The matrix has a strong influence on several mechanical properties of the composite, such as the transverse modulus and strength, the shear properties and the properties in compression. Physical and chemical characteristics of the matrix such as melting or curing temperature, viscosity and reactivity with fibres influence the choice of the fabrication process. Hence, proper selection of the matrix material for a composite system requires that all these factors be taken into account (Agarwal and Broutman 1990).

Epoxy resins, polyester and vinylester are the most common polymeric matrix materials used with high-performance reinforcing fibres. They are thermosetting polymers with good processibility and good chemical resistance. Epoxies have, in general, better mechanical properties than polyesters and vinylesters, and outstanding durability, whereas polyesters and vinylesters are cheaper. On the other hand, polymer-modified cement-based mortars are the most common materials when the matrix is of the inorganic binder type.

2.4 Fibres

A great majority of materials are stronger and stiffer in the fibrous form than as a bulk material. A high fibre aspect ratio (length/diameter ratio) permits very effective transfer of load via matrix materials to the fibres, thus enabling full advantage of the properties of the fibres to be taken. Therefore, fibres are very effective and attractive reinforcement materials. Fibres can be manufactured in continuous or discontinuous (chopped) form, but here only continuous fibres are considered. Such fibres have a diameter in the order of 5-20 μm, and can be manufactured as unidirectional or multi-directional reinforcement, sometimes in the form of textiles (e.g. in the case of inorganic binders). The fibres used for strengthening all exhibit a linear elastic behaviour up to failure and do not have a pronounced yield plateau as for steel.

There are mainly three types of fibres that are used for strengthening of civil engineering structures, namely glass, aramid and carbon fibres. It should be recognised that the physical and mechanical properties can vary a great for a given type of fibre as well of course the different fibre types.

Glass fibres for continuous fibre reinforcement are classified into three types: E-glass fibres, S-glass and alkali resistant AR-glass fibres. E-glass fibres, which contain high amounts of boric acid and aluminate, are disadvantageous in having low alkali resistance. S-glass fibres are stronger and stiffer than E-glass, but still not resistant to alkali. To prevent glass fibre from being eroded by cement-alkali, a considerable amount of zircon is added to produce alkali resistance glass fibres; such fibres have mechanical properties similar to E-glass. An important aspect of glass fibres is their low cost.

Aramid fibres were first introduced in 1971, and today are produced by several manufacturers under various brand names. The structure of aramid fibre is anisotropic and gives higher strength and modulus in the fibre longitudinal direction. The diameter of aramid fibre is approximately 12 μm. Aramid fibres respond elastically in tension but they exhibit non-linear and ductile behaviour under compression; they also exhibit good toughness, damage tolerance and fatigue characteristics.

Material	Elastic modulus (GPa)	Tensile strength (MPa)	Ultimate tensile strain (%)
Carbon			
High strength	215-235	3500-4800	1.4-2.0
Ultra high strength	215-235	3500-6000	1.5-2.3
High modulus	350-500	2500-3100	0.5-0.9
Ultra high modulus	500-700	2100-2400	0.2-0.4
Glass			
E	70	1900-3000	3.0-4.5
S	85-90	3500-4800	4.5-5.5
Aramid			
Low modulus	70-80	3500-4100	4.3-5.0
High modulus	115-130	3500-4000	2.5-3.5

Table 2: Typical properties of fibres (Feldman 1989, Kim 1995).

Carbon fibres are normally either based on pitch or PAN, as raw material. Pitch fibres are fabricated by using refined petroleum or coal pitch that is passed through a thin nozzle and stabilised by heating. PAN fibres are made of polyacrylonitrile that is carbonised through burning. The diameter of pitch-type fibres measures approximately 9-18 μm and that of the PAN-type measures 5-8 μm. The structure of this carbon fibre varies according to the

orientation of the crystals; the higher the carbonation degree, the higher the orientation degree and rigidity as a result of growing crystals. The pitch base carbon fibres offer general purpose and high strength/elasticity materials. The PAN-type carbon fibres yield high strength materials and high elasticity materials. Typical properties of various types of fibre materials are provided in Table 2. Note that values in this table are only indicative of static strength of unexposed fibres. Design values of the composite material systems should account both for the presence of matrix (see "rule of mixtures" below) and for reductions due to long-term loading, environmental exposure etc. (such reductions are normally supplied by the manufacturer).

2.5 Composite materials

Advanced composites as strengthening materials consist of a large number of small, continuous, directionalized, non-metallic fibres with advanced characteristics, bundled in a resin or inorganic matrix. Depending on the type of fibre (Section 2.4) they are referred to as CFRP (carbon fibre based), GFRP (glass fibre based) or AFRP (aramid fibre based); when different types of fibres are used, the material is called "hybrid". Typically, the volume fraction of fibres in advanced composites equals about 50-70% for strips and about 25-35% for sheets. Given also that the elastic modulus of fibres is much higher than that of the matrix, it becomes clear that the fibres are the principal stress bearing components, while the matrix transfers stresses among fibres and protects them. Different techniques are used for manufacturing (e.g. pultrusion, hand lay-up), detailed descriptions of which are outside the scope of this document. As externally bonded reinforcement for the strengthening of structures, advanced composite materials are made available in various forms, which are described in Section 3.

Basic mechanical properties of advanced composites may be estimated if the properties of the constituent materials (fibres, matrix) and their volume fractions are known. Details about the micromechanics of composite materials are not considered here. However, for the simple – yet quite common - case of unidirectional fibres, one may apply the "rule of mixtures" simplification as follows:

$$E_f = E_{fib} V_{fib} + E_m V_m \tag{1}$$

$$f_f \approx f_{fib} V_{fib} + f_m V_m \tag{2}$$

where E_f = Young's modulus of fibre-reinforced material in fibre direction, E_{fib} = Young's modulus of fibres, E_m = Young's modulus of matrix, V_{fib} = volume fraction of fibres, V_m = volume fraction of matrix, f_f = tensile strength of fibre-reinforced material in fibre direction, f_{fib} = tensile strength of fibres and f_m = tensile strength of matrix. Note that in the above equations $V_{fib} + V_m = 1$. Also, typical values for the volume fraction of fibres in prefabricated strips are in the order of 0.50 – 0.65.

As the rule of mixtures is an approximation of the micro-mechanical behaviour of fibre composites, a more detailed prediction of the stress-strain behaviour should be obtained through tensile testing. Hence the material properties should be given for the composite material directly, so to reflect the fibre and matrix characteristics as well as the micro-structural aspects such as fibre diameter, distribution and parallelism of fibres, local defects, volume fractions and fibre-matrix interfacial properties.

Typical commercial products where composite materials of the fibre-reinforced polymer type (FRP) in the form of prefabricated strips have the properties given in Table 3, where the

properties for mild steel are also given for comparison.

Material	Elastic modulus E_f (GPa)	Tensile strength f_f (MPa)	Ultimate tensile strain ε_{fu} (%)
Prefabricated strips			
Low modulus CFRP strips	170	2800	1.6
High modulus CFRP strips	300	1300	0.5
Mild steel	200	400	25*

* Yield strain = 0.2%

Table 3: Typical properties of prefabricated FRP strips and comparison with steel.

In case of prefabricated strips the material properties based on the total cross-sectional area can be used in calculations and are usually supplied by the manufacturer (see Table 3). In case of in-situ resin impregnated systems, however, the final composite material thickness and with that the fibre volume fraction is uncertain and may vary. For this reason a calculation based on the properties for the total system (fibres and matrix) and the actual thickness is not appropriate. Note that manufacturers sometimes supply the material properties for the bare fibres. Because of this difference in approach, one should be careful when comparing properties of different systems. Furthermore it is very important that in calculations the appropriate material properties for the applied system are used. In the following the difference between both approaches is explained and elucidated with the example given in Table 4 (*fib* 2001).

Assumed properties for fibres and matrix:
E_{fib}=220 GPa f_{fib} = 4000 MPa
E_m= 3 GPa f_m = 80 MPa

Cross-sectional area				Composite material properties			Failure load	
A_{fib} (mm^2)	A_m (mm^2)	A_f^* (mm^2)	V_{fib} (%)	E_f [eq. (1)] (MPa)	f_f [eq. (2)] (MPa)	Ultimate strain (%)	(kN)	(%)
70	0	70	100	220000	4000	1.818	280.0	100.0
70	30	100	70	154900	2824	1.823	282.4	100.9
70	70	140	50	111500	2040	1.830	285.6	102.0

* In case of a strip with a width of 100 mm dividing this value by 100 mm gives the thickness of the strip (respectively 0.7 mm, 1.0 mm and 1.4 mm).

Table 4: Example showing the effect of volume fraction of fibres on the composite material properties.

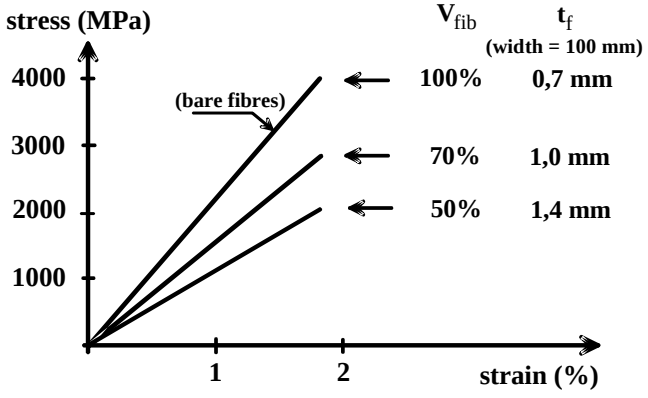

Fig. 2: Stress strain relations corresponding to various fibre volume fractions V_{fib} in Table 4.

Due to the fact that the stiffness and strength of the fibres (E_{fib} and f_{fib}) is much higher than respectively the stiffness and strength of the matrix (E_m and f_m), the properties of the composite material (E_f and f_f) are governed by the fibre properties and the cross-sectional area of the bare fibres. When the composite material properties are based on the total cross-sectional area (fibres and matrix) this means that, compared to the properties of the bare fibres, the stiffness and strength is less. It may be obvious that the strength and stiffness of the total system is not affected because this reduction is compensated by an increase of the cross-sectional area compared to the cross-sectional area of the fibres. So, there is a strong relation between the fibre volume fraction and the composite material properties to be used in calculations. This is illustrated in Table 4 and Figure 2 (*fib* 2001). For certain chosen properties of the fibres and the matrix, the effect of the volume fraction of the fibres on the composite material properties is shown. For a constant amount of fibres (cross-sectional area = 70 mm^2) the failure load and strain at failure is only very little affected by an increase of the amount of matrix. The composite material properties to be used in calculations based on the total cross-sectional area, however, are strongly influenced.

The example given above demonstrates that for a comparison of composite material properties it may not be sufficient only to compare values for strength and/or stress-strain relations. It is important also to know the composition of the composite material to which the given property belongs. In case of uncertainty about the thickness (like with in-situ resin or mortar impregnated systems) it may be more convenient to base calculations on the fibre properties and fibre cross-sectional area than on properties for the total system. The latter approach is still possible; however, the material properties and thickness (cross-sectional area) as specified by the manufacturer should then be used and not the actual thickness that is realised in practice.

As mentioned, in case of in-situ impregnated systems, one may calculate the properties of the composite material based on those of the bare fibres only. In this case the second term in eq. (1)-(2) may be ignored, V_{fib} should be taken equal to 1 and the dimensions of the externally bonded reinforcement (e.g. cross-sectional area) should be calculated based on the nominal dimensions of the fibre sheets or fabrics. If this approach is adopted, the resulting property (e.g. elastic modulus, tensile strength) should be multiplied by a reduction factor r, to account for the efficiency of the fibre-resin system and for the sheet or fabric architecture. This factor should be provided by the composite material system supplier based on testing. Alternatively, the composite material supplier could provide directly the properties of the in-situ impregnated system (e.g. thickness, elastic modulus, tensile strength) based on testing. To illustrate this, we may assume that a sheet has a nominal thickness t_{fib} and elastic modulus E_{fib} (both calculated based on bare fibre properties). After impregnation, the composite material has a thickness t_f and an elastic modulus E_f. The two systems are equivalent according to the condition: $t_{fib}E_{fib}r = t_fE_f$.

3 Composite material systems

A variety of externally bonded reinforcement systems exist, related to the constituent materials, the form and the strengthening technique. In general, these can be subdivided into "wet lay-up" (or "cured in-situ") systems and "prefab" (or "pre-cured") systems. In the following, an overview is given of the different forms of these systems. Techniques for FRP strengthening are given in Section 4.

3.1 Wet lay-up systems

- Dry unidirectional fibre *sheet* and semi-unidirectional *fabric* (woven or knitted), where fibres run predominantly in one direction partially or fully covering the structural element. Installation on the concrete surface requires saturating resin usually after a primer has been applied. Two different processes can be used to apply the fabric:
  - the fabric can be applied directly into the resin which has been applied uniformly onto the concrete surface,
  - the fabric can be impregnated with the resin in a saturator machine and then applied wet to the sealed substrate.
- Dry multidirectional *fabric* (woven or knitted), where fibres run in at least two directions. Installation requires saturating resin or inorganic binders. The fabric is applied using one of the two processes described above.
- Resin pre-impregnated uncured unidirectional *sheet* or *fabric*, where fibres run predominantly in one direction. Installation may be done with or without additional resin.
- Resin pre-impregnated uncured multidirectional *sheet* or *fabric*, where fibres run predominantly in two directions. Installation may be done with or without additional resin.
- Dry fibre *tows* (untwisted bundles of continuous fibres) that are wound or otherwise mechanically placed onto the concrete surface. Resin is applied to the fibre during winding.
- Pre-impregnated fibre *tows* that are wound or otherwise mechanically placed onto the concrete surface. Product installation may be executed with or without additional resin.
- Multidirectional *textiles* with fibres in at least two directions. Installation on the concrete surface is accomplished using an inorganic binder.

3.2 Prefabricated elements

- Pre-manufactured cured straight *strips*, which are installed typically through the use of adhesives. Sometimes application of strips with multidirectional fibres is possible using mechanical fasteners (e.g. powder-activated nails). The strips are typically in the form of thin ribbons, rods or grids that may be delivered in a rolled coil. Normally, the strips are pultruded. In case they are laminated, also the term *laminate* instead of *strip* may be used.
- Pre-manufactured cured shaped *shells*, *jackets* or *angles*, which are installed through the use of adhesives. They are typically factory-made curved or shaped elements or split shells that can be fitted around columns or other elements.

4 Techniques for strengthening with composites

4.1 Basic technique

The basic composite material strengthening technique, which is most widely applied, involves the manual application of either wet lay-up (so-called hand lay-up) or prefabricated systems by means of cold cured adhesive bonding. This is the so-called classical FRP strengthening technique. Common in this technique is that the external reinforcement is

bonded onto the concrete surface with the fibres as parallel as practically possible to the direction of principal tensile stresses. Typical applications of the hand lay-up and prefabricated systems are illustrated in Figure 3.

(a) (b)

Fig. 3: (a) Hand lay-up of CFRP sheets or fabrics. (b) Application of prefabricated strips.

4.2 Special techniques

Besides the basic technique, several special techniques have been developed. Without aiming to provide a complete overview of these special techniques, a number of them are briefly explained in the following sections.

4.2.1 Automated wrapping

The strengthening technique through automated winding of tow or tape was first developed in Japan in the early 90s and a little later in the USA. The technique, shown in Figure 4, involves continuous winding of wet fibres under a slight angle around columns or other structures (e.g. chimneys, as has been done in Japan) by means of a robot. Key advantage of the technique, apart from good quality control, is the rapid installation.

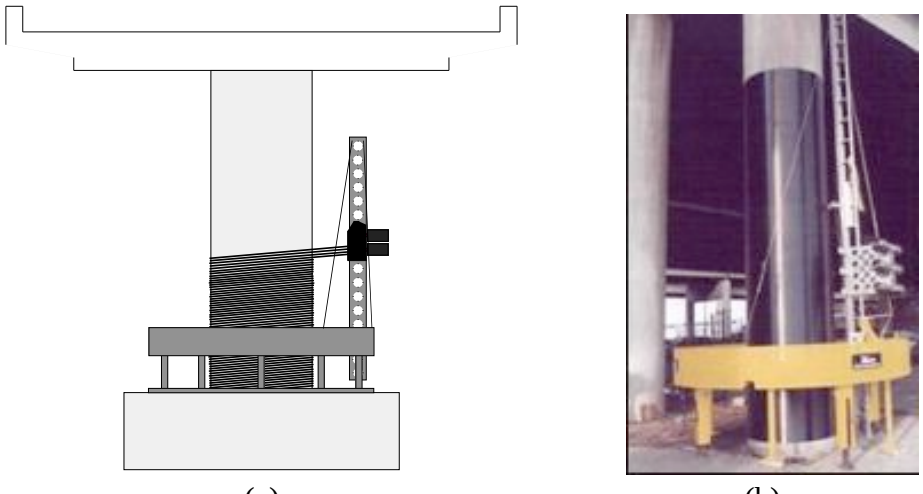

(a) (b)

Fig. 4: Automated RC column wrapping. (a) Schematic. (b) Photograph of robot-wrapper.

4.2.2 Prestressed FRP

In some cases it may be advantageous to bond the external FRP reinforcement onto the concrete surface in a prestressed state. Both laboratory and analytical research (e.g. Triantafillou et al. 1992, Deuring 1993) has shown that prestressing represents a significant contribution to the advancement of the FRP strengthening technique. Recently some methods have been developed to prestress the FRP under real life conditions (Luke et al. 1998).

Prestressing the strips prior to bonding has the following advantages:

- provides stiffer behaviour as at early stages most of the concrete is in compression and therefore contributing to the moment of resistance.
- crack formation in the shear span is delayed and the cracks when they appear are more finely distributed and narrower (crack widths are also a matter of bond properties).
- closes cracks in structures with pre-existing cracks.
- improves serviceability and durability due to reduced cracking.
- improves the shear resistance of the member as the whole concrete section will resist the shear, provided that the concrete remains uncracked.
- the same strengthening is achieved with smaller areas of stressed strips compared with unstressed strips.
- with adequate anchorage, prestressing may increase the ultimate moment of resistance by avoiding failure modes associated with peeling-off at cracks and the ends of the strips.
- the neutral axis remains at a lower level in the prestressed case than in the unstressed one, resulting in greater structural efficiency.
- prestressing significantly increases the applied load at which the internal steel begins to yield compared to a non-stressed member.
- The technique has also some disadvantages:
- it is more expensive than normal strip bonding due to the greater number of operations and equipment that is required.
- the operation takes somewhat longer.
- the equipment to push the strip up to the soffit of the beam must remain in place until the adhesive has hardened sufficiently.

The concept for applying a prestressed FRP strip is shown schematically in Figure 5. A schematic illustration and a photograph of stressing devices is given in Figure 6a and 6b, respectively.

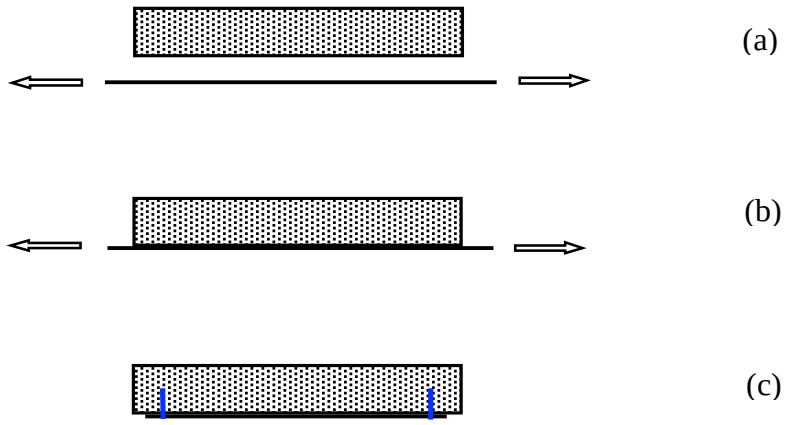

Fig.5: Strengthening with prestressed FRP strips: (a) prestressing; (b) bonding; (c) end anchorage and FRP release upon hardening of the adhesive.

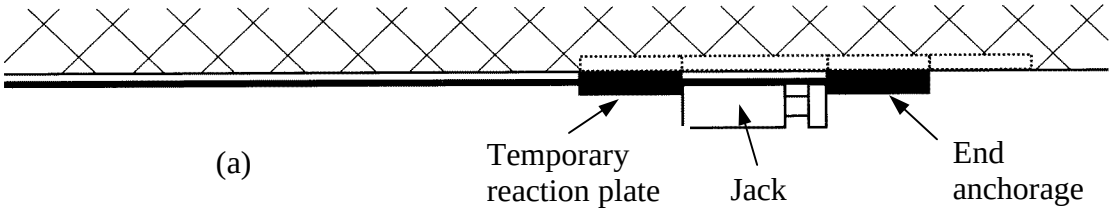

(a)

(b)

Fig. 6: (a) Schematic illustration and (b) photograph of active anchorages.

When the prestressing force is too high, failure of the beam due to release of the force will occur at the two ends, due to the development of high shear stresses in the concrete just above the FRP. Hence the design and construction of the end zones requires special attention. Tests and analysis have shown that if no special anchorages are provided at the ends, FRP strips shear-off (from the ends) with prestress levels in the order of only 5-6% of their tensile strength (for CFRP). But a technically and economically rational prestress would require a considerably higher degree of prestressing, in the range of 50% of the FRP tensile strength, which may only be achieved through the use of special anchorages applying vertical confinement (see Figure 5c). Such systems have been developed for research purposes as well as practical applications (Figure 6).

Prestressing of column jackets (active confinement) can be achieved by pretensioning the fibre bundles during winding or with unstressed jackets by making use of, e.g., expansive mortar or injection of mortar or epoxy under pressure.

4.2.3 Fusion-bonded pin-loaded straps

Another interesting development of the FRP strengthening technique involves replacing solid and relatively thick strips (Figure 7a) by the system shown in Figure 7b, known as pin-loaded strap (Winistoerfer and Mottram 1997). The strap comprises a number of non-laminated layers formed from a single, continuous, thin tape, which consists of fibres in a *thermoplastic* matrix. The outside, final layer of the tape is fixed to the previous layer by a fusion bonding process. Such a system enables the individual layers to move relative to each other, thus reducing the unwanted secondary bending stresses. Careful control of the initial tensioning process allows interlaminar shear stress concentrations to be reduced, so that a uniform strain distribution in all layers is achieved.

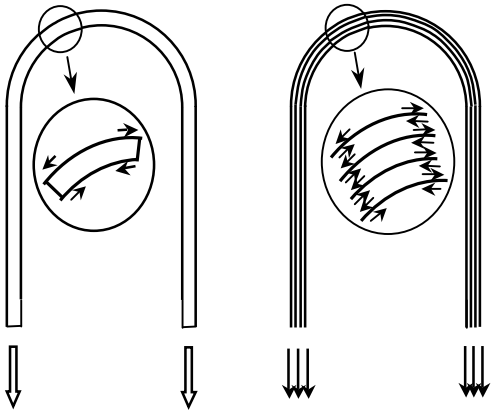

Fig. 7: Wrapping with (a) thick strips and (b) non-laminated straps.

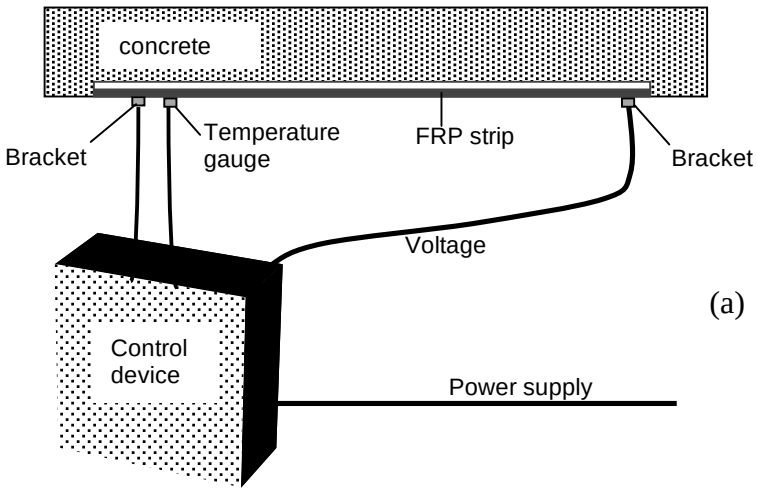

(b)

Fig. 8: Fast curing using heating device: (a) Schematic, (b) Photograph of end brackets.

4.2.4 In-situ fast curing using heating device

Instead of cold curing of the bond interface (curing of the two-component epoxy adhesive under environmental temperature), heating devices can be used. In this way it is possible to reduce curing time, to allow bonding in regions where temperatures are too low to allow cold

curing, to apply the technique in winter time, to work with prepreg FRP types, etc.

Different systems for heating can be used, such as electrical heaters, IR (infrared) heating systems and heating blankets. For CFRP the system illustrated in Figure 8 is also possible. This system takes advantage of the electrical conductivity of carbon fibres. It uses a special heating device to pass an electric current through CFRP strips during the strengthening process. The control unit allows the desired curing temperature to be maintained within a narrow range.

Controlled fast curing enables not only rapid application of the strengthening technique (e.g. full curing at 70 ^{o}C may be achieved in 3 hours) but also increases the glass transition temperature of the adhesive.

(a)

(b)

(c)

Fig. 9: Examples of prefab shapes for strengthening. (a) Angle, (b) application of angles, (c) shell.

4.2.5 Prefabricated shapes

Prefab type of composite material systems are mostly applied in the form of straight strips. However, these prefab systems can also be produced in other forms, depending on the foreseen application. By shaping them, prefab systems can be employed in applications where normally the more flexible wet lay-up systems are used. For shear strengthening of beams, pre-manufactured angles can be used as shown in Figure 9a-b. Figure 9c shows prefab shells or jackets which can be used for the confinement of circular and rectangular columns. In this case, the shells should be fabricated with sufficiently small tolerances. For

new structures, FRP castings may be used. These act as formwork during construction, and as external reinforcement for the loaded structure.

4.2.6 Near-surface mounted reinforcement

Near-surface mounted reinforcement may be thought of as a special method of supplementing reinforcement to concrete structures. According to this method, the composite materials in the form of strips or rods are placed into slits or grooves, respectively, which are cut into the concrete structure with a depth smaller than the concrete cover. Typically CFRP strips e.g. with a thickness of 2 mm and a width of 20 mm are bonded into these slits (Figure 10).

Bond tests and beam tests have been carried out to study the mechanical behaviour of the system (Blaschko and Zilch 1999, De Lorenzis et al. 2004). It was shown that a higher anchoring capacity compared with CFRP strips bonded onto the surface of a concrete structure is obtained. The mechanical behaviour is stiffer under serviceability loads but more ductile in the ultimate limit state. The tensile strength of the CFRP can be reached in beams with additional reinforcement consisting of strips in slits, if there is enough load carrying capacity of the compression zone in the concrete and for shear. The bond behaviour with high strength and ductility allows to bridge wide cracks without peeling-off. Moreover the strips are protected against demolition. Hence, the FRP material can be used more efficiently if it is glued into slits instead of on the surface.

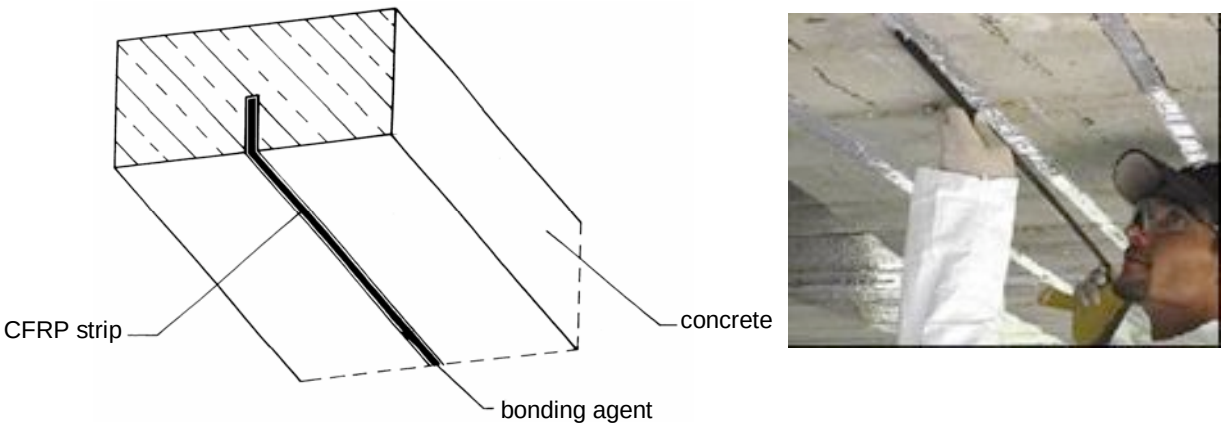

Fig. 10: CFRP strips glued into slits.

4.2.7 FRP impregnation by vacuum

FRP impregnation by vacuum is quite common in the plastics industry. Vacuum impregnation is, to some extent, comparable with wet lay-up. The concrete element to be strengthened according to this method is pre-treated in the same manner as for the other methods (i.e. through sandblasting, grinding or water blasting). The surface is cleaned carefully, primer is applied and after curing of the primer the fibres are placed in predetermined directions. It is important that sheets or fabrics have channels where the resin can flow, otherwise special spacing material must be used. A vacuum bag is placed on top of the fibres, the edges of the bag are sealed and a vacuum pressure is applied. Two holes are made in the vacuum bag, one for the outlet where the vacuum pressure is applied and one for the inlet where the resin is injected (Figure 11). In order to achieve an acceptable vacuum

pressure, a special sealant of epoxy putty can be used along the sides of the beam at the underside of the vacuum bag. Sealing must be effective to a very high level.

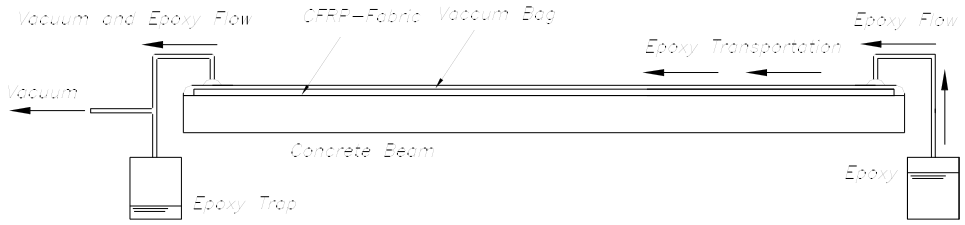

Fig. 11: Strengthening with vacuum injection system.

Vacuum impregnation has several advantages over traditional wet lay-up. The first advantage is that with this method it is possible to avoid hand contact with the epoxy adhesive and waste at the work site can be kept to a minimum. Furthermore, the quality of the composite can be improved. However, this method requires a large investment and there can be some difficulties in achieving a high degree of vacuum with surfaces of rough texture or in complicated geometries and locations. This implies higher costs for the strengthening work. For this application, a low viscosity cold-cured epoxy adhesive is used.

4.2.8 Mechanically-fastened FRP

A strengthening method has been developed in the past few years (e.g. Lamanna et al. 2001) where the strengthening strips are entirely mechanically attached to the concrete surface using multiple small, distributed powder actuated fasteners, sometimes in combination with anchor bolts at the strip ends, without any bonding (Figure 12). This system requires simple hand tools, lightweight materials and minimally trained labour. Unlike the conventional method of adhesively bonding FRP strips to the concrete surface, this strengthening technique does not require significant surface preparation and allows for immediate use of the strengthened structure.

(a)

(b)

Fig. 12:(a) Mechanically-fastened FRP. (b) Detail of end anchorage with a combination of anchors and powder actuated nails.

RC elements strengthened with the conventional method (of adhesively bonding FRP strips) exhibit a tendency to fail in a brittle fashion, with a sudden debonding of the strip. However, suitably designed mechanically fastened strips enable a more ductile failure, due to

the partial shear connection at the strip concrete-interface as a result of strip compression failure at the points of contact with the fasteners, possibly combined with fastener pull-out and/or bending. One of the key requirements for this desirable failure mechanism to be activated is the proper design of strips with fibres in many directions, so that sudden shearing type of failures in the strips may be avoided.

4.2.9 Application of textile-reinforced mortar (TRM) jacketing

Despite its great advantages over other conventional techniques in a variety of applications, the FRP strengthening technique suffers from some problems associated with the epoxy resins, including the problematic behaviour at high temperatures and the relatively high cost. One possible solution to alleviate these problems would be the mere replacement of resins with inorganic binders. However, as a consequence of the granularity of the mortar, penetration and impregnation of conventional fibre sheets is very difficult to achieve; also, mortars cannot wet individual fibres, unlike resins. Bond conditions in cementitious composites could be improved and fibre-matrix interactions could be made tighter when continuous fibre sheets are replaced by textiles. These materials comprise fabric meshes made of long woven, knitted or even unwoven fibre rovings in at least two (typically orthogonal) directions (Figure 13).

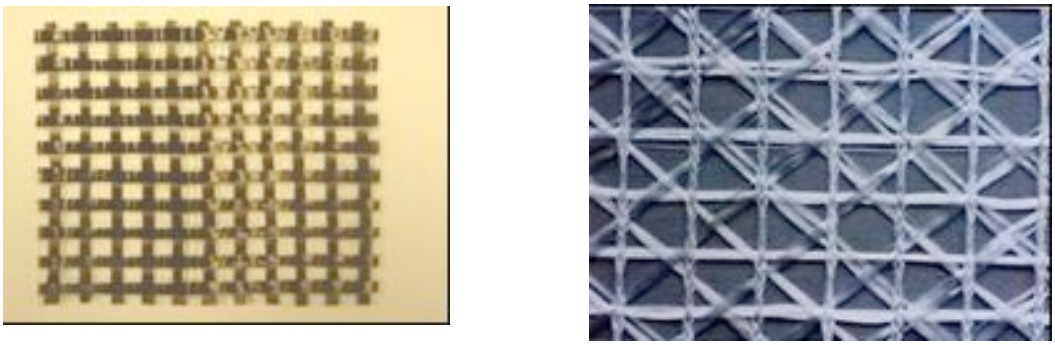

Fig. 13: (a) Bidirectional carbon fibre and (b) multidirectional glass fibre textiles.

Fig. 14: Textile-reinforced mortar (TRM) jacketing.

The density, that is the quantity and the spacing, of rovings in each direction can be controlled independently, thus affecting the mechanical characteristics of the textile and the degree of penetration of the mortar matrix through the mesh. The combination of textiles

with mortars has led to the development of the so-called TRM-strengthening technique (Figure 14), which appears quite promising for jacketing of RC members (Triantafillou et al. 2006, Triantafillou and Papanicolaou 2006).

5 Applications of composites and some design considerations

5.1 General

Composites have found their way as strengthening materials of reinforced concrete elements (such as beams, slabs, columns etc.) in several thousands of applications worldwide, where conventional strengthening techniques may be problematic. For instance, one of the popular techniques for upgrading RC elements has traditionally involved the use of steel plates epoxy-bonded to the external surfaces (e.g. tension zones) of beams and slabs. This technique is simple and effective as far as both cost and mechanical performance is concerned, but suffers from several disadvantages: corrosion of the steel plates resulting in bond deterioration; difficulty in manipulating heavy steel plates in tight construction sites; need for scaffolding; and limitation in available plate lengths (which are required in case of flexural strengthening of long girders), resulting in the need for joints. Replacing the steel plates with composites provides satisfactory solutions to the problems described above. Another common technique for the strengthening of RC structures involves the construction of reinforced concrete (either cast in-place or shotcrete) jackets around existing elements to enhance the shear resistance and/or ductility. Jacketing is clearly quite effective as far as strength, stiffness and ductility is concerned, but it is labour intensive, it often causes disruption of occupancy and it provides RC elements, in many cases, with undesirable weight and stiffness increase. Jackets may also be made of steel; but in this case protection from corrosion is a major issue. The conventional jackets may be replaced with composites wrapped around RC elements, thus providing substantial increase in strength (axial, shear, torsional) and ductility without much affecting the stiffness.

All necessary design situations, load combinations and limit states should be considered in the re-design of structures with externally applied composite reinforcement. The design of the strengthening system has to reflect the effects of the additional reinforcement provided to the cross sections (designed assuming *full composite action*) and the ability of transferring forces by means of the bond interface (verification of *debonding*) in bond-critical situations (e.g. flexural strengthening, shear strengthening with open jackets). In addition, detailing rules and special provisions need to be considered. Design calculations are based on analytical or (semi-) empirical models.

5.2 Material models

For *Serviceability Limit State* (SLS) verifications, a linear stress-strain response is considered for the constituent materials and the partial safety factors of the materials are taken equal to 1.0. In the case of fibre-reinforced composites, reference will be made to the following relationship:

$$\sigma_f = E_{fk}\varepsilon_f \tag{3}$$

where E_{fk} is the characteristic value of the secant modulus of elasticity. Normally, the lower

bound characteristic value $E_{fk0.05}$ is used for the design. In some verifications, when a higher modulus results in lower reliability, it is necessary to refer to the upper bound value $E_{fk0.95}$. When the elastic modulus is not considered as a fundamental variable in the equation, reference may be made to the mean value E_{fm}.

The tensile stress-strain behaviour of composites for the *Ultimate Limit State* (ULS) verifications can be idealised by means of a linear elastic response to failure:

$$\sigma_f = E_{fu}\varepsilon_{fu} \leq f_{fd} \tag{4}$$

where $E_{fu} = f_{fk} / \varepsilon_{fuk}$ is the modulus of elasticity at ultimate, based on the characteristic values of the tensile strength and ultimate strain, and f_{fd} = design tensile strength.

When the design is governed by the SLS or an ULS corresponding with bond failure, the composite material strain at ultimate is rather limited. In this situation, which will often be the case in flexural strengthening or in shear strengthening with open jackets, the composite material stress σ_f at the ULS is considerably lower than the tensile strength, so that the design tensile strength is generally not governing. In this case the design tensile strength f_{fde} is:

$$f_{fde} = \frac{f_{fk}}{\gamma_f}\frac{\varepsilon_{fue}}{\varepsilon_{fum}} \tag{5}$$

where ε_{fue} is the effective ultimate strain, ε_{fum} is the mean ultimate strain and γ_f is the material safety factor for fibre-reinforced composites.

Values for γ_f are suggested in Table 5 (*fib* 2001). These are mainly based on the observed differences in the long-term behaviour of composites (basically depending on the type of fibres), as well as on the influence of the application method. The proposed factors are subject to further study.

If the ULS verification involves *fracture* of the composite material, the ratio $\varepsilon_{fue}/\varepsilon_{fum}$ normally equals 1, as the effective ultimate strain ε_{fue} expected in-situ will not significantly differ from the mean strain ε_{fum} obtained through uniaxial tensile testing, and as small variations are accounted for in the material safety factor γ_f. However in particular cases, the effective failure strain ε_{fue} may be significantly lower as result of wrapping around very sharp corners, application of a large number of layers, multi-axial state of stress, etc.

A limited value of the failure strain may also be considered as a simplified design alternative. In this case, the ULS verification restricts excessive deformations in the composite materials, rather than verifying the related failure mode itself.

If the ULS verification involves *bond failure*, it is expected that this will develop through shearing in the concrete. In this case the material safety factor is taken as that for concrete failure ($\gamma_f = \gamma_{f,b} = \gamma_c$).

FRP type	Application type A[(1)]	Application type B[(2)]
CFRP	1.20	1.35
AFRP	1.25	1.45
GFRP	1.30	1.50

(1) Application of prefab systems under normal quality control conditions. Application of wet lay-up systems if all necessary provisions are taken to obtain a high degree of quality control on both the application conditions and the application process.

(2) Application of wet lay-up systems under normal quality control conditions. Application of any system under difficult on-site working conditions.

Table 5: Composite material safety factors γ_f.

5.3 Flexural strengthening

Reinforced concrete elements, such as beams and slabs, may be strengthened in flexure through the application of composites to their tension zones, with the direction of fibres parallel to that of high tensile stresses. The concept is illustrated in Figure 15, which also shows a practical application. The analysis for the limit states for such elements may follow well-established procedures for reinforced concrete structures, provided that: (a) the contribution of external reinforcement is taken into account properly; and (b) special consideration is given to the issue of bond between the concrete and the external reinforcement, through the use of an appropriate bond model. Central to the analysis of these elements is the identification of all the possible failure modes. These failure modes may be divided into two types: (a) those where full composite action of concrete and external reinforcement is maintained until the concrete reaches crushing in compression or the composite material fails in tension (such failure modes may also be characterized as "classical") and (b) those where composite action is lost prior to type (a) failure, due to debonding of the composite material. Debonding of the external reinforcement is dealt with through the use of a proper bond model, which allows the calculation of the maximum force carried by the composite material based on force – bond length relations (e.g. Fig. 16). A schematic illustration of the various failure modes is given in Figure 17.

Typical load – deflection curves for RC elements strengthened in flexure are given in Figure 18, illustrating the distinct characteristics if the behaviour such as the decrease in ductility with the increase in strength.

Fig. 15: Flexural strengthening of RC beam with CFRP strips.

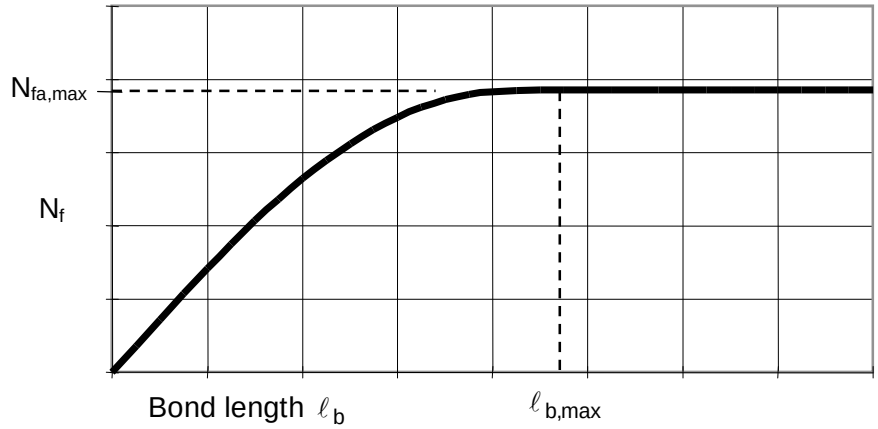

Fig. 16: Tensile force in the fibre-reinforced composite and maximum anchorable force as a function of bond length

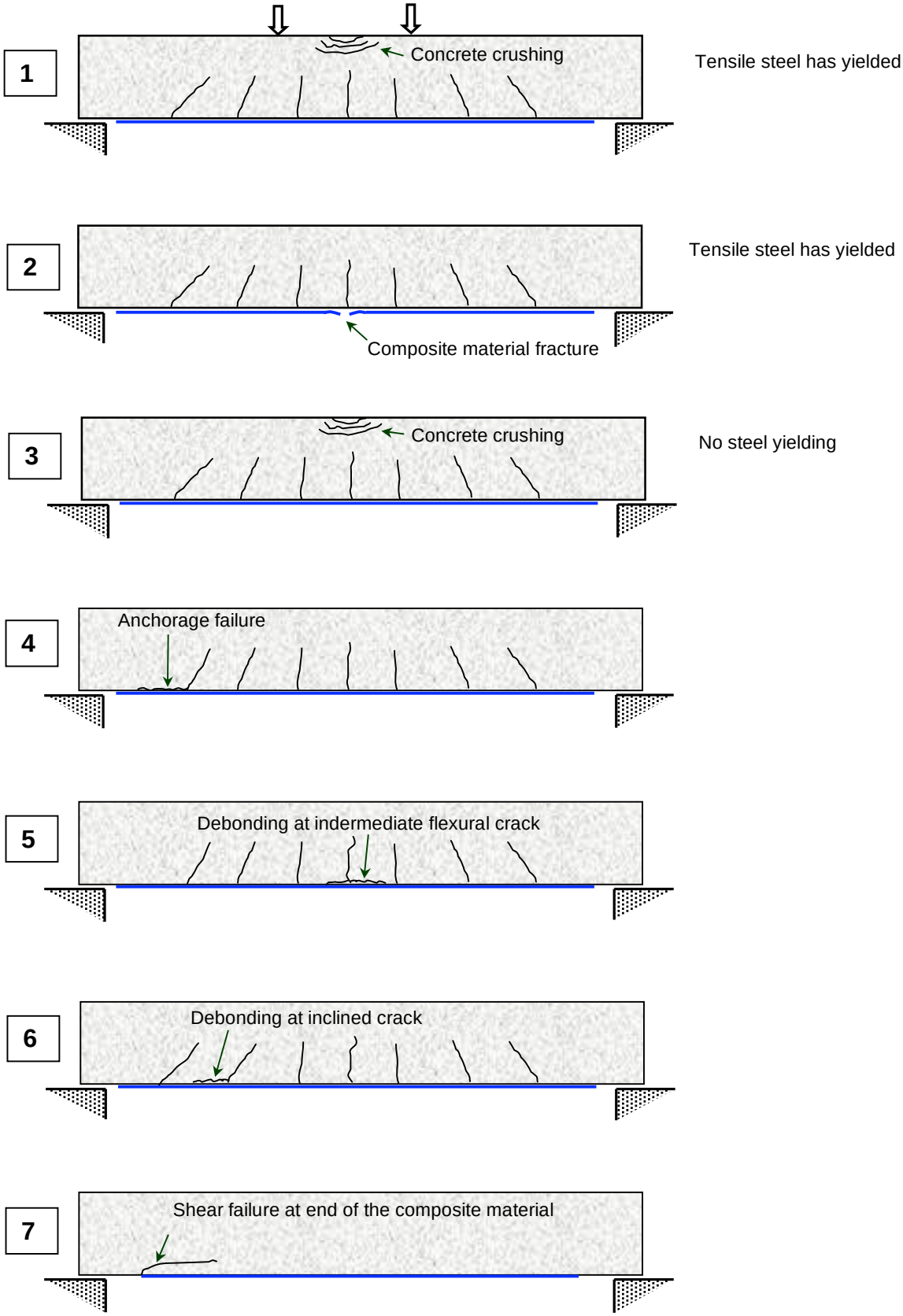

Fig. 17: Full composite action (1-3), loss of composite action (4-6) and end-shear (7) failure modes associated with flexural strengthening.

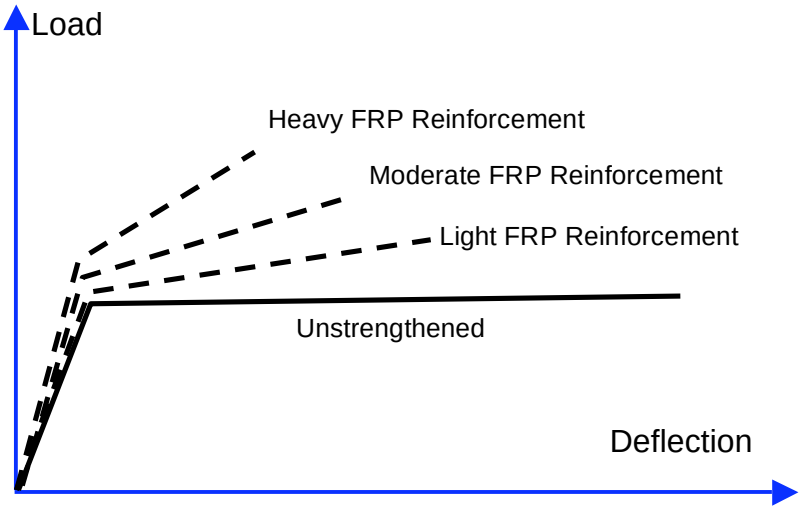

Fig. 18:Load-deflection curves for beams strengthened with FRP in flexure.

5.4 Shear strengthening

Shear strengthening of RC members (e.g. columns, beams, shear walls) using composites may be provided by bonding the external reinforcement with the principal fibre direction as parallel as practically possible to that of maximum principal tensile stresses, so that the effectiveness of the external reinfocement is maximised (see Figure 19 for the dependence of the composite material elastic modulus, E_{fu}, on the fibre orientation). For the most common case of structural members subjected to transverse loads, that is perpendicular to the member axis (e.g. beams under gravity loads or columns under seismic loads), the maximum principal stress trajectories in the shear-critical zones form an angle with the member axis which may be taken roughly equal to 45^o. However, it is normally more practical to attach the external reinforcement with the principal fibre direction perpendicular to the member axis (Figure 20).

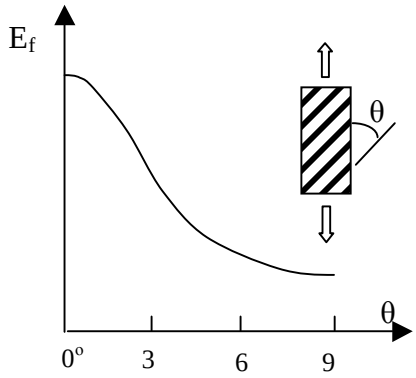

Fig. 19: Dependence of composite material elastic modulus on fibre orientation

According to the model of Triantafillou (1998), the external reinforcement may be treated in analogy to the internal steel stirrups, accepting that the composite materials carry only normal stresses in the principal material direction (Figure 21). It is assumed that at the ultimate limit state in shear (concrete diagonal tension) the composite develops an effective stress in the principal material direction, σ_{fde} (note: this is not the principal tensile stress, which may be assumed perpendicular to the crack), which is, in general, less than the tensile failure stress, f_{fd}. This effective stress depends on the type of jacket (closed versus open), the type of fibres, the thickness of the jacket and (for open jackets) on the strength of the substrate (concrete).

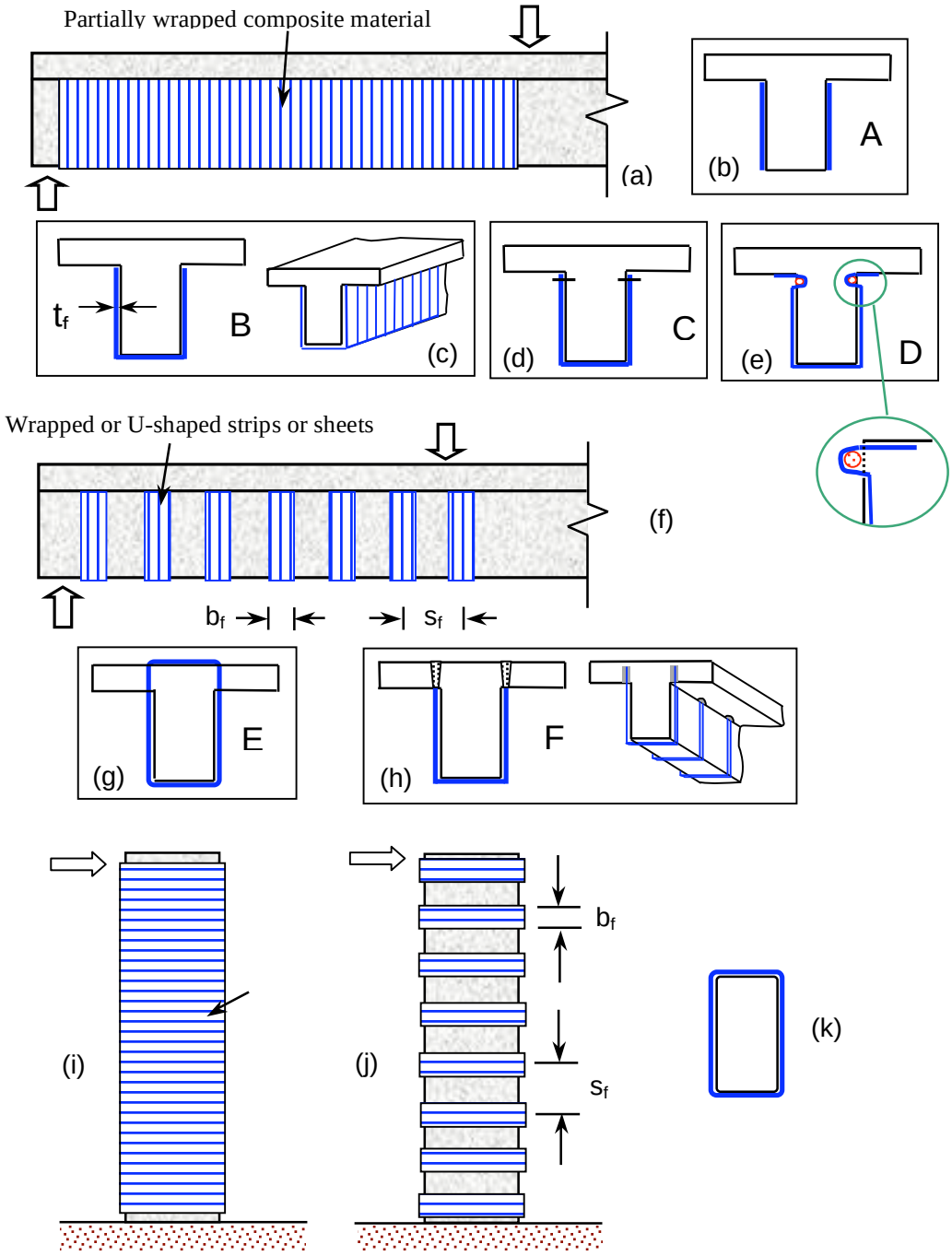

Fig. 20: *Schematic illustration of RC element strengthened in shear with externally bonded composites: (a)-(e) sheets or fabrics bonded to the web of beams; (f)-(h) wrapped or U-shaped strips applied to beams; (i)-(k) four sided wrapping of columns.*

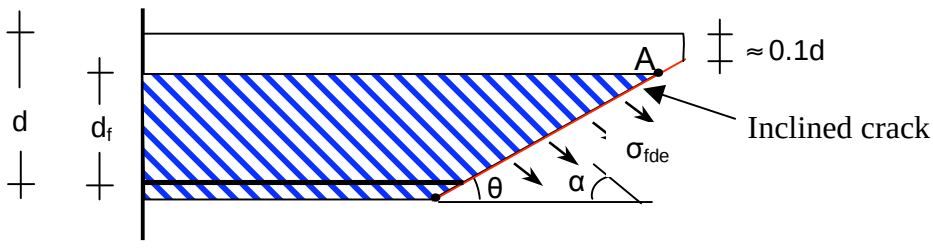

Fig. 21: Contribution of composite materials to shear resistance.

Typical results of the cyclic loading response of RC elements strengthened with composites in shear is illustrated in Figure 22, which shows that composite material jacketing suppresses brittle shear-type failures and enables flexural yielding and substantial ductility.

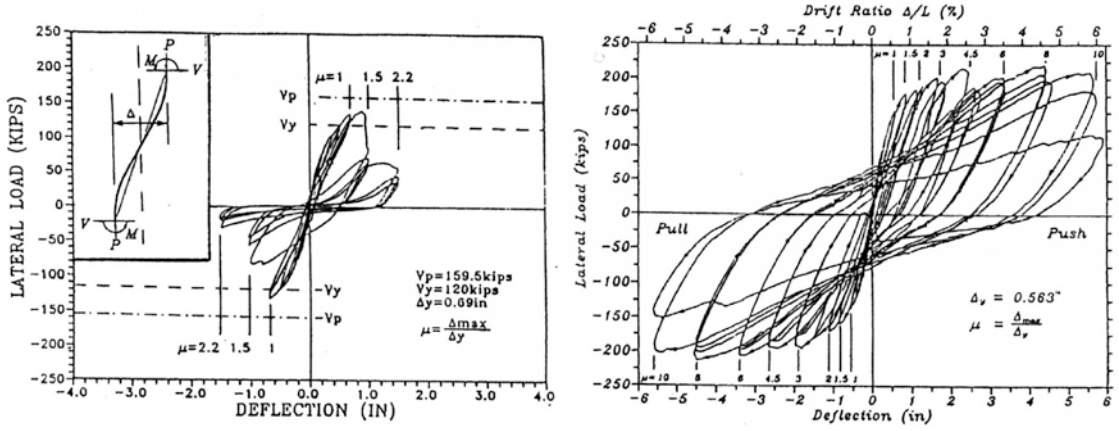

(a) (b)

Fig. 22: Lateral force-displacement response of shear-critical rectangular columns: (a) as-built; (b) retrofitted with GFRP jacket (Priestley and Seible 1995).

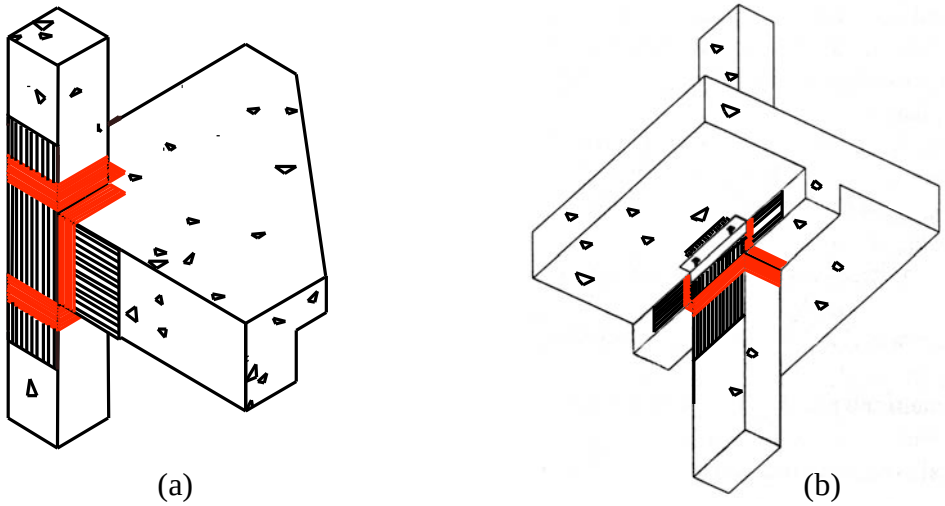

(a) (b)

Fig. 23: Typical composite material configurations for beam-column joint strengthening. (a) exterior joint, (b) interior joint.

5.5 Increase of member capacity through confinement

Enhancement of deformation capacity of seismicly deficient columns, as well as of axial load capacity of columns in need to carry higher axial forces is best achieved through concrete confinement. The stress-strain response of concrete confined with composites is shown schematically in Figure 24. The figure displays a nearly bilinear response with sharp softening and a transition zone at a stress level that is near the strength of unconfined concrete f_{cd}. After this stress the tangent stiffness changes a little, until the concrete reaches its ultimate strength f_{ccd} when the jacket reaches tensile failure at a stress f_{fde} which is, in general, less than the uniaxial tensile strength. This reduction is attributed to several reasons, including: (a) the triaxial state of stress in the composite material (due to axial loading and confining action, but also due to bending, e.g. at corners of low radius); and (b) the quality of execution (potential local ineffectiveness of some fibres due to misalignment, and overstressing of others; damaged fibres at sharp corners or local protrusions etc).

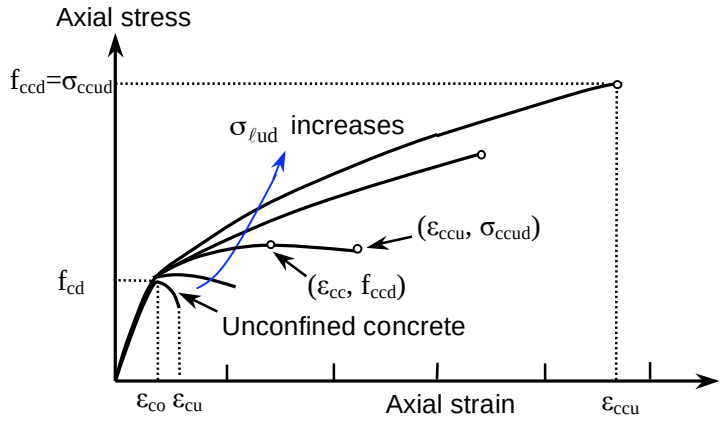

Fig. 24: Axial stress-strain response of concrete confined with composites.

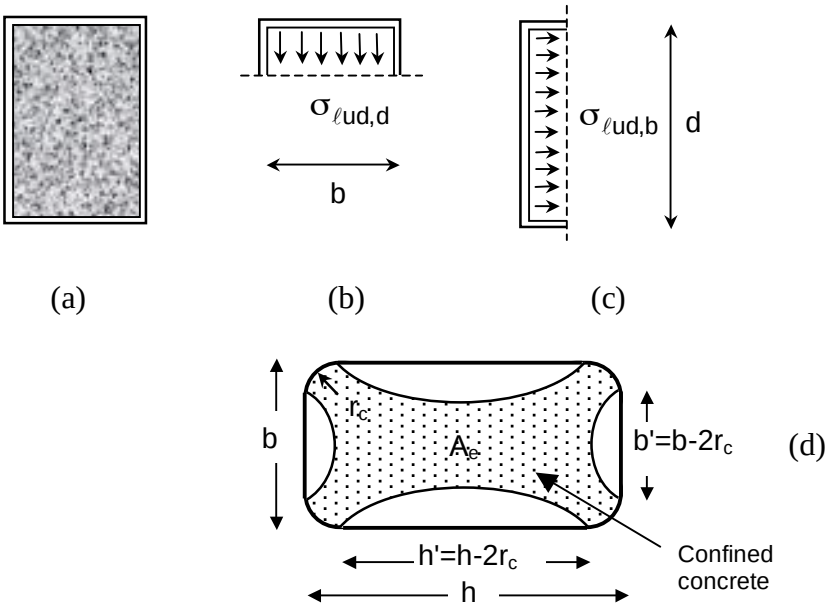

Fig. 25: (a)-(c) Approximate average confining stresses and (d) effectively confined area in columns with rectangular cross section.

Analytical and experimental studies of the stress-strain response of concrete confined with composites have been conducted by several researchers. Most of the available models give the stress at ultimate strain f_{ccd} and the associated strain ε_{ccu} as functions of the respective unconfined values f_{cd} and ε_{cu} as well as of the confining stress at ultimate $\sigma_{\ell ud}$ as follows:

$$\frac{f_{ccd}}{f_{cd}} = 1 + k_1 \left(\frac{\sigma_{\ell ud}}{f_{cd}} \right)^m \tag{6}$$

$$\varepsilon_{ccu} = \varepsilon_{cu} + k_2 \left(\frac{\sigma_{\ell ud}}{f_{cd}} \right)^n \tag{7}$$

where k_1, k_2, m and n are empirical constants. For circular cross sections of diameter D the ultimate confining stress (at failure of the jacket) equals

$$\sigma_{\ell ud} = \frac{2 t_f f_{fde}}{D} \tag{8}$$

where t_f is the thickness of the jacket. For rectangular cross sections $\sigma_{\ell ud}$ may be taken (approximately) as the mean confining stress in each direction (Figure 25), which depends on the confinement effectiveness factor α:

$$\acute{o}_{\ell ud} = \frac{\sigma_{\ell ud,b} + \sigma_{\ell ud,d}}{2} = \frac{1}{2}\left(\alpha \frac{2t_f}{d} f_{fde} + \alpha \frac{2t_f}{b} f_{fde} \right) = \alpha \frac{(b+d)}{bd} t_f f_{fde} \quad (9)$$

For the most common case of continuous jackets with fibres in the direction perpendicular to the member axis, the confinement effectiveness coefficient is defined as the ratio of effectively confined area (A_e in Figure 25d) to the total cross sectional area A_g.

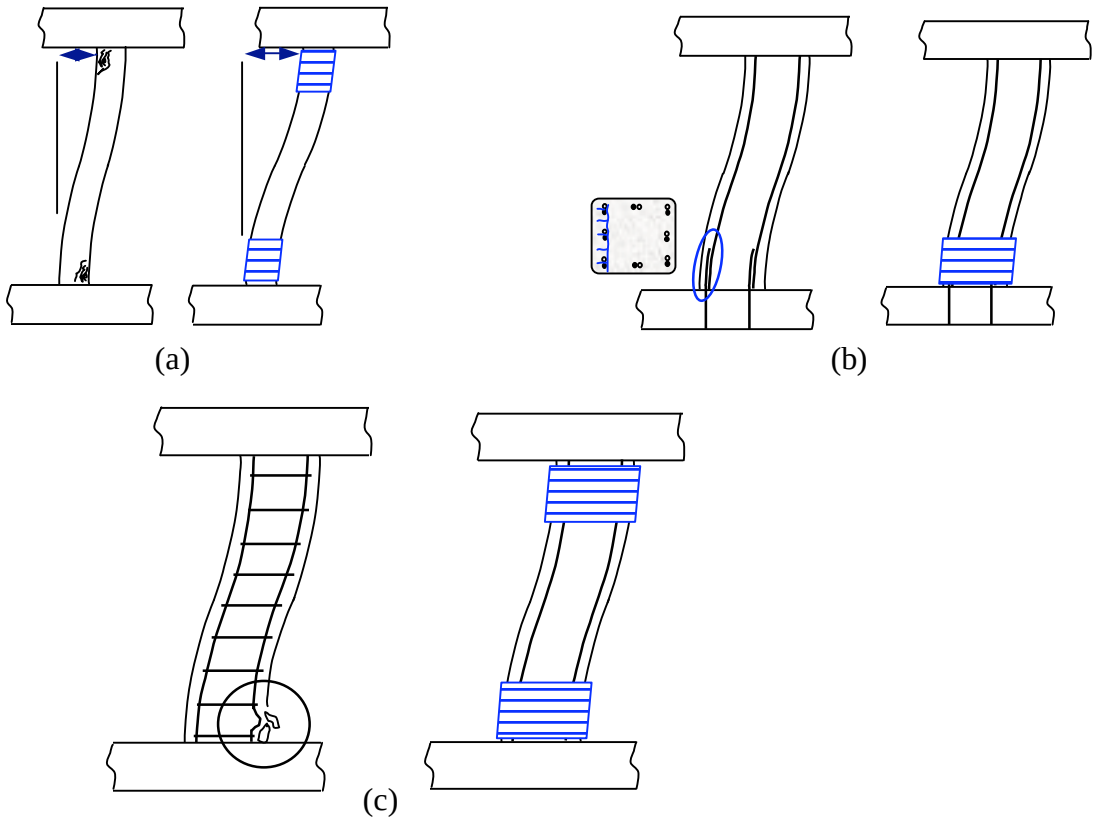

Fig. 26: Confinement of columns with composite materials to: (a) Increase lateral deformations (i.e. chord rotations). (b) Prevent lap splice failure. (c) Delay rebar buckling.

In summary, confinement of RC with composites has the following four favourable effects:

(a) Increase of axial load capacity,
(b) Increase of member lateral deformations (or chord rotations) due to improved plastic hinging (Figure 26a),
(c) Lap splice clamping (Figure 26b), and
(d) Delay of longitudinal rebar buckling (Figure 26c).

Existing models may be used to select the proper jacket thickness for each of the four cases given above.

References

Agarwal, B. D. and Broutman, L. J. (1990), *Analysis and performance of fibre composites*, John Wiley & Sons.

Antonopoulos, C. P. and Triantafillou, T. C. (2002), Analysis of FRP-strengthened RC beam-column joints. *Journal of Composites for Construction, ASCE*, 6(1), 41-51.

Antonopoulos, C. P. and Triantafillou, T. C. (2003), Experimental investigation of FRP-strengthened RC beam-column joints. *Journal of Composites for Construction, ASCE*, 7(1), 39-49.

Blaschko, M. and Zilch, K. (1999), Rehabilitation of concrete structures with CFRP strips glued into slits. In *Proceedings of the 12th International Conference on Composite Materials*, Paris, July 5-9.

De Lorenzis, L., Lundgren, K. and Rizzo, A. (2004), Anchorage length of near-surface mounted fibre-reinforced polymer bars for concrete strengthening – experimental investigation and numerical modeling. *ACI Structural Journal*, 101(2), 269-278.

Deuring, M. (1993), *Strengthening of RC with prestressed fibre reinforced plastic sheets*. EMPA Research Report 224, Dübendorf, Switzerland (in German).

Feldman, D. (1989), *Polymeric building materials*, Elsevier Science Publishers Ltd., UK.

fib (2001), Bulletin 14, *Externally bonded FRP reinforcement for RC structures*.

Hollaway, L. C. and Leeming, M. B. (1999), *Strengthening of reinforced concrete structures, using externally-bonded FRP composites in structural and civil engineering*, Woodhead Publishing.

Kim, D.-H. (1995), *Composite structures for civil and architectural engineering*, E & FN Spon, London.

Lamanna, A. J., Bank, L. C. and Scott, D. W. (2001), Flexural strengthening of RC beams using fasteners and FRP strips. *Journal of Composites for Construction, ASCE*, 8(3), 203-210.

Luke, P. S., Leeming, M. B. and Skwarski, A. J. (1998), ROBUST results for carbon fibre. *Concrete Engineering International*, 2(2), 19-21.

Mays, G. C. and Hutchinson, A. R. (1992), *Adhesives in civil engineering*, Cambridge University Press.

Priestley, M. J. N. and Seible, F. (1995), Design of seismic retrofit measures for concrete and masonry structures, *Construction and Building Materials*, 9(6), 365-377.

Täljsten, B. (1994), *Strengthening of existing concrete structures with epoxy bonded plates of steel or fibre reinforced plastics*. Doctoral Thesis, Luleå University of Technology.

Triantafillou, T. C., Deskovic, N. and Deuring, M. (1992), Strengthening of concrete structures with prestressed fibre reinforced plastic sheets. *ACI Structural Journal*, 89(3), 235-244.

Triantafillou, T. C. (1998), Shear strengthening of reinforced concrete beams using epoxy-bonded FRP composites. *ACI Structural Journal*, 95(2), 107-115.

Triantafillou, T. C., Papanicolaou, C. G., Zisimopoulos, P. and Laourdekis, T. (2006), Concrete confinement with textile reinforced mortar (TRM) jackets, *ACI Structural Journal*, accepted for publication.

Triantafillou, T. C. and Papanicolaou, C. G. (2006), Shear strengthening of RC members with textile reinforced mortar (TRM) jackets, *Materials and Structures, RILEM*, accepted for publication.

Winistoerfer, A. and Mottram, T. (1997), The future of pin-loaded straps in civil engineering applications. In *Recent Advances in Bridge Engineering, Proceedings of the US-Canada-Europe Workshop on Bridge Engineering*, ed. U. Meier and R. Betti, EMPA Switzerland, 115-120.

Detailing, technological aspects and durability

György L. Balázs
Budapest University of Technology and Economics, Hungary

1. Detailing rules

1.1 General

Detailing rules give practical information on the location, arrangement and limitations for the FRP reinforcement required by considerations such as minimum ductility, functional requirements, adequate anchorage, applicability of calculation models, practical durability measures, friendliness of execution, etc.

Compared to other fields of the EBR strengthening method (e.g. design for bending), detailing is much less supported by available test results. This is a field where future research is definitely needed. Most of the existing design specifications on EBR strengthening do not contain any or very limited amount of detailing rules.

1.2 Detailing with respect to strengthening lay-out

1.2.1 Flexural strengthening

Flexural strengthening is provided by axially oriented fabrics of pultruded strips or cured in situ fabrics bonded to the top or bottom faces of the member or to the sides (Fig. 1).

In the anchorage zones no additional transverse reinforcement is required if adequate anchorage is provided by bond stresses and debonding is resisted by concrete tensile stresses.

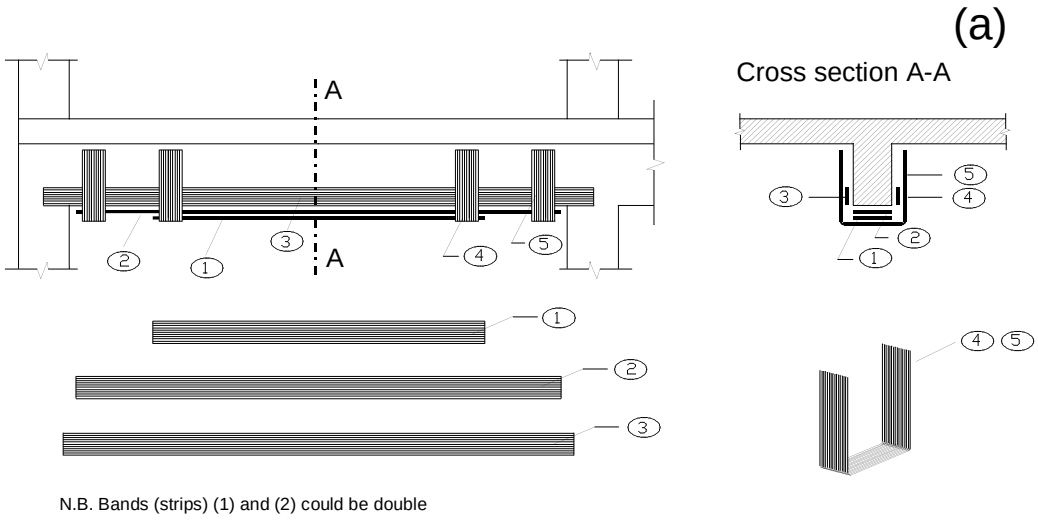

Fig. 1: Flexural reinforcement with possible shear anchorages (fib Bulletin 14)

1.2.1.1 General recommendations

The following recommendations should apply (Deutsches Institut für Bautechnik, 1998):

- Maximum spacing $s_{f,max}$ between strips:

$s_{f,max}$ $\leq 0.2\ \ell$ (ℓ = span length)

≤ 5 h (h = total depth)

$\leq 0.4\ \ell_c$ (ℓ_c = length of cantilever)

- *Minimum distance* to the edge of the beam should equal the concrete cover of the internal reinforcement.
- *Lap joints of strips* should only be provided in sections where the maximum tensile force in the EBR does not exceed 60% of the tensile force at ultimate. The lap length should be calculated according to the verification of the end anchorage (see Chapter 4 of *fib* Bulletin 14), where f_{ctm} should equal 10 N/mm^2 (bond strength of the adhesive). Joints are allowed for static loading only. Nevertheless, it is strongly recommended here that lap joints should be avoided; they are absolutely not necessary, because FRP can be delivered in the required length.
- *Permissible radii* of bends should be given in the product description for the strips. Permissible radii of fabrics need not be specified. However, it is recommended that sharp edges of the section be mechanically rounded before application. In this case, a minimum radius of 30 mm is recommended.
- *Crossing of strips* is allowed, with bonding in the crossing area.

1.2.1.2 Case of several layers

If several strips are to be applied, it is recommended to apply the one next to the other rather than the one onto the other. In this latter case, more than 3 layers of pultruded strips or 5 layers of cured in-situ fabrics are not recommended to apply unless proved by experimental evidence. In any case, recommendations of the EBR supplier must be followed.

By applying several layers of prestressed strengthening strips, reduction of prestressing due to the successive release of prestressing forces should be considered.

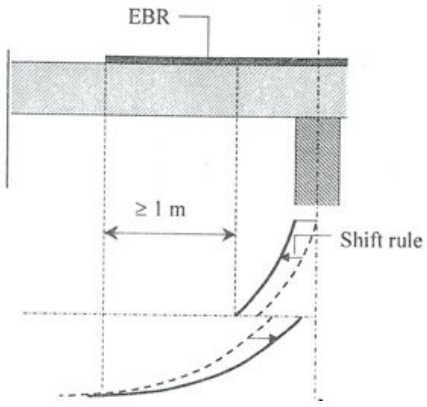

Fig.2: Anchorage above internal supports (fib Bulletin 14)

1.2.1.3 Anchorage zone

If strengthening is applied in the span of simply supported beams, the distance between the face of the support and the end of the strip should not exceed 50 mm. In the case of applying strips or fabrics over supports of continuous beams or slabs, the strips or fabrics should be anchored in the compression zone (Fig. 2).

Anchoring of EBR (especially if the strips are staggered) can be ensured by applying bonded FRP “strirrups” that enclose the longitudinal strips at their ends. The use of such

strirrups is strongly recommended. Note that these stirrups are not considered to be the part of the shear reinforcement but are responsible to keep the longitudinal strips in their position and to prevent peeling-off.

1.2.2 Shear strengthening

Shear strengthening can be provided by.

- factory made L-shaped CFRP strips,
- continuous sheets.

The externally bonded shear reinforcement generally covers four or three sides of the element but in some cases only two sides. Appropriate anchorage is strongly recommended. Practical solutions are given in Fig. 5-2 of Chapter 5 of *fib* Bulletin 14. It is important to note that in principle there are two different cases:

1. Proper anchorage of the shear strengthening system [Fig. 5-2 b, eq. (5-4 a, c) in *fib* Bulletin 14)],
2. Side or U-shaped shear strengthening system [Fig. 5-2 a, eq. (5-4 b) in *fib* Bulletin 14].

Anchorage failure, debonding failure and FRP fracture are accounted for in design through the effective FRP strains described in Section 5.1 [eq. (5-4 a-c) in *fib* Bulletin 14.)].

Proper anchorage means a fully wrapped or a system that is properly anchored in the compression zone, as shown in Fig. 3 and Fig. 4. Where practically possible, it is recommended to use for anchoring the whole height of the compression zone, to guarantee an anchoring as good as possible. FRP strips at the sides of the beam only are not recommended as in this case there is a lack of anchorage in both the compression and tension zone.

For the case of insufficient anchorage in the compression zone, the usable height (inner lever arm) has to be reduced, so that the member has a fictitious lower ultimate bending resistance. The principle is illustrated in Fig. 5. Until better calculation methods become available, it is recommended to calculate according to this proposal.

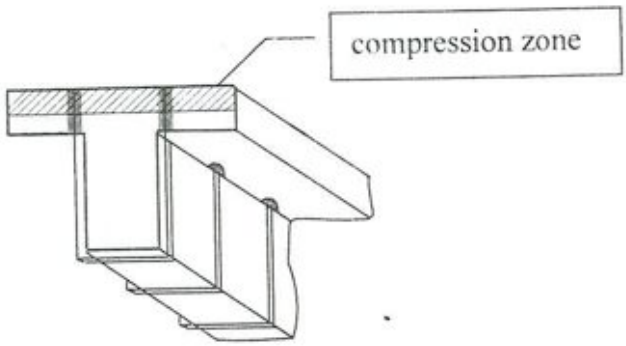

Fig. 3: Anchorage in the compression zone (fib Bulletin 14)

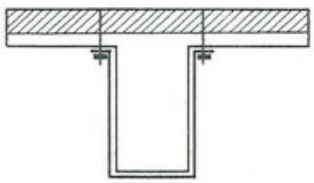

Fig. 4: Alternative anchorage in the compression zone (fib Bulletin 14)

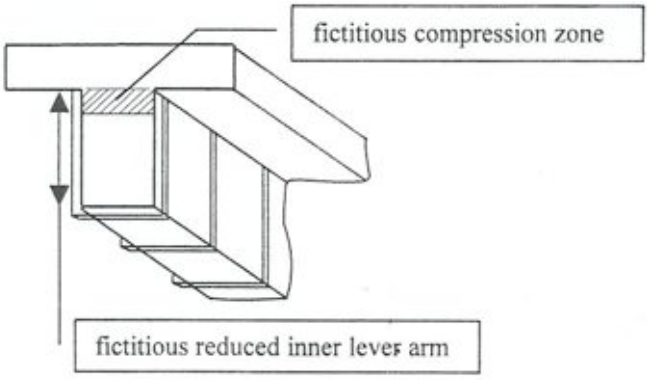

Fig. 5: No anchorage: Reduction of the usable height for bending resistance (fib Bulletin 14)

1.2.3 Confinement

Compressed members can be effectively confined by externally bonded reinforcement with horizontally or spirally running fibres. The number of superimposed layers (maximum number of layers 20-25 or according to the material supplier's recommendation) is obtained by the analysis described in Chapter 6 of *fib* Bulletin 14.

Concerning the application of EBR on rectangular columns or pier walls with large aspect ratio, the EBR does not actually confine the internal concrete structure if just applied to the surface. In order to achieve confinement, the EBR jacket need to be constrained on both sides along the length through the use of dowels or bolts that anchor the jacket to the pre-existing structure, thereby creating shorter distances which are confined between bolts (Karbhari and Seible, 1998).

In case of eccentric compressive loads of high magnitude, longitudinally directed fibres can be also applied. These fibres are to be anchored with transverse fibres at the top as well as the bottom of the member.

Class 0	Structures located in dry environment with low content of humidity Example: indoor structures
Class 1	Structures that can be subjected to freeze-thaw and minor content of humidity Example: protected outdoor structures
Class 2	Structures located in a humid environment Example: outdoor structures which are not in direct contact with water or subjected to extreme rain (e.g. facades)
Class 3	Structures located in a very humid environment or in direct contact with water or/and environment with high temperature and high humidity Example: part of quay-, bridge- or dam structures in direct contact with water

Table 1: Environmental classes (Täljsten, 1999)

1.2.4 Humidity and moisture issues

When applying an FRP system, especially in the case of fabrics that can wrap the total surface of the element, water can accumulate at the bond line. Therefore in the case of flexural strengthening of beams or of slabs it is recommended to leave a gap to provide vapour transfer space. In the case of shear strengthening, a gap every 300 mm should be left exposed. Detailed recommendations can be found in Mack and Holt (1999).

In the case of column strengthening, practice suggests leaving a gap of 30 to 50 mm of

concrete unwrapped at the connection between the column and footing and/or cap beam face. Indeed excessive flexural strength in the plastic hinge region due to the contact between the column jacket and the adjacent member may possibly result in undesired moment and shear forces in footings and cap beams during seismic response. A gap is then needed but it also leaves a path for excess water to enter through any irregularities between the FRP and the concrete. Water should be prevented from seeping in between the FRP and the concrete surface by sealing the gap with a water barrier (epoxy resin or paint).

When dealing with humidity and moisture problems, structures to be strengthened can be divided into environmental classes as shown in Table 1.

The total surface can be wrapped for classes 0 and 1, special investigations are needed for class 2 and full wrapping should be avoided for class 3.

1.3 Special anchorages

1.3.1 General

Bolts, U-shaped sheets or L-shaped strips (Meier and Bleibler, 1999) are recommended at the ends of the EBR to resist concentrations of peel and shear stresses in the region where these stresses exceed the pull-off strength of the concrete times γ_m.

With respect to bolted systems, it is not adequate to drill through the strengthening strip omitting special provisions and merely fixing with a bolt, as drilling holes through unsupported composites severs the unidirectional fibres. As compressive forces can weaken the strip further and as it is not possible for the forces in the strip to be transmitted into the bolt, the end tabs should be designed to take the full forces in the strip to be transmitted into the bolt, the end tabs should be designed to take the full force to be anchored. Alternatively, FRP EBR with multidirectional fibres at the location of the bolts can be used in an effective way (Matthys and Blontrock, 2000). Bolted systems should be positioned at suitable spacing and anchored in the concrete to a depth beyond the steel reinforcement. The bolts should be supplied with large washers and tightened up to a specified torque to prevent crushing of the composite materials.

In general, anchoring devices that may influence the integrity of the strengthening system are not recommended. For example, at holes that are necessary when bolts are applied, interlaminar shear failure or splitting of the strip may initiate. Moreover, holes reduce the cross section of the strip.

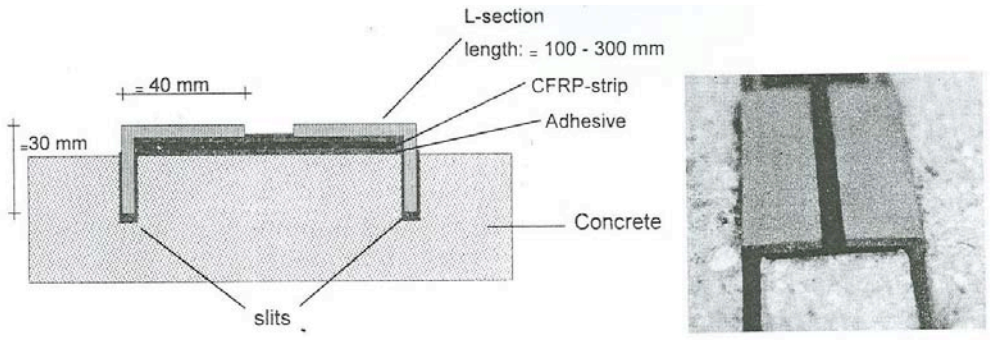

Fig. 6: Anchorage for CFRP strips, special anchorage system (Zehetmaier, 2000) (fib Bulletin 14)

1.3.2 Device for CFRP strips

The basic scheme of tests made with special anchoring devices for CFRP strips is shown

in Fig. 6. With this mechanical anchorage a significant increase in anchored tensile force can be obtained. This system can be applied in case of strengthening slabs (where no wrapping is possible), local strengthening and as an anchorage for prestressed strips. A minimum concrete cover of about 20 mm is required.

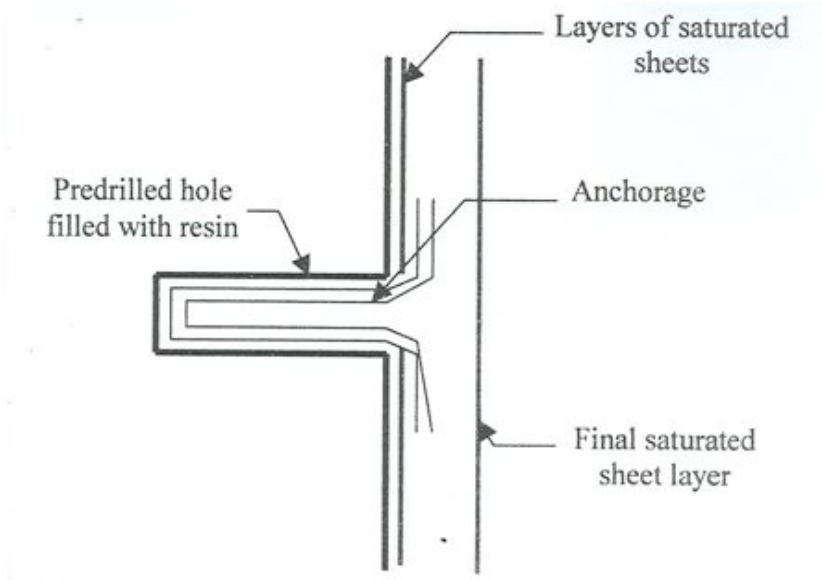

Fig. 7: Section of the anchor system (fib Bulletin 14).

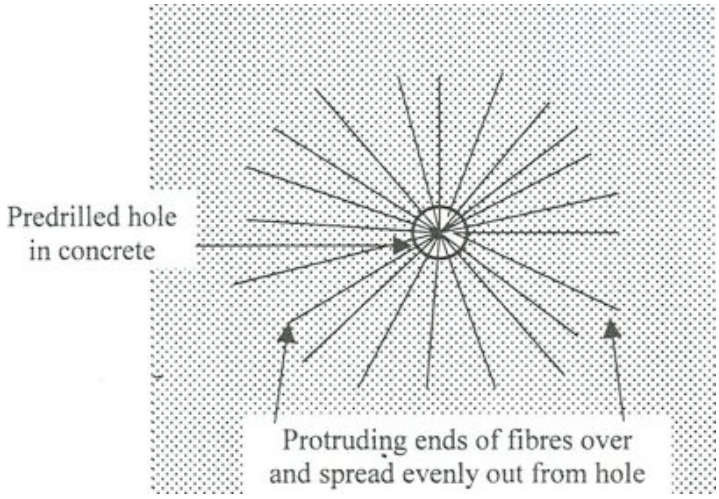

Fig. 8: Top view of the anchor system (fib Bulletin 14)

1.3.3 Device for sheets

The following patented anchor system (see Fig. 7 and 8) is a way to bond a composite to a concrete structure in addition to the normal adhesive that is used (Neuner and Falabella, 1996). A hole is drilled in the concrete, debris is blown out and epoxy adhesive is applied on the structure. A layer of continuous sheet reinforcement impregnated with an epoxy resin is applied. A glass tow is then forced through the impregnated fabric into the predrilled hole and the ends are splayed outwards in a circle. A final layer of resin-impregnated fabric is applied and allowed to cure.

Concrete blocks made with and without this type of anchors and with glass composite extending outwards from a flush cut edge have been tested. The composite ends were tabbed

and shear tests were performed by gripping the tabs and the blocks and pulling apart under tension. The results were concrete failures in both cases with the anchors showing about two times increase in shear strength versus specimens without anchors (Neuner and Falabella, 1996).

2 Technological aspects

EBR strengthening is a technique where technological aspects have high importance. Adequate quality can only be reached if careful execution is provided.

2.1 Initial requirements

The following requirements should be fullfilled:

a. minimum content tensile strength: 1.5 N/mm^2
b. maximum water content of substance: 4 mass%
c. minimum surface temperature of concrete: +5°C.

(a)

(b)

Fig. 9: Circular application of FRP strips on a silo (Balázs, Almakt, 2000) (fib Bulletin 14)
a) application of FRP to the substance
b) gluing of the two surfaces

2.2 Steps of execution

Application of FRP strips is carried out in the following steps.

1. Mechanical cleaning of substance (e.g. by sand blasting) in order to reach slightly rough surface.
2. Removal of dust from the concrete surface.
3. Cutting of FRP strips to design size.
4. Cleaning of FRP strips from carbon dust.
5. Mixing of adhesive (A+B components).
6. Application of adhesive both to the substance and to the FRP (potlife of adhesive should be considered) (Fig. .9a and b).
7. Rolling (or pushing) of FRP into the adhesive (elimination of air bubbles). Final thickness of adhesive should be 1 to 1.5 mm.
8. Cover layer to the FRP by the adhesive (if required).
9. Fire protection (if required).
10. UV protection (if required).

Steps 8, 9 and 10 are needed only if required.

Application of wraps is similar to that of strips, however, above point 4 is irrelevant and in case of point 6 the adhesive to FRP is applied after placing it.

An important application rule is that FPP does not need supporting during hardening of adhesive owing to its low weight.

2.3 Quality control

Adequate quality of the execution can be reach by considering the following requirements:

- certified material properties both for FRP and adhesive
- qualified and trained workers for execution
- appropriate cleaning of surfaces (dust free surface is needed)
- continuous bond should be provided (checks by destructive or non-destructive testing).

3 Durability

Short-term characteristics of FRPs can be more or less easily determined, however, long-term properties may require specific considerations. Present chapter intends to give an overview on long-term characteristics of FRP-s (Balázs, Borosnyói, 2001) (Table 2).

Long-term characteristics		
Environmental influences		*Mechanical properties*
- alkalis	- thermal effects	- creep,
- chloride ions	- fire	- relaxation,
- water	- freeze/thaw	- fatigue
- UV radiation	- combined effects	

Table 2: Long-term influences related to the behaviour of FRP

3.1 Effect of alkaline environment

Concrete is highly alkaline due to the high calcium hydroxide content of hardened cement stone (pH 12.5 to 14) that may need special attention for durability of FRP (Fig. 10.).

Carbon fibres cannot absorb liquids and are resistant to acid, alkali and organic solvents, therefore, do not show considerable deterioration in any kind of harsh environment (Machida, 1993; Tokyo Rope, 1993).

Deterioration of glass fibres in alkaline environment is well known. Therefore, the duty of resins is of great importance in protection of glass fibres. Experimental studies of GFRP reinforcement embedded in concrete or under accelerated aging tests in strong alkaline solutions have demonstrated that glass fibres show significant degradation due to alkali, independently of the of resin (Sen et al, 1993; Tannous and Saadatmanesh, 1998; Uomoto and Nishimura, 1999). Decrease in tensile capacity can be in the range of 30 to 100 percent according to saturation and acting time. Best protection is ensured with vinyl ester resin. Results of accelerated tests usually show more deterioration than tests with embedded reinforcement. Rate of deterioration of glass fibres in alkaline environment is highly dependent on the type of fibres.

Aramid fibres may also suffer deterioration in alkaline environment, however, to a less degree than glass fibres and may depend on the actual fibre product (Uomoto and Nishimura, 1999). Decrease in tensile capacity can be 25-50 percent (Rostásy, 1997).

Alkaline environment can deteriorate links between molecules of resins. Similarly to the resistance against water absorption the alkaline resistance of vinyl ester resins is the best while epoxy and polyester resins can give sufficient and poor resistance, respectively (Machida, 1993).

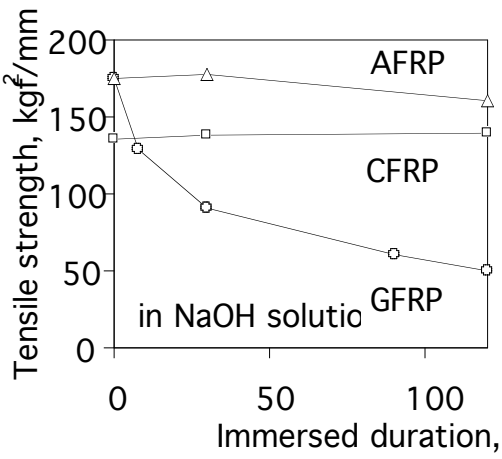

Fig. 10: Effect of alkali on tensile strength (after Uomoto-Ohga, 1996) (fib Bulletin 14)

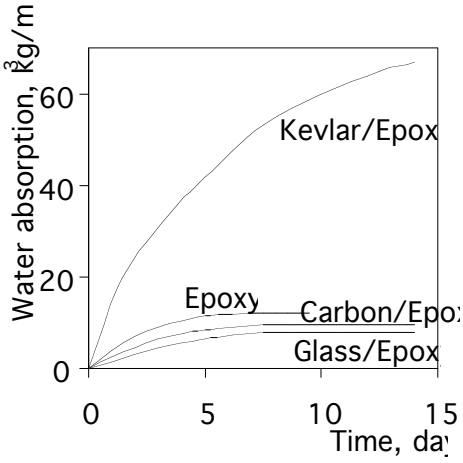

Fig. 11: Water absorption of FRPs (after Piggott, 1980) (fib Bulletin 14)

3.2 Effect of chloride ions

CFRP and AFRP reinforcements are insensitive to chloride ions, however aramid fibres seem to be inapplicable in marine environment due to difficulties initiated by swelling (Sen et al, 1998a; Sen et al, 1998b). Experimental studies demonstrated that GFRP reinforcements can be seriously deteriorated in marine environment or in presence of de-icing salts led to corrosion induced failure (Saadatmanesh and Tannous, 1997).

3.3 Effect of ultraviolet rays

Polymeric materials can be considerably degraded by ultraviolet rays (Piggott, 1980). Embedded FRP reinforcements are protected from direct sunlight, however, when stored outdoors or applied as external reinforcement can be exposed to ultraviolet rays. On one hand, deterioration of GFRP and CFRP materials are attributed to the degradation of resin matrix. After 2500 hours of exposure to direct sunlight decrease in tensile strength and in Young's modulus was less than 10 percent and negligible, respectively (Kato et al, 1997). Aramid fibres themselves may deteriorate due to UV radiation.

3.4 Effect of moisture and water

In fresh concrete contact of water and FRP reinforcement is evident. Material changes associated with water are usually of the resins. Water can absorb into polymer chains and can create weak chemical reactions causing considerable changes in characteristics (e.g. strength, Young's modulus, bond). These effects are mostly reversible, however, swelling of resin can cause micro-cracks in the matrix that can initiate fibre debonding and higher permeability. In general it can be stated that vinyl ester resins show the best resistance to water absorption, epoxy resins can provide sufficient resistance, while polyester resins usually have poor performance (Machida, 1993).

For what concerning fibres, carbon and glass fibres cannot absorb water on the contrary to aramid fibres (Uomoto and Nishimura, 1999). Water absorption of aramid fibres causes reversible decrease in tensile strength, Young's modulus or relaxation and irreversible decrease in fatigue strength (Piggott, 1980). Decrease in characteristics of AFRP due to water absorption is about 15-25% (Gerritse, 1993). According to swelling of AFRP reinforcement bond cracking can be induced by wet/dry cycles (e.g. in splash zones of marine structures) that cause deterioration (Sen et al., 1998a). Fig. 2 indicates water absorption capacity of variours FRPs.

3.5 Combined and other effects

Effect of water and alkaline absorption is clearly accelerated by increasing temperature. Rate of degradation of GFRP and AFRP can be doubled by the change of temperature from 20°C to 60°C (Rostásy, 1997; Tannous and Saadatmanesh, 1998).

Degradation of AFRP due to ultraviolet rays can be accelerated by wet/dry cycles of marine splash zone (Uomoto and Ohga, 1996)

As it is well known, carbonation of concrete has important role on the corrosion of ordinary reinforcement. Research work on the effect of carbonation on durability of FRP reinforcement is very limited. Available data shows large scatter, however, carbonation seems to have no effect on the durability of FRP reinforcements (Sheard et al, 1997).

3.6 Thermal actions on FRP reinforcements

3.6.1 General considerations

In the case of FRPs thermal actions can influence both mechanical characteristics and bond behaviour. As indicated in Table 3 coefficient of thermal expansion (CTE) of fibres, resins, FRPs and concrete are differing from each other. In the longitudinal direction FRPs

have lower or nearly identical CTEs than that of concrete, however, in the transverse direction – governed mostly by the resin – have 5 to 8-times higher values. In specific cases, when high temperature variation takes place the large difference between CTEs can lead to high radial pressure on the surface of the reinforcement that can cause longitudinal splitting of concrete cover. It reflects on the importance of sufficient concrete cover especially if AFRP reinforcement is applied. Critical concrete cover (whenever splitting occurs) of AFRP tendons with sand coated surface was found to have 2.8×∅ (Taerwe and Pallemans, 1995). Authors found sufficient concrete cover of 2.5×∅ to CFRP tendons with sand coated surface for pretensioned application with ten hours heat curing of maximum temperature of 75°C (Balázs and Borosnyói, 2001).

Thermal effects can also have influence on aging of resins, in this way the residual strength of FRP reinforcements. Experimental data on change of long-term residual strength of FRPs due to thermal cycles are not available.

Tensile strength and Young's modulus of FRPs are functions of the temperature. Under service temperature of concrete structures (-20 to +60°C) the change in Young's moduli of CFRP, AFRP and GFRP reinforcements are decrease of 10, 25, 35 percent, respectively (Rostásy, 1996). Change in tensile strength is attributed to only higher temperatures when deterioration of resin occurs.

Material	Coefficient of thermal expansion, $\times 10^{-6}$ 1/K	
	longitudinal	transverse
carbon fibre	–0.9…+0.7	8…18
aramid fibre	–6.0…–2.0	55…60
glass fibre	5…15	5…15
resins	60…140	
CFRP	–0.5…1.0	20…40
AFRP	–2.0…–1.0	60…80
GFRP	7…12	9…20
concrete	6…13	

Table 3: Coefficients of thermal expansion of fibres, resins, FRPs and concrete

3.7 Effect of elevated temperature

Polymeric materials are usually flammable or harming in case of fire. Therefore, theoretically the resin determines the temperature/fire resistance of FRPs. Resins soften, melt or catch fire above 150-200°C. The fibres themselves can more or less able resist higher temperatures: aramid up to 200°C, glass to 300-500°C and carbon to 800-1000°C (Rostásy, 1996).

3.8 Effect of freezing and thawing

In many civil engineering applications reinforced concrete members are subjected to large number of freezing/thawing cycles (mostly combined with water and chloride ion penetration into concrete). However, experimental data on the influence of such effects on the durability of FRP reinforcements is very limited. Due to freezing/thawing cycles (combined with water and chloride ion diffusion) degradation of fibres, resin and interfacial bond is possible. According to micro cracking of concrete under freezing/thawing cycles bond between concrete and FRP can be also injured.

References

Balázs, G.L. and Almakt, M.M. (2000) Strengthening with CFRP – Hungarian experiences, *Concrete Structures 2000*, pp. 52-60.

Balázs, G.L. and Borosnyói, A. (2001) Long-term behaviour of FRP", *ASCE Proceedings,* Int. Workshop on Composites in Construction: A Reality, Capri, Italy, pp. 84-91.

"Deutsches Institut für Bautechnik (1998), Authorisation No. Z-36.12-54.

Karbhari, V. M. and Seible F. (1998) Design considerations for the use of fibre reinforced polymeric composites in the rehabilitation of concrete structures, In Proceedings of NIST Workshop on Standard Development for the Use of FRP for the Rehabilitation of Concrete and Masonry Structures, Tucson, Arizona, pp. 203-210.

Mack, J. K. and Holt, E. E. (1999) The effect of vapor barrier encapsulation of concrete by FRP strengthening systems, Proc. 44th International SAMPE Symposium and Exhibition, Long Beach, California.

Matthys, S. (2000) Innovaties in uitwending gelijmde vezelcomposietwapening vor de versterking van betonconstructies: Experimenteel onderzoek, In Proceedings colloquium "Betonversterking met uitweinding gelijmde wapening: staal en kunststof', Belgiche Vereniging tot Studie, Beproeving en Gebruik der Materialen (BSVM).

Meier, H. and Bleibler, A. (1999) The latest R&D in Structural Strengthening with bonded CFRP plates, In Proceedings of Structural Faults & Repair-99, London.

Neuner, J. and Falabella, R. (1996) Composite anchor system – flatwise tensile and shear testing, Internal Report, Hexcel Corporation.

Balázs, G. L. and Borosnyói, A. (2001) Prestressing with CFRP Tendons, Proc. of UEF Intern. Conference on High Performance Materials in Bridges and Buildings, Kona, Hawaii

Gerritse, A. (1993) Aramid-based prestressing tendons, Alternative Materials for the Reinforcement and Prestressing of Concrete, Ed. Clarke, Chapman & Hall, London, 172-199.

Kato, Y., Yamaguchi, T., Nishimura, T. and Uomoto, T. (1997) Computational Model for Deterioration of Aramid Fibre by Ultraviolet Rays, Proc. 3rd Int. Symp. FRPRCS-3, Japan Concrete Institute, Vol. 2., pp. 163-170.

Machida, A. (1997) Recommendation for Design and Construction of Concrete Structures Using Continuous Fibre Reinforcing Materials, JSCE, Tokyo.

Piggott, M. R. (1980) Load Bearing Fibre Composites, Pergamon Press, Oxford.

Rostásy, F. (1997) On Durability of FRP in Aggressive Environment, Proc. 3rd Int. Symp. FRPRCS-3, JCI, Vol. 2, pp. 107-114.

Saadatmanesh, H., Tannous, F. E. (1997) Durability of FRP Rebars and Tendons, Proc. 3rd Int. Symp. FRPRCS-3, JCI, Vol. 2., pp. 147-154.

Sen, R., Mariscal, D. and Shahawy, M. (1993) Durability of Fibreglass Pretensioned Beams, *ACI Structural Journal*, V. 90, No. 5, pp. 525-533.

Sen, R., Shahawy, M., Rosas, J. and Sukumar, S. (1998) Durability of Aramid Pretensioned Elements in a Marine Environment, *ACI Structural Journal*, V. 95, No. 5, pp. 578-587.

Sen, R., Shahawy, M., Rosas, J. and Sukumar, S. (1998) Durability of Carbon Pretensioned Elements in a Marine Environment, *ACI Structural Journal*, V. 95, No. 6, pp. 716-724.

Sheard, P., Clarke, J., Dill, M. and Hammersley, G. – Richardson, D. (1997) EUROCRETE – Taking Account of Durability for Design of FRP Reinforced Concrete Structures, Proc. 3rd Int. Symp. FRPRCS-3, JCI, Vol. 2., pp. 75-82.

Tannous, F. E. and Saadatmanesh, H. (1998) Environmental Effects on the Mechanical Properties of E-Glass FRP Rebars, *ACI Materials Journal*, V.95, No. 2, pp. 87-100.

Tokyo Rope (1993), Technical Data on CFCC®, Tokyo Rope Mfg. Co., Ltd. Manual, Tokyo

Uomoto, T. and Ohga, H. (1996) Performance of Fibre Reinforced Plastics for Concrete Reinforcement, Proc. 2nd ACMBS Conference, Montreal, CSCE, 1996, pp. 125-131.

Uomoto, T. and Nishimura, T. (1999) Deterioration of Aramid, Glass and Carbon Fibres Due to Alkali, Acid and Water in Different Temperatures, Proc. 4th Int. Symp. FRPRCS-4, ACI SP-188, American Concrete Institute, pp. 515-522.

Strengthening of RC beams with FRPs and FRP anchorages

Ugurhan Akyuz
Middle East Technical University, Ankara, Turkey

1. Flexural strengthening of beams

1.1 Introduction

RC beams which have insufficient flexural capacity should be appropriately strengthened. Bonding of steel plates or post-tensioning of steel plates are some of the methods most commonly used. These methods have difficulties in application. For RC beams strengthened with externally applied steel plates, corrosion is another problem.

In the last decade, with the improvements in technology, a promising technique was developed for strengthening of structures, aiming at less disturbance and shorter time of application. Fibre reinforced polymers (FRP), made of high-modulus fibres bonded with a resin matrix, have increasingly been used for strengthening, because of their superior properties. Compared to steel, FRPs possess many advantages: good corrosion resistance, high strength to weight ratio, electromagnetic neutrality and ease of handling. If the labour cost and losses due to interruption of services are considered, strengthening with FRPs provides overall the most-cost effective solution.

FRPs are generally constructed of high performance fibres such as carbon (CFRP), aramid (AFRP) or glass (GFRP). By selecting among the many available fibres, geometries and polymers, the mechanical and durability properties can be adapted accordingly. Such a synthetic quality makes FRP a good choice for civil engineering applications.

This contribution is mainly based on Teng et al. 2002, where reference is made for details.

1.2 Methods of flexural strengthening

The first study on RC beams strengthened with CFRP sheets was done at the Swiss Federal Laboratory for Material Testing and Research (Meier *et al.* 1993). Strengthening of RC beams is generally done by bonding an FRP sheet to the beam as shown in Figure 1. It is very important that the RC beam should be prepared prior to the application of FRP sheet. Unevenness of the beam surface must be corrected. This preparation is very critical, especially if the FRP sheet is going to be constructed on site in a wet lay-up process. In some cases, prefabricated FRP plates are used; then preparation of the bonding surface of the FRP plate can be necessary.

Bonding of FRP sheets to the bottom surface of the beam is the most common strengthening technique of RC beams for flexure (Figure 1).

There are basically two schemes for the adhesion of the FRP sheet: i) wet lay-up, ii) adhesive bonding of prefabricated FRP plate. The former method is the most commonly used due to its greater flexibility for field application. Epoxy resin is applied to the concrete surface and FRP sheets are impregnated in place using rollers. In the later method, prefabricated FRP plates are cut according to the application and bonded to the RC beam by using epoxy. The wet lay-up method is very sensitive to unevenness of the beam surface, which leads to debonding. On the other hand, the prefabricated FRP plate method, due to material uniformity and quality control is not sensitive to unevenness of the beam surface. To prevent debonding

FRP U-shaped strips can be bonded to the ends of the sheet (Figure 2). It should be mentioned that debonding at the plate ends is very brittle and occurs with no prior indication of failure.

U-shaped FRP strips as well are formed through the wet lay-up method. If feasible, FRP strips can also be wrapped around the beam near the ends of the FRP sheet. However, in most of the beam cases wrapping is not possible. It is noted that wrapping can delay debonding only up to a certain limit (Smith and Teng 2001a).

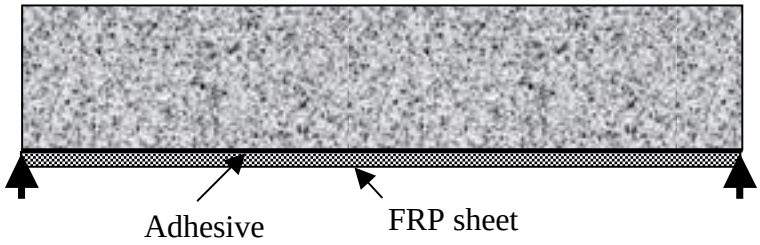

Fig.1: RC beam strengthened with an unstressed FRP sheet

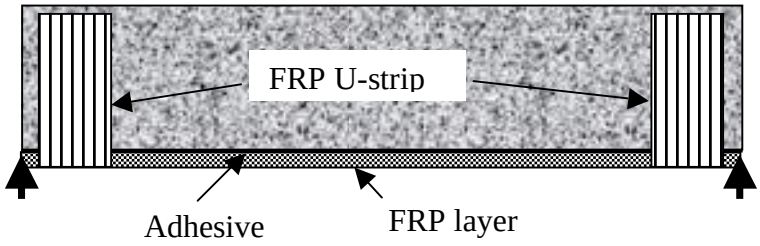

Fig. 2: Strengthened RC beam with FRP U-strip

1.3 Failure modes

There are basically four types of failure in a RC beam strengthened with FRP:

- Flexural failure
- Shear failure
- Debonding of plate end failure
- Intermediate crack-induced interfacial debonding failure.

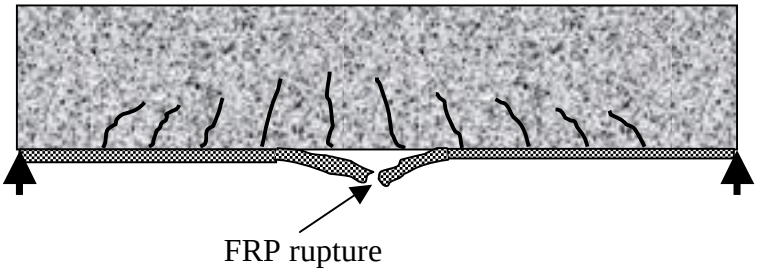

Fig. 3: Flexural failure

1.3.1 Flexural failure

Flexural failure generally occurs when there is no debonding at the ends of FRP sheet. In a flexural failure either the FRP sheet is ruptured or the concrete is crushed in compression (Figure 3). Although this failure is very similar to the flexural failure of RC beams, it is a very brittle failure. It should be kept in mind that flexural strengthening of RC beams using FRP

sheets leads to a strength gain (up to 76%) but causes a reduction in ductility.

1.3.2 Shear failure

In a RC beam strengthened in flexural using FRP sheets, the shear failure mode can be more critical. FRP sheets placed at the tension zone of RC beam have little contribution to shear resistance. Thus the shear capacity of an RC beam dictates the failure mode. In such cases, the shear capacity of RC beam must be increased, so that flexural failure precedes shear failure. Although in a RC beam strengthened with FRP sheets flexural failure is brittle, it is still more ductile than shear failure.

1.3.3 Plate-end debonding failure

Before ultimate capacity of the strengthened beam is reached, premature failure may occur due to end debonding (Figure 4). Separation of the concrete cover at one of the two ends is the most commonly seen failure mode. In this mode of failure, first a crack forms, it propagates up to the tension reinforcement and then progresses horizontally along the steel. This process leads to the separation of the concrete cover.

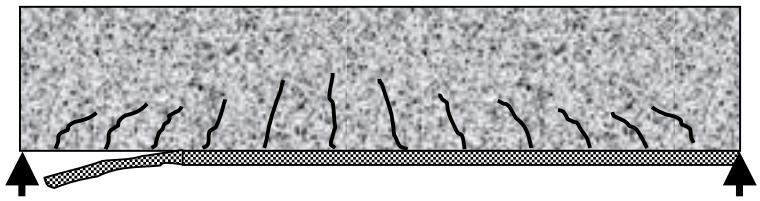

Fig. 4: Plate-end debonding failure

1.3.4 Intermediate crack-induced interfacial debonding failure

Debonding may occur at a flexural crack near mid-span that propagates towards one end. This is intermediate crack-induced interfacial debonding failure (Figure 5). It is also a very brittle and premature mode of failure.

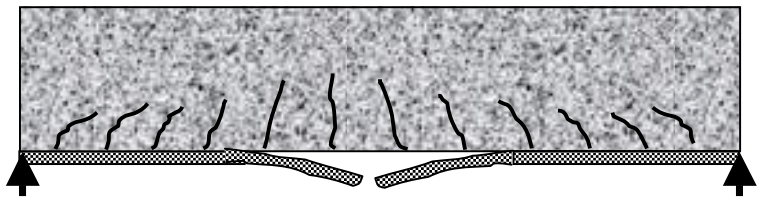

Fig. 5: Intermediate crack-induced interfacial debonding failure (from Teng et al. 2002)

2 Shear strengthening of RC beams with FRPs

2.1 Introduction

RC beams fail due to either flexure or shear. The former is the desirable mode of failure since it is more ductile. Shear failure is very brittle. It is already mentioned that, an RC beam strengthened in flexure with an FRP sheet exhibits a brittle behaviour, even though it fails due to a flexural failure mode, but it is still more ductile than shear failure mode. It is extremely important to examine the shear capacity of RC beams that are going to be strengthened in flexure. Recently, use of FRP sheets or FRP strips attracts more attention in strengthening of RC beams in shear. Versatility of FRP is a benefit for shear strengthening.

It is known that bonding of FRP sheets to the tensile zone of RC beams has insignificant contribution to the shear capacity. It is also evident that side bonding with longitudinally placed fibres has very little contribution. When a RC beam must be strengthened both in flexure and in shear, shear strengthening must be applied first.

This chapter is based on Teng *et al.* 2002, to which the reader is referred for details.

2.2 Methods of shear strengthening

Strengthening of RC beams in shear is done basically in three different schemes: i) by bonding of FRP sheets to the sides of the RC beam only, ii) by bonding FRP U-strips to both the sides and the tension face of the RC beam (U jacketing), iii) by wrapping FRP around the whole cross-section of the RC beam. While strengthening RC beams in shear, fibre orientation must be carefully chosen to control the shear cracks, keeping in mind that FRPs are strong only in the fibre direction. Here reversed cyclic loading, such as earthquake loads, should be carefully taken into account.

A suitable strengthening method must be selected according to the:

- Accessibility (whether wrapping is possible or not)
- Strengthening requirement (reversed cyclic loading or monotonic)
- How much increase in shear capacity is needed

Among the three different schemes, side bonding only is the easiest to apply and needs the least amount of FRP, but it is the most vulnerable to debonding and the least effective. In U jacketing, beam ends must be rounded and normal U-jackets must be used. This scheme is less vulnerable to debonding compared to side bonding. Although it is acting as mechanical anchor for flexural strengthening with FRP, it may need mechanical anchors at the free ends of the U. Among the three different schemes, wrapping is the most effective and less vulnerable to debonding. However, in most of the cases, it is not feasible or very difficult due to the inaccessibility of at least one side of the beam.

2.3 Failure modes

There are basically three types of shear failure occur in a RC beam strengthened with FRP:

- Shear failure with FRP rupture
- Shear failure without FRP rupture
- Shear failure due to FRP debonding

2.3.1 Shear failure with FRP rupture

This failure generally occurs with a diagonal shear crack (Figure 6). First a vertical flexural crack occurs and propagates diagonally towards the loading point. As the width of the crack increases, the strain in the FRP increases, and the FRP ruptures when it reaches its ultimate strain. Rupture of the FRP leads to brittle failure of the RC beam.

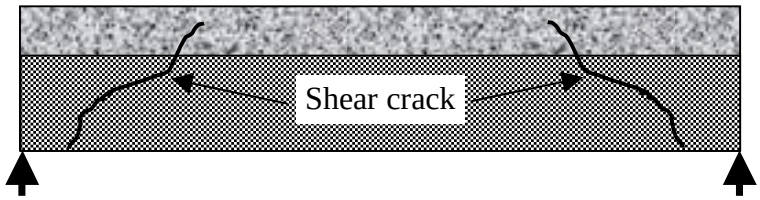

Fig. 6: Shear failure with FRP rupture

2.3.2 Shear failure without FRP rupture

This is very similar to the shear failure with rupture, except that FRP does not rupture and can carry loads after the concrete fails (Chajes *et al.* 1995).

2.3.3 Shear failure due to FRP debonding

This is the most commonly seen failure mode for side bonding and U jacketing (Figure 7). On the side of the beam debonding of FRP occurs first, and then beam fail in a brittle manner.

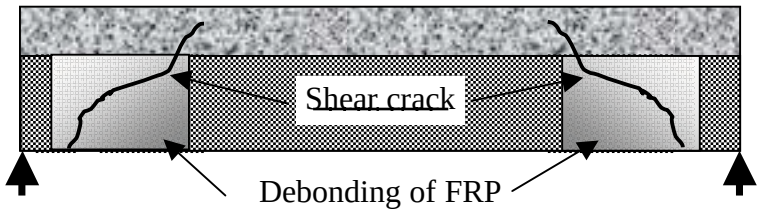

Fig. 7: Shear failure due to FRP debonding

3 FRP anchorages

3.1 Introduction

Knowing that strengthening with FRP is successful for member repair, it was used in rehabilitation of undamaged structures with a new technique in which the goal was system improvement rather then member rehabilitation. This technique is called seismic retrofitting by carbon fibre sheet (SR-CF system). In the SR-CF system, the existing hollow clay tile infill walls are basically employed as members that can carry shear force like RC walls. This is done by partially covering the hollow clay tile infill walls with diagonally glued carbon fibre sheets, provided that the edges of the sheet are connected to the peripheral column, beam and slab using special connections. Here, the carbon fibre sheet behaves like a tensile bracing, and increases the shear resistance of the wall as well as its lateral stiffness.

The most important point in SR-CF application is the performance of the special connection, because this application is based on the load transfer from hollow clay tile infill wall covered with CFRP to the frame members. This can be possible with proper connection details. For this purpose, special devices namely, carbon fibre reinforced polymer (CFRP)

anchors, were developed. The effectiveness of SR-CF system highly depends on the capacity of CFRP anchors. When this connection is lost, the load-transmitting function fails.

3.2 Types of CFRP anchors

There are basically two types of CFRP anchors, depending on how they are prepared:

i) Type-1 CFRP anchors,

ii) Type-2 CFRP anchors.

Before giving the details of these types, it should be emphasized that adhesive anchors transfer the applied load to the concrete through the bond surface along the embedment depth. Therefore to have an effective bonding, manufacturers usually suggest 2-3 mm free space between the concrete and the anchor for the adhesive.

3.2.1 Type-1 CFRP anchors

Type-1 anchors are prepared by rolling the CFRP sheet around itself, such that it has a cylindrical form (Figure 8). To secure that CFRP anchors do not deviate from their cylindrical form, they were tied. Then, the rolled CFRP sheets are embedded into epoxy resin so that a 10 mm portion from the bottom is covered with epoxy. By the time the end of the anchor hardens, some portion of the CFRP sheet, equal to the embedment depth, is coated with epoxy and inserted into drilled holes. With the help of a 10 mm stiff portion from the bottom of the CFRP anchor, one can push the epoxy coated cylindrical sheet into the hole filled with epoxy by means of a very thin steel wire.

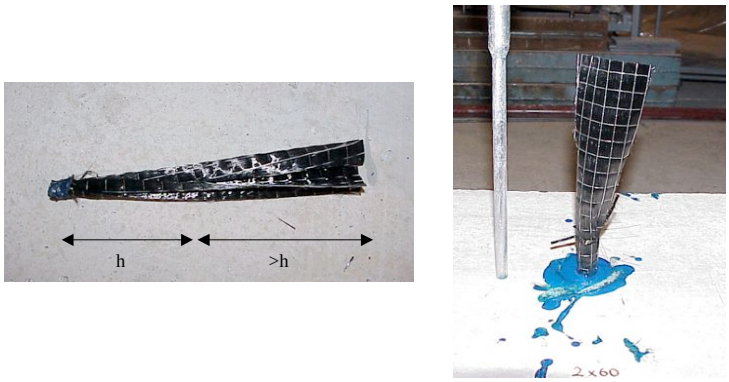

(a) (b)

Fig.8: a) Rolled CFRP sheet (left) and b) CFRP anchor embedded into concrete (right)

3.2.2 Type-2 CFRP anchors

Unlike Type-1 anchors, these CFRP anchors are prepared completely outside the hole and then installed into the concrete. In this type, first the desired width of the CFRP sheet is cut and coated with epoxy resin. Then, the epoxy coated CFRP sheet is rolled over a silicon rod 10 mm longer than the embedment depth (Figure 9). This technique provides straight anchors in which the fibres of the CFRP sheets are oriented in the same alignment. The part of the anchor that is rolled around the silicon rod is embedded into the drilled hole and bonded there. The extra part of the silicon rod is cut just at the concrete level.

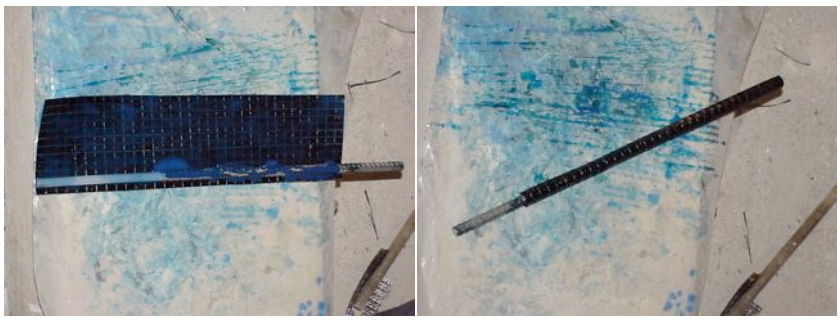

Fig. 9: Epoxy coated CFRP sheet rolled around silicon and steel rod

3.3 Mechanical properties of CFRP anchors

There are several parameters that affect the capacity of adhesively bonded CFRP anchors. Among them, the most important are the anchor hole diameter, the CFRP sheet width, the embedment depth and the concrete compressive strength.

Adhesive anchors transfer the applied load to the concrete through bond along the embedment depth. To have an effective bonding, manufacturers usually suggest 2-3 mm free space between concrete and anchor for the adhesive.

The tensile capacity of CFRP anchors is proportional to sheet width. However, the increase in tensile capacity of CFRP anchors is not linearly proportional to the sheet width: tensile capacity of the anchors do not increase in the same amount with the sheet widths.

In a recent study (Gokhan and Akyuz, 2005) the maximum tensile load capacities are obtained for CFRP anchors for a certain embedment depth. This indicates that there is an effective bond length beyond which load capacity does not increase. The increase in tensile load capacities can be assumed linear up to the effective embedment depth. In the mentioned study, this effective depth was reported as 100 mm.

For shallow embedment depths, the concrete compressive strength, if it is in the range of 10 to 20 MPa, does not significantly affect the tensile capacity of CFRP anchors. However, as the embedment depth increases, the effect of concrete compressive strength becomes more important.

3.4 Failure modes

Anchors are primarily loaded through attachments to the embedded anchors. The loading can be in tension and/or in shear. They may also be subjected to bending, depending on the details of shear transfer through the attachment. The behaviour and failure modes of anchors in tension are of primary importance in this study.

There are four primary failure modes for adhesive anchor dowels which are subjected to pure tensile loading. These are

a) Anchor failure,
b) Concrete splitting failure,
c) Concrete cone failure, and spacing and edge cone failure,
d) Pull-out failure.

3.4.1 Anchor failure

The strength of the anchor controls failure when the embedment depth of the anchor is sufficient to preclude concrete failure and when the spreading forces are sufficiently high or

the bearing area is sufficiently large to preclude an anchor slip failure. The ductility at which failure occurs by rupture of the anchor depends on the type of anchor and the embedment depth.

For given material properties and anchor dimensions, this case defines the upper limit for the tensile load carrying capacity. If the embedment depth of the anchor is sufficient for the anchor not to fail due to tension in the concrete, then the corresponding failure is shown in Figure 10. In this type of failure, the anchor reaches its maximum tensile capacity under the applied direct tension load. Since CFRP is a brittle material, this failure is very brittle.

3.4.2 Splitting failure of concrete

Splitting failure is characterized by the propagation of a crack in a plane containing the anchor. This failure mode may occur only if the dimensions of the concrete are so small that the anchors are placed very close to an edge or too close to each other. The failure load is usually smaller than needed for a concrete cone failure.

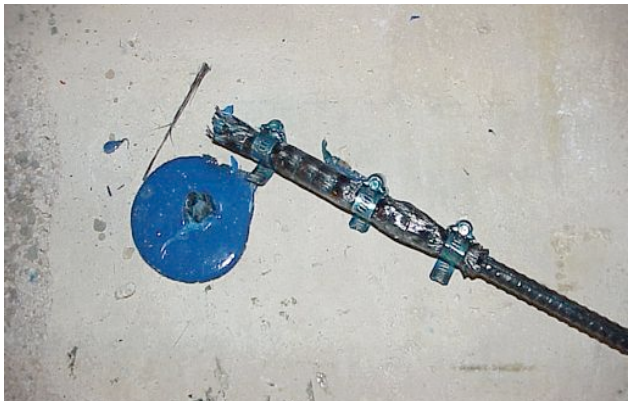

Fig. 10: CFRP failure

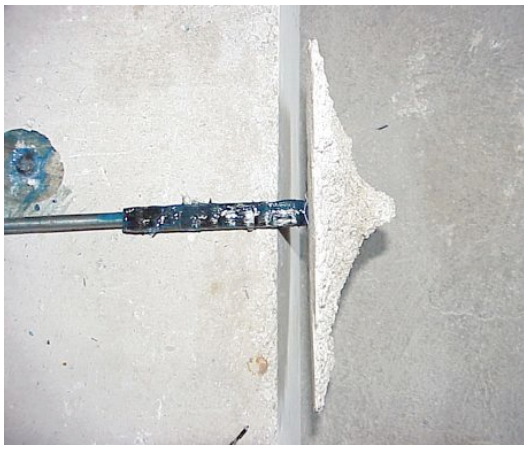

Fig. 11: Concrete cone failure

3.4.3 Concrete cone failure

When the anchor load is transferred to concrete through bond, the maximum stress occurs near the surface and diminishes with depth. If the embedment depth of an anchor is insufficient to develop the tensile strength of the anchor, then a pullout cone failure of the concrete is the expected failure mode. In addition, when the spacing of anchors or the location

with respect to an edge interferes with the development of the full cone strength of an anchor, its capacity is reduced. Consequently, for anchors which do not have sufficient embedment depth to provide the failure of the anchor itself, the tensile capacity of the anchor is limited with the cone capacity. For the case in which the tensile strength of the concrete is the main parameter to determine the capacity of the anchor (shallow anchors), some of the methods which are widely accepted are the concrete capacity (CC) method and the 45^{o} cone method. It should not be forgotten that all models are based on some similar conditions or assumptions to simplify the calculations. One of these conditions is the spacing between neighbouring anchors. To eliminate the interaction between neighbouring anchors, the spacing between successive anchors is chosen at least equal to twice the embedment depth.

In agreement with the definitions given above, when the embedment depth is shallow the observed failure is due to tensile capacity of the concrete. In Figure 11, a picture of the concrete cone failure observed during the tests is given for an embedment depth of 50 mm.

3.4.4 Pullout failure

Pullout failure is a typical failure mode for wedge anchors at moderate to deep embedment depths in lower strength concrete, where the crushing of the concrete at the wedges allows the anchor to pull through. The pullout capacity of adhesive anchors increases with increasing embedment depth. However, after a certain depth the increase is not proportional to embedment depth. This is due to high bonding effect resulting in high load transfer to the concrete at the top of the anchor. The bond stress is no longer uniform and if the tensile load is sufficiently high, failure initiates with a concrete failure in the upper portion of the concrete and then bond fails in the remainder of the embedment depth. The bond stress distribution along the embedment depth of the anchor prior to failure is given in Figure 12.

Figures 13 and 14 show the pictures of a pullout failure together with a slip and a concrete cone at the top. In Figure 13, the failure area can be seen clearly. This figure shows the importance of spacing between neighbouring anchors. It is obvious that anchors which are too close to each other can not provide the full capacity of the concrete.

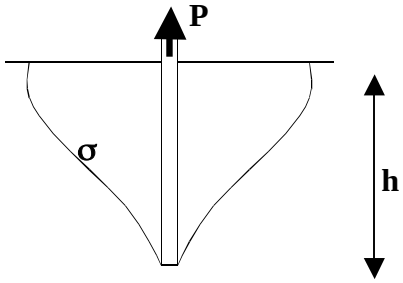

Fig. 12 Bond stress distribution along embedment depth of the anchor

Fig. 13: Pullout failure of CFRP anchor

Figure 14 shows the part of the failed anchor inside the crushed concrete. For this specific anchor, embedment depth was 70 mm. At the upper part near the surface, there occurs a shallow concrete cone with an approximate depth of 50 mm. The remaining 20 mm part fails due to slip of the anchor from the concrete. Therefore, one can conclude that the tensile load causes a bond failure between the epoxy resin and the concrete surface after the concrete cone has occurred.

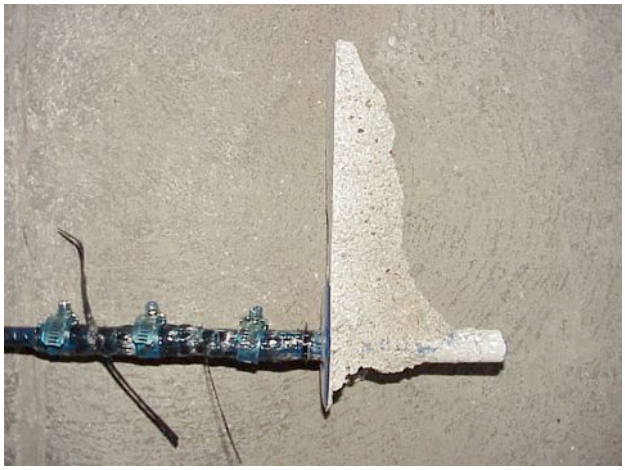

Fig. 14: Side view of the failed CFRP anchor

3.5 Strength model

There are several methods in the literature that can be used to predict the strength of adhesive steel anchors. However, there is not any successive way of predicting the tensile capacities of CFRP anchors yet. Eq. (1) is used to give an idea about the tensile capacity of the CFRP sheet used to prepare the anchor.

$$P_{FRP} = w \times t \times f_u \tag{1}$$

On the other hand, the effect of the concrete strength can be considered by calculating the tensile capacity of the concrete cone given in Figure 16 as:

$$P_{CONE} = 0.33\sqrt{f_c}\left(d + \frac{h}{\tan\theta}\right)\frac{\pi h}{\sin\theta} \qquad h < 50\,\text{mm} \qquad (2a)$$

$$P_{CONE} = 0.33\sqrt{f_c}\left(d + \frac{50}{\tan\theta}\right)\frac{\pi \times 50}{\sin\theta} + \tau_{ave} \times \pi d \times (h - 50) \qquad h > 50\,\text{mm} \qquad (2b)$$

In Eqs. (2), f_c is concrete compressive strength, h is embedment depth of anchor dowel, d is hole diameter, θ is the crack angle, and τ_{ave} is the average shear stress of the concrete through the embedment depth. CFRP anchors with embedments deeper than 50 mm have a shallow cone followed by a slip through the remaining part in failure. The concrete cone depth is almost equal to 50 mm for all embedment depths. Therefore, for embedment depths greater than 50 mm, to represent the bond failure Eq. (2b) is proposed.

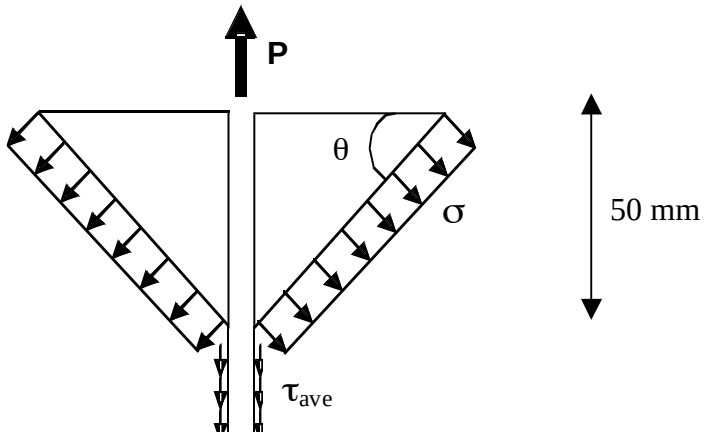

Fig. 15: Stress distribution along the embedment depth of the anchor

References

Chajes, M.J., Januszka, T.F., Mertz, D.R., Thomson, T.A., Jr, and Finch, W.W. Jr (1995). Shear strengthening of reinforced concrete beams using externally applied composite fabrics. *ACI Structural Journal*, Vol. 93, No. 3, pp. 295-303.

Meier, U., Deuring, M., Meier, H. and Schwegler, G. (1993). CFRP bonded sheets. FRP Reinforcement for Concrete Structures: Properties and Applications, edited by A. Nanni, Elsevier Science, The Netherlands.

Ozdemir, G. and Akyuz, U., 2005. Tensile capacities of CFRP anchorages, ACI Special Publication, Vol. 230, pp 39 – 56, October 1, 2005.

Smith, S.T., Teng, J.G. (2001). Interfacial Stresses in plated RC beams. Engineering Structures, Vol. 23, pp. 857-871.

Teng, J.G., Chen, J.F., Smith, S.T. and Lam, L. (2002). FRP Strengthened RC Structures. John Wiley and Sons, Ltd. England.

Modelling aspects and design issues for anchorages, shear strengthening and confinement

Giorgio Monti
Universita di Roma "La Sapienza", Italy

1 Introduction

A regulatory document was issued by the National Research Council (CNR) of Italy on the use of FRP for strengthening structures: "Instructions for Design, Execution and Control of Strengthening Interventions by Means of Fibre-reinforced Composites" (2004), denoted as CNR-DT 200/04. This document, described in more details in the following, was inspired by the *fib* Bulletin n. 14 (2001) "Externally bonded FRP reinforcement for RC structures" and, moving further, sets for the first time in Italy clear standards for production, design and application of FRP for reinforced concrete and masonry constructions. It is also conceived with an informative and educational spirit, which is crucial for the dissemination, in the professional sphere, of the mechanical and technological knowledge needed for an aware and competent use of such materials.

As a matter of fact, a unique situation exists in Italy for as regards the preservation of existing constructions, which is the result of the combination of two aspects:

- seismic hazard over the whole of the national territory, recently refined by a new seismic zonation, with medium-high intensity over a large portion of it, the highest expected PGA being 0.35g for a 475 years return period;
- extreme variety of the built environment, perhaps with no comparison in the entire world.

Construction typology in Italy encompasses examples reckoned as Country's (and world's) historical, architectural and cultural heritage – which include buildings of various function and importance, such as palaces, temples, churches, cloisters, theatres, spas, memorials, city walls, castles, simple dwellings, civil engineering works as bridges harbours and aqueducts – dating back to more than 2000 years ago, throughout the ancient- middle- modern- and contemporary ages, down to those built in the 20th century.

The former are largely made of masonry, although under this name again a great quantity of techniques and materials are indicated, from those using stone of various natures, squared or not, regularly placed or loose, or clay bricks of different quality, or combinations of them, and binders extremely different in nature, in application ways and in ageing conditions.

Instead, the latter mainly consist of reinforced concrete constructions, if not uniform, at least more homogeneous.

This has motivated the growth of two clearly distinct fields of research and application of fibre-reinforced polymers (FRP): one for (generally old) masonry and one for (relatively recent) reinforced concrete constructions.

The first studies in both fields have started in the beginning of the 1990s by some pioneering groups. Their research strived at finding new solutions for increasing the safety of existing constructions, that could compete with the more developed and usual ones of mortar injections, concrete jacketing, steel tying and plating, base isolation, integrative bracings (dissipative or not).

In ten years, the interest has spread so widely and rapidly that nowadays FRP has become one of the most active and prolific research fields in Italy. In the last three years, ten

interuniversity research projects have been funded on a 3-year basis by the Italian Ministry of University and Scientific Research, being recognized of national interest, gathering more than 20 different university departments nationwide to cooperate on the most diverse FRP-related topics.

The most important testimony of the intense activity in Italy is the above mentioned CNR-DT 200/2004, which is a code of practice with a volunteer character but in the same time an official normative value.

The document is the result of a remarkable joint effort of almost all academics and researchers involved in this field and of the representatives of major production and application companies, as well as of contractors using FRP for strengthening artefacts. Thus, the code naturally incorporates the experience and knowledge gained in ten years of studies, researches and applications of FRP in the country.

In the following sections, before introducing and commenting the new Italian FRP code, a review is offered of three peculiar aspects of FRP-strengthening, namely, adhesion, shear and confinement, with emphasis on the theoretical bases that constitute the background to the design equations contained in the code.

2 FRP-concrete adhesion

2.1 Introduction

The effectiveness of strengthening techniques employing FRP relies on the adhesion between the FRP plate/sheet and the concrete surface of the element to be strengthened, both in uncracked and cracked concrete zones. One important aspect, peculiar to this technique, concerns the anchorage failure that occurs in a plate/sheet bonded to a concrete surface. Many studies, both theoretical and experimental, have been carried out on FRP-concrete adhesion (for a list see, *e.g.*, Chen and Teng 2001). A clear distinction between two different cases exists: a) in un-cracked zones, b) in cracked zones. In both cases, beyond a certain applied force, a crack could form and propagate parallel to the bonded FRP plate/sheet near or along any weak interface in the plate/adhesive/concrete packet. This has been observed to be the most common anchorage failure mode for: a) plates/sheets bonded on the beam sides for shear strengthening, or, b) for beams and slabs flexurally strengthened with FRP strips bonded along the soffit, with debonding developing at a major crack and propagating towards the plate end (see *e.g.*, Chaallal et al. 1997, Teng et al. 2000). Under these conditions, all possible failure modes for FRP plates bonded to concrete have been thoroughly discussed by Chen and Teng (2001) based on extensive experimental database search with a valuable reference list of experimental tests. There, it was shown that experimented anchorage zones mostly failed in the concrete a few millimeters beneath the concrete/adhesive interface. This failure mode is referred to as “debonding in the concrete” (*fib* 2001). Other theoretically possible failure modes (*e.g.*, interfacial failure between either the adhesive and the concrete or the adhesive and the plate) have seldom been observed, thanks to the high quality of the commercially available adhesives. Different failure modes, such as debonding of the concrete cover, have not been considered here, because attention is devoted to debonding only. Also, it is assumed that the plate thickness is small enough not to activate peeling mechanisms, due to stresses normal to the bonded surface.

When mechanical fastening is not used, the efficiency of the strengthening element depends on the correct design of its anchorage zone. Various predictive equations are available in the literature for determining the anchorage strength associated to a given anchorage length, mostly for uncracked concrete zones, while for cracked zones still some

aspects need to be clarified. The maximum stress taken by an FRP plate/sheet depends on its anchorage length, along which it is transferred through a bond mechanism from the FRP to the concrete surface. In this section, the response of an FRP sheet bonded both to uncracked concrete, and to cracked zone is described. The presence of cracks considerably modifies the resisting mechanism, in that an interaction develops between the two ends of the FRP sheet/plate between two adjacent cracks. The relevant code equations used to determine both the debonding strength and the optimal anchorage length (or effective bonded length), in both uncracked and cracked concrete zones, are described later in Section 5.3.

2.2 FRP anchored in uncracked concrete zones (Mode I)

It is instructive to stepwise follow the response of an FRP bonded plate/sheet to uncracked concrete, with particular attention to the penetration of both cracking and debonding from the plate/sheet pulled end, where the load is applied, well into the anchored interface. This gives valuable information on the resisting mechanism and the development of failure.

Figure 1 shows the force vs. displacement diagram at the pulled end of a numerical model of a sample FRP anchorage zone of length L = 400 mm, subjected to an increasing applied force up to failure.

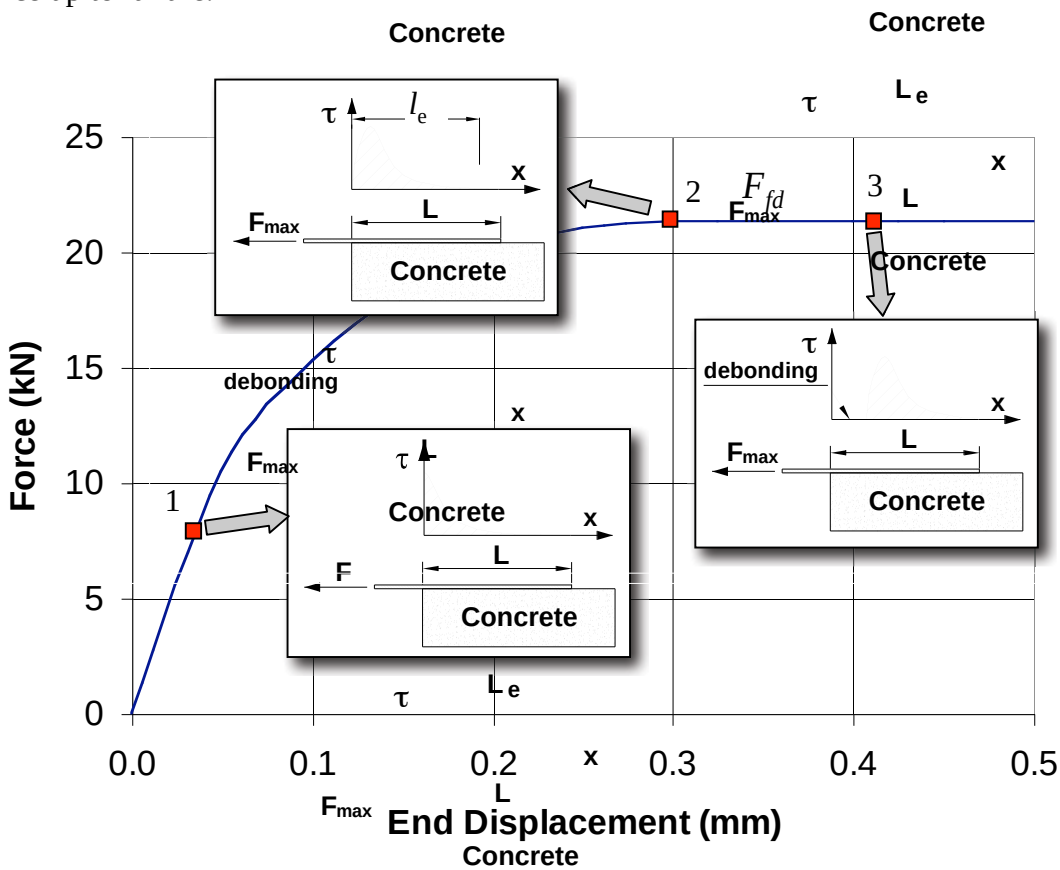

Fig. 1: Force-slip response of the example anchored FRP sheet, with characteristic points and corresponding bond fields.

In Figure 1 three characteristic points along the response curve, denoted by square marks, are noted: 1) the first one, separating the linear from the non-linear response, corresponds to the attainment of the maximum bond strength and to the initiation of interface cracking at the pulled end; 2) the second corresponds to the attainment of the ultimate slip at the pulled end and to the initiation of debonding; here the maximum anchorage force (that is, the debonding

force) F_{fd} is achieved and the involved bonded length is termed “effective” and denoted by l_e; and, 3) the third point corresponds to the debonding penetration into the anchored length. The corresponding bond distributions are depicted in the boxes within Figure 1.

A series of observations can be made:

- by subjecting the pulled end to increasing end displacement beyond point 2, the bond stress shape does not change (unless the bond-slip parameters slightly vary along the length, as commonly occurs in experimental tests) and rigidly moves towards the free end,
- thus, the load carrying capacity F_{fd} (proportional to the area under the bond field) does not change beyond point 2; if divided by the FRP cross-section area, it is called *debonding strength* and denoted by f_{fd},
- further displacements at the pulled end, beyond point 2, are due to the elongation of the (penetrating) debonded FRP portion, under a constant axial force F_{fd},
- the debonding penetration lasts until the bond shape reaches the free end; in a sense, the longer the sheet length ($L > l_e$), the higher the anchorage ‘ductility’ (even though a proper design criterion should not rely on it),
- the “effective” bonded length is a key point in the design of FRP-strengthening of reinforced concrete elements. It guarantees a complete stress transfer between FRP and concrete, thus avoiding premature debonding that would impair the strengthening measure.

2.3 FRP anchored in cracked concrete zones (Mode II)

The response of an FRP sheet anchored to a beam, in both a constant and a variable bending moment zone is considered (Figure 2). Between two adjacent cracks, at a spacing s_{rm}, a beam slice can be analysed, with the FRP sheet subjected to two opposite tensile forces at the cracks. Two cases are studied: 1) the slice size s_{rm} is larger than twice the effective length l_e, and 2) the slice size s_{rm} is smaller than twice the effective length l_e.

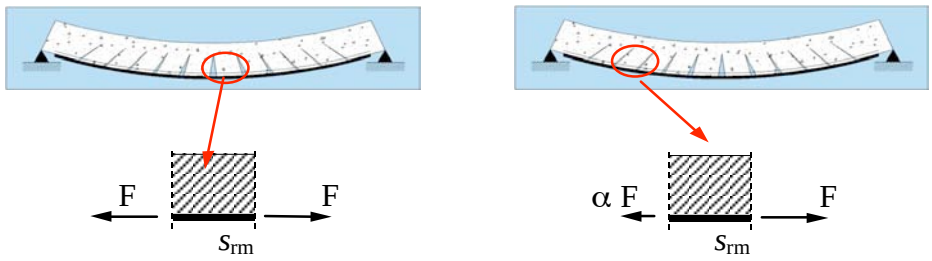

Fig.2: Beam slices in constant (left) and variable (right) bending moment zones.

2.3.1 Case: $s_{rm} \geq 2l_e$ in a constant bending moment zone

Figure 3 shows the bond stresses and the force along the FRP sheet at the onset of debonding. The bond stress is normalized with respect to the adhesion strength. The force is normalized with respect to the anchorage strength. No interaction takes place between the two ends of the sheet (at midpoint both the bond stress and the force are zero), because the available bonded length is sufficient to equilibrate the applied force. The two parts of the

sheet behave in the same way as shown in Figure 1, therefore the anchorage strength (*i.e.*, the applied force at the onset of debonding, which is equal to the area under the bond stress curve) is the same for uncracked concrete zones. Note that interface cracking (*i.e.*, where the normalized bond stress reaches ± 1) progresses from the two ends towards the slice midpoint.

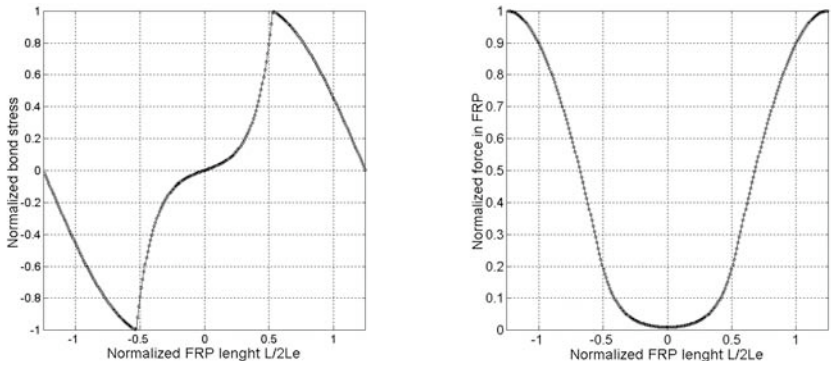

Fig.3: ULS: (a) Bond stress along the FRP; (b) Force along the FRP for $s_{rm} \geq 2l_e$.

2.3.2 Case: $s_{rm} < 2l_e$ in a constant bending moment zone

Figure 4 shows the bond stresses and the force along the FRP sheet at the onset of debonding. In this case there is interaction between the two ends of the sheet (at midpoint both bond stress and force are non zero), because the available bonded length is insufficient to equilibrate the applied force and therefore the two parts "hook" to each other. Figure 4(a) shows that the area under the bond stress is lower than in the previous case, while Figure 4(b) shows that the anchorage strength is higher than that pertaining to uncracked concrete zones.

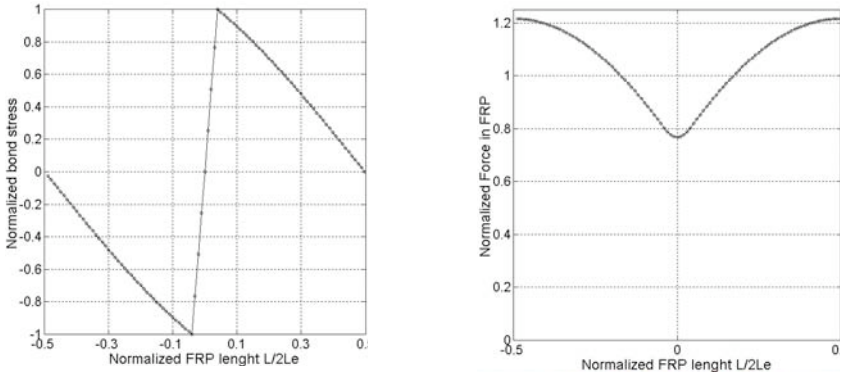

Fig. 4: ULS: (a) Bond stress along the FRP; (b) Force along the FRP for $s_{rm} < 2l_e$.

2.3.3 Response in variable bending moment zones

The same remarks above can be extended to the case of variable bending moment zones. The FRP sheet is subjected to different forces at the two ends (for illustrative purposes, a ratio of 1/3 has been chosen). The same diagrams as in the previous figures are shown in Figures 5 and 6. It is seen that, as expected, debonding occurs on the more stressed end (on the right) giving rise in both cases to the same anchorage strength as that pertaining to uncracked concrete zones.

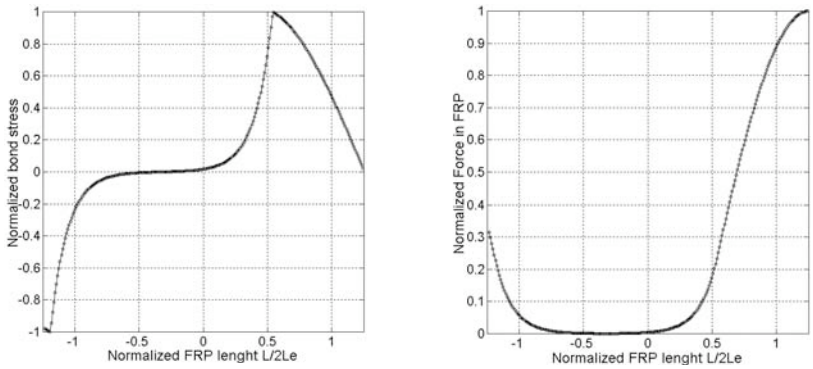

Fig. 5: Same as Fig. 3, in a variable bending moment zone.

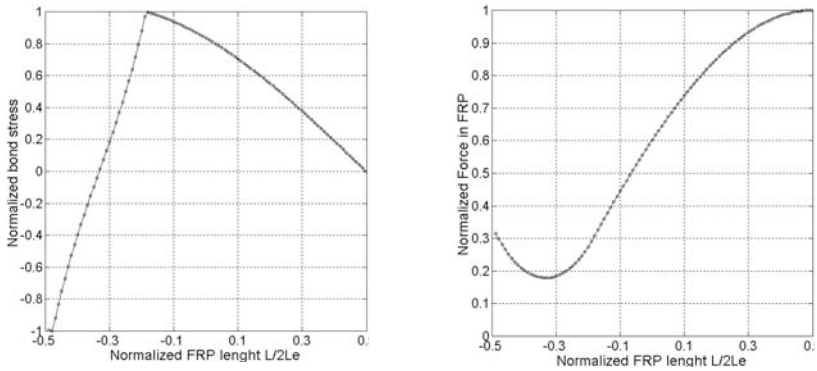

Fig. 6: Same as Fig. 4, in a variable bending moment zone.

Note how the available bond length is divided between the two sheet parts in proportion to the applied force: that subjected to a higher force requires a longer bond length. Note also that interface cracking progresses only from the pulled end on the right.

The behaviours commented above have direct consequences on the design equations of FRP anchorages, which have to include this beneficial effect when in the presence of cracked concrete. This will be commented later in Section 5.3, where it will be shown that this phenomenon is accounted for through a coefficient that increases the debonding strength under cracked conditions.

3 Shear strengthening

3.1 Introduction

This section presents the results of an experimental/analytical study that supported the Italian FRP code development. The objective is to explain the rationale behind the design equations presented hereafter in Section 5.5 and to describe the underlying mechanisms of the shear strengthening of reinforced concrete beams with FRP.

The strengthening configurations considered are those depicted in Figures 7 and 8.

In such developments, three aspects are of paramount importance and should be included in a mechanics-based model. The first regards the shear resisting mechanism that develops when FRP strips/sheets are side bonded, rather than U-jacketed or wrapped, to the element; in this case, a different mechanism than the Moersch truss activates, that is, a “crack-bridging” mechanism, similar in nature to those of aggregate interlock, dowel effect and concrete tooth. The second aspect regards the evaluation of the contribution of the FRP transverse

strengthening to the shear capacity; as opposed to the case of steel transverse reinforcement, which is always considered as yielded, FRP is instead subjected to a variable tensile stress along the crack profile, which is usually expressed as an effective stress. The third aspect regards the evaluation of the relative contributions to the shear capacity of concrete, steel and FRP at ultimate; it is not guaranteed that both concrete and stirrups can exploit their maximum strength when in the presence of FRP strengthening.

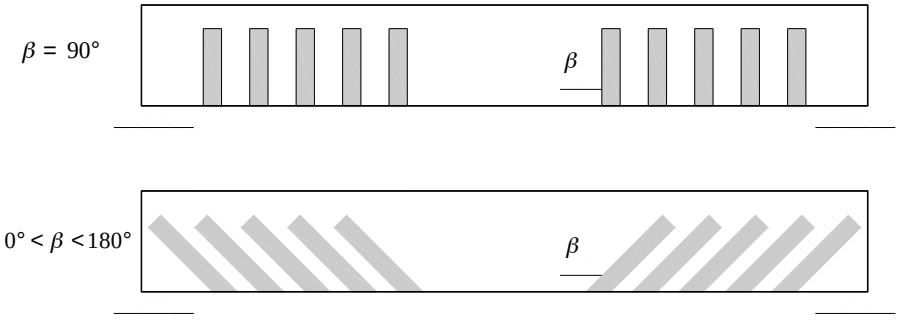

Fig. 7: FRP shear strengthening configurations on the beam length.

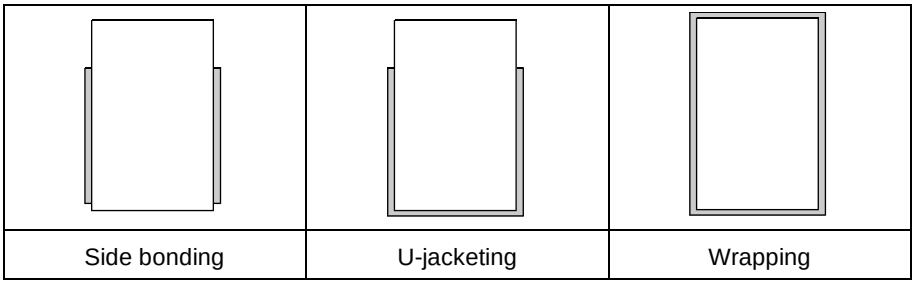

Fig.8: FRP shear strengthening configurations on the cross-section.

These aspects are treated in detail in this section according to the following method: through the definition of the generalised constitutive law of a bonded FRP sheet, of the compatibility imposed by the shear crack opening, and of the appropriate boundary conditions depending on the strengthening configuration, analytical expressions of the stress field in the FRP sheet crossing a shear crack are obtained. The expressions obtained are presented later on. These are closed-form equations of the effective strength of FRP strips/sheets used for shear strengthening, as function of both the adopted strengthening configuration and some basic geometric and mechanical parameters. The FRP contribution is then added to those of concrete and steel. The equations accuracy has been verified through correlation studies with experimental results obtained from the literature and from laboratory tests on purposely under-designed real-scale beam specimens, strengthened with different FRP schemes.

3.2 Design equations for FRP shear strengthening

This section tries to provide a coherent analytical framework to describe the behaviour of RC elements FRP-strengthened in shear, following previous efforts made by other authors (Täljsten 1997, Triantafillou 1998, Khalifa et al. 1998). The theory presented aims at producing closed-form expressions to describe the FRP stress distribution $\sigma_{f,cr}(x)$ along a shear crack (as qualitatively sketched in Figure 9), as opposed to regression-based formulas (Triantafillou & Antonopoulos 2000). Once this is correctly defined, the FRP resultant across

the crack can be computed and the FRP contribution to the resisting shear be found. The analytical developments (shown in more detail in Monti and Liotta 2005) arrive at defining three predictive equations for the three typical strengthening configurations: Side Bonding (S), U-jacketing (U) and Wrapping (W) (see Figure 8).

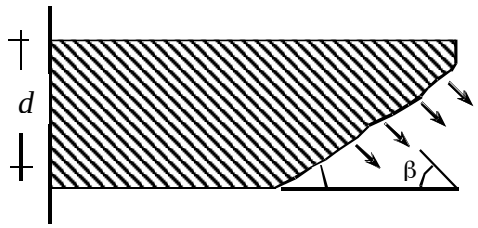

Fig. 9: Stress distribution along an FRP sheet crossing a shear crack.

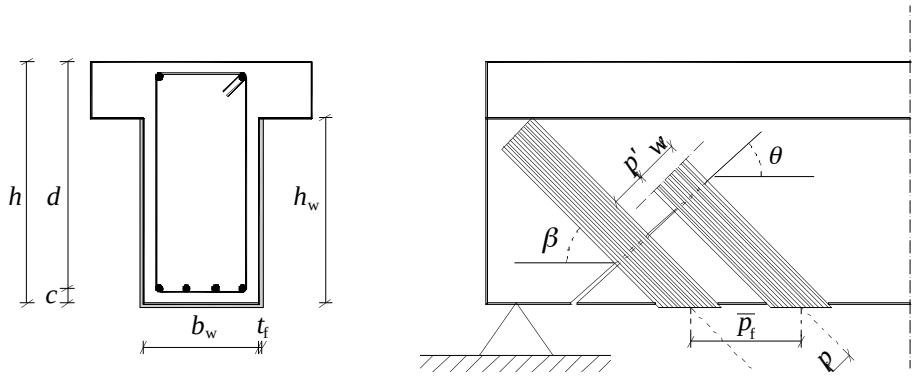

Fig. 10: Geometry notation for shear strengthening

In the following developments, the following hypotheses are made (notation in Figure 10):

- Shear cracks are evenly spaced along the beam axis, and inclined with angle θ,
- At the ULS the cracks depth is equal to the internal lever arm z = 0.9 d,
- In the case of U-jacketing (U) and wrapping (W), the resisting shear mechanism is based on the Moersch truss, while in the case of side bonding (S), because the Moersch truss cannot form as the tensile diagonal tie is missing, a different resisting mechanism of "crack-bridging" is considered to develop.

In order to fully characterize the physical phenomenon, the following aspects must be analytically defined: the failure criterion of an FRP strip/sheet bonded to concrete, the stress-slip constitutive law, the compatibility equations (*i.e.*, the crack opening), and the boundary conditions (*i.e.*, the available bonded lengths on both sides of the crack depending of the different configurations).

3.2.1 Generalised failure criterion of an FRP strip/sheet bonded to concrete

The criterion includes the two cases of: a) straight strip/sheet, and b) strip/sheet wrapped around a corner. Two quantities are used from the discussion in the previous Section 2: the *effective bonded length* l_e and the *design debonding strength* $f_{fdd}(l)$, whose equations are given later in Section 5.3 when presenting the Italian code.

The ultimate strength of the FRP strip/sheet, which includes the case when it is wrapped around a corner rounded with a rounding radius r_c, is:

$$f_{\mathrm{fu}}(l_{\mathrm{b}},\delta_{\mathrm{e}},R) = f_{\mathrm{fdd}}(l_{\mathrm{b}}) + \left\langle \phi_{\mathrm{R}} \cdot f_{\mathrm{fu}} - f_{\mathrm{fdd}}(l_{\mathrm{b}}) \right\rangle \cdot \delta_{\mathrm{e}}, \text{ where: } \delta_{\mathrm{e}} = \begin{cases} 0 & \text{free end} \\ 1 & \text{end around a corner} \end{cases} \quad (1)$$

where it can be seen that the debonding strength depends on the available bonded length l_{b} and $\langle \cdot \rangle$ denotes that the bracketed expression is zero if negative. It is noted that the sheet wrapped around a corner attains a fraction ϕ_R of the ultimate strength f_{fu} of the FRP sheet depending on the coefficient ϕ_{R} as function of the rounding radius r_{c} with respect to the beam width b_{w} (Campione and Miraglia 2003):

$$\phi_{\mathrm{R}} = 0.2 + 1.6 \frac{r_{\mathrm{c}}}{b_{\mathrm{w}}}, \qquad 0 \le \frac{r_{\mathrm{c}}}{b_{\mathrm{w}}} \le 0.5 \quad (2)$$

When $l_b \geq l_e$, the expression for the ultimate strength of the FRP strip/sheet, wrapped around a corner with a radius R, reduces to:

$$f_{\mathrm{fu,W}}(R) = f_{\mathrm{fdd}} + \left\langle \phi_{\mathrm{R}} \cdot f_{\mathrm{fu}} - f_{\mathrm{fdd}} \right\rangle \quad (3)$$

3.2.2 Generalised stress-slip constitutive law

The generalised stress-slip law $\sigma_{\mathrm{f}}(u, l_b, \delta_e)$ of FRP strips/sheets bonded to concrete, including both cases of free end or wrapped around a corner, is shown in Figures 11 and 12.

3.2.3 Compatibility (crack width)

Considering a reference system with the origin fixed at the upper limit of the shear crack and with abscissa x along the crack itself (Figure 13), the crack width (normal to the crack axis) along the shear crack can be expressed as $w = w(x)$.

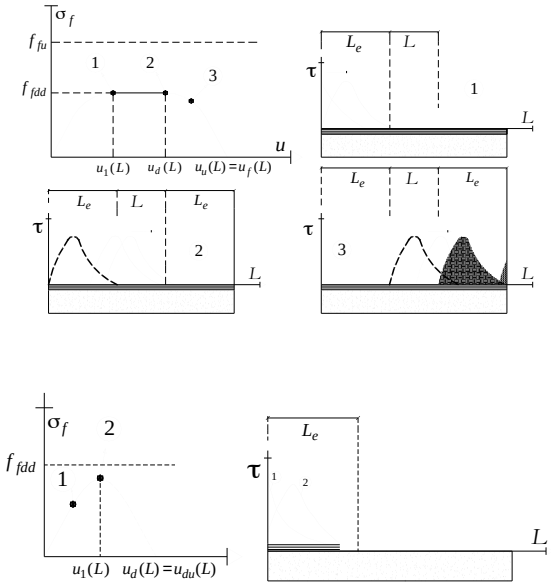

Fig. 11: Stress-slip law for the case of FRP strip/sheet with free end and with: sufficient bond length (top), and small bond length (bottom).

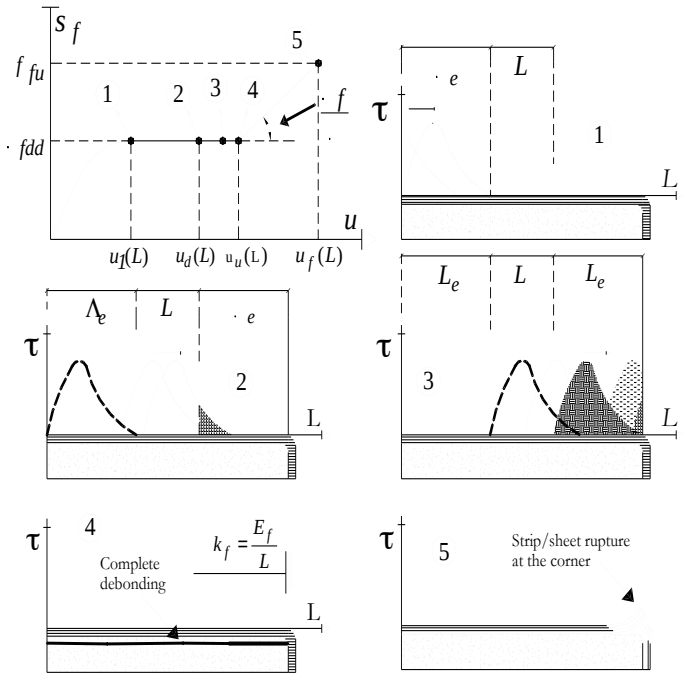

Fig. 12: Stress-slip law for the case of FRP strip/sheet wrapped around a corner.

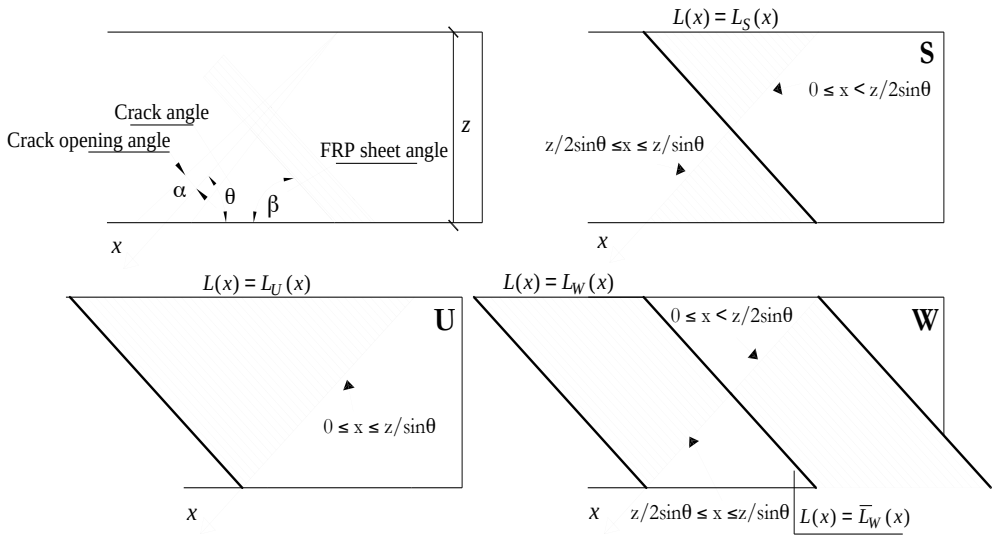

Fig. 13: Boundary conditions (available bond length) for three strengthening configurations: S = Side bonding, U = U-jacketing, and W = Wrapping.

3.2.4 Boundary conditions (available bond length)

The boundary conditions refer to the available bond length $L(x)$ on both sides of the shear crack and should be defined according to the strengthening scheme adopted: either S=Side bonding, U=U-jacketing, W=Wrapping (Figure 13).

3.2.5 FRP stress profile along the shear crack

In order to obtain the stress profile in the FRP sheet along the crack as a function of both the crack opening and the available bond length on both sides of the crack itself, one has to substitute into the constitutive law $\sigma_f(u, l_b, \delta_e)$: a) the compatibility equation $u = u(\alpha, x)$, b) the boundary condition $l_b = l_b(x)$ given according to the strengthening configuration, and c) the end constraint given by the appropriate value of δ_e. Figure 14 qualitatively depicts the $\sigma_{f,cr}(x)$ profiles along the crack for the three different strengthening configurations considered, when sheets are used. In the configuration S, the stress profile is truncated towards the end of the crack, where the available length tends to zero. In the configuration U, the stress profile remains constant where the available length allows the full debonding strength to be developed throughout the crack length. In the configuration W, the stress profile rises towards the end of the crack, where, after complete debonding, the sheet is restrained at both ends and subjected to simple tension up to its tensile strength.

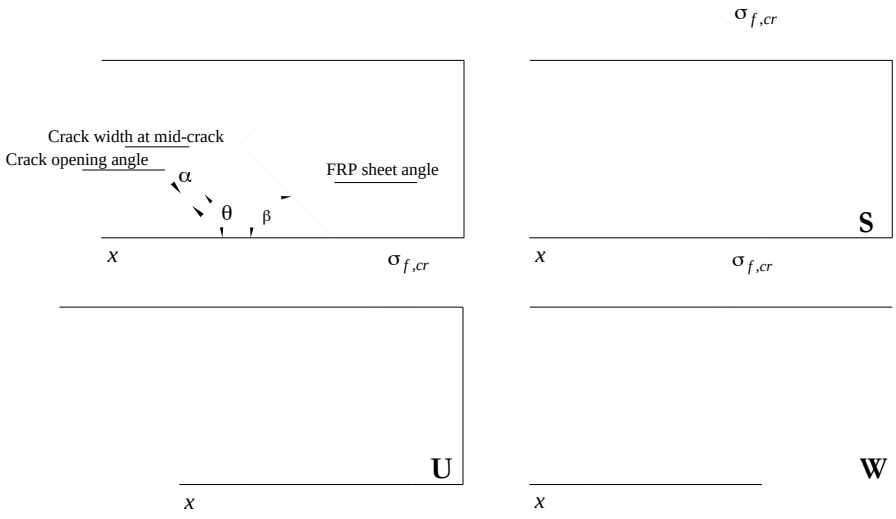

Fig.14: Typical stress profiles in FRP sheets along the shear crack for three strengthening configurations: S = Side bonding, U = U-jacketing, and W = Wrapping.

3.2.6 Determination of FRP contribution to the shear strength

The objective is to obtain the maximum contribution of the FRP strips/sheet to the shear strength. This means to identify, among all possible shapes of the FRP stress profile $\sigma_{f,cr}[u(\alpha,x),l_b(x)]$, which changes with the crack opening α, the one having the maximum integral intensity.

3.2.7 Effective stress in the FRP sheet

To this aim it is expedient to define an *effective stress* in the FRP sheet, inclined to an angle β as the FRP fibres, as the mean FRP stress field $\sigma_{f,cr}(x)$ along the shear crack length $z/\sin\theta$:

$$\sigma_{fe}(\alpha) = \frac{1}{z/\sin\theta} \cdot \int_0^{z/\sin\theta} \sigma_{f,cr}[u(\alpha, x), l_b(x)]\, dx \qquad (4)$$

which might be regarded as an equivalent constant FRP stress block along the shear crack.

3.2.8 Effective debonding strength

The maximum of the FRP effective stress, which is termed the *effective debonding strength* f_{fed}, is found by imposing:

$$\frac{d\sigma_{fe}[x_u(\alpha)]}{d\alpha} = \frac{d\sigma_{fe}(x_u)}{dx_u} \cdot \frac{dx_u(\alpha)}{d\alpha} = 0 \tag{5}$$

where the chain rule has been used. Solution of this last equation allows to determine the FRP stress profile with the maximum area, that is, the effective strength of the FRP shear strengthening.

The obtained expressions of the effective debonding strength are given in terms of readily available geometrical and mechanical quantities of both the FRP strengthening and the RC beam and are then used to compute the FRP contribution to the overall shear strength, together with that of concrete and transverse reinforcement. These equations, adopted in the new Italian FRP code, are given in Section 5.5.

4 Confinement

4.1 Introduction

The strengthening of vertical elements in reinforced concrete, either columns or bridge piers, has different implications depending on whether the strengthening measure is carried out on a conventional structure or on a structure in a seismic area.

For conventional structures, the objective is usually to increase the bearing capacity, and therefore the strengthening measures aims either at enlarging the cross sectional area or at enhancing the compressive strength of concrete by applying a confining action. Such measures are generally applied in buildings where live loads have increased consequent to a change in use. In the case of bridge piers, which can usually rely on adequate safety levels with respect to the vertical loads, confining measures are applied in cases when concrete is heavily damaged or if required by a live load increase (*e.g.*, third lane construction, etc.).

In the structures built in seismic areas according to obsolete codes, the flexural capacity is generally adequate, as a result of the conservative design assumptions inherent in the elastic design approach. It is known that obsolete codes focused on the strength aspects while only making implicit reference to the concepts of ductility and dissipation capacity, and, which is more important, gave no provisions to ensure stability of the response in the post-elastic range. Ductility is the property of being able to deform through several cycles of displacements much larger than the yield displacement, without significant strength degradation. Displacement ductility as high as 6 to 8 may be needed sometimes.

Existing structures built according to obsolete codes – as assessed either from original project drawings or through *in-situ* inspections after destructive seismic events – systematically show insufficient transverse reinforcements and thus lack the confinement necessary for ensuring a ductile response. In Figure 15 the lateral collapse mechanism of a column with insufficient transverse reinforcement is shown.

At displacement ductility 2 to 3, spalling of the cover concrete occurs in the plastic hinge zones, where inelastic deformations concentrate. Unless the core concrete is well confined by close-spaced transverse hoops or spirals, crushing extends into the core, the longitudinal

reinforcement buckles, and rapid strength degradation follows. This behaviour can even be accelerated when transverse reinforcement is lapped in the cover concrete, as is often the case in old constructions. The hoops then loose effectiveness at laps, when concrete spalls out.

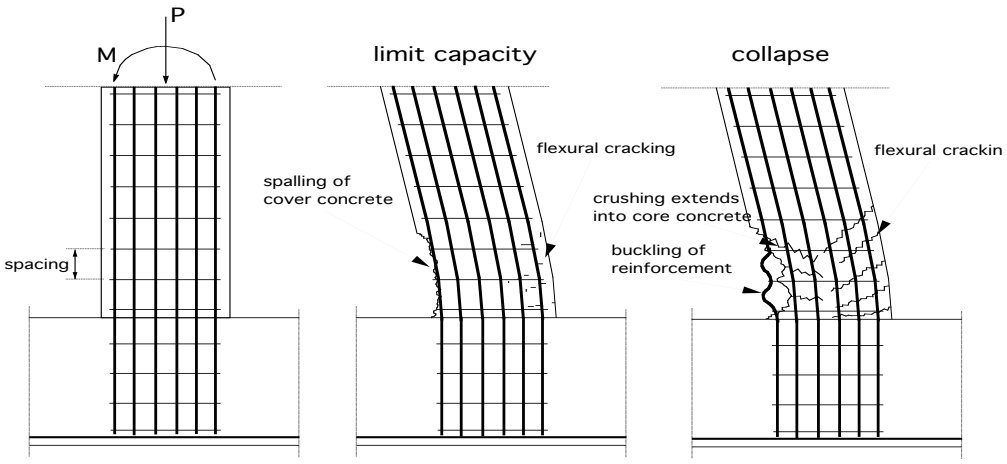

Fig. 15: Lateral collapse mechanism of an under-designed column.

Common retrofitting techniques of columns typically aim at increasing the available ductility by enhancing the confinement action in the potential plastic hinge region. However, enhancement of the flexural strength can be sought in lap-spliced zones or when longitudinal reinforcement is terminated prematurely.

It is already well known that confinement of concrete enhances its strength and ductility. Therefore, improved confinement will increase the ability of a column to withstand repeated cycles of loading beyond the elastic limit and tend to prevent column failure due to degradation of flexural capacity. Debonding of longitudinal reinforcement lap-splices and formation of plastic hinges at regions of termination of longitudinal reinforcement can also be prevented by adequate confinement.

When necessary, retrofitting techniques are sometimes directed at increasing flexural strength. This retrofit method should be used carefully: increased flexural capacity will increase the forces transferred to the foundation and the superstructure/column connections, and will also result in increased column shear force. Since failure of the foundation or brittle shear failure of the columns are usually more critical than excessive flexural yielding, this method should only be used when loss of flexural strength results in a collapse mechanism, and not without taken precautions.

4.2 FRP wrapping

Until a few years ago, the only available techniques for upgrading vertical structural elements were the traditional ones in reinforced concrete and steel. Only in the last decade have fibre reinforced polymers (FRP) been recognised as an effective strengthening technique for degraded or inadequate reinforced concrete members. The remarkable properties of FRP, such as high specific strength, and mostly also high specific stiffness, low thickness and weight, and resistance to corrosion, allow them to be applied in a construction site without serious difficulties. An FRP jacket can consist of active or passive layers, or a combination, of different FRP materials. Normally carbonfibre and/or fibreglass are used, sometimes also aramid-fibres like Kevlar™ or Twaron™, in combination with a resin matrix, usually epoxy. Numerous combinations can be made, which is one of the main advantages of FRP jackets.

Experimental studies and pilot applications have demonstrated that, by wrapping vertical elements with FRP jackets placed on one or more layers, a confining action on the concrete is obtained that enhances both strength and ductility of the whole element. In the case of columns, FRP composite jacketing techniques have been shown to have performance capabilities comparable to and in some cases better than columns retrofitted through the application of conventional methods.

The confinement action so obtained is of the "passive" type, that is, it develops only consequent to the transverse dilation of the compressed concrete core that stretches the confining device, which thus applies an inward confining pressure (Figure 16). "Active" confinement action can be obtained by pre-tensioning the sheets prior to application. Generally, carbon fibres (CFRP) are preferred in those cases where the objective is the bearing capacity increase of the column, while glass fibres (GFRP) are more suitable, thanks to their higher deformability, to cases where a ductility increase is sought instead.

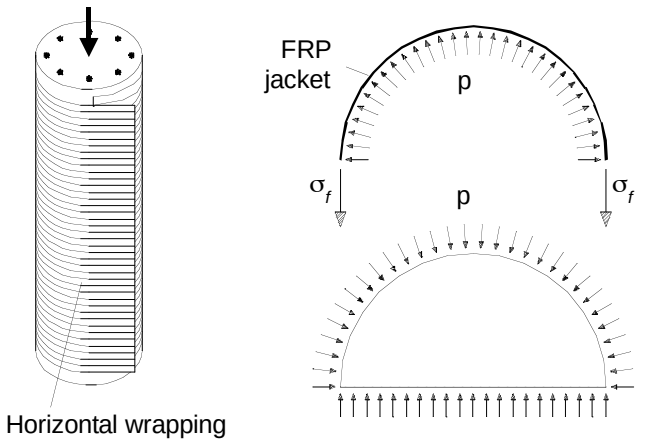

Fig. 16: Confining columns with FRP, taking advantage of the transverse dilation of the compressed concrete core under axial load.

4.3 Types of FRP wrapping

Different types of column FRP wrapping systems have been investigated and developed based on material types, form and process of application.

They can be classified into five categories based on the method of processing/installation (Karbhari et al. 2001):

(a) wet lay-up process using fabric, tape or individual tow;
(b) prepreg in the form of tow, tape or fabric;
(c) prefabricated shells;
(d) resin infusion processes;
(e) external composite cables or prefabricated strips.

In technique a) the column can be wrapped with either mono- or multi-layer FRP sheets, or even with FRP strips placed in spirals or rings (see also Figure 18(a)). Applications of this technique are amply reported for both buildings columns and bridge piers (see for ex., ACI 1996, Neale and Labossiere 1997, Tan 1997). Laying-up of prepreg tape is a straightforward, very fast construction principle, but it is more difficult to control, since it is carried out by hand completely, and there are concerns related to the quality control of resin mix, attainment of good wet-out of fibres with uniform resin impregnation without entrapment of excessive

voids, good compaction of fibres without excessive wrinkling of the predominantly hoop-directed fibres, control of cure kinetics and achievement of full cure, and aspects related to environmental durability during and after cure.

In the case of wet winding tow or tape (b), the process may be automated, although resin impregnation is still through the use of wet bath and/or spray, and many concerns are the same as those described for the lay-up process. Moreover, the necessity of curing under elevated temperatures (usually in the range of 80-150°C) can cause problems if the substrate concrete is very moist resulting in water vapour driven blistering in the curing composite jacketing.

Technique c), involving the use of cables or prefabricated strips, has not been investigated to a large extent as yet.

In technique d) a wrapping machine is used for automatically winding the fibres around the column (see also Figures 17(b), 18(b)). The machine, built for the first time in Japan in the 80ies (ACI 1996), has been designed for the upgrade of bridge piers, but it can be used for buildings columns, as well. The automated wrapping device is set up around the column. The fibres, wound on reels, are placed in the fibres winding head, and moving upwards are wound around the column, pre-impregnated with the resin. After winding, a curing blanket is placed. Winding angle, fibre volume fraction, and thickness are fully computer controlled. With this device it is possible to wind the fibres while pre-tensioning them, so to obtain an active jacketing system, independent of the concrete lateral dilation. The disadvantage of such device is that, in the presence of non-levelled soils, preliminary calibration operations are required, which sensibly slow down its use. The same effect can be actually obtained with the other systems, by injecting either expanding mortar or epoxy in pressure between the jacket and the column surface.

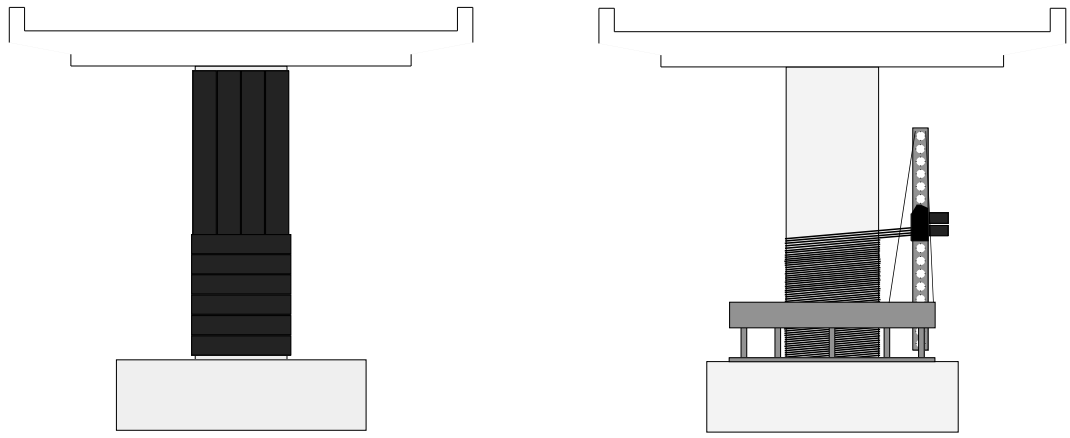

a) Prepreg tape lay-up b) Automated fibre wrapping system

Fig. 17: Schematic examples of FRP wrappings (from fib bulletin 14).

Technique e) consists in the application around the column of two prefabricated half shells (Figure 18(a)) that can be, depending on its cross-sectional shape, either circular (for ex., Nanni and Norris 1995) or rectangular (for ex., Ohno et al. 1997). In alternative, full circular shells with a vertical slit can be opened and placed around the column (for ex., Xiao and Ma 1997). This is a very simple system in any *in situ* application, and affords a high level of materials quality control due to controlled factory-based fabrication of shells. However, the shells must be realised with strict tolerance with respect to the piers dimensions. In case of multiple layers, they must be properly positioned to ensure the desired collaboration of the entire jacketing system. Prefabricated shells can be used as formworks, also functioning as transverse reinforcement; in the case of rectangular sections, the confining action of the shells

is less effective and it is generally preferred to modify the column cross-sectional shape (as explained hereafter).

Finally, in the case of resin infusion (f), the dry fabric is applied manually and resin is then infused using vacuum with cure being under ambient conditions.

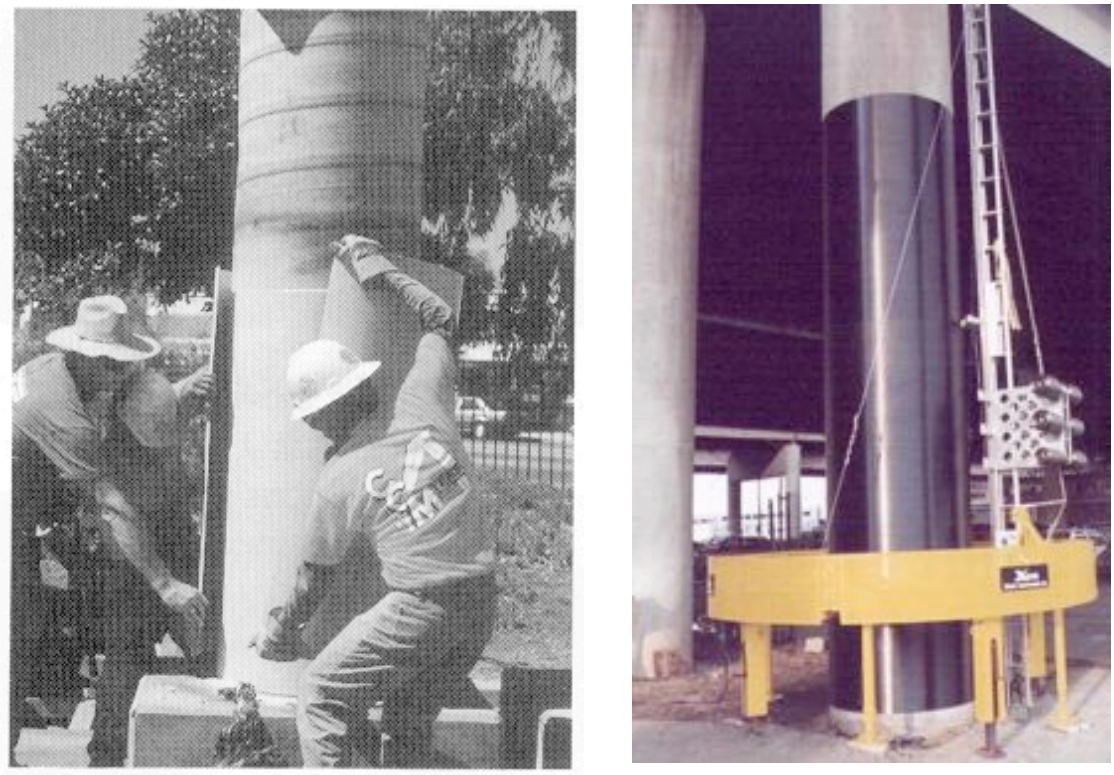

a) b)

Fig.18: (a) Positioning prefabricated FRP shells; (b) automated wrapping system (from fib bulletin 14).

It is worth recalling that the increase in strength obtainable by FRP-wrapping is not significant as that in ductility. However, when necessary, upgrading techniques of columns aim at enhancing the flexural capacity. In this case, capacity design criteria should be applied (as, for ex., expressed in Eurocode 2 - EN 1992), because an increased flexural capacity in the column introduces higher forces in the beam-column joint (or in the footings) and it amplifies the shear action in the column itself. Because these resisting mechanisms are of the brittle type, it is mandatory to avoid them, by strengthening them as well.

The purpose of confining a column is therefore either enhancing its load carrying capacity or its ductility under lateral actions, such as those induced by earthquakes. Both cases are included in the FRP code presented hereafter and will be discussed in Section 5.6. Moreover, the confining device offers a transverse constraint to the longitudinal bars, preventing them from buckling, and avoids the spalling of the concrete cover. This technique can also be used to prevent premature slippage of rebars in lap-splicing zones, or to avoid rebars pullout in anchorage zones, as discussed in Section 5.7.

It is extremely important to understand that, in case of members with rectangular cross-section, the confining action is less effective than for the circular. In fact, due to the long distance between the corners, the composite does not actually confine the internal concrete structure if just applied to the surface. In these cases, reinforcing fibres are often loose and unable to provide confinement. If the aspect ratio is larger than 2, it is appropriate to inscribe the section within an elliptical shape cast in (preferably light) concrete, which is subsequently

FRP-wrapped (Figure 19). If this solution is not viable, due to the evident weight increase, the corners must be rounded in order to avoid excessive stress concentrations in the sheets folded around them (the radius is about 15 to 25 mm, depending on the specifications given by the FRP jacket supplier and on the available concrete cover thickness). Design issues relevant to the above described cases are dealt with in Section 5.6.

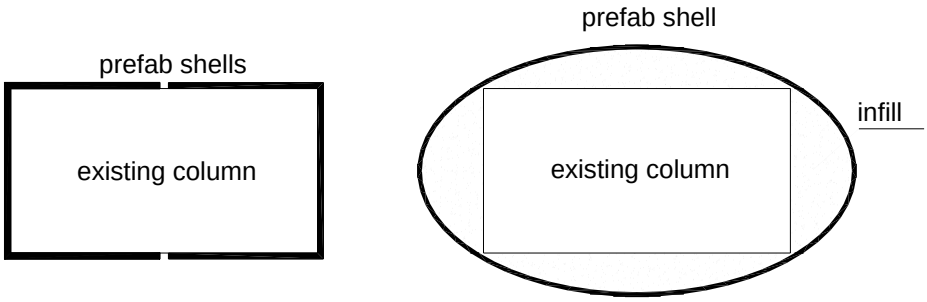

Fig. 19: Ovalisation of a rectangular section prior to wrapping.

4.4 Concrete strength and ductility

In the last three decades the behaviour of confined concrete has been deeply studied in countless researches, whose results are now well known and established. All of those studies deal with concrete confined by steel, which, after yielding, exerts a constant confining pressure. This allowed all researchers to relate the confined concrete properties as if under hydrostatic pressure, expressed in terms of the steel yield strength, thus avoiding to tackle the complex problem of concrete dilation and of its interaction with the confining device itself.

This standpoint had to change with the innovative introduction of FRP confining devices: FRP is an elastic material, and as such it does not yield; as a consequence, it exerts a continuously increasing confinement action on concrete (Spoelstra and Monti 1999).

The response of FRP-confined concrete turns out to be completely different from the steel-confined one, and this opened the way to a remarkable research effort that in the last few years has produced a number of valuable studies, both experimental and analytical, with the common aim of clarifying all new aspects in this phenomenon.

The strength increase in confined concrete originates from a known fact: unconfined concrete under uniaxial compression up to 90% of its strength reduces in volume; beyond this value, it dilates. A confining pressure opposing such dilation remarkably improves its performance.

The most relevant findings of all experimental studies on FRP-confined concrete are condensed in Figures 20 and 21. In Figure 20 the (normalized) behaviour of (both Glass and Carbon) FRP-confined concrete are compared to the more familiar steel-confined concrete. All stress and strain quantities are normalized with respect to the unconfined concrete strength and to the corresponding strain, respectively.

In the stress-strain relation, Figure 20 top-left, it is seen that the (G-C)FRP-confined concretes show an ever-increasing branch, as opposed to the steel-confined one, which, after reaching the peak strength, decays on a softening branch. Concrete degradation is proportional to the lateral strain: the increasing confinement action of the elastic FRP limits the lateral strain thus delaying the degradation; on the other hand, when steel yields, which occurs at 2.5 normalized axial strain, degradation of concrete takes place, because steel offers a zero stiffness to the lateral dilation of concrete.

The increasing confinement action of the elastic FRP limits the lateral strain thus delaying degradation. As regards the ultimate strain, and implicitly ductility, it should be noted that, notwithstanding the low ultimate strain of the FRP-jackets, the concrete ultimate strain is

comparable (CFRP) or even greater (GFRP) than that obtained with steel.

As regards the concrete ultimate strain, which influences the ductility attained through confinement, it should be noted that, notwithstanding the low strain values in the FRP-jackets, in these cases the concrete ultimate strain is comparable or even greater than that obtained through the use of a ductile confining device, *i.e.* steel.

This different behaviour suggests that, when FRP jackets are used, the ultimate axial strain of concrete is only weakly governed by the ultimate confinement pressure (proportional to the FRP strength), whereas it is mostly dependent on the FRP ultimate deformation. This is proven by the fact that the fibreglass-confined specimen shows an almost twice as large deformability than the carbonfibre-confined one, although the ultimate confinement pressure of the latter is roughly 50% larger.

In Figure 20 (top, right), the lateral strain vs. axial strain relation is shown. It can be observed that the slope of the branches depends on the stiffness of the confining device (which can also be observed in the previous diagram): steel and CFRP start with almost the same slope, but after steel yields at 2.5 normalized axial strain, it departs towards higher lateral strains.

GFRP shows a more stable behaviour, in the sense that it starts with a higher slope (meaning that concrete has a higher initial lateral dilation), which however remains constant until the jacket fails. CFRP reduces the initial lateral strain, but its effectiveness has a shorter duration, due to its lower extensional ultimate strain.

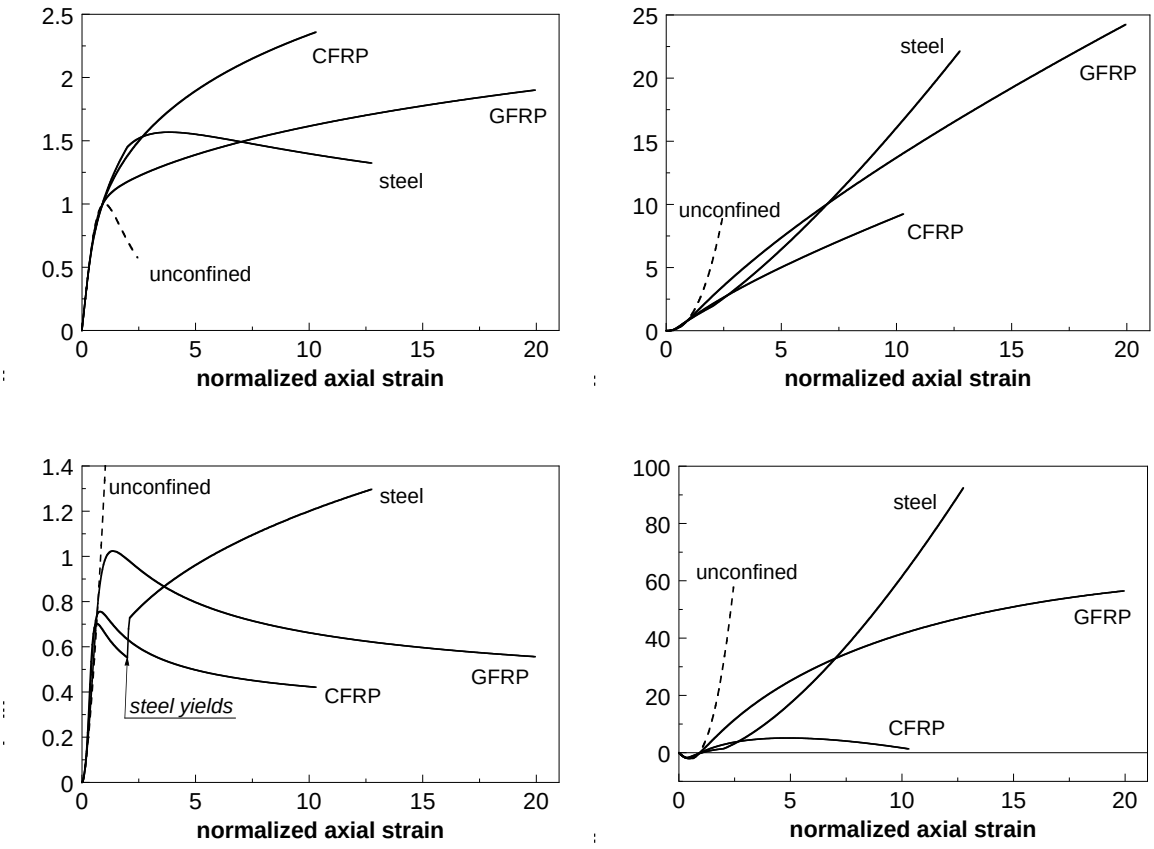

Fig. 20: Schematic behaviour concrete confined with steel, CFRP and GFRP: axial stress vs. axial strain (top, left), lateral strain vs. axial strain (top, right), volume strain vs. axial strain (bottom, left), dilation rate vs. axial strain (bottom, right).

This can be better appreciated in Figure 20 (bottom, left), where the dilation rate is expressed as function of the axial strain. The dilation rate $\mu = \Delta\varepsilon_l / \Delta\varepsilon_c$ is defined as the rate

of increase of the lateral strain $\Delta\varepsilon_l$ to the corresponding axial strain increment $\Delta\varepsilon_c$. It is seen that when steel yields a discontinuity occurs, due to the abrupt change in modulus; after this, the dilation rate increases indefinitely. On the other hand, for the two FRP, it constantly decreases towards an asymptotic value. Note that the position of the point where the confinement action starts becoming effective (that is, when the branches depart from the unconfined one) depends on the stiffness of the confining device: the GFRP-confined concrete departs later than the other two. This is the point where a sufficient lateral pressure develops that prevents the lateral dilation of concrete from increasing unrestrained.

In Figure 20 (bottom, right), it is interesting to observe from the volume strain vs. axial strain curve that for the CFRP jacket the volumetric strain first decreases, as expected, then reverts to zero and beyond a certain level of axial strain the ever increasing confinement pressure curtails the volumetric expansion and inverts its direction.

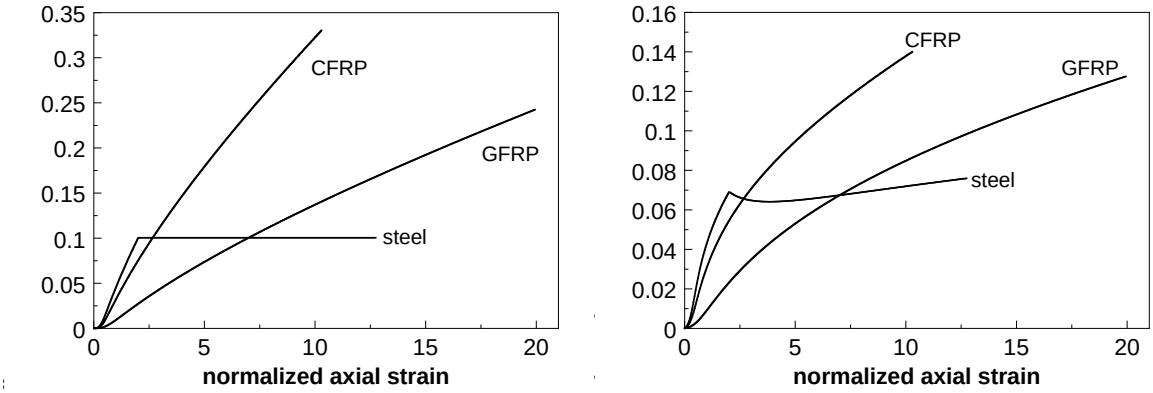

Fig. 21: Comparison of confinement effectiveness on concrete confined with steel, CFRP and GFRP.

In Figure 21, left, the confinement effectiveness (lateral stress vs. axial strain) for all three types of jackets is compared. It is explicitly shown what expected, that is, before yielding the steel jacket exerts a higher confining action, which however remains constant after yield, whereas the FRP jackets show a monotonically increasing confinement, thus arriving at applying a confinement action twice (GFRP) or thrice (CFRP) that of steel, with the same volumetric ratio. In Figure 21, right, it is interesting to compare the jacket effectiveness expressed in terms of ratio of the lateral stress to the *current* axial stress. The steel jacket effectiveness after yield is only due to the softening behaviour of concrete, whereas in the other two cases it is the elastic behaviour of the FRP jackets that increases the ratio. Here, it should be evident how the two FRP materials reach almost the same level of effectiveness, but at different axial strain levels, which renders more attractive the use of GFRP jackets that also exploit ductility while maintaining the same effectiveness of CFRP jackets.

The idea emerges from these graphs that CFRP should be used to provide concrete with higher strength increase and moderate ductility, whereas GFRP should be used to provide higher ductility and moderate strength increase. This findings will be the basis of the confinement equations of the Italian FRP Code that are presented in Section 5.6.

5 The new FRP code in Italy

The CNR-DT 200/2004: 'Instructions for Design, Execution and Control of Strengthening Interventions by Means of Fibre-reinforced Composites' (2004) includes the following sections:

- Materials,
- Basic concepts of FRP strengthening and special problems,

- Strengthening of reinforced concrete and prestressed concrete structures,
- Strengthening of masonry structures (not treated here).

5.1 Materials

The section on materials has a prevailing informative character and contains the fundamental information needed to obtain a basic knowledge of the composite materials, of their components (fibres, matrices, and adhesives) and of their physical and mechanical properties. It also includes an annex describing the most usual production techniques and some basic notions on the mechanical behaviour of composites.

The most notable aspect is that a possible classification of composites usually adopted for structural strengthening is proposed, and some appropriate criteria for product qualification and acceptance are introduced. Moreover, the concept is introduced of FRP as a strengthening *system*, enforcing all applicators to sell fibre-reinforced material and bonding agent as a certified package.

It is widely recognised that the design of a FRP strengthening system is a critical process. The various components (fibres, resin and the support) have different mechanical properties and roles but must be selected and designed to work together in a unique system. Therefore the properties of the components, their interactions and the properties of the final FRP must be well known and defined. The chapter on materials provides both general information on the mechanical, physical and chemical properties of FRP materials and indications for the qualification of the components and the systems on use in the reinforcement of civil engineering structures.

Specific sections of the chapter are dedicated to the main components, namely the fibres and the textiles, the resin and the adhesives. For each of them the main properties are discussed and some examples of the technical data sheets that should be provided with the products are reported. For all the mechanical, physical and chemical properties that must be determined or verified, reference is made to the appropriate testing procedures and the relevant European and American standards. The terms and quantities that are commonly used in the textile or chemical fields and are not familiar to civil engineers are properly explained.

An informative section is dedicated to the different reinforcing systems. The main aim is to clarify that the material properties can be referred to the total cross-sectional area for the prefabricated strips. On the contrary when in-situ resin impregnated systems are used, the final FRP thickness varies with the amount of resin and cannot be known in advance. For this reason the calculations may be based on the properties of the bare fibres but a reduction factor should be included to account for the efficiency of the system and for other detrimental variables such as the textile architecture or possible misalignments of the fibres.

It is known that conventional materials used in the civil engineering field are covered by standard specifications that both ensure the properties of the materials and provide standard procedures for the tests. The CNR-DT 200 document suggests two levels of qualification for the FRP materials that imply a set of mechanical and physical tests for the definition of short-term or long-term material properties respectively. The complete systems are also classified in two categories. In both cases all the basic components of the FRP must be tested and certified while a series of tests on the complete system in full scale and with the proper substrate must be performed for class A systems. Certified systems of this class have the advantage of being subject to less severe safety factors.

5.2 Basic concepts

It is stated that the design of the FRP strengthening intervention must meet with the requirements of strength, serviceability and durability. In case of fire, the strengthening resistance must be adequate to the prescribed exposure time.

The design working life of the strengthened structure is taken equal to that of new structures, which implies that the design actions to be considered are those of the current design codes for new constructions.

Safety verifications are performed for both the serviceability and the ultimate limit states. The format is that of the partial factor method. The design values of both materials and products properties are obtained from the characteristic values, affected by the appropriate partial factors.

A rather innovative point (following the indications of EN 1990) is that the design properties X_d of the existing materials in the structure to be strengthened are obtained as function of the number of tests performed to acquire information on them:

$$X_d = \frac{\eta}{\gamma_m} m_X (1 - k_n V_X) \tag{6}$$

where η (<1) is a conversion factor, accounting for special design problems (related to environmental conditions and long duration phenomena), γ_m is the material partial factor, m_X is the mean value of the property X resulting from the number n of tests, k_n is given as function of n and the coefficient of variation V_X is supposed known. This latter can be assumed equal to 0.10 for steel, to 0.20 for concrete and to 0.30 for masonry and timber.

The partial factor γm of FRP for ultimate limit states verifications, in case the failure mechanism is FRP rupture, is taken as 1.1 under quality control and to 1.25 in other situations; while it is taken as 1.2 under quality control and to 1.5 in other situations, in case the failure mechanism is FRP debonding.

The design capacity is given by:

$$R_d = \frac{1}{\gamma_{Rd}} R\{X_{d,i}; a_{d,i}\} \tag{7}$$

where $R\{\cdot\}$ is the function describing the relevant mechanical model considered (e.g., flexure, shear, confinement, etc.) and γ_{Rd} is a partial factor accounting for the uncertainties in the above capacity model (equal to 1.0 for flexure, to 1.2 for shear, and to 1.1 for confinement); the function arguments are, in general, a set of mechanical and geometrical properties, of which $X_{d,i}$ and $a_{d,i}$ are the design value and the nominal value of the *i*-th quantity, respectively.

An essential and innovative aspect is related to the safety verifications in presence of fire. It is suggested that the load combination for exceptional situations, where E_d is the design value of the indirect thermal action due to fire, refers to the following situations:

a) Exceptional event in the presence of strengthening ($E_d \neq 0$), in case the strengthening was designed for a predefined fire exposure time. In this case, the service actions of the *frequent combination* are to be considered. The elements capacity, appropriately reduced to account for the fire exposure time, should be computed with the partial factors relevant to the exceptional situations.

b) After the exceptional event ($E_d = 0$), in the absence of strengthening. In this case, the service actions of the *quasi-permanent combination* are to be considered. The elements capacity, appropriately reduced to account for the exposure time to fire, should be computed with the partial factors relevant to the exceptional situations.

5.3 Anchorages

Two different collapse modes for debonding are considered: end debonding (mode I as explained in 2.2) and intermediate debonding for flexural cracking (mode II as explained in 2.3).

The optimal anchorage length or effective bonded length (Figure 22) is given as (units in mm):

$$l_e = \sqrt{\frac{E_f \cdot t_f}{2 \cdot f_{ctm}}} \tag{8}$$

where E_f is the modulus of FRP in the fibres direction, t_f is the thickness of FRP and f_{ctm} is the concrete mean tensile strength.

The design debonding strength for end debonding (Mode I) is:

$$f_{fdd} = \frac{1}{\gamma_{f,d} \cdot \sqrt{\gamma_c}} \cdot \sqrt{\frac{2 \cdot E_f \cdot \Gamma_{Fk}}{t_f}} \tag{9}$$

$$\text{with } \Gamma_{Fk} = 0.03 \cdot k_b \cdot \sqrt{f_{ck} \cdot f_{ctm}} \quad \text{(forces in N, lengths in mm)} \tag{10}$$

where Γ_{Fk} is the characteristic value of fracture energy of bond between concrete and FRP, k_b is a scale/covering coefficient ≥ 1, $\gamma_{f,d}$ is the debonding partial factor, and f_{ck} is the concrete characteristic strength.

The design debonding strain for intermediate debonding (Mode II) is:

$$\varepsilon_{fdd} = \frac{k_{cr} \cdot f_{fdd}}{E_f} \tag{11}$$

where k_{cr} is a coefficient assumed equal to 3.0, in the absence of a more detailed definition.

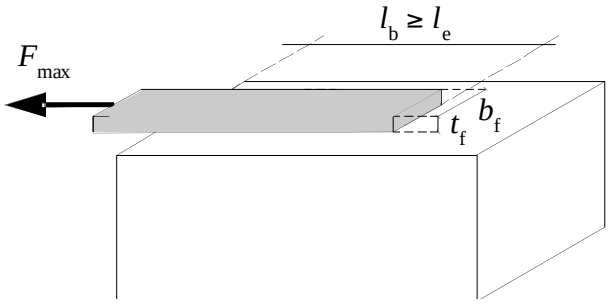

Fig. 22: Notation for anchorages.

5.4 Flexure without and with axial load

The flexural capacity is attained when either the concrete compressive strain reache its ultimate value or when the FRP tensile strain reaches its ultimate value $\varepsilon_{fd} = \min(\eta_a \varepsilon_{fu}/\gamma_f, f_{ffd}/E_f)$ where the first value corresponds to failure and the second to the design debonding as previously defined. The flexural capacity is then given as (notation in Figure 23):

$$M_{\mathrm{Rd}} = \frac{1}{\gamma_{\mathrm{Rd}}} \cdot \left[\psi \cdot b \cdot x \cdot f_{\mathrm{cd}} \cdot (d - \lambda \cdot x) + A_{\mathrm{s2}} \cdot \sigma_{\mathrm{s2}} \cdot (d - d_2) + A_{\mathrm{f}} \cdot \sigma_{\mathrm{f}} \cdot d_1 \right] \tag{12}$$

where the neutral axis x is found by solving:

$$0 = \psi \cdot b \cdot x \cdot f_{\mathrm{cd}} + A_{\mathrm{s2}} \cdot \sigma_{\mathrm{s2}} - A_{\mathrm{s1}} \cdot f_{\mathrm{yd}} - A_{\mathrm{f}} \cdot \sigma_{\mathrm{f}} \tag{13}$$

in which ψ and λ are non-dimensional coefficients representing the intensity and the position of the compressive concrete resultant, respectively. However, the strengthened capacity cannot be considered as greater than the 60% of initial capacity.

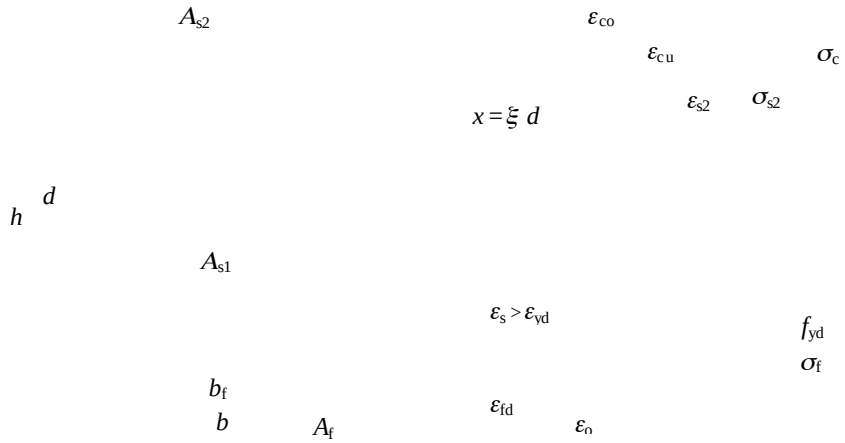

Fig.23: Notation for flexural strengthening and collapse modes.

When in the presence of axial force N_{sd}, the flexural capacity can be evaluated by means of the two equations above, substituting the first member of the former by N_{sd}. Longitudinal fibres must be accurately confined in order to avoid their debonding as well as the spalling of the support material.

As an alternative, the following procedure can be adopted (Monti and Alessandri 2005).

In the sections under axial load, the ULS design requires the dimensioning of the FRP strengthening in order to satisfy the following inequality:

$$M_{\mathrm{Sd}} \leq M_{\mathrm{Rd}}(N_{\mathrm{Sd}}) \tag{14}$$

where M_{Sd} is the design moment demand and M_{Rd} is the design moment capacity of the strengthened section under the acting design axial load, N_{Sd}.

One preliminarily evaluates the tensile reinforcement mechanical ratio, μ_s, and that of the FRP strengthening, μ_f, given, respectively, by the following relations:

$$\mu_{\mathrm{s}} = \frac{A_{\mathrm{s1}} \cdot f_{\mathrm{yd}}}{0.85 \cdot f_{\mathrm{cd}} \cdot b \cdot d} \tag{15}$$

$$\mu_{\mathrm{f}} = \frac{b_{\mathrm{f}} \cdot t_{\mathrm{f}} \cdot f_{\mathrm{fd}}}{0.85 \cdot f_{\mathrm{cd}} \cdot b \cdot d} \tag{16}$$

where A_{s1} and f_{yd} are, respectively, the area and the design yield strength of the existing tensile steel rebars; f_{cd} is the compressive design strength of the existing concrete; b and d are, respectively, the width and depth of the existing concrete section; b_f and t_f are, respectively, the width and thickness of the new FRP strengthening; f_{fd} is the design FRP strength.

The following non-dimensional expressions are useful for the following developments:

$$n_{Sd} = \frac{N_{Sd}}{0.85 \cdot f_{cd} \cdot b \cdot d} \tag{17}$$

$$m_{Sd} = \frac{M_{Sd}}{0.85 \cdot f_{cd} \cdot b \cdot d^2} \tag{18}$$

Having selected the FRP width and mechanical properties, in the design phase one has to determine its thickness t_f.

By starting from a guess value (usually, one layer) one computes the strengthening mechanical ratio, μ_f, and then proceeds by iterations as follows.

Step 1

Compute the value of the parameter η defined as:

$$\eta = n_{Sd} + \mu_s \cdot (1-u) + \mu_f \tag{19}$$

Step 2

Compute the boundary values η_i (i = 0, 1, 2, 3) of the above parameter as:

$$\eta_0 = -\mu_s \cdot u\,, \quad \eta_1 = \frac{2}{3} \cdot \frac{r}{r+1}\,, \quad \eta_2 = 0.8 \cdot \frac{1.75 \cdot r}{1.75 \cdot r + 1}\,, \quad \eta_3 = 0.51 + \mu_f \cdot (1-r)\,, \tag{20}$$

where:

- u is the ratio between compressive steel, A_{s2}, and tensile steel, A_{s1};
- $r = 2/1000\,\varepsilon_{fd}$.

Step 3

From the following table, by comparing the value of the parameter η with the boundary values of Step 2, identify the collapse mode of the strengthened section (Figure 24) and compute the relevant value of the parameter $W_{(mr)}(\eta)$.

Collapse mode	η	$W_{(mr)}(\eta)$
1a	$\eta_0 \le \eta \le \eta_1$	$W_{(1a)}(\eta) = \frac{1}{2} \cdot \left\{ \eta_0 + \frac{\eta_1 \cdot (1-\eta_1) - \eta_0}{\eta_1 - \eta_0} \cdot (\eta - \eta_0) \right\}$
1b	$\eta_1 \le \eta \le \eta_2$	$W_{(1b)}(\eta) = \frac{1}{2} \cdot \left\{ \eta_1 \cdot \eta_2 + \left[1 - (\eta_1 + \eta_2) \right] \cdot \eta \right\}$
2	$\eta_2 \le \eta \le \eta_3$	$W_{(2)}(\eta) = \frac{1}{2} \cdot \left\{ \eta_2 \cdot (1-\eta_2) + \frac{(0.75-\eta_3) - \eta_2 \cdot (1-\eta_2)}{\eta_3 - \eta_2} \cdot (\eta - \eta_2) \right\}$

Step 4

Compute the non-dimensional resisting moment of the FRP-strengthened section, $m_{Rd}(n_{Sd})$, as follows:

$$m_{Rd}(n_{Sd}) = W_{(mr)}(\eta) + \frac{1}{2} \cdot \left[\mu_s \cdot (1+u) + \mu_f \right]. \tag{21}$$

Step 5

Verify that:

$$m_{Rd}(n_{Sd}) \ge m_{Sd} \tag{22}$$

If this is not satisfied, then increase the FRP thickness, t_f, and therefore the mechanical strengthening ratio, μ_f, and iterate again from Step 1.

5.5 Shear and torsion

Shear strengthening configurations can be in the form of side bonded, U-jacketed and wrapped FRP strips/sheets. The design shear strength of the strengthened element is given as:

$$V_{\mathrm{Rd}} = \min\left\{V_{\mathrm{Rd,ct}} + V_{\mathrm{Rd,s}} + V_{\mathrm{Rd,f}}, V_{\mathrm{Rd,max}}\right\} \tag{23}$$

where $V_{\mathrm{Rd,ct}}$, $V_{\mathrm{Rd,s}}$ and $V_{\mathrm{Rd,f}}$ are the concrete, transverse steel and FRP contribution, respectively, while $V_{\mathrm{Rd,max}}$ is the shear producing collapse in the compressed diagonal concrete strut.

The FRP contribution to the overall strength is given based on the chosen strengthening configuration. For side bonding (with notation in Fig: 10):

$$V_{\mathrm{Rd,f}} = \frac{1}{\gamma_{\mathrm{Rd}}} \cdot \min\left\{0.9d, h_{\mathrm{w}}\right\} \cdot f_{\mathrm{fed}} \cdot 2t_{\mathrm{f}} \cdot \frac{\sin\beta}{\sin\theta} \cdot \frac{w_{\mathrm{f}}}{p_{\mathrm{f}}} \tag{24}$$

where the partial safety factor γ_{Rd} is equal to 1.20, while for U-jacketing and wrapping:

$$V_{\mathrm{Rd,f}} = \frac{1}{\gamma_{\mathrm{Rd}}} \cdot 0.9d \cdot f_{\mathrm{fed}} \cdot 2t_{\mathrm{f}} \cdot (\cot\theta + \cot\beta) \cdot \frac{w_{\mathrm{f}}}{p_{\mathrm{f}}} \tag{25}$$

where f_{fed}, termed effective debonding strength, is given, in the case of side bonding, as:

$$f_{\mathrm{fed}} = f_{\mathrm{fdd}} \cdot \frac{z_{\mathrm{rid,eq}}}{\min\left\{0.9d, h_{\mathrm{w}}\right\}} \cdot \left(1 - 0.6\sqrt{\frac{l_{\mathrm{eq}}}{z_{\mathrm{rid,eq}}}}\right)^2 \tag{26}$$

with:

$$z_{\mathrm{rid,eq}} = z_{\mathrm{rid}} + l_{\mathrm{eq}}, \quad z_{\mathrm{rid}} = \min\left\{0.9d, h_{\mathrm{w}}\right\} - l_{\mathrm{e}} \cdot \sin\beta, \quad l_{\mathrm{eq}} = \frac{s_{\mathrm{f}}}{f_{\mathrm{fdd}} / E_{\mathrm{f}}} \cdot \sin\beta \tag{27}$$

where l_{e} is the optimal anchorage length given in (8), s_{f} is the ultimate debonding slip assumed as 0.2 mm and E_{f} is the elastic modulus of FRP reinforcement in fibres direction.

In the case of U-jacketing and wrapping, respectively, it is given by:

$$f_{\mathrm{fed}} = f_{\mathrm{fdd}} \cdot \left[1 - \frac{1}{3}\frac{l_{\mathrm{e}}\sin\beta}{\min\left\{0.9d, h_{\mathrm{w}}\right\}}\right] \tag{28}$$

$$f_{\mathrm{fed}} = f_{\mathrm{fdd}} \cdot \left[1 - \frac{1}{6}\frac{l_{\mathrm{e}}\sin\beta}{\min\left\{0.9d, h_{\mathrm{w}}\right\}}\right] + \frac{1}{2}(\phi_{\mathrm{R}} \cdot f_{\mathrm{fd}} - f_{\mathrm{fdd}}) \cdot \left[1 - \frac{l_{\mathrm{e}}\sin\beta}{\min\left\{0.9d, h_{\mathrm{w}}\right\}}\right] \tag{29}$$

where f_{fd} is the FRP design strength, and:

$$\phi_{\mathrm{R}} = 0.2 + 1.6\frac{r_{\mathrm{c}}}{b_{\mathrm{w}}}, \qquad 0 \le \frac{r_{\mathrm{c}}}{b_{\mathrm{w}}} \le 0.5 \tag{30}$$

is a coefficient depending on the rounding radius r_{c} with respect to the beam web width b_{w}.

With regards to strengthening in torsion, this is obtained through the application of wrapping strips/sheets at an angle of 90° to the element axis. The design torsional strength of

the strengthened element is given as:

$$T_{Rd} = \min\left\{T_{Rd,s} + T_{Rd,f}\,, T_{Rd,max}\right\} \tag{31}$$

where $T_{Rd,s}$ and $T_{Rd,f}$ are the transverse steel and FRP contribution, respectively, while $T_{Rd,max}$ is the torque producing collapse in the compressed diagonal concrete strut. The FRP contribution to the torsional strength is given as:

$$T_{Rd,f} = \frac{1}{\gamma_{Rd}} \cdot 2\, f_{fed} \cdot t_f \cdot b \cdot h \cdot \frac{w_f}{p_f} \cdot \cot\theta \tag{32}$$

where f_{fed} is given by (20) and γ_{Rd} is equal to 1.20.

5.6 Confinement

This aims both at increasing the ultimate strength in elements under axial load, and the ductility in FRP-confined elements under axial load and flexure. In case of elements with circular cross-section of diameter D, the confined/unconfined concrete strength ratio is:

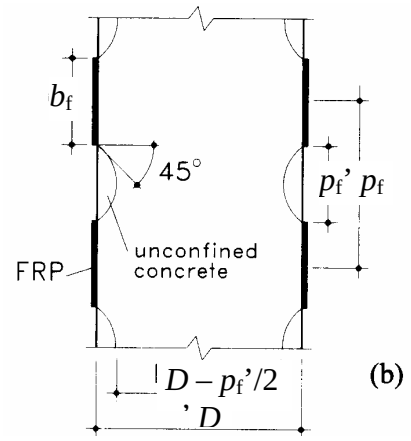

Fig.24: Notation for confinement (from fib bulletin 14).

$$\frac{f_{ccd}}{f_{cd}} = 1 + 2.6\left(\frac{f_{l,eff}}{f_{cd}}\right)^{2/3} \tag{33}$$

while the ultimate concrete strain is:

$$\varepsilon_{ccu} = 0.0035 + 0.015\sqrt{\frac{f_{l,eff}}{f_{cd}}} \tag{34}$$

where both depend on the confinement pressure exerted by the FRP sheet, given as:

$$f_{l,eff} = k_{eff} \cdot f_l \text{ , with: } f_l = \frac{1}{2}\rho_f\, E_f\, \varepsilon_{fd,rid} \tag{35}$$

where k_{eff} is an efficiency factor (≤ 1), E_f is the FRP modulus of elasticity, $\varepsilon_{fd,rid}$ is the FRP reduced design strain, defined in the following, and ρ_f is the geometric strengthening ratio, depending on the cross-section shape (circular or rectangular):

$$\rho_f = \frac{4 t_f b_f}{D \cdot p_f} \text{ or } \rho_f = \frac{2 \cdot t_f \cdot (b+d) \cdot b_f}{b \cdot d \cdot p_f} \tag{36}$$

with t_f and b_f thickness and height of the generic FRP strip, p_f strips distance, D diameter of the circular section, or b and d transverse dimensions of the rectangular section (Figure 24).

The efficiency factor is given as:

$$k_{eff} = k_H \cdot k_V \cdot k_\alpha \tag{37}$$

where k_H, horizontal efficiency factor, is equal to 1.0 for circular sections and to:

$$k_H = 1 - \frac{b'^2 + d'^2}{3 \cdot A_g} \tag{38}$$

for rectangular sections, with $b' = b - 2r_c$, $d' = d - 2r_c$ and A_g = area of the cross-section; and the vertical efficiency factor, k_V, is:

$$k_V = \left(1 - \frac{p'_f}{2\, d_{min}}\right)^2 \tag{39}$$

where p'_f is the net distance between adjacent strips and d_{min} is the minimum transverse dimension of the element; the angle efficiency factor, k_α, when the fibres are wrapped at an angle α_f with respect to the element axis, is:

$$k_\alpha = \frac{1}{1 + (\tan \alpha_f)^2} \tag{40}$$

Finally, the reduced design strain is:

$$\varepsilon_{fd,rid} = \min\{\eta_a \varepsilon_{fk} / \gamma_f ;\ 0.004\} \tag{41}$$

where η_a and γ_f are the environment conversion factor and the partial factor of the FRP strengthening, respectively.

5.7 Seismic strengthening with FRP

It should be underlined that this portion of the code applies once the requirement to assess a particular building has been established. The conditions under which seismic assessment of individual buildings – possibly leading to retrofitting – are required are addressed in the recently issued Italian seismic code (OPCM 3431 5/2005).

The code offers the possibility, as an alternative to more traditional strengthening techniques, to use composite materials to seismically upgrade under-designed reinforced concrete structures. The objective is that of strengthening buildings that do not meet the safety requirements stated by the current seismic codes, with respect to one or more limit states, under the design seismic action.

It is assumed that a preliminary analysis has been performed on the existing structure and that the strengthening intervention is designed based on the outcomes of the assessment phase.

Both the assessment and the retrofitting analyses must comply with the indications given by the most recent seismic codes, with particular reference to: a) assessment of the seismic safety, b) safety requirements, c) protection levels (intensity of the seismic action), d) methods of analysis, e) verification criteria, f) material characteristics to be uses in the safety verifications.

For as regards the criteria for the selection of the FRP strengthening, it is recognized that stiffness irregularities cannot be solved by applying FRP. An intervention performed with FRP is classified as a selective technique. Strength irregularities can be adjusted by strengthening a selected number of elements, however, attention should be paid that the global ductility is not reduced.

The design of a strengthening intervention with FRP should include the following activities: a) justification of the intervention type, b) selection of techniques and/or materials, c) preliminary dimensioning of the strengthening intervention, d) structural analysis accounting for the characteristics of the upgraded structure.

The above principles apply to any construction typology, both reinforced concrete, masonry, steel and timber. In the following sections, specific rules for buildings made from reinforced concrete are dealt with.

From the seismic standpoint, FRP strengthening is regarded as a selective intervention technique, aiming at: a) increasing the flexural capacity of deficient members, with and without axial load, through the application of composites with the fibres placed parallel to the element axis, b) increasing the shear strength through the application of composites with the fibres placed transversely to the element axis, c) increasing the ductility (or the chord rotation capacity) of critical zones of beams and columns through FRP wrapping (confinement), d) improving the efficiency of lap splice zones, through FRP wrapping, e) preventing buckling of longitudinal rebars under compression through FRP wrapping, f) increasing the tensile strength of the panels of partially confined beam-column joints through the application of composites with the fibres placed along the principal tensile stresses.

A relevant innovation concerns the definition of the inspiring principles of the intervention strategies: a) all brittle collapse mechanism should be eliminated, b) all “soft story” collapse mechanism should be eliminated, and c) the global deformation capacity of the structure should be enhanced, either: c1) by increasing the ductility of the potential plastic hinge zones without changing their position, or c2) by relocating the potential plastic hinge zones by applying capacity design criteria. In this latter case, the columns should be flexure-strengthened with the aim of transforming the frame structure into a high dissipation mechanism with strong columns and weak beams.

Failure of brittle mechanisms such as shear, lap splicing, bar buckling, and joint shear should be avoided. For shear, the same criteria apply as for the non-seismic case, with the exception that side bonding is not allowed and FRP strips/sheets should only be applied orthogonal to the element axis. For lap splices of length L_s, adequate FRP confinement should be provided, having thickness:

$$t_{\mathrm{f}} = \frac{\max\{b,d\}}{2\cdot E_{\mathrm{f}}}\cdot\left(1000\cdot\frac{f_l}{k_H} - E_{\mathrm{S}}\right) \tag{42}$$

where E_s = steel modulus, and f_{l} = confinement pressure:

$$f_{\mathrm{l}} = \frac{A_{\mathrm{s}}\cdot f_{\mathrm{y}}}{\left[\frac{u_{\mathrm{e}}}{2\cdot n} + 2\cdot(d_{\mathrm{b}} + c)\right]\cdot L_{\mathrm{s}}} \tag{43}$$

where u_{e}= perimeter of the cross section inscribed in the longitudinal bars, of which n are spliced, and c = concrete cover. For bar buckling, adequate FRP confinement should be provided, having thickness:

$$t_{\mathrm{f}} = \frac{10\cdot n\cdot\max\{b,d\}}{E_{\mathrm{f}}} \tag{44}$$

where n = total number of longitudinal bars under potential buckling.

For case a) above, when eliminating potential brittle failure mechanisms, the relative strengthening modalities are quite straightforward. The most common case is that of potential shear failure, for which a strengthening of the shear mechanism should be sought. More peculiar cases are those of longitudinal bars lap splices and buckling. In the former case, due to either bond degradation in splices or insufficient splice length, the relevant regions of potential plastic hinge formation should be adequately confined through an FRP wrapping; in the latter case of bar buckling, the strengthening intervention should consist in confining the potential plastic hinge zones where the existing transverse reinforcement cannot prevent the bars post-elastic buckling.

For case b) above, specific consideration should be given to potential "soft storey" collapse mechanisms, which can develop in the absence of walls, due to the contemporary formation of plastic hinges on top and bottom of all columns at a certain story. In such cases, the strengthening intervention should aim at increasing the flexural capacity in those zones, with the objective of inhibiting the hinges formation. It is emphasized that in no case one should aim at increasing the ductility of such collapse mechanisms.

For case c), when all possible brittle and storey mechanisms are eliminated, one could ascertain to which extent the structure could exploit its ductility. This can be done, for example, through a nonlinear pushover analysis, now adopted and codified in the most modern seismic codes. Usually, one is requested to check if the structure can actually ensure a given ductility, expressed by a pre-selected behaviour factor, or, which is the same, it is able to attain a given target displacement obtained from the displacement spectrum. Such analysis allows to identify all those elements whose local collapse, due to ductility exhaustion, prevents the structure from exploiting its global ductility and from reaching the target displacement.

At this stage, one could face two different situations: c1) the number of local collapses is not significant, or c2) the number of local collapses is significant.

In the former case (c1), it comes all too natural to increase the deformation capacity of only those elements that collapse before the global target displacement is attained. The deformation capacity of beams and columns can be measured by the chord rotation θ, that is, the rotation of the chord connecting the element end section with the contraflexure section (shear span). Generally, the plastic deformation capacity is controlled by the compressive behaviour of concrete. An intervention of FRP-confinement on such elements (usually columns) increases the ultimate compressive strain of concrete, thus determining a ductility increase of the element.

In the latter case (c2), the collapses are so numerous that a different strategy should be pursued: the overall resisting mechanism is changed into one where the request of ductility is spread over a larger number of elements. This can be achieved by relocating all potential plastic hinges in the columns to the framing beams, by applying the capacity design criteria. The application of the capacity design criteria implies the elimination of all potential plastic hinges in columns. In "weak column-strong beam" situations, typical of frame structures designed for gravity loads only, the columns sections are under-designed both in geometry and reinforcement. In such case, it is necessary to increase their flexural strength with the objective of changing the structure into a "strong column-weak beam" situation. It should be noted that, pursuing this strategy implies an increase of shear demand on columns due to the flexural capacity increase. It is therefore necessary to perform the required shear verifications, and to eventually increase the shear strength in order to avoid brittle failure modes.

It might be superfluous to mention the dramatic importance of a unified approach in the mechanical models describing the ultimate deformability and strength of FRP-strengthened elements.

As a matter of fact, for what concerns the evaluation of the deformation capacity of FRP-strengthened existing RC elements under cyclic load, this has been deemed as a research

priority for over 10 years now; as a result, a relatively large number of analytical models that describe the “axial load - bending - shear” cyclic response of RC structural members with FRP has been proposed, together with empirical formulae derived from experimental observations. However, such large number of available models and related research work denotes also the difficulties that currently exist in finding a unified and undisputed approach, which should include both a mechanics-based view of all FRP-strengthening modalities and a sound reliability-based framework. This stems in part from the relatively limited accuracy shown by some of the proposed models, as well from the difficulty in extrapolating results obtained from a limited experimental sample, which, for as much complete as it might be, always fails short of representing the full range of peculiarities of the response of FRP-strengthened RC elements under cyclic actions.

6 Conclusions

The peculiarity of Italy, highly seismic and endowed with a built environment unique extremely various and rich of cultural value, renders all research in this field a continuous and challenging task.

This nationwide effort has resulted in a first regulatory document (CNR-DT 200/2004), that was conceived both for regulating a rapidly growing professional and technical market, as well as for an informative and educational purpose. The document is deemed of great importance for the dissemination, in the professional sphere, of the physical and technological knowledge necessary to conscious and competent use of FRP in strengthening.

A version in English of the document is under preparation and will be available in summer 2005.

In this section, three aspects of paramount importance in FRP-strengthening have been dealt with, namely, anchorages, shear and confinement, with the aim of understanding the mechanics behind the design equations.

References

ACI 440.2R-02 (2002). Guide for the Design and Construction of Externally Bonded FRP Systems for Strengthening Concrete Structures. *American Concrete Institute*, Committee 440.

Adhikary, B. B. and Mutsuyoshi, H. (2004). Behavior of Concrete Beams Strengthened in Shear with Carbon-Fiber Sheets. *Journal of Composites for Construction*, ASCE, 8, 258

Aiello, M.A., and Pecce, M. (2001). Experimental Bond Behavior between FRP Sheets and Concrete, *Structural Faults and Repair Conference*, 4-6 July, 2001.

American Concrete Institute (1996). State-of-the-art report on fiber reinforced plastic reinforcement for concrete structures. *ACI Report 440R-96*, 1996, Detroit, Michigan, USA.

Antonopoulos, C.P., and Triantafillou, T.C. (2002). Analysis of FRP-Strengthened RC Beam-Column Joints. *J. of Composites for Construction*, ASCE, 6, 41.

Antonopoulos, C.P., and Triantafillou, T.C. (2003). Experimental Investigation of FRP-Strengthened RC Beam-Column Joints. *J. of Composites for Construction*, ASCE, 7, 39.

Aprile, A., and Benedetti, A. (2004). Coupled flexural-shear design of R/C beams strengthened with FRP. *Composites: Part B*, Elsevier, 35, 1-25.

Aprile, A., Spacone, E., and Limkatanyu, S. (2001). Role of Bond in Beams Strengthened with Steel and FRP Plates. *Journal of Structural Engineering*, ASCE, 127(12), pp. 1445-1452.

Arduini, M., and Nanni, A. (1997). Behavior of precracked RC beams strengthened with carbon FRP sheets. *Journal of Composites for Construction*, ASCE, 1(2), 63–70.

Arduini, M., Di Tommaso, A., and Nanni, A. (1997). Brittle failure in FRP plate and sheet bonded beams. *ACI Structural Journal*, 94(4), 363–369.

Ascione, L., and Feo, L. (2000). Modeling of composite/concrete interface of RC beams strengthened with composite laminates. *Composites: Part B*, Elsevier, 31(6/7), 535–40.

Ascione, L., and Feo, L. (2002). Strengthening of cracked RC beams with FRP sheets: an experimental investigation. *International Conference on Composites Engineering (ICCE/9)*, San Diego, USA.

Barboni, M., Bendetti, A., and Nanni, A. (1997). Carbon FRP Strengthening of Doubly Curved Precast PC Shell. *Journal of Composites for Construction*, ASCE, 1(4), 168–174.

Brosens, K., and Van Gemert, D. (1999a). Anchorage design for externally bonded carbon fiber reinforced polymer laminates. *Proc. 4th Int. Symposium on FRP Reinforcement for Concrete Structures*, Baltimore, USA, pp. 635-645.

Brosens, K., and Van Gemert, D. (1999b). Stress analysis in the anchorage zones of externally bonded CFRP laminates. *Proc. of the Int. Conference on Infrastructure Regeneration and Rehabilitation – Improving the Quality of Life Through Better Construction, A Vision for the Next Millennium*, Sheffield, June 28th – July 2nd, 931-940.

Camata, G., Corotis, R., and Spacone, E. (2004). Simplified Stochastic Modeling and Simulation of Unidirectional Fiber Reinforced Composites. *Probabilistic Engineering Mechanics*, 19(1-2), 33-40.

Camata, G., Spacone, E., Al Mahaidi, R., and Saouma, V. (2004). Analysis of Test Specimens for Cohesive Near-Bond Failure of FRP-Plated Concrete. *Journal of Composites for Construction*, ASCE, in press.

Campione, G., and Miraglia, N. (2003). "Strength and strain capacities of concrete compression members reinforced with FRP". *Cement and Concrete Composites*, Elsevier, 25, 31-41.

CEN (1991), "Eurocode 2: Design of concrete structures – Part 1-1: General rules and rules for buildings", EN 1992-1-1, Comité Européen de Normalisation (CEN), Brussels.

Ceroni F., Manfredi G., Pecce M. (2001). Cracks width in RC beams strengthened with carbon fabrics. *Proc. of the Fifth Conference on Non-Metallic Reinforcement for Concrete Structures,FRPRCS5*, Thomas Telford, Cambridge, UK, 16-18 July, Vol.2, 917-926.

Ceroni F., Pecce M., Matthys S. (2003). Tension Stiffening of RC Ties Strengthened with Externally Bonded FRP Sheets, *J. of Composites for Constructions*, ASCE, 8(1).

Ceroni F., Pecce M. (2004). Modelling of Tension Stiffening behaviour of RC ties strengthened with FRP sheets, *J. of Composites for Constructions*, ASCE.

Chaalal, O., Nollet, M.-J., and Perraton, D. (1997). Experimental investigation of RC beams strengthened in flexure with externally bonded CFRP strips. *Proc. Annual Conference of the Canadian Society for Civil Engineering*, Part 6 (of 7), Sherbrooke, Canada.

Chen, J.F., and Teng, J.G. (2001). Anchorage strength models for FRP and steel plates bonded to concrete. *Journal of Structural Engineering*, ASCE, 127(7), 784-791.

Chen, J.F., Yang, Z.J., and Holt, G.D. (2001). FRP for steel plate-to-concrete bonded joints: Effects of test methods on experimental bond strength. *Steel & Composite Structures – An International Journal*, 1(2), 231-244.

Deniaud, C. and Cheng J.J.R. (2004). Simplified shear design method for concrete beams strengthened with FRP. *ASCE Journal of Composites for Construction*, 8(5), 425-433.

fib Bulletin 14 (2001). Externally bonded FRP reinforcement for RC structures. fédération internationale du béton, Lausanne.

Holzenkämpfer, P. (1994). Ingenieurmodelle des Verbundes geklebter Bewehrung für Betonbauteile. *Dissertation*, Technische Universität Braunschweig, Germany (in German).

Ianniruberto, U. and Imbimbo, M. (2000). Shear resisting contribution of composite for RC beams strengthened with FRP sheets, *Proceedings International Conference Advancing with Composite 2000*, Milan, May, 233-241.

Ianniruberto, U. and Imbimbo, M. (2002). Experimental analysis on the shear behaviour of RC beams strenghtened with GFRP sheets. *Proc. Third International Conf. on Composites in Infrastructure, ICCI '02*, San Francisco, California, 10-12 June.

JSCE (1995). State-of-the-Art-Report on Continuous Fibre Reinforcing Materials. *Concrete Engineering Series 3*, Japan Society of Civil Engineering, Japan.

Karbhari, V.M., and Gao, Y. (1997). Composite jacketed concrete under uniaxial compression – verification of simple design equations. *J. of Materials in Civil Engineering*, ASCE, 9(4), 185-193.

Khalifa, A., Gold, W. J., Nanni, A. and Aziz, A. M. I. (1998). Contribution of externally bonded FRP to shear capacity of rc flexural members. *ASCE Journal of Composites for Construction*, 2(4), 195-202.

Maeda, T., Asano, Y., Sato, Y., Ueda, T., and Kakuta, Y. (1997). A study on bond mechanism of carbon fiber sheet. *Proc. 3rd Int. Symposium on Non Metallic (FRP) Reinforcement for Concrete Structures*, Japan Concrete Institute, Sapporo, Vol. 1, 279-285.

Mander, J.B., Priestley, M.J.N., and Park, R. (1988). Theoretical stress-strain model for confined concrete, *Journal of Structural Engineering*, ASCE, Vol. 114(8), 1804-1826.

Manfredi, G., Monti, G. (2005). FRP strengthening in seismic zones. *ACI Convention*, New York, USA, April.

Micelli, F. Annaiah, R and Nanni, A. (2002) Strengthening of Short Shear Span Reinforced Concrete T Joists with Fiber-Reinforced Plastic Composites, *Journal of Composites for Construction*, ASCE, 6, 264

Miller, B., and Nanni, A. (1999). Bond between CFRP sheets and concrete. *Proceedings, ASCE 5th Materials Congress*, Cincinnati, OH, L.C. Bank, Editor, May 10-12, 1999, 240-247.

Mirmiran, A., Shahawy, M., Samaan, M., El Echary, H., Mastrapa, J.C., and Pico, O. (1998). Effect of column parameters on FRP-confined concrete, *J. Composites for Construction*, ASCE, 2(4), 175-185.

Monti, G. (2001). Confining concrete with FRP: Behavior and Modeling. *Workshop "Composite in Construction: A Reality"*, July, Capri, Italy.

Monti, G., Nisticò, N., and Santini, S. (2001). Design of FRP jackets for upgrade of circular bridge piers. *Journal of Composites for Construction*, ASCE, 5(2), 94-101.

Monti, G., Santini, S. (2002). Reliability-based calibration of partial safety coefficients for FRP. *Journal of Composites for Construction*, ASCE, 6(3).

Monti, G., and Barbato, M. (2003). Fiber-Section FE of FRP-Strengthened RC Beam in Flexure, Shear and Confinement. *Proceedings of the 6th International Symposium on Fibre-Reinforced Polymer (FRP) Reinforcement for Concrete Structures (FRPRCS-6)*, Singapore.

Monti, G., Renzelli, M., and Luciani, P. (2003). FRP Adhesion to Uncracked and Cracked Concrete Zones. *Proceedings of the 6th International Symposium on Fibre-Reinforced Polymer (FRP) Reinforcement for Concrete Structures (FRPRCS-6)*, Singapore, July, 183-192

Monti, G., Santinelli, F., Liotta, M.A. (2004). Mechanics of FRP shear strengthening of RC beams. *Proc. ECCM 11*, Rhodes, Greece, May.

Monti, G. (2004). FRP research in Italy – Towards a New Code for FRP Strengthening. *Proc. 2nd International Conference on FRP Composites in Civil Engineering - CICE 2004*, (invited speaker), Adelaide, Australia, December.

Monti, G., Santinelli, F., Liotta, M.A. (2004). Shear strengthening of beams with composite materials. *Proc. 2nd International Conference on FRP Composites in Civil Engineering - CICE 2004*, Adelaide, Australia, December.

Monti, G., Alessandri, S. (2005). Design equations for FRP-strengthening of columns. Proceedings of the 7th International Symposium on Fibre-Reinforced Polymer (FRP) Reinforcement for Concrete Structures (FRPRCS-7), New Orleans, USA, November.

Monti, G., Liotta, M.A. (2005). FRP-strengthening in shear: tests and design equations. *Proceedings of the 7th International Symposium on Fibre-Reinforced Polymer (FRP) Reinforcement for Concrete Structures (FRPRCS-7)*, New Orleans, USA, November.

Nanni, A. and Norris, M.S. (1995). FRP jacketed concrete under flexure and combined flexure-compression, *Construction and Building Materials*, 9(5), 273-281.

Neale, K.W. and Labossiere, P. (1997). State-of-the-art report on retrofitting and strengthening by continuous fibre in Canada. *Non-Metallic (FRP) Reinforcement for Concrete Structures, Proc. 3rd Int. Symposium*, Sapporo, Japan, 25-39.

Neubauer, U., and Rostasy, F. S. (1997). Design aspects of concrete structures strengthened with externally bonded CFRP plates. *Proc. 7th Int. Conference on Structural Faults and Repair, ECS Publication*, Edinburgh, Scotland, Vol. 2, 109-118.

Niedermeier, R. (1997). Gemischte Bewehrung bei klebearmierten Bauteilen (Mixed reinforcement in concrete members with externally bonded reinforcement). *Munchner Massivbau-Seminar*, Technische Universität München, Germany (in German).

Ohno, S., Miyauchi, Y., Kei, T. and Higashibata, Y. (1997). Bond properties of CFRP plate joint. *Non-Metallic (FRP) Reinforcement for Concrete Structures, Proc. 3rd Int. Symposium*, Sapporo, Japan, 241-248.

Pecce M., Manfredi G., and Cosenza E. (2000). Experimental response and code models of GFRP RC beams in ultimate and serviceability conditions. *Journal of Composites for Construction*, ASCE, 4(4), November, 182-190.

Pellegrino, C and Modena, C. (2002) Fiber Reinforced Polymer Shear Strengthening of Reinforced Concrete Beams with Transverse Steel Reinforcement *ASCE Journal of Composites for Construction*, 6, 104

Priestley, M.J.N., Seible, F., Xiao, Y., and Verma, R. (1994). Steel jacket retrofitting of reinforced concrete bridge columns for enhanced shear strength. *ACI Structural J.*, 91(4), 394-405.

Prota, A., Nanni, A., Manfredi, G., and Cosenza, E. (2003). Capacity Assessment of RC Subassemblages Upgraded with CFRP. *Journal of Reinforced Plastics and Composites*, Sage, 22(14), 1287-1304.

Purba, B.K., and Mufti, A.A. (1999). Investigation on the behavior of circular concrete columns reinforced with CFRP jackets, *Canadian J. of Civil Engineering*, 26, 590-596.

Realfonzo, R., Prota, A., Manfredi, G., and Pecce, M. (2002). Flexural Strength of FRP-confined RC Columns. *Proc. 1st fib Congress*, October, Osaka, Japan.

Saadatmanesh, H., Ehsani, M.R., and Li, M.W. (1994), Strength and ductility of concrete columns externally reinforced with fiber composite straps, *ACI Structural J.*, 91(4), 434-447.

Saafi M, Toutanji HA, and Li Z. (1999). Behavior of concrete columns confined with fiber reinforced polymer tubes. *ACI Materials Journal*, 96(4), 500-509.

Samaan, M., Mirmiran, A., and Shahawy, M. (1998). Model of concrete confined by fiber composites. *Journal of Structural Engineering*, ASCE, Vol. 124(9), 1025-1031.

Seible, F., Hegemier, G. A., Priestley, M. J. N. and Innamorato, D. (1995). Developments in bridge column jacketing using advanced composites. *Proc. National Seismic Conference on Bridges and Highways*, San Diego, CA, USA.

Seible, F., Priestley, M.J.N., and Innamorato, D. (1995). Earthquake retrofit of bridge columns with continuous fiber jackets, Volume II, Design guidelines, *Advanced composite technology transfer consortium*, Report No. ACTT-95/08, University of California, San Diego, USA.

Spadea, G., Bencardino. F., and Swamy, R.N. (1998). Structural behaviour of composite RC beams with externally bonded CFRP. *Journal of Composite for Construction,* ASCE, 2(3), 132–137.

Spoelstra, M. R., and Monti, G. (1999). FRP-confined concrete model. *Journal of Composite for Construction*, ASCE, 3(3), 143-150.

Spoelstra, M.R., Monti, G. (1999). FRP-confined concrete model. *Journal of Composites for Construction, ASCE*, Vol. 3, No. 3.

Täljsten B. (1997). Strengthening of concrete structures for shear with bonded CFRP-fabrics. *Recent advances in bridge engineering, Advanced rehabilitation, durable materials, nondestructive evaluation and management*, Eds. U. Meier and R. Betti, Dübendorf, 57-64.

Täljsten, B. (1994), Plate Bonding, Strengthening of existing concrete structures with epoxy bonded plates of steel or fibre reinforced plastics, *Doctoral Thesis*, Luleå University of Technology, 1994:152D.

Täljsten, B. and Elfgren, L. (2000), Strengthening concrete beams for shear using CFRP-materials, Evaluation of different application methods. *Journal of Composites, Part B.*

Tan, K.H. (1997). State-of-the-art report on retrofitting and strengthening by continuous fibers, Southeast Asian perspective – Status, prospects and research needs. *Non-Metallic (FRP) Reinforcement for Concrete Structures, Proc. 3rd Int. Symposium*, Sapporo, Japan, 13-23.

Teng, J.G., Chen, J.F., Smith, S.T., and Lam, L. (2000). RC structures strengthened with FRP composites. *The Hong Kong Polytechnic University*, Hong Kong, China.

Thomsen, H., Spacone, E., Limkatanyu, S., and Camata, G. (2003). Failure Mode Analyses of Reinforced Concrete Beams Strengthened in Flexure with Externally Bonded Fiber Reinforced Polymers. *Journal of Composites for Construction*, ASCE, 8(2), 123-131.

Toutanji, H.A. (1999). Stress-strain characteristics of concrete columns externally confined with advanced fiber composite sheets, *ACI Materials J.*, 96(3), 397-404.

Triantafillou, T. C., Deskovic, N. and Deuring, M. (1992), Strengthening of concrete structures with prestressed fiber reinforced plastic sheets. *ACI Structural Journal*, 89(3), 235-244.

Triantafillou, T. C. (1998). Shear strengthening of reinforced concrete beams using epoxy-bonded FRP composites. *ACI Structural Journal*, 95(2), March-April, 107-115.

Triantafillou, T. C. and Antonopoulos, C. P. (2000). Design of concrete flexural members strengthened in shear with FRP. *ASCE Journal of Composites for Construction*, 4(4), 198-205.

Xiao, Y. and Ma, R. (1997). Seismic retrofit of RC circular columns using prefabricated composite jacketing, *J. of Structural Engineering*, ASCE, 123(10), 1357-1364.

Xiao, Y., Martin, G. R., Yin, Z. and Ma, R. (1995). Retrofit design of existing reinforced concrete bridge columns using prefabricated composite jacketing. *Proc. National Seismic Conference on Bridges and Highways*; December 10-13, San Diego, CA, USA.

Ye, L. Yue, Q. Zhao, S and Li, Q. (2002). Shear Strength of Reinforced Concrete Columns Strengthened with Carbon-Fiber-Reinforced Plastic Sheet. ASCE *Journal of Structural Engineering*, 128, 1527

Yuan, H., and Wu, Z.S. (1999). Interfacial fracture theory in structures strengthened with composite of continuous fiber. *Proc. Symposium of China and Japan: Science and Technology of 21st Century*, Tokyo, Sept., 142-155.

Yuan, H., Wu, Z.S., and Yoshizawa, H. (2001). Theoretical solutions on interfacial stress transfer of externally bonded steel/composite laminates. *J. Struct. Mech. and Earthquake Engrg.*, Tokyo.

Zilch, K., Niedermeier, R., and Blaschko, M. (1996). Bond failure modes of flexural members strengthened with FRP. *Proc. 2nd Int. Conference on Composites in Infrastructures*, H. Saadatmanesh and M. R. Ehsani, eds., 315-327.

FRP retrofitting of reinforced concrete two-way slabs

Barış Binici and Oguzhan Bayrak
Middle East Technical University, Ankara, Turkey

1 Introduction

Reinforced concrete slabs are among the most commonly used structural elements. They have been used in many forms for structural systems such as flat plates, flat slabs, waffle slabs, and two-way slab with beams. Their design, initially conducted at the risk of the designer in early 1900s, has come a long way with advances in understanding the two-way load transfer mechanisms and extensive experimental studies. Especially, flat plate and flat slab structural systems are widely popular around the world due their advantages such as economical formwork, shorter construction time, less total building height with more clear space and architectural flexibility.

There are mainly two motivations for the retrofit of existing infrastructure including the reinforced concrete slabs. Firstly, the structural system designed and detailed for prescribed forces using a given code at a given time may be subjected to forces and displacements higher than those considered in the initial design during its lifetime. Examples can be the changes in use of the whole or a part of the structural system or changes in the prescribed design forces due to an increased seismicity of the area. These and similar situations increase either force or deformation demands on the structural elements. Secondly, there may be situations where the intended design force and/or displacement capacity of a structural member may be insufficient. A recent study might have pointed out the fact that the old design and construction practice may have led to unsafe designs. In addition, time dependent deterioration in the structural elements may result in reduced capacities. The particular examples for existing flat plate systems are non-ductile slab-column connections designed only to carry vertical loads and slab-column connections that are deficient with regard to continuous bottom bar requirements that were introduced in the late 1980s. Whether it is due to the changes in demand or capacity, structural upgrades may be needed for the reinforced concrete structural systems.

Fibre reinforced polymers (FRPs), previously used in aerospace and defense industries have emerged as a feasible alternative for structural retrofit in the last decade. Advantages of FRPs such as being light weight, high strength, resistant to corrosion and ease of application have made them popular in the upgrades of structural elements. Among different types of FRP materials, carbon fibre-reinforced polymers (CFRPs) and glass fibre-reinforced polymers (GFRPs) are used extensively in the structural engineering field. CFRPs have elasticity moduli comparable to that of steel and their ultimate strength range from about 800 to 4000MPa. On the other hand, lower cost GFPRs have ultimate uniaxial strength values ranging between 500 to 2000 MPa with elasticity moduli equal to about half that of CFRPs.

FRPs have found wide range of applications for reinforced concrete columns for shear and axial strength enhancement and for beam retrofit for shear and flexural strength improvement. Recent studies have shown that FRPs can also be successfully used in the retrofit of reinforced concrete slabs and slab-column connections. This section explains in detail upgrade of slab-column connections to enhance punching shear capacity and lateral deformation capacity of slab-column connections when subjected to combined gravity shear and seismically induced deformations. Following that, flexural strengthening of slabs by bonding FRPs on the tension side of the slabs is described.

2 Punching shear strengthening

2.1 Introduction

Use of fibre reinforced polymers as external shear reinforcement for punching shear strengthening has many advantages over other strengthening methods such as use of bolts, rebars acting as shear reinforcement or, externally built drop panels and capitals. The greatest advantages are due to favorable material properties such as light weight, high strength and ease of handling and applications. Superior material properties of these materials and ease of application (i.e. reduced labor costs) have led to the increased popularity of FRPs for strengthening and rehabilitation of structural components. Besides the advantages outlined above, there are additional advantages for their utilization in strengthening slab-column connections. As flat-plate structural systems are preferred for their versatile characteristics due to absence of beams, upgrade procedure should be such that flexible and aesthetic aspects of these systems are preserved after rehabilitation. Local increases in slab thickness or column size around the connection area may not be tolerated and they may bring additional costs in addition to rehabilitation costs. When FRPs are used for punching shear strengthening, slab thickness does not increase as a result of the application. Another advantage is the ease of detailing of FRP strips to form closed stirrups. During the application, FRP strips are saturated with bonding agent and the composite matrix is then applied to the concrete surface. At this stage of application, the composite material is flexible, easy to work with and it can be formed into any given shape for detailing purposes. For applications where FRPs are used as shear reinforcement, flexible nature of the material allows them to be wrapped around any shape, to be anchored by FRP overlaps, and to form closed loops as stirrups. Considering these advantages, the use of FRP as shear reinforcement for punching shear strength increase of reinforced concrete flat-plates was adopted in this study. However, it is well appreciated that somewhat lower stiffness of this costly material needs to be considered in punching shear upgrades.

In order to eliminate the punching failure due to an inclined shear crack at the face of the loaded area, shear reinforcement in the form of CFRPs should span the inclined crack and help to carry the shear as shown in Figure 1 schematically. For existing slabs, this can be achieved by drilling holes along the depth of the slab, and providing CFRPs in the vertical direction to pass through the expected failure plane. As the inclined crack forms around the concentrically loaded area, closest CFRP stirrups start carrying forces and the critical perimeter is shifted to the next set of CFRP stirrups with the formation of a new inclined crack. In this way, the length of the shear critical section can be increased resulting in an increased punching shear capacity of the slab-column connection. Based on this hypothesis, failure can take place i) inside the shear reinforced region due to sudden loss of load carrying capacity as a result of CFRP rupture, ii) outside the shear reinforced zone due to an inclined crack that develops outside the shear reinforced zone, iii) in flexure.

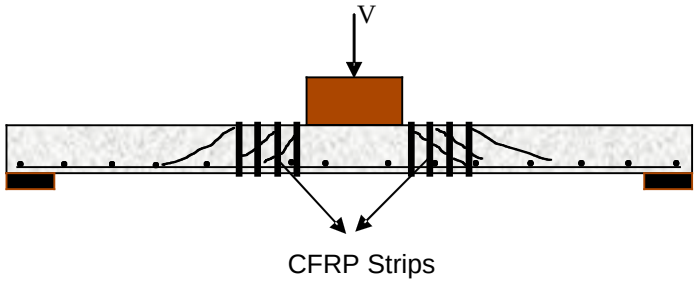

Fig. 1 Postulated shear response (Binici, 2003)

2.2 Strengthening methodology

The upgrade of the flat plates starts with arranging drilling locations around the slab-column connection region. In practice drilling through the slab may damage the existing longitudinal reinforcement. However, it is important to appreciate the fact that flexural strengthening can be achieved by bonding additional FRP strips on the tension face of the slab. Therefore, available flexural capacity should be checked and additional flexural strengthening should be provided in case of a potential damage to the longitudinal reinforcement in the connection region.

FRP stirrup installation and details of the proposed stitching technique are shown in Figure 2. Prior to upgrading, hole ends should be chamfered to eliminate sharp corners, which makes FRP vulnerable to early rupture. FRP strips cut to predetermined width are impregnated with epoxy and weaved through the vertical holes to form closed loops in the vertical plane.

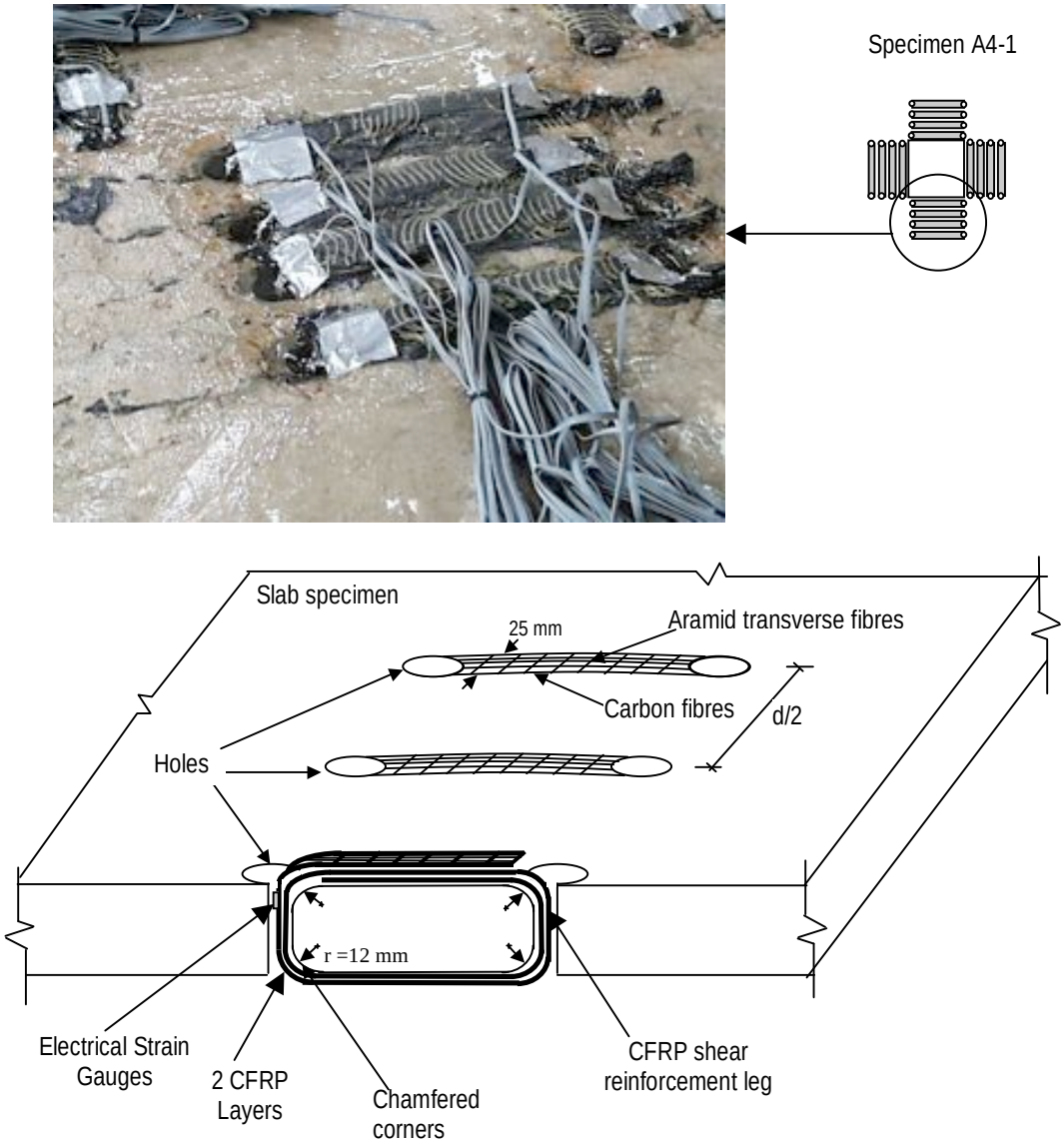

Fig. 2 Installation of external CFRP stirrups (Binici, 2003)

FRP anchorage is ensured by overlapping the FRP strips on the compressive side of the slab between the holes. Figure 3 shows the plan view of some of the previously investigated

strengthening patterns and stitching details (i.e. placement of CFRP stirrups). The first FRP stirrup is generally located d/4 away from the column face in both directions, and spacing of FRP stirrups is d/2 for the remaining strips (Figure 2). After the installation of FRP shear reinforcement, the holes are filled with epoxy and the slab is left for curing (Figure 2).

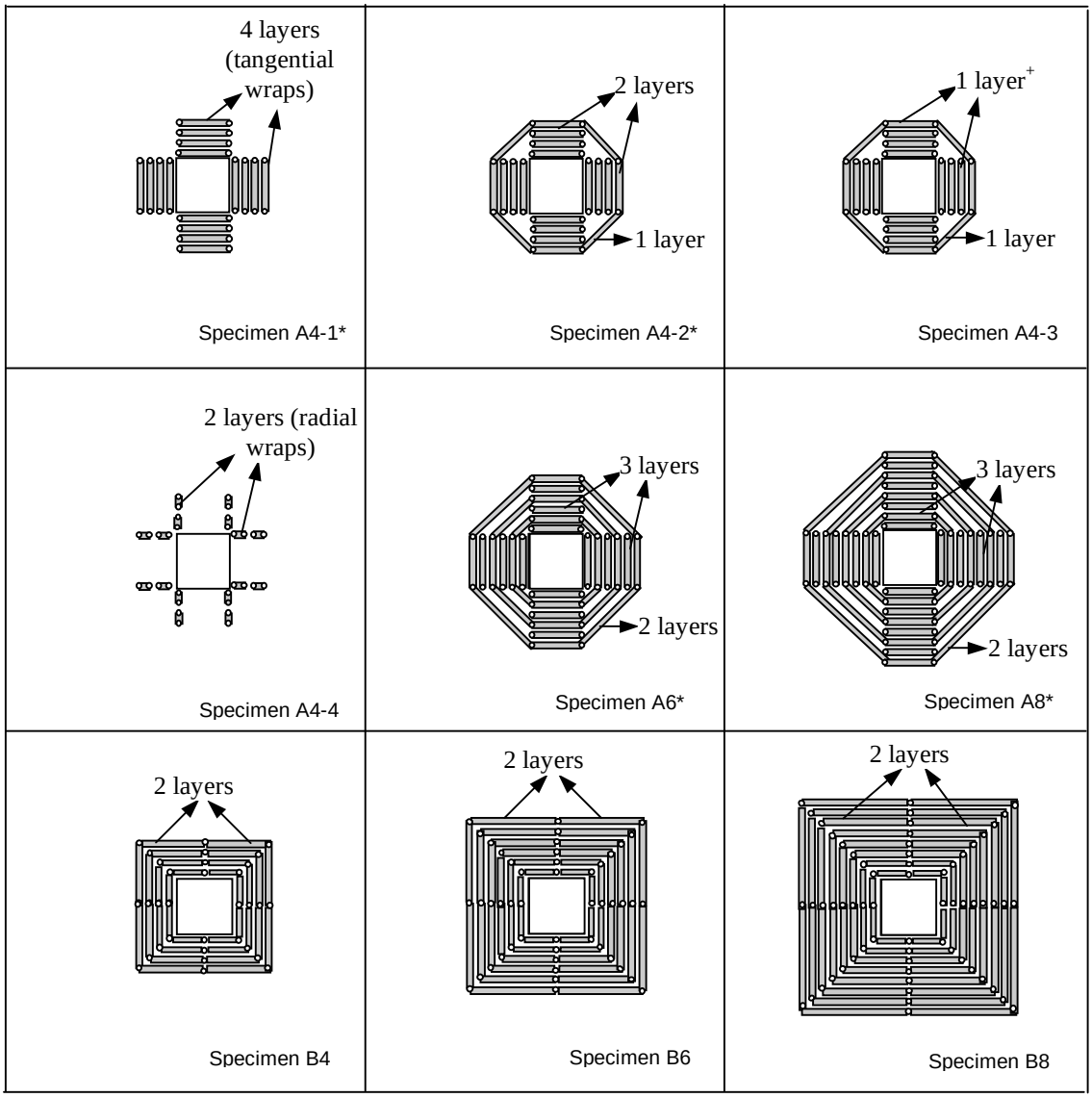

+: 1 layer corresponds to 25mm wide and 1mm thick CFRP strip.

*: Previously reported in Reference 6

: CFRP strips ∘ : Location of holes and shear reinforcement legs

: Loading plate

Fig. 3 Plan View of FRP stitching configurations (Binici, 2003)

2.3 Concentric shear capacity enhancement

The results of experiments [Binici, 2003; Binici and Bayrak, 2003, 2005] conducted on 2000 mm x 2000 mm x 150 mm reinforced concrete slabs are discussed in this section. The reinforcement ratio of all the slabs was about 1.76% and all the tests were conducted by applying a concentrated force in a displacement controlled mode on a 305 mm x 305 mm central area simulating the column. Load deflection measurements from concentric punching

shear tests are shown in Figure 4. The net deflection under the load application point was calculated by subtracting the measured support deformations from the measured average central deflections. Summary of test results are presented in Table 1. The increases in load carrying capacity were between 20 to 50% for Pattern A specimens, and 54 to 59% for Pattern B specimens relative to Control-1. The flexural capacity of test specimens was computed using a yield line analysis consisting of two lines extending from each column corner forming corner levers [Binici 2003]. For specimens strengthened using pattern-A CFRP stirrup arrangements, it can be observed that the ratio of ultimate load to flexural capacity increased with increasing number of CFRP perimeters. However for Pattern B specimens, this ratio was between 1.03 and 1.07 and was not affected by the number of CFRP perimeters used. Although flexural capacity according to the yield line method was reached for specimens A6, A8, B4, B6, and B8, extensive yielding did not occur, and punching failures occurred after some yielding in the repaired zone. Displacement ductilities, defined as the ratio of deflection at the ultimate load divided by the deflection at first yield was about 1.0 for control specimens. For specimens with pattern A, displacement ductility ranged from about 1.5 to 2.0. On the other hand, higher displacement ductilities (between 2.5 to 2.6) were observed for specimens strengthened with Pattern B. It was also possible to see that as the area of the CFRP strengthened zone increased the maximum load carrying capacity and displacement ductility values tended to increase (Table 1).

Specimen	Punching Failure Surface Locations	Ultimate Load, V_u (kN)	V_u / V_{flex}*	Load at First Yield, V_y (kN)	Deflection at First Yield, Δ_y (mm)	Deflection at Ultimate Load, Δ_u (mm)	% Increase in load capacity compared to Control 1	% Increase in displacement capacity compared to Control 1	Displacement Ductility, Δ_u / Δ_y	Post Punching Capacity (kN)
Control 1	-	494	0.68	487	11.0	11.3	-	-	1.03	139
Control 2	-	510	0.70	469	8.3	9.6	-	-	1.15	251
A 4-1	Inside	595	0.81	549	11.5	14.6	20.3	29.5	1.27	165
A 4-2	Outside	668	0.91	493	10.2	18.9	35.1	67.6	1.85	173
A 4-3	Inside	618	0.85	488	10.7	18.0	25.1	59.8	1.69	173
A 4-4	Inside	600	0.82	463	10.6	18.8	21.5	66.6	1.78	116
A 6	Outside	721	0.99	562	12.3	19.8	45.9	75.8	1.61	204
A 8	Outside	744	1.02	546	10.2	20.7	50.5	83.1	2.02	555
B 4	Outside	756	1.04	501	9.9	16.2	53	131.9	2.64	271
B 6	Outside	752	1.03	482	9.5	24.1	52.1	113.9	2.53	351
B 8	Outside	778	1.07	539	10.6	27.6	57.5	144.5	2.59	583

*: $V_{flex} = 8m\left(\frac{a}{a-r} - 3 + 2\sqrt{2}\right) = 8(90.3)\left(\frac{1981}{1981-304} - 3 + 2\sqrt{2}\right) = 730\,kN$ ($Constant$ *for all specimens*)

Table 1 Summary of concentric test results

Failure surfaces and inclined cracks of the two specimens are shown in Figure 5. It can be observed that upon retrofitting with FRPs, punching failure surface is shifted outside the reinforced zone resulting in higher concrete resistance on a larger perimeter. It is possible to say that as the CFRP area of the CFRP reinforced zone increases, higher strength increases can be achieved. The observed crack angles were between 22 and 35 degrees both for the reference specimens and the upgraded ones, the only difference being the location of the inclined cracks.

The post punching capacity of test specimens are compared in Table 1. As the number of FRP perimeters increased, the increased dowel contribution from longitudinal reinforcement resulted in higher post punching capacity. The number of bars engaged for dowel resistance was higher for Pattern B specimens compared to Pattern A specimens with a similar number of FRP perimeters. Hence, Pattern B specimens had higher post punching load carrying capacities than those of Pattern A. The existence of continuous compressive bars in specimen Control-2 resulted in an increased post punching capacity compared to that of specimen

Control-1. It is interesting to observe that specimens A8, B4, B6 and B8 had higher residual capacities than that of specimen Control-2, which complies with requirements of integrity steel.

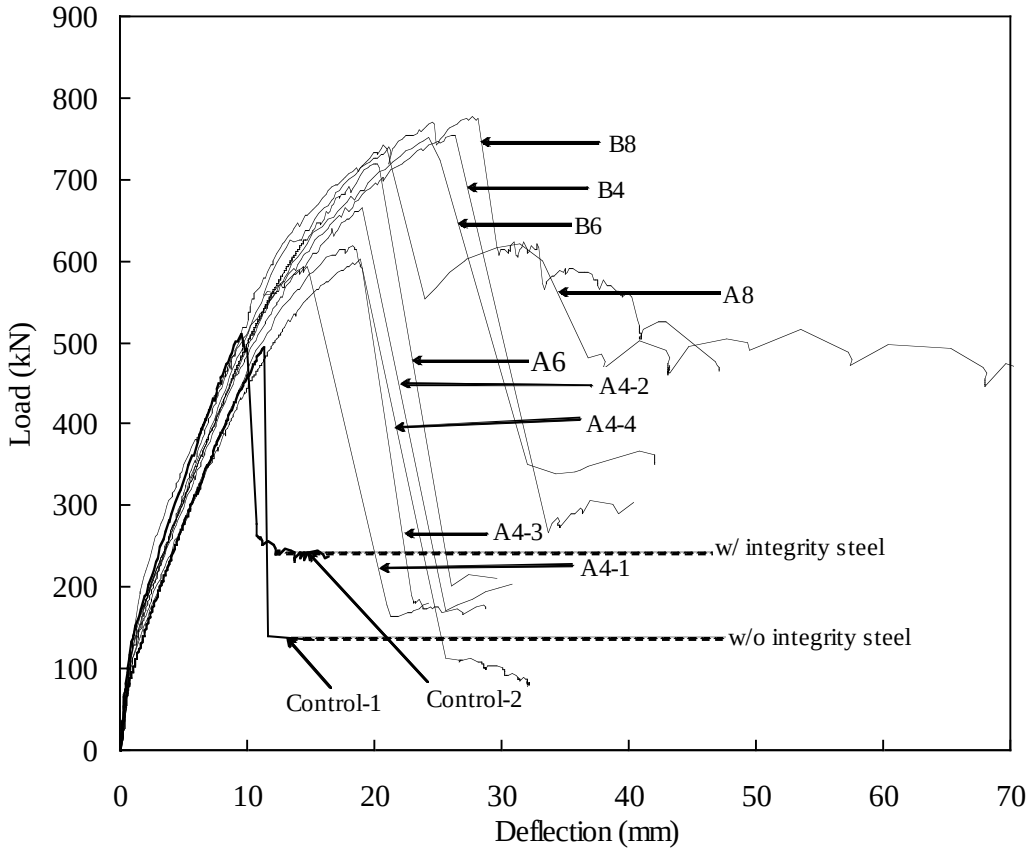

Fig. 4 Load-deflection behaviour of concentric tests (Binici, 2003)

Strength increases in specimens with respect to Control-1 versus the ductility of the specimens are plotted in Figure 6. Increased ductility is observed with increased strength. The dashed trend line shows the relationship between strength and ductility. As the flexural capacities of the specimens are reached, the relationship becomes asymptotic to some multiple of flexure capacity divided by the yield line, meaning further increase in ductility without significant increase in strength and change of failure mode from punching shear to flexure.

Specimen A4-3 failed inside the shear reinforced zone due to rupture of CFRP strips at the corners. The measured maximum vertical CFRP strain ((~0.0096)) was about 80% of the ultimate strain capacity of CFRP strips from uniaxial tension tests. This high strain level in the vertical direction is an indication of possibly higher strains attained at the corners of CFRP strips which are vulnerable to rupture. In addition to that, based on the assumption of similar strains in concrete and CFRP, it is possible to say that concrete contribution inside the shear reinforced zone has already vanished under strains almost 2.5 times that of the crushing strain of concrete (~0.0035). This shows that shear reinforced zone can not successfully sustain large strains without loss of concrete contribution and CFRP rupture. The vertical CFRP strain level obtained in specimen A4-2 (~0.004) can be accepted as the maximum attainable strain without causing any significant damage in the shear reinforced zone.

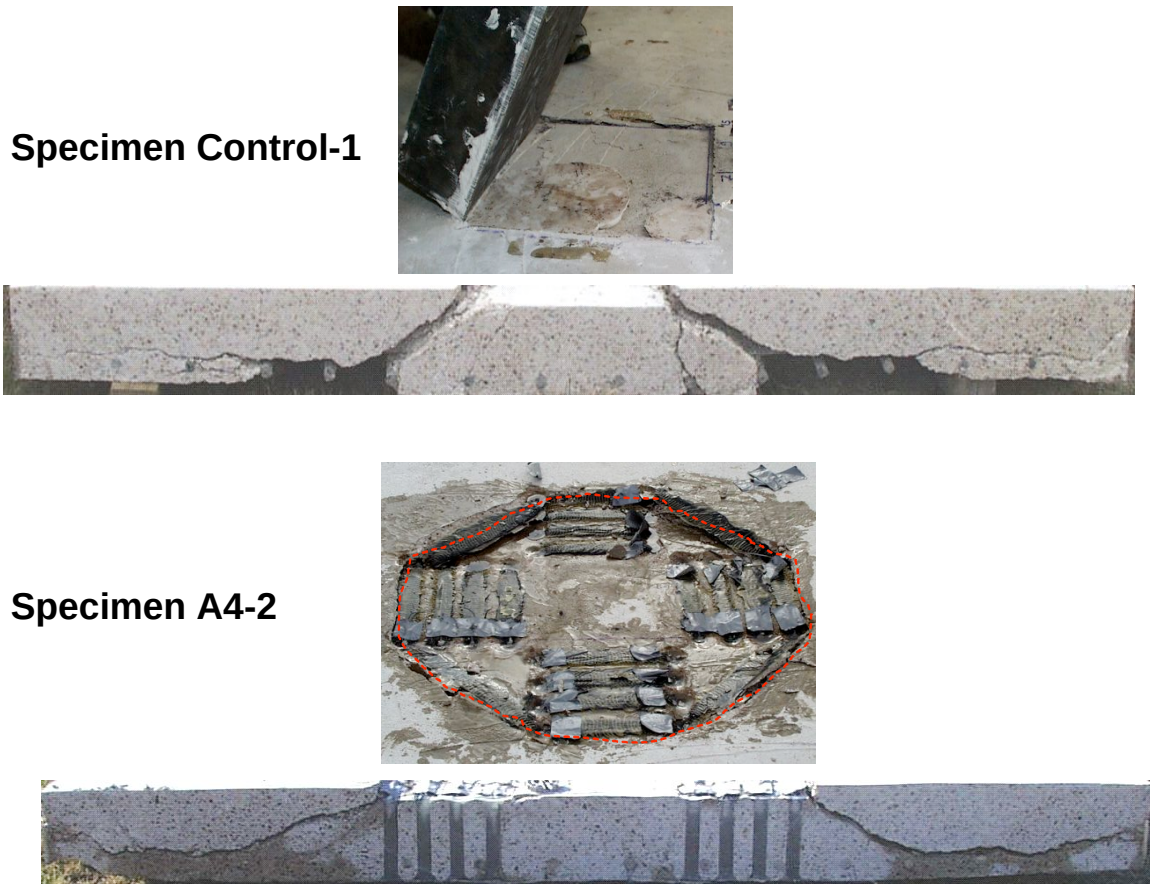

Fig. 5 Failure surfaces and inclined cracks (Binici, 2003)

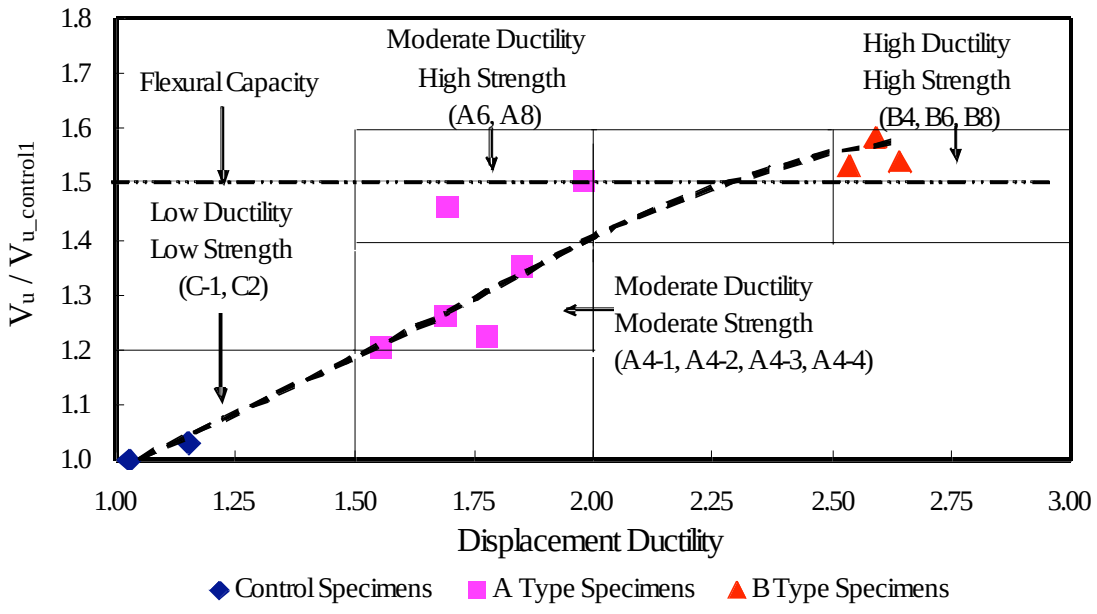

Fig. 6 Performance of FRP Retrofit (Binici, 2003)

2.4 Seismic upgrade

Flat plate structures are also commonly used in moderate and low seismic zones as lateral force resisting systems whereas they are coupled with shear walls or moment resisting frames

in high seismic zones. The ductility of these systems is generally limited by the deformation capacity of the slab-column connections. Punching shear failure is the governing failure mode in the presence of pronounced gravity and lateral load combinations. The ductility of the slab-column connections can be enhanced with the use of shear reinforcement (Stirrups, stud rails etc.) for new construction and the risk of punching shear failure can be highly reduced when the connection is designed and detailed properly. There have been a number of other research efforts to understand lateral load behaviour of flat plate systems under constant gravity shear. Experiments were conducted on isolated slab-column connections and on flat plate sub. The results of the experiments provided information on the lateral stiffness, strength, ductility, cyclic behaviour of the slab-column connections of reinforced concrete flat plate systems. It was found that gravity shear is the most important factor affecting the ductility of the connections under cyclic load reversals. One of the most important results from these studies is shown in Figure 7 where the gravity shear ratio, V_g/V_o (ratio of shear due to gravity loads (V_g) to concentric punching shear capacity (V_o) is plotted against the maximum interstorey drift ratio attained by the slab column connection. It can be observed that there is a drastic decrease in the available deformation capacity with increasing gravity shear ratio. Based on this result, a consensus was reached to limit the gravity shear to 0.4 to obtain sufficient ductility and lateral deformation capacity in the individual slab-column connections.

The FRP retrofit scheme discussed in the previous section can also enhance the lateral deformation capacity of the slab-column connections. A typical interior connection having a gravity load ratio of about 0.4 is strengthened using two patterns as shown in Figure 8. The connections are then subjected to reversed cyclic displacement excursions to simulate earthquake induced demands.

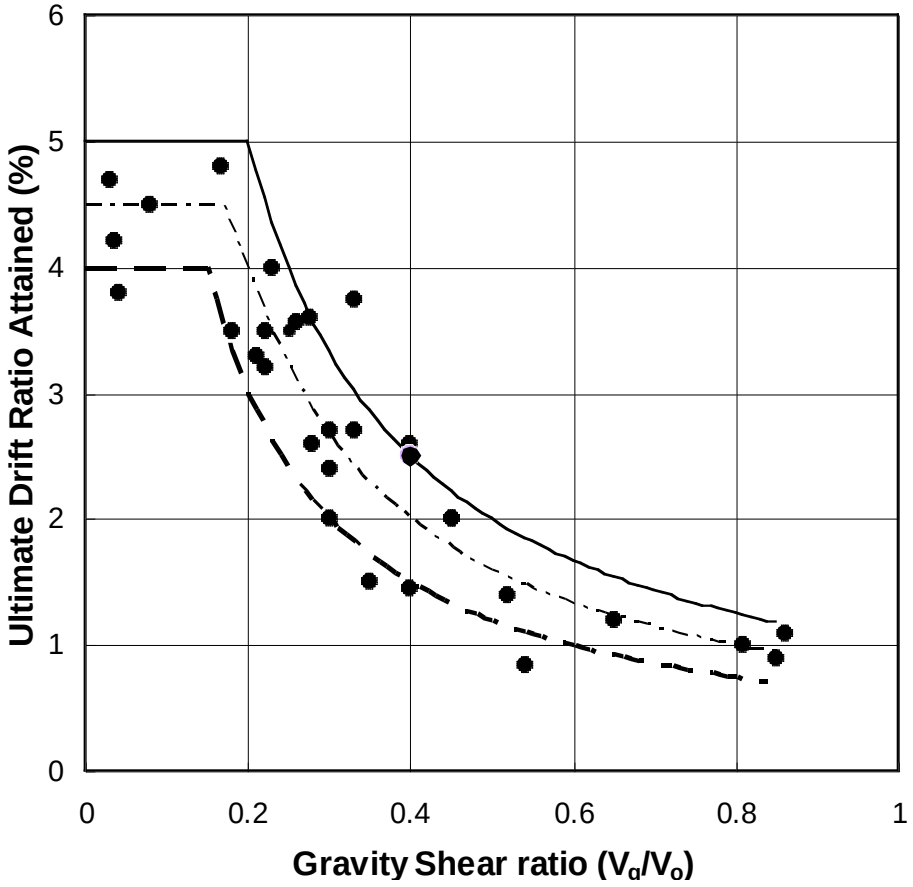

Fig. 7 Effect of gravity shear ratio on ultimate drift capacity (Dots are experimental points, lines are bounds for the experiments)

The experimental results from reversed cyclic slab-column connection tests [Stark et. al.

2005] are briefly summarized in this section. All the specimens were 2400 mm x 2400 mm x 115 mm with a column size of 300 mm x 300 mm. Lateral load versus drift ratio and moment-rotation results for test specimens C-02 (without any upgrades), A4-S and B4-S are shown in Figures 9 to 11. Control specimen, C-02 exhibited punching shear failures that resulted in a significant drop in lateral load. At a drift ratio of about 2%, cracks began to open and considerable pinching occurred in the lateral load-deformation plots. Concrete began to spall around each specimen's column base plate, on the bottom slab face, prior to punching shear failure. When upgraded with CFRP shear reinforcement, specimens A4-S and B4-S (Figures 10 and 11) had significant increases in ductility and energy dissipation capacities when compared with control specimens. The upgraded test specimens displayed similar behaviour to the control specimens until 2.5% inter-storey drift, but specimens A4-S and B4-S did not experience a punching shear failure while subjected to combined gravity and lateral loads. Both upgraded specimens sustained substantial reinforcing bar yielding. Flexural cracks on the top slab face of specimens A4-S and B4-S opened wider as drift excursions increased. Increased crack widths augmented pinching in the load-displacement hysteresis loops at larger drift-ratios.

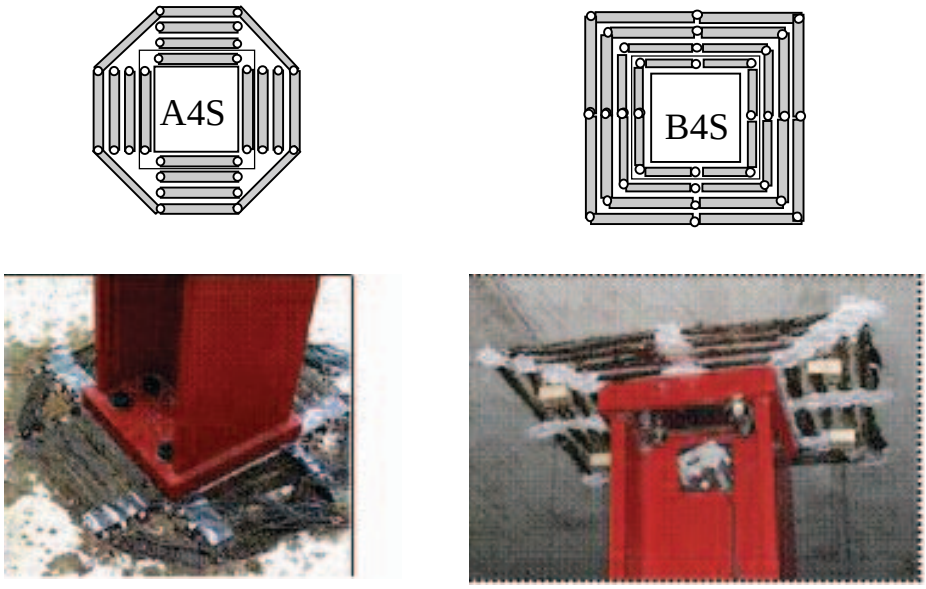

Fig. 8 Connection upgrade configurations (Stark 2003)

The poor inelastic behaviour displayed by specimen C-02 was eliminated in upgraded specimens A4-S and B4-S. After achieving a maximum lateral load of 41.7 kN, specimen A4-S retained 80% of the maximum resisted lateral load up to an inter-storey drift of 8.3% in one direction. Following the initial strength degradation, the lateral load carrying capacity increased after an applied drift of 7%, due to the onset of strain hardening in the reinforcing steel bars. The maximum lateral load resisted by specimen B4-S was 48.4 kN. After reaching the peak lateral load peak, specimen B4-S demonstrated a strength decay of 12.5% until CFRP stirrup rupture at the outermost shear reinforcement perimeter occurred at 8.3% inter-storey drift. This resulted in a 41% decrease in lateral load resistance on the completion of the applied drift-cycle. For specimen C-02, punching shear failure initiated at 0.023 radians and completed at 0.017 radians in the next cycle, which corresponded to applied moments of 38.6 kN-m and 24 kN-m, respectively. Upgraded specimens A4-S and B4-S attained greater rotational capacities without failing in two-way shear because of the additional CFRP shear reinforcement. The maximum recorded connection rotation for specimen A4-S was 0.06 radians. Specimen B4-S had a maximum connection rotation of 0.067 radians before a CFRP strand rupture occurred. The increased joint rotational capacity permitted the longitudinal

reinforcing steel to deform well into the inelastic range, which allowed further energy dissipation.

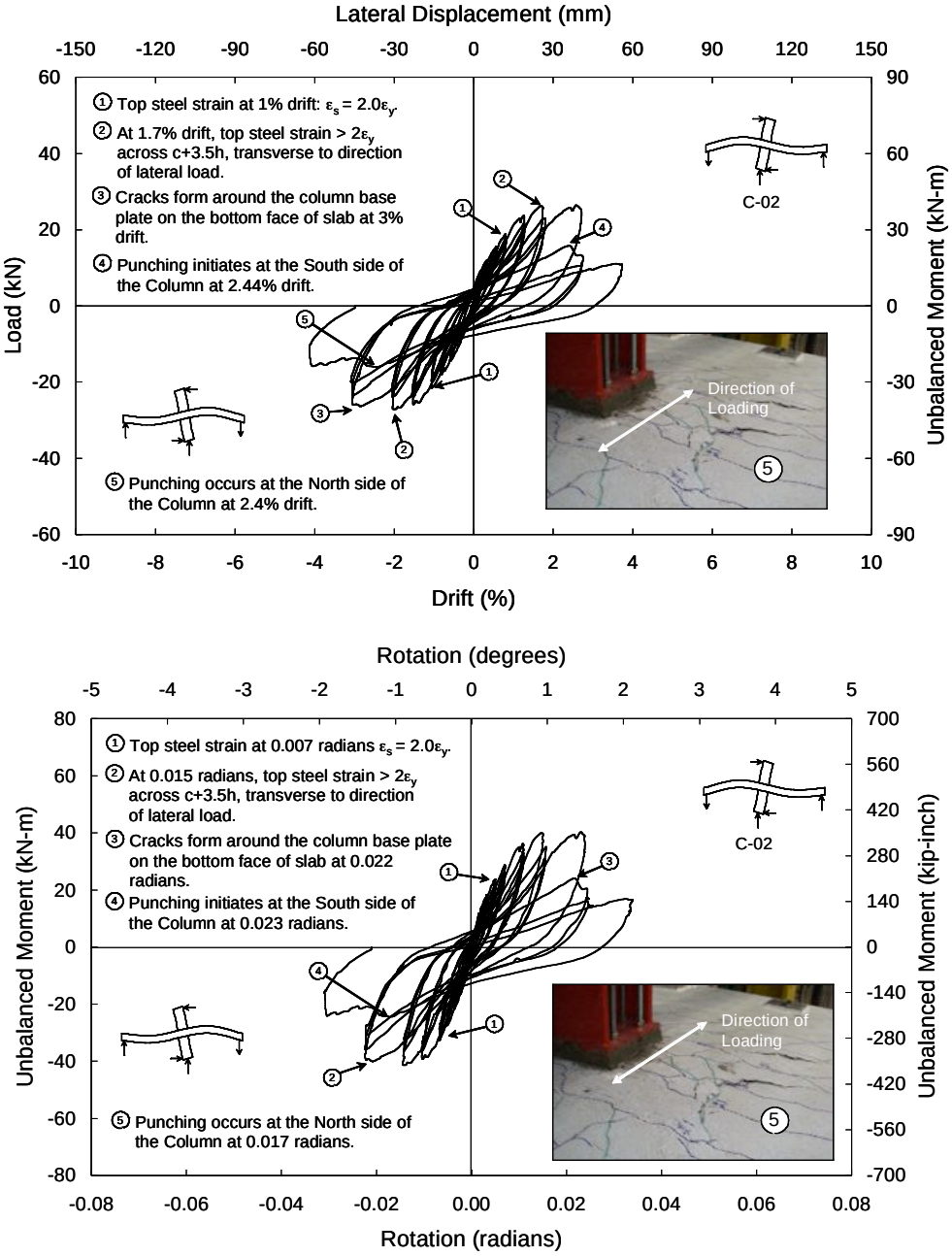

Fig. 9 Load-deformation behaviour of specimen C-02 (Stark 2003)

2.5 Retrofit design

Punching shear strength, v_c is calculated as the smallest of the following three expressions for an upgraded interior slab-column connections [ACI 318-02, 2002]:

$$v_c = \min\{\frac{1}{3}\sqrt{f_c}\ ;\quad (\frac{\alpha_s}{(b_o/d)}+\frac{1}{2})\frac{1}{3}\sqrt{f_c}\ ;\quad (\frac{1}{2}+\frac{1}{B})\frac{1}{3}\sqrt{f_c}\ \} \qquad (1)$$

where f_c is the compressive strength of concrete in MPa, d is the average effective depth in mm, α_s is 10 for interior connections, and B is the aspect ratio of the column section ($B \geq 1.0$), b_o is the critical perimeter located d/2 away from the column face or from the outermost shear

reinforcement depending on the existence of shear reinforcement (Figure 12). The ultimate load carrying capacity outside the shear reinforced zone, V_u^o then is calculated by:

$$V_u^o = v_c b_o d \tag{2}$$

When CFRPs are used as externally installed stirrups, the shear capacity inside the shear reinforced zone, V_u^i is computed by:

$$V_u^i = V_c + V_{FRP} = \frac{1}{4}\sqrt{f_c}bd + \varepsilon_{eff}\, E_{FRP} A_{FRP} \frac{d}{s} \le V_{cmax} \tag{3}$$

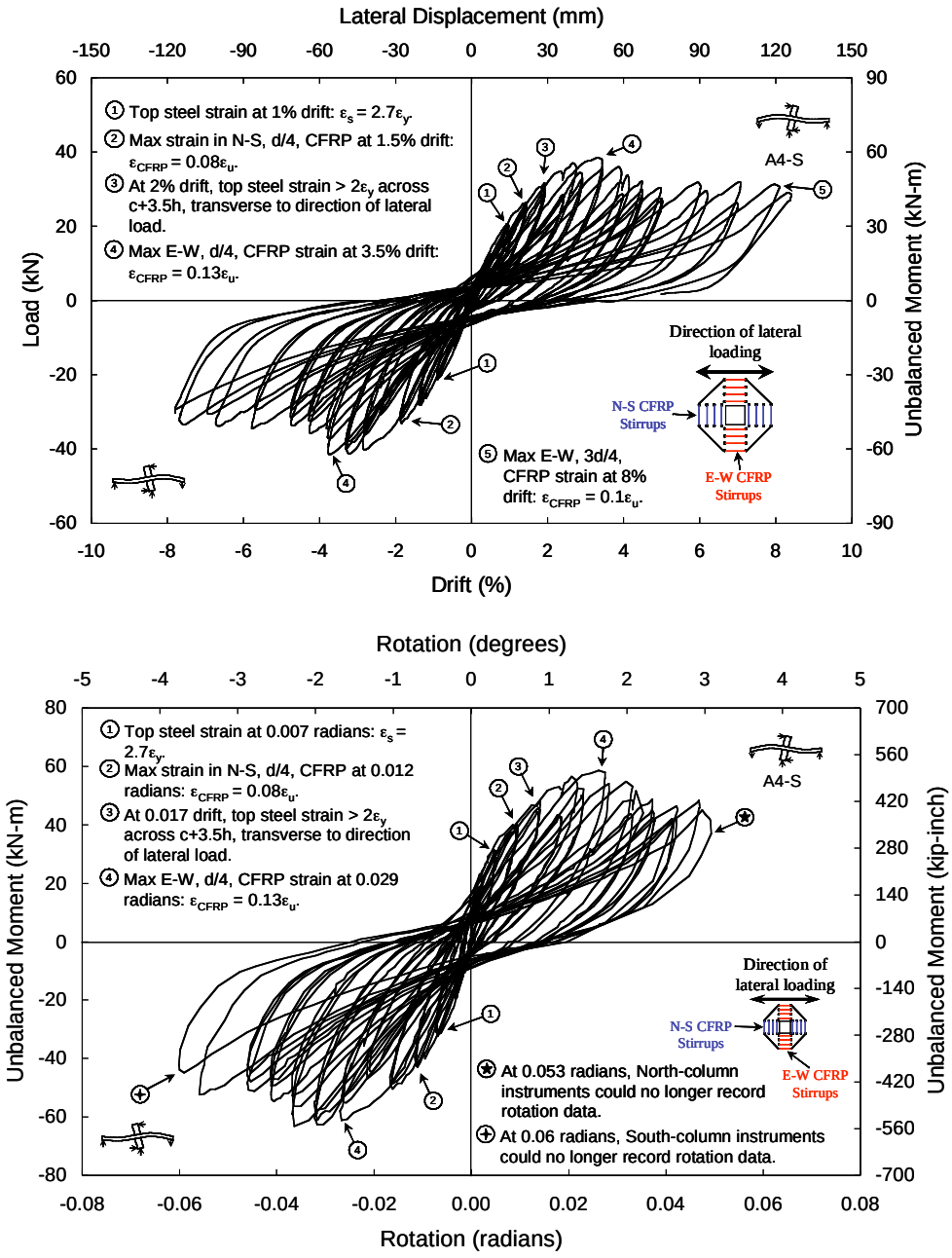

Fig. 10 Load-deformation behaviour of specimen A4-S (Stark 2003)

V_c is the concrete contribution inside the shear reinforced zone, b is the critical perimeter located at a distance of $d/2$ from the column face. V_{FRP} is the force that needs to be carried by

FRP, E_{FRP} is the Modulus of Elasticity of FRP, A_{FRP} is the cross-sectional area of FRP per perimeter. V_{cmax} is the maximum allowable capacity associated with concrete crushing at the connection and taken as two times the strength computed using Equation 1. In upgraded reinforced slab- column connections, the punching shear capacity, V_n, is the smallest of the capacity inside the shear reinforced zone, V_u^i, and outside the shear reinforced zone, V_u^o. Number of CFRP perimeters is selected such that punching shear strength outside the FRP reinforced zone is sufficient for the imposed shear demand. Following that, FRP amount is designed using Eq. (3) such that failure of FRP reinforced zone is avoided prior to failure outside the shear reinforced zone.

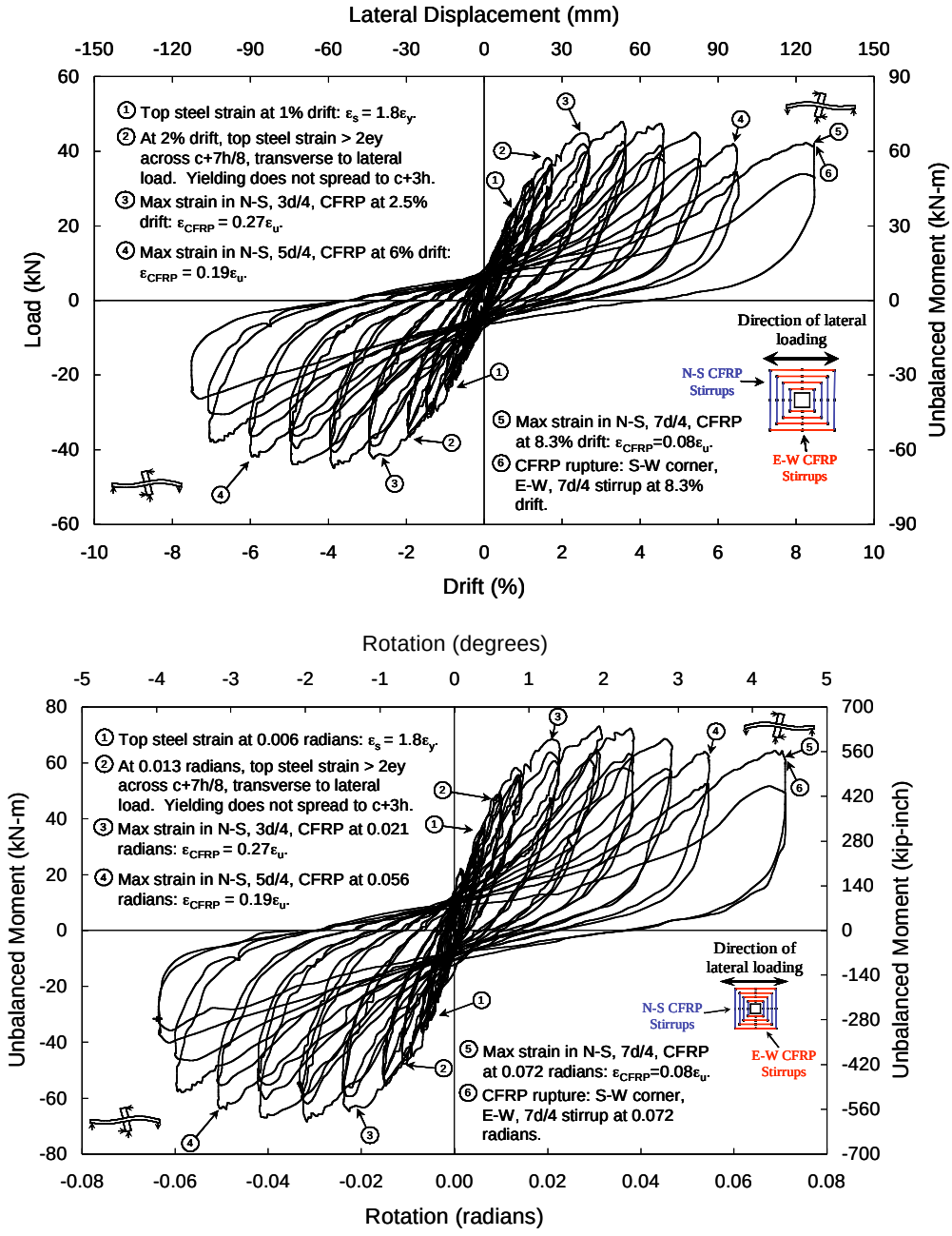

Fig. 11 Load-deformation behaviour of specimen B4-S (Stark 2003)

In the case of combined shear and unbalanced moment, a similar design methodology is followed. First the number of CFRP perimeters are selected such that punching shear strength

outside the shear reinforced is sufficient to carry the shear and unbalanced moment demand.

This is accomplished by satisfying the following equation:

$$v_u^o = \frac{V_u}{b_o d} + \frac{\gamma_v M_u}{(J^o / c)} \le v_c \tag{4}$$

where V_u is the gravity shear, M_u is the unbalanced moments acting on the connection, b_o is the critical perimeter located d/2 away from the outermost shear reinforcement, and c is the distance from the column centerline to the critical perimeter. For rectangular strengthening patterns (d in Figure 12):

$$J^o = \frac{d(b_1)^3}{6} + \frac{(b_2)d^3}{6} + \frac{d(b_2)(b_1)^2}{2} \tag{5}$$

where b_1 and b_2 are the side lengths of the critical perimeter parallel and perpendicular to the direction of the moment transfer.

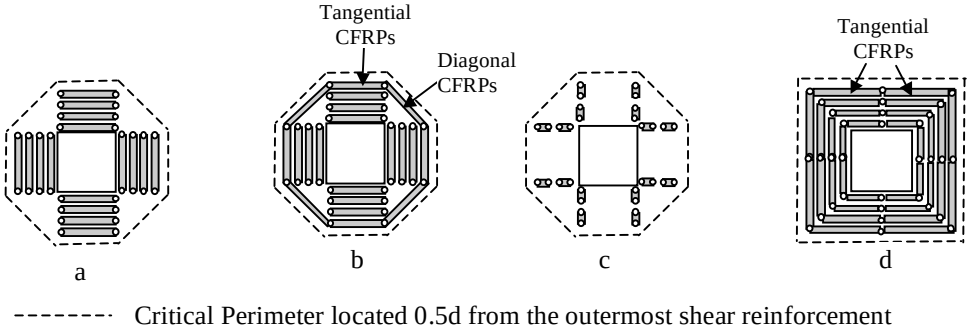

Fig. 12 Location of critical perimeters outside the shear reinforced zone (Binici, 2003)

It is assumed that part of the unbalanced moment, $\gamma_f M_u$ is resisted by flexure within the strip with width $c+3h$ along the direction of moment transfer, where h is the thickness of the slab and $\gamma_v M_u$ by eccentricity of shear. This assumption requires that:

$$\gamma_v + \gamma_f = 1 \tag{6}$$

The γ_v factor for computing the fraction of the unbalanced moment transferred by eccentricity of shear is given by:

$$\gamma_v = 1 - \frac{1}{2/3 + \sqrt{c_x / c_y}} \tag{7}$$

where c_x, and c_y are the column side length parallel and perpendicular to the direction of moment transfer, respectively.

Once the capacity outside the shear reinforced zone is evaluated, the amount of CFRP that ensures punching outside the shear reinforced zone can be found using the following expression:

$$v_u = \frac{V_u}{bd} + \frac{\gamma_v M_u}{(J/c)} = v_c + v_{FRP} = \frac{1}{4}\sqrt{f_c} + \frac{0.004 E_{FRP} A_{FRP}}{bs} \tag{8}$$

J and b in Eq. (8) are computed for the critical perimeter located d/2 away from the column face. The concrete contribution, v_c is similar to that given in Eq. (1).

To summarize, the following procedure (the flowchart in given in Figure 13) can be used to clarify the design steps for upgrade of slab-column connections using externally installed CFRPs:

1) Determine geometric and material properties of the connection. Evaluate the target shear and unbalanced moment demand.
2) Confirm that required punching shear strength is within the acceptable range and maximum permissible shear stress is not exceeded.
3) Assume number of FRP perimeters and strengthening pattern.
4) Calculate the effective shear stress (Equation 4) by computing *J* from Equ. 5 for a critical perimeter located *d*/2 from the outermost shear reinforcement.
5) Compare v_u with the concrete strength, v_c outside the shear reinforced zone. If $v_u < v_c$, proceed to step 6, otherwise go to step 3.
6) Compute required amount of FRP reinforcement per leg from Eq. (8).
7) Detail the FRP shear reinforcement. Use closed loops for FRP anchorage overlapped at the slab surfaces. For pattern A, use diagonal stirrups anchored in alternative directions to eliminate punching failure inside the shear reinforced zone. For pattern B use FRP stirrups anchored on the slab surface with CFRP overlaps parallel to the column faces. The cross sectional area of diagonal stirrups in pattern A should not be less than half the cross-sectional area of primary CFRP stirrups used in the last CFRP perimeter parallel to the column side. CFRP configurations should be similar to b and d shown in Figure 12.

Based on the observations from cyclic tests, the plastic rotation capacity of an FRP retrofitted connection can be taken as 0.05 radians as long as a capacity-based design is followed for the FRP design to eliminate punching shear failures. To achieve this, first, negative and positive moment capacities (M_u^+, M_u^-) based on an effective width of column width plus three times slab thickness is computed assuming that yield strength of steel reinforcement is 25% than its nominal value. Then, the unbalanced moment transferred to the connection upon reaching flexural capacity of the effective width is computed using Eq. (9).

$$M_{un} = \frac{M_u^+ + M_u^-}{\gamma_f} \tag{9}$$

The number of CFRP stirrup perimeters is selected to ensure that punching shear failure of the section outside the shear reinforced zone is prevented prior to reaching flexural capacity of the slab. Accordingly, Eq. (4) needs to hold for the selected configuration such that average shear stress at a section located d/2 away from the outermost shear reinforcement (Figure 12) is smaller than the concrete shear strength. Once punching shear capacity of the critical perimeter outside the shear reinforced zone is sufficient to allow flexural capacity to be achieved, amount of CFRP required per perimeter is determined assuming a concrete contribution inside the shear reinforced zone and area of CFRP stirrup leg per perimeter is found from Eq (8).

3 Flexural Strengthening

Fibre reinforced polymers can easily be utilized to strengthen existing reinforced concrete slabs and slabs on grade to enhance flexural capacity, to avoid excessive slab deformations and to reduce stress concentrations around regions of cutouts. The idea of bonding FRP sheets on the tension side of the slab is similar to the well known method of flexural strengthening reinforced concrete beams in flexure by bonding FRP sheets. FRPs can easily be installed from the tension side of the slab with little occupancy disturbance while resulting in minimal slab thickness increases. A brief description of an experimental program on flexural strengthening of slabs is described in what follows.

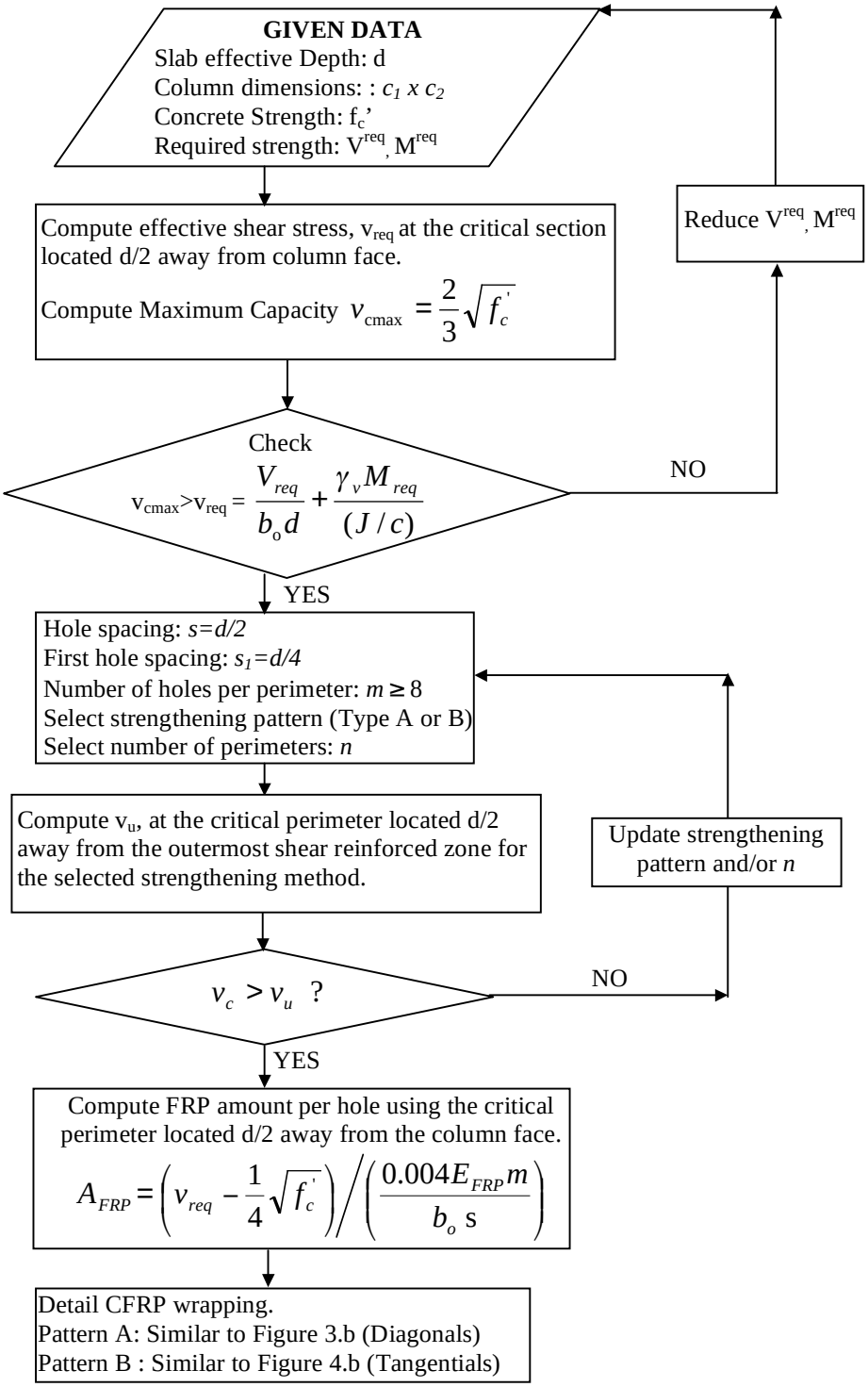

Fig. 13 Design for shear and unbalanced moment transfer (Binici, 2003)

A total of fifteen full-scale tests were conducted under out-of-plane flexural loading conditions [Mosalam 2002]. The results of these tests are applicable to reinforced concrete slabs, unreinforced slabs-on-grade (under expansive soil and uplift pressures), as well as reinforced and unreinforced concrete walls subjected to static out-of-plane loads.

Five control (three unreinforced and two steel reinforced) full-scale slab specimens (without composites) were tested initially. For repair applications, the maximum load was determined by the development of repairable cracks the size of 1.5mm for unreinforced specimens and the yielding of the steel for steel reinforced control specimens. For the repair evaluation, five pre-cracked full-scale specimens were tested up to ultimate failure. Another

"undamaged" five slabs were tested up to ultimate failure. The purpose of these tests was to evaluate the ultimate strength, and to identify mode of failures of both repaired and retrofitted slabs specimens under gravity loading conditions. Two extremes were considered for the reinforcements; for example, the first set of tests was conducted on slabs with non-structural steel wire mesh simulating the extreme condition of corroded steel ($\rho \sim 0$), where composite is the primary reinforcing system. For specimen with steel reinforcements, a typical reinforcement ratio was used (ρ =0.3%) according to ACI-318 recommendations. All the specimens had plan dimensions of 2650 mm x 2650 mm with a slab thickness of about 76 mm. Concrete strength was 28MPa whereas the reinforcing steel was Grade 60 with a yield strength of about 450MPa. Three FRP composite strengthening systems evaluated in this program, namely; carbon/epoxy wet lay-up system, E-glass/epoxy wet lay-up system, carbon/epoxy prefabricated strips. Prior to the application of composites, the top surfaces of concrete were grinded, and cleaned of dirt, dust, and other foreign matters. For the pre-cracked specimens, the cracks and surface adjacent to cracks or other areas of application were cleaned and low viscosity epoxy, was gravity-fed to fill the surface and penetrate through the smaller cracks of the pre-cracked specimens. After the epoxy treatment, FRPs cut to predetermined sizes were impregnated into epoxy and bonded on the tension sides of the slabs. Typical application of the wet lay-up procedure is shown in Figure 14. All specimens were tested in a water-bag structural frame in an inverted position to observe cracking and FRP delamination. The hydraulic pressure loading was applied uniformly to each specimen until ultimate failure occurred. The applied pressure was controlled by a data acquisition computer program connected directly to the loading frame. The load followed a quasi-static ramp-loading regime and a loading frequency of 3.45 kPa/minute was used.

a) Wet-layup application b) Composite layup application

Fig. 14 Flexural strengthening of slabs (Mosalam, 2002)

Load deformation responses of precracked unreinforced specimen and repaired specimen using FRP laminates is shown in Figure 15. Thus, the use of FRP laminates succeeded not only in restoring the strength of the pre-cracked slab, but also in upgrading its strength capacity to 6.4 times as compared to the control specimens. In addition, the repaired specimens were able to deflect more than 41mm before failure, thus giving an ample visual warning before ultimate collapse. Crack pattern at ultimate failure of the FRP repaired specimen is shown in Figure 16. It can be observed that a well distributed cracking resembling the yield lines spanning along the diagonals were observed. The observations of crack propagation revealed that failure occurred progressively as a result of crack extension followed by shear failure and FRP debonding.

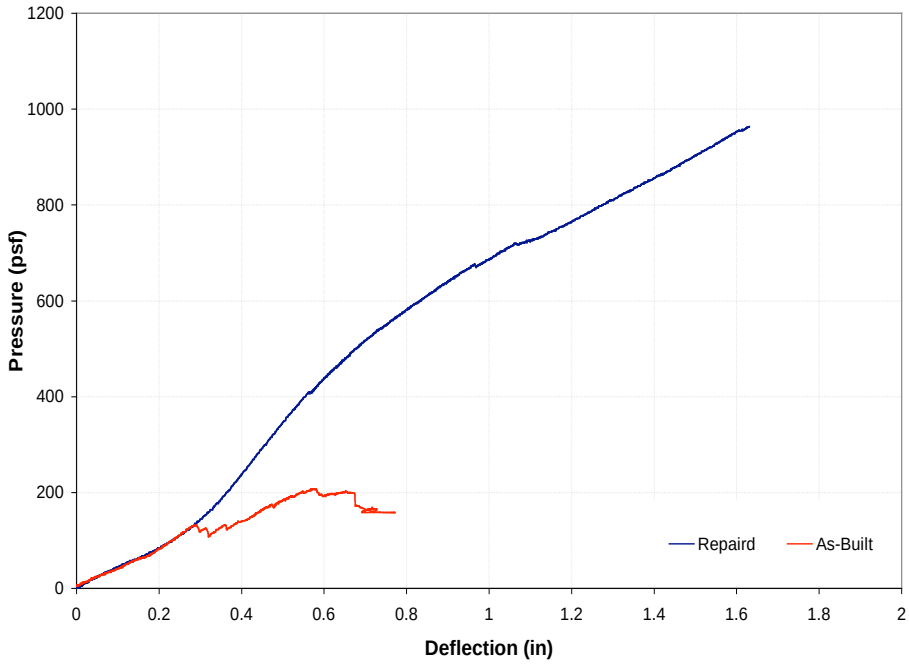

Fig. 15 Load-deformation behaviour of as built and repaired specimens (ρ = 0 %) (Mosalam, 2002)

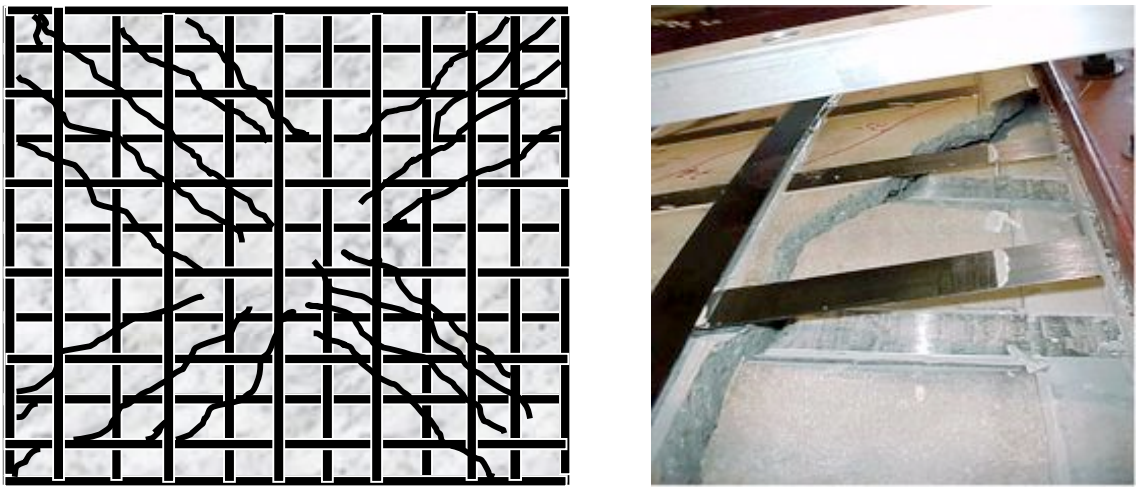

Fig. 16 Observed cracking and failure modes of repaired specimens (ρ = 0 %) (Mosalam, 2002)

Figure 17 shows the load-deflection curves for GFRP retrofitted as built specimens with a reinforcement ratio of about 0.3%. As shown in this figure, the behaviour was linear up to a load level of 330 psf (15.84 kPa) after which non-linearity was observed up to the ultimate load. The ultimate capacity of this specimen was 1,187.6 psf (57 kPa) with maximum mid-span deflection of 2.772" (70.4 mm). As compared to the as-built slab specimen, the ultimate capacity of the strengthened specimen is 2.86 times the capacity of the as-built reinforced specimen (414.72 psf (20 kPa) vs. 1,187.6 psf (57 kPa)). The first major local failure was a large shear crack that was developed near one edge of the slab. The laminate in the neighborhood of this crack locally debonded in a cohesive manner (Figure 18). The ultimate failure mode was a combination of cohesive debonding of the edge laminates followed by a sudden shear failure of the unstrengthened concrete near the support. The progression of local failure is shown in Figure 18. the maximum-recorded composite tensile strain was about 0.6%. The strain level is much less of the ultimate strain of the GFRP obtained from the coupon tests (about 30% of the ultimate strain of 2.1%).

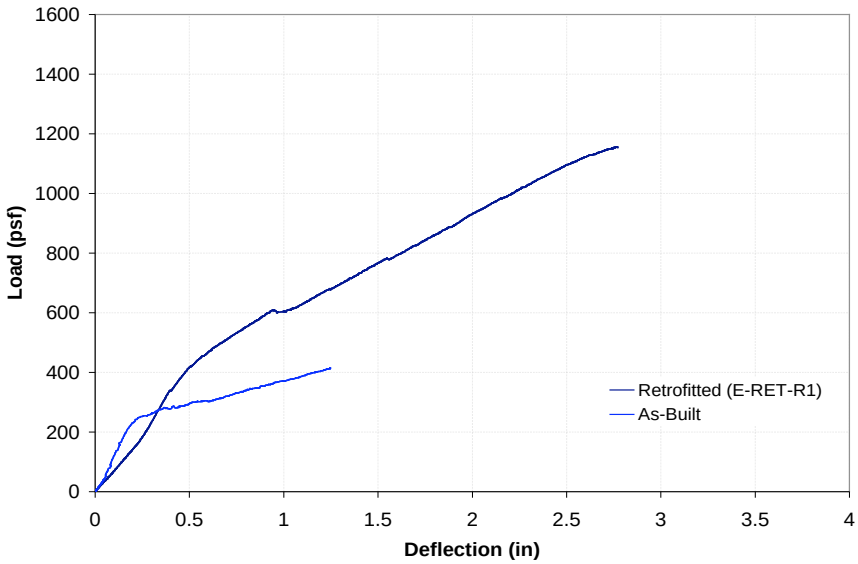

Fig. 17 Load-deformation behaviour of as built and repaired specimens (ρ = 0.3 %) (Mosalam, 2002)

Fig. 18 Observed cracking and failure modes of repaired specimens (ρ = 0.3 %) (Mosalam, 2002)

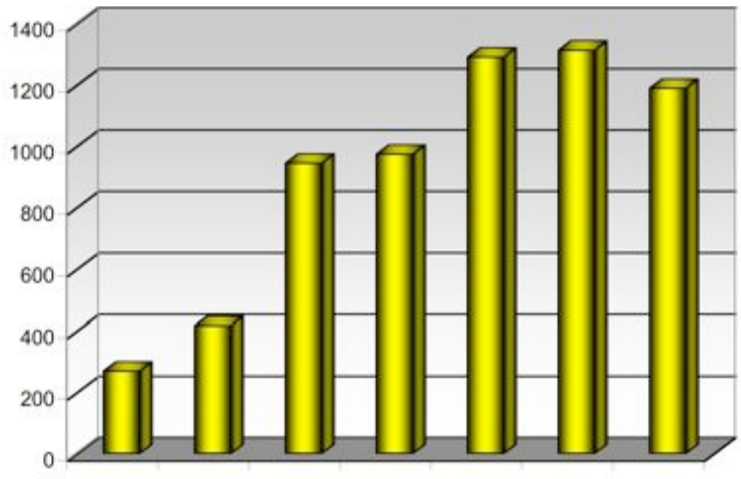

Fig. 19 Strength comparison of various repaired/retrofitted slabs (Mosalam, 2002)

Strength comparisons between various specimens are shown in Figure 19. It can be observed that significant strength enhancements can be obtained through the use of the wet or composite lay-ups. From the observed failure modes it is important to say that FRP debonding from an inclined shear crack determines the ultimate load carrying capacity.

Retrofit design for flexural capacity enhancement can be performed using classical reinforced concrete flexure theory. Accordingly, sectional analysis of a unit width slab region can be conducted as shown in Figure 20. In this case, section analysis is used based on normal assumptions of strain compatibility (linear strain distribution along the depth of the flexural member) between concrete, internal steel reinforcement and external FRP composite laminates. The enhancement of the equivalent axial tensile force (T_{FRP}) (Figure 20) provided by the composite laminate of effective thickness t_f, oriented at angle θ to the direction of the flexural member axis is limited by the following expression:

$$T_{frp} = t_f \; f_{eff} \cos^2 \theta \, / unit \; width \tag{10}$$

where:

$$f_{eff} = E_f \; \varepsilon_{eff} \leq 0.75 \varepsilon_{fu} \tag{11}$$

In Eq. (11) ε_{eff} is similar to the effective strain values suggested for beam flexural strengthening using FRPs. Available experimental results suggest using a maximum value of about 0.6% and 0.4 % for ε_{eff} to estimate effective ultimate strength of FRPs bonded to slabs with no visible cracks and with visible cracking, respectively. The ultimate moment capacity per unit width of the slab is computed by:

$$M_n = [T_s (d_s - \frac{a}{2}) + T_{frp} (h - \frac{a}{2})] \tag{12}$$

where T_s is the force in the steel reinforcement, d_s is the effective depth of the steel reinforcement, h is the effective depth of the FRP, and a is the height of the equivalent rectangular stress block for concrete in compression.

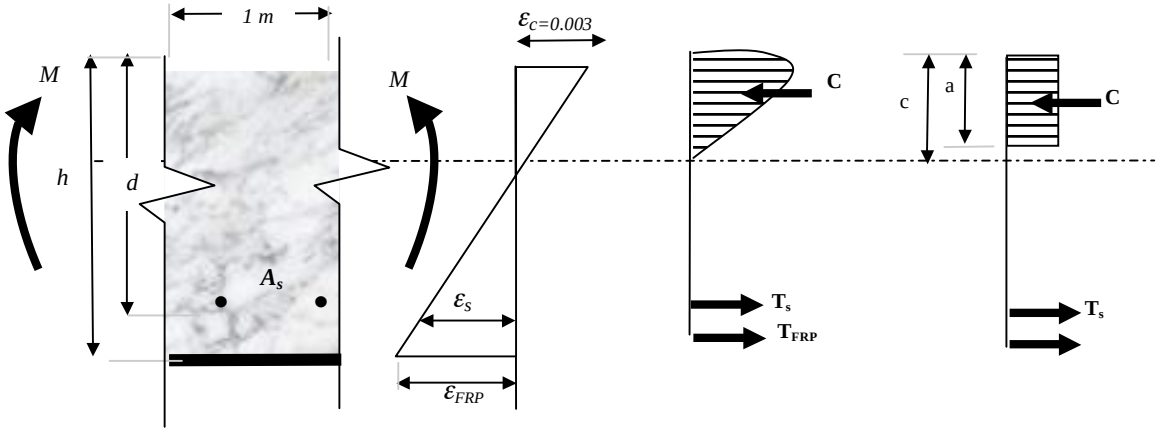

Fig. 20 Sectional analysis of a unit width slab

References

ACI Committee 318. (2002) Building Code Requirements for Structural Concrete (ACI 318-02). *American Concrete Institute*, Farmington Hills, Michigan.

Binici B. (2003) Punching Shear Strengthening of Reinforced Concrete Slabs Using Fibre Reinforced Polymers. *Dissertation Submitted to the Faculty of Engineering for partial fulfilment of the requirements for the Doctoral Degree*, The University of Texas at Austin, 279 p.

Binici B. and Bayrak,O. (2003) Punching Shear Strengthening of Reinforced Concrete Flat Plates Using Carbon Fibre Reinforced Polymers. American Society of Civil Engineers, *Journal of Structural Engineering*, Vol. 129. No.9, 1173-1182.

Binici B. and Bayrak, O. (2005) Use of Fibre Reinforced Polymers in Slab-Column Connection Upgrades. *American Concrete Institute, Structural Journal*, Vol. 102, No.1, 93-102.

Binici B. and Bayrak, O. (2005) Upgrading of Slab-Column Connections Using Fibre Reinforced Polymers. *Engineering Structures*, Vol. 27, No.1, pp. 97-107.

Mosalam A. (2002) Structural Evaluation of SCCI-FRP Composite Systems (TufLam) for Flexure Repair and Upgrade of Reinforced Concrete Floor Slabs, Slabs-on-Grade, and Out-of-Plane RC Walls. California State University, Fullerton, Test Report No. SRRS-SCCI, 79 p.

Stark, A. (2003) Seismic Upgrade of Flat-Plate Slab-Column Connections using Carbon Fiber Reinforced Polymer Stirrups. *Dissertation Submitted to the Faculty of Engineering for partial fulfilment of the requirements for M.Sc Degree*, The University of Texas at Austin, 233 p.

Stark, A., Binici B., and Bayrak, O. (2005) Seismic Upgrade of Reinforced Concrete Slab-Column Connections Using Carbon Fibre-Reinforced Polymers. *American Concrete Institute, Structural Journal*, Vol. 102, No.2, 324-333.

Overview of seismic strengthening strategies for concrete structures

Zekai Celep
Istanbul Technical University, Turkey

1. Introduction

Strengthening of a structural system can be defined as a process to upgrade the system to a safety level which is acceptable for public safety. Seismic strengthening is a difficult, complex and expensive process. The process consists of several steps. It starts with examination and evaluation of the building in question. The second step is the development of alternative strengthening options and the examination of each alternative in view of its technical and financial feasibility, in order to find the optimum solution. The final step is the design of the added elements and the intervention to existing structural elements, and the preparation of the application drawings.

The present Turkish seismic code was prepared in 1998. Although it states in its introduction that "strengthening of the existing structures should conform to the code as well", it is written specifically for the seismic design of new concrete structures. It is intended to regulate design and construction. However, after the Marmara Earthquake of 1999 it became clear that application of the code requirements to strengthening problems gives rise to various difficulties which can not be overcome easily. Numerous strengthening projects have been carried out by extending or even sometimes disregarding some of the requirements of the code and by using common engineering judgment to make the strengthening process technically and financially feasible. However, it is felt that a new chapter should be added to the seismic code in order to regulate and improve strengthening design and its application, as well as to prevent non-engineered applications as much as possible. On the other hand, it is hoped that such a new chapter will provide nationally recognized minimum requirements for making existing buildings more resistant to earthquakes.

A draft of the seismic code has recently been published and presented to the engineering community with the above mentioned objectives. The present contribution is prepared in the light of the 2005 draft of the seismic code. It gives only limited information in this respect. Strengthening of the concrete structural system as well as its elements is discussed and a few strengthening examples are presented. Detailed information can be found in the Draft itself (Turkish Ministry of Public Works and Settlement, 2005).

2. Evaluation of existing and strengthened concrete structures

General evaluation principles for existing buildings are intended to check whether the building has an acceptable level of seismic safety as defined in the Code. On the other hand, the same evaluation principles can be applied for strengthened buildings, to check whether the level of performance obtained is acceptable. The evaluation principles are based on the seismic performance of buildings. Building performance can be described quantitatively in terms safety afforded by building occupants during and after the seismic event considered. Performance characteristics are directly related to the extent of damage that would be sustained by the building.

2.1. General requirements

In the evaluation of existing buildings, the as-built information of the structure is of prime importance. Data related to the structural system and its elements should be carefully obtained. Depending on the information related to the available data, a *knowledge factor* is introduced. This factor is used in the evaluation of the capacity of the cross sections and of structural elements to account for possible uncertainties (Table 1). The capacity of the sections and of elements is evaluated by using the capacity strength of concrete and steel. The capacity strength of steel is the characteristic yield stress. However, the capacity strength of concrete is evaluated by using the concrete core test results, as well as the knowledge factor of the structure.

When no construction documents of the building are available, or when they are missing, as-built documents should be prepared. In that case the level of knowledge is assumed to be *limited*. When all drawings are available and when they conform to the existing condition completely, the level of knowledge is *comprehensive*. In the case in-between, the level of knowledge is called *medium*.

Level of knowledge	**Knowledge factor**
Limited	0.75
Medium	0.90
Comprehensive	1.00

Table 1: Knowledge factor

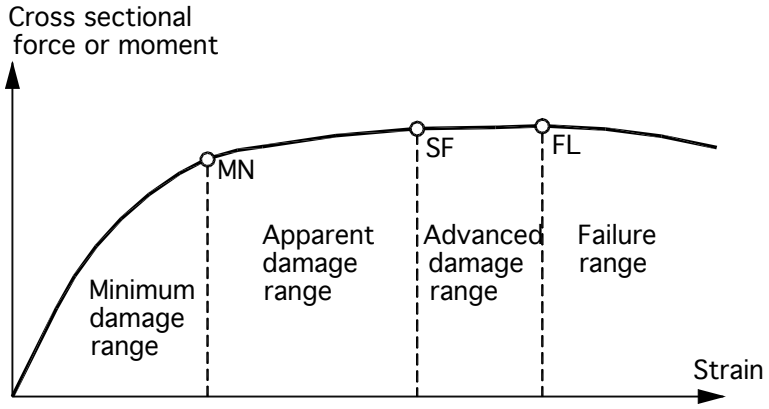

Fig. 1: Damage ranges for ductile sections and elements and their limits

Structural elements of the existing building are classified in two groups, with respect to their failure types: ductile (deformation-controlled) elements and brittle (force-controlled) elements. The typical example of ductile elements are those which fail due to bending moments. Elements which fail due to shearing force, or those which are subjected to large axial force ($N_d > 0.7 f_d A_c$) are considered to be brittle elements. Damage zones of ductile elements and their limits are shown in Figure 1. As seen in this Figure, their inelastic behaviour can be taken into consideration in the evaluation of the existing structure.

Brittle elements are assumed to behave elastically and to fail without displaying any inelastic deformation.

Structural elements are also classified in two groups, depending to their transverse reinforcement at their ends where plastic hinges normally form. When the transverse

reinforcement there conforms to the requirements given in the code for new structural elements, then the element is considered to be *confined*. When the transverse reinforcement required by the code for new structural elements does not exist, then the element is considered as an *unconfined* one. The acceptable deformations of a cross section, and consequently those of the structural elements, at a specific performance level depend on the characterization of their confinement. For these two types of elements, two different deformation limits are defined, depending on their performance levels. The deformation limits for confined elements are larger than those of the unconfined ones.

Compared to the seismic design of new concrete structures, the evaluation analysis of an existing structure provided by the draft Code has the following differences:

a. In the design process, the elastic seismic base shear force is reduced by applying the reduction factor R_a, in order to take into account the inelastic capacity of the structural system. In the linear elastic evaluation procedure, the seismic base shear force is not reduced; however, a factor which represents the ratio of the inelastic capacity to the elastic one is evaluated for each element separately, by considering their failure modes. Since the nonlinear inelastic evaluation is not a force-based procedure and since the behaviour of the structure beyond the elastic range is considered, such a reduction is not employed.
b. In the design process of new concrete structures, the seismic base force is increased for those buildings which are important for the community, by using an importance factor depending on building occupancy. In the evaluation procedure, the importance factor is not employed, because different performance levels are taken into account for buildings having different occupancy types and importance.
c. In the design process of new concrete structures, the seismic forces are applied by considering an accidental eccentricity ratio of 0.05, in order to take into account the non-uniform distribution of storey mass. In the evaluation procedure, a uniform distribution of storey mass is assumed and an accidental eccentricity is not employed.
d. In the evaluation process, considerable importance is given to short columns controlled by brittle failure.
e. In the evaluation process of the structural system, the plastic moment capacity of the beam cross sections are calculated taking into account the reinforcement in the beam section, as well as the slab reinforcement in the effective width of the section.
f. The nonlinear static evaluation procedure of the structural system is carried out by considering the moment of inertia of cracked sections. This assumption increases the period of the structure and probably decreases the corresponding base shear force. On the other hand, it increases the corresponding seismic displacement demands. Similarly, the elastic behaviour of the soil (soil-structure interaction) can be taken into account, possibly having similar effect on the analysis results as the moment inertia of the cross section.

2.2. Building performance levels

Building performance levels are a measure of damage level under the seismic event. They are defined as a combination of the performance levels of the structural elements, such as beams and columns. Three building performance levels are defined (Figure 2):

a. *Immediate Occupancy (IO)*: In the post-earthquake damage state, no permanent drift is expected, the structural system substantially retains its original strength and stiffness, and minor hairline cracking and limited yielding of steel are possible at a few locations. However, no concrete crushing is expected. In terms of damage level of

structural elements; all columns are in the minimum damage range. Less than 10 % of beams could be in the apparent damage range.

b. *Life Safety (LS)*: In the post-earthquake damage state, certain residual lateral strength and stiffness remain, the gravity-load bearing system works, and limited damage and spalling of concrete in beams and columns are expected. In terms of damage level of structural elements, less than 20 % of the beams could be in the advanced damage range, while columns in the advanced damage range carry less than 20 % of the base shear force. The contribution to base shear of the columns having the two end sections in the advanced damage range is not be more than 30 %.
c. *Collapse Prevention (CP)*: In the post-earthquake damage state, limited residual stiffness and strength remain, large permanent drifts are expected, extensive cracking and hinge formation in beams and columns are possible. However, load bearing columns function. In terms of damage level of structural elements, all beams and columns are in the advanced damage range or in lower damage ranges. The contribution of columns in the failure damage range to the base shear force is not be more than 20 %. At the same time, the contribution to base shear of those columns that have the two end sections in the higher than the minimum damage range is not be more than 30 %.

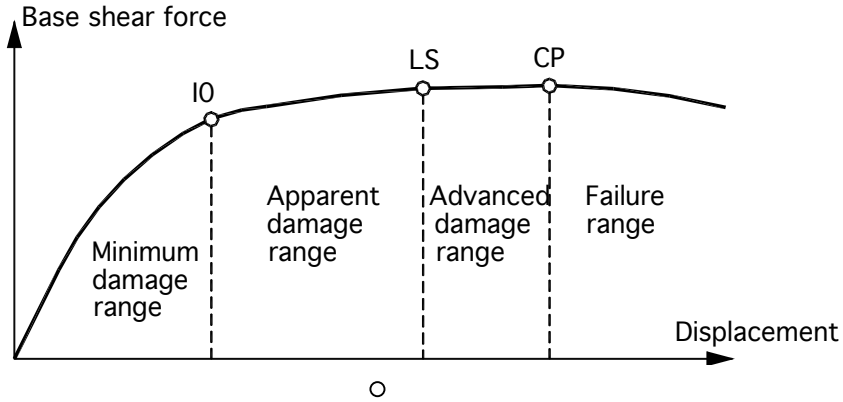

Fig. 2: Building performance levels and damage ranges

Occupancy of building	Earthquake having probability of exceedance		
	50%/50 years	10%/50 years	2%/50 years
Buildings to be utilized immediately after the earthquake (Hospitals, health wards, fire fighting buildings, telecommunication and energy generation and distribution facilities, transportation stations, administration buildings, emergency planning stations, etc.)		IO	LS
Intensively and long-term occupied buildings (Schools, dormitories, hostels, military barracks, prisons, museums, etc.)	IO		LS
Intensively and short-term occupied buildings (Theatre and concert halls, sport facilities, etc.)		LS	CP
Buildings containing hazardous materials (Buildings storing toxic, explosive and flammable materials, etc.)		IO	CP
Other buildings (those not defined above, such as residential and office buildings, hotels, industrial facilities, etc.)		LS	

Table 2: Performance levels for existing buildings under seismic effect

In Table 2 earthquake events are given in probabilistic terms, i.e., in terms of their probability of exceedance in 50 years. Table 3 shows the mean return periods of these events and the ratio of their elastic response spectra to that of the earthquake with 10% probability of exceedance in 50 years.

Earthquake	Probability of exceedance	Mean return period (years)	Factor to be applied to elastic response spectra
Service	50%/50 year	72	0.5
Design	10%/50 year	474	1.0
Maximum	2%/50 year	2475	1.5

Table 3: Definition of probabilistic earthquake levels

2.3. Analysis procedures

The performance level of a building can be found by performing one of the two possible types of analysis of its structural system. The two types are linear elastic analysis and the nonlinear (inelastic) analysis. The first type of analysis can be performed by applying the equivalent earthquake load method and the modal combination method. Linear procedure is appropriate, when the expected level of nonlinearity in the structural system is low. The equivalent earthquake load method is recommended, when higher mode effects are not significant.

2.3.1. Linear elastic procedure

This procedure can be applied either using the *Equivalent Earthquake Load Method* or the *Modal Combination Method*. The equivalent earthquake load method is acceptable for buildings, if their height is not more than 25m and the number of storeys is not more than eight. In all other cases, the modal combination method is to be applied.

For each structural element, damage ranges are determined by evaluation of *r*-factors (demand/capacity ratios).

In ductile elements the *r*-factor is obtained by dividing the earthquake demand to the residual (i.e., available) capacity. The residual capacity is defined as the difference between the capacity and the demand due to vertical (gravity) loads. It is anticipated that the elastic demand may exceed the actual strength of the element; this overload is taken into account by introducing the corresponding *r*-factors. This factor can be seen as an indirect measure of the nonlinear deformation capacity of the element.

For brittle elements the *r*-factor is the ratio of the force demand due to gravity loads in combination with earthquake loads, to the force capacity. Since nonlinear deformations are not permitted in brittle elements, force demands should not exceed the force capacity.

2.3.2. Nonlinear inelastic procedure

This procedure incorporates directly the nonlinear load-deformation characteristics of the structural elements, by assuming that the building is subjected to monotonically increasing lateral loads representing inertia forces, until a target displacement is reached. When the distribution of the lateral load conforms to the first effective mode shape, the method is called

Incremental Equivalent Earthquake Load Method. By using a suitable modal combination, the contributions of the higher modes can be taken into account accordingly. Then the procedure is called *Incremental Modal Combination Method*.

The nonlinear static evaluation procedure is known as *Pushover Analysis* method. The pushover analysis assesses the structural performance by estimating the strength and deformation capacities of the structural elements and performing a static nonlinear analysis. These capacities are compared with the corresponding seismic demands at the desired performance levels. The assessment is based on the estimation of important structural parameters, such as, global and interstorey drifts or element deformations and forces. The analysis accounts for the inelastic behaviour of the structural elements, as well as for the redistribution of internal forces, under the assumption that the inelastic deformations can be concentrated at specific sections, namely the plastic hinges. Generally, plastic hinges may be assumed to form at the ends of structural components. The target displacement is the maximum value of the seismic displacement expected at the top of the building under the earthquake considered. It can be calculated by considering the effects of nonlinear response on displacement amplitudes.

A building which does not meet the performance requirements should be strengthened. This can be done by strengthening the individual elements, or the structure as a whole. By applying the evaluation procedure discussed above, it can be decided whether the strengthened structural system satisfies the performance requirements. A trial-and-error process is required to find an acceptable and feasible strengthening procedure (Figure 3).

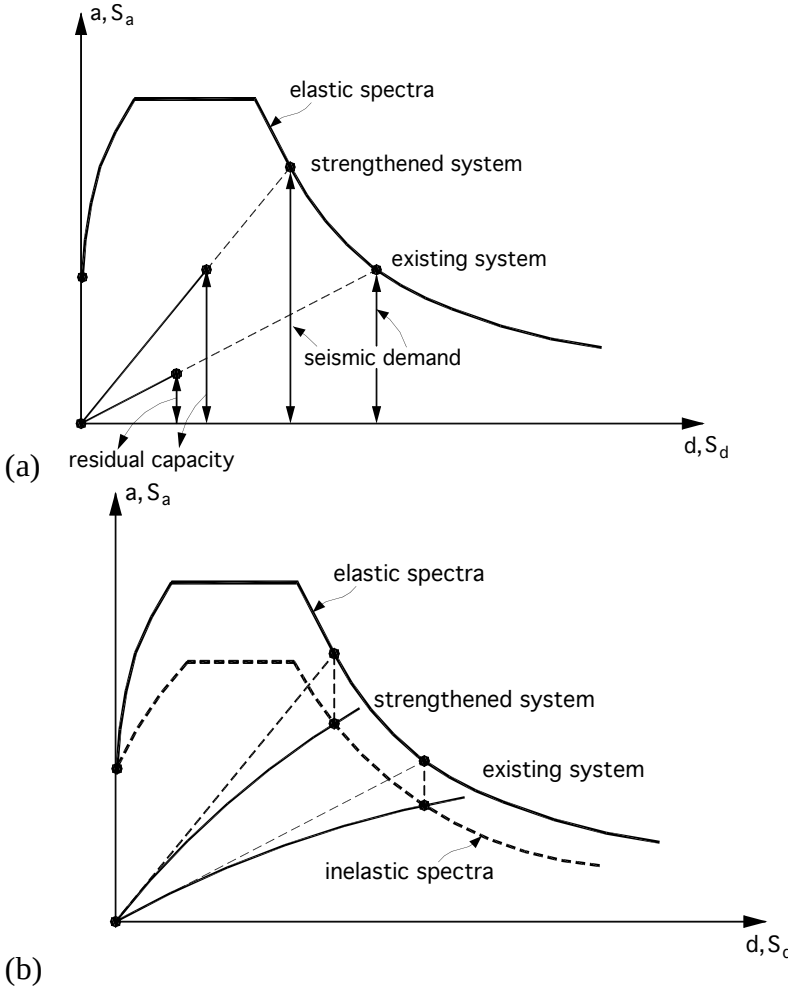

Fig. 3: Strengthening structural system by using (a) the linear elastic procedure; (b) the nonlinear inelastic procedure

3. Strengthening of concrete structures

3.1. Strengthening of structural elements

Local intervention of deficient elements of the structural system is a possible method for strengthening It can be done by increasing ductility and/or strength of the elements.

a. The ductility of a structural element can be increased by adding external transverse reinforcement in the confinement zones. Instead of conventional lateral reinforcement, steel bands or FRP can be used. Consequently, the deformation limits of the element will increase and it may be possible to satisfy the corresponding requirements for this specific element at the desired performance level. This process is applicable in beams as well as in columns. This type of intervention does not increase the moment capacity of the member. By adding a concrete layer around a column section (jacketing), the ductility of the structural element can be increased as well. The minimum concrete layer is specified as 100mm. The shear and axial force capacity of the section should be obtained by taking into account the properties of confined concrete. However, to account for possible uncertainties, the capacity of the new section should be reduced by 10%.
b. The axial, shear or bending resistance of columns can be increased by increasing the cross sectional area. Suitable lateral and longitudinal reinforcement should be provided in the new section. Continuity of the longitudinal reinforcement between storeys should be maintained. Shear and axial force capacity of members should be obtained by taking into account the added longitudinal and lateral reinforcement. However, to account for possible uncertainties, the capacity of the new section should be considered as reduced by 10%.

3.2. Strengthening of structural systems

Strengthening of structural systems is usually done by adding shear walls. Depending on the architectural layout, co-axial new shear walls can be added to the existing plane frames. It is also possible to add the shear walls eccentrically with respect to the frame system. It is recommended that two shear walls should be added in each direction. When the planar area of the building is small, a total of just three shear walls may be acceptable.

Seismic forces develop mainly in the existing building and they should be transferred to the added shear walls. For this reason, the integration of the existing structure with the added shear walls is of great importance. The forces transferred to shear walls should be transferred to the soil through a suitable foundation. When a shear wall does not have a proper foundation layout, the foundation may tend to uplift, because the soil does not take tensile stresses. In this case the shear wall will not be able to carry the expected seismic forces (Bayülke, 1999; Celep et al, 2005; Penelis et al 1997).

3.3. Other retrofitting and improvement strategies

The following retrofitting techniques can be considered in various cases:

a. *Removal of existing irregularities*: Irregularities appear often due to the presence of discontinuity in the structural system. Simple removal of structural irregularities may be sufficient to reduce demands predicted by the analysis to an acceptable level.

Addition of shear walls can be effective corrective measures for the removal or reduction of torsional irregularity and of irregularity due to soft or weak storeys. Irregularity due to vertical discontinuity in columns and shear walls can be corrected, by extending them through the zone of discontinuity.

b. *Mass reduction*: If the seismic analysis shows that structural deficiencies are attributable to excessive building mass, mass reduction may be an effective retrofitting strategy. It can be done by decreasing the number of storeys, as well.
c. *Seismic isolation*: If the seismic evaluation results show that the structural deficiencies are related to excessive seismic force or displacement demands, seismic isolation may be an effective retrofitting strategy. In the present state, base isolation in existing buildings is very costly. Its application may be feasible only for special buildings having historical value or importance in the society.
d. *Use of FRP*: FRP can be used to provide confinement to columns and bridge piers, or to increase the shear strength of shear walls and masonry walls. Their application is easy and clean. However their cost is relatively high.

4. Examples

Various retrofitting examples are given in this Section.

4.1. Slabs

Slabs support gravity loads and transmit seismic loads developed within the structure to columns and shear walls. When the computational checks show that the slab resistance is insufficient; the slab can be strengthened by increasing its thickness and by placing additional reinforcement (Figure 4). The integration of the existing and the new layers of the slab, i.e. the force transfer between the old and the new concrete layer, is of prime importance. For this purpose, steel dowels or anchors can be used. However this can also be accomplished by roughening the surfaces of the existing slab or by applying resin coatings onto the interface (Figure 5).

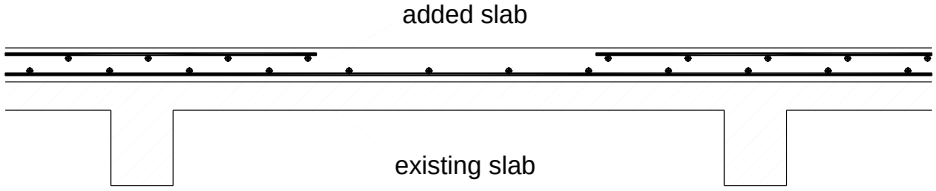

Fig. 4: Strengthening of a slab

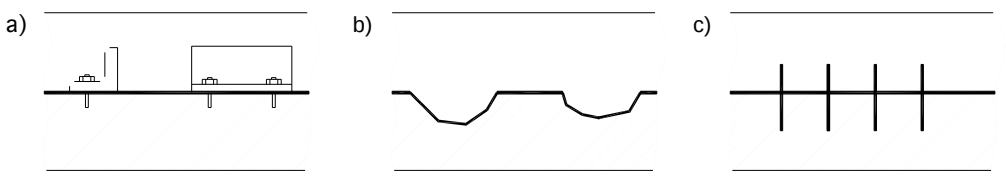

Fig. 5: Integration of the new and existing slab

4.2. Beams

In the case of beams, and depending on the desired degree of strengthening, reinforced concrete jacketing can be applied to one, two and three sides of the beam (Figure 6). Here the key is the extension of the reinforcement in the support sections, so that an increase in the bending capacity of the sections can be achieved.

Strengthening of beams is a difficult and expensive application and it should be avoided, whenever possible.

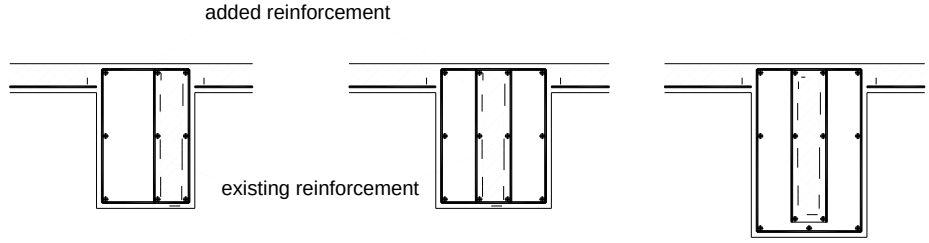

Fig. 6: Jacketing of beams

4.3. Columns

Jacketing of columns is a very common application. Depending on the inadequacy in seismic resistance of the column and on the architectural layout, jacketing can be applied at one, two or three sides of the column (Figure 7 and 8). If the jacketing is applied over the entire perimeter of the column, its effectiveness is quite high. In case of full jacketing, the integration of the existing and of the new parts of the column can be achieved by roughening the corresponding surfaces. In other cases, use of anchorage dowels in addition is recommended.

When the jacketing is limited to the storey height, the degree of confinement, and the axial and shear capacity of the element increase. When the column has insufficient bending moment capacity, then the longitudinal reinforcement of the jacketing should be extended through the slabs between storeys (Figure 9).

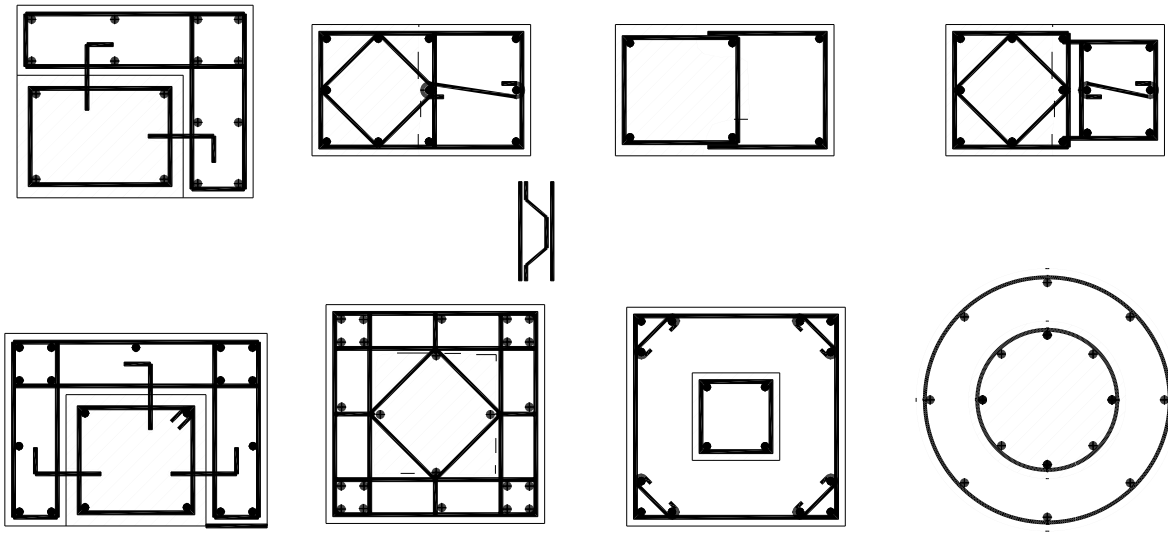

Fig. 7: Jacketing of columns

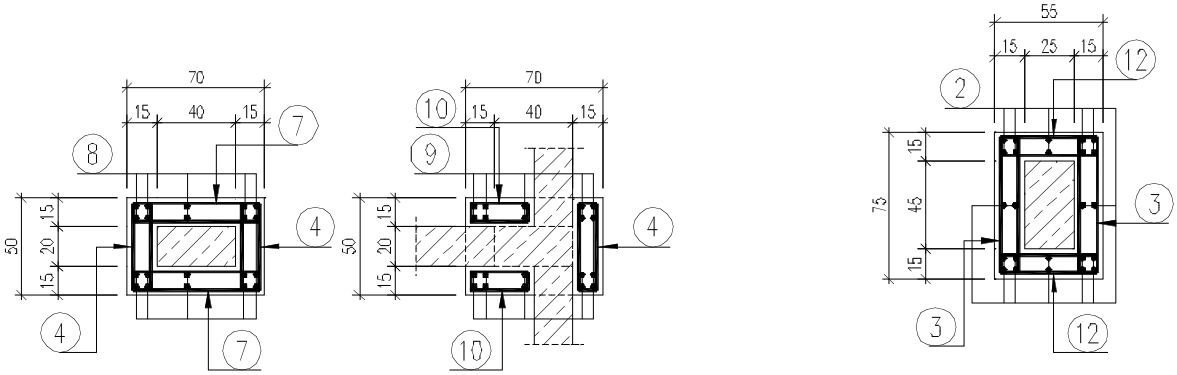

Fig. 8: Jacketing of columns

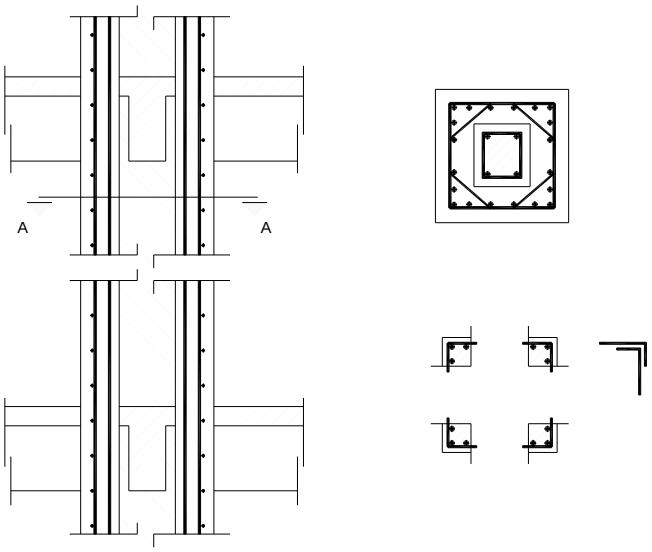

Fig. 9: Column jacketing over the full height of the storeys

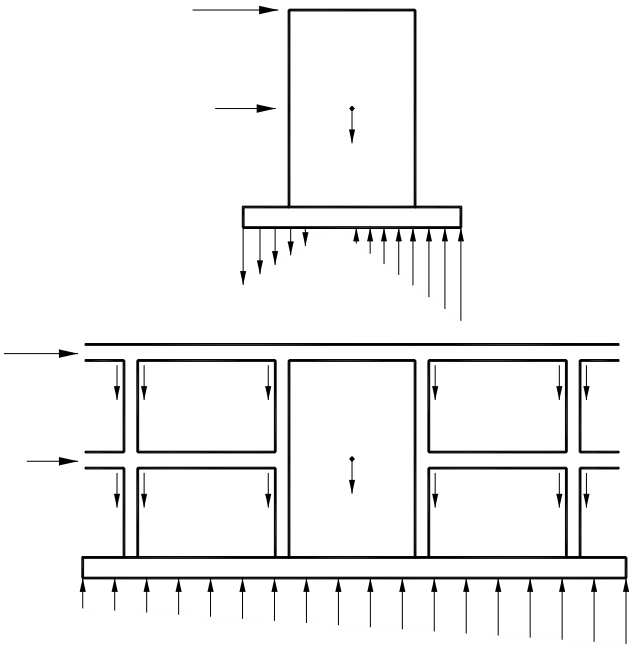

Fig. 10: Added shear wall and its foundation

4.4. Addition of new shear walls

The seismic resistance of a structure can be improved by addition of new shear walls that have large lateral stiffness and bending moment and shear capacities and can carry large seismic forces. In case of addition of shear walls, special care should be taken to ensure the force transfer between the new and the existing structural elements and between the structural system and its foundation. A spread footing is not recommended for an added shear wall, because soil cannot develop tensile stresses that arise due to the large moments and the low axial load. A combined footing that includes the columns around the new wall is recommended (Figure 10).

A typical configuration of the added shear wall and its reinforcement is given in Figure 11.

Figure 12 shows a shear wall added externally. In this case construction can be relatively easy. However this application requires more care for integration of the added and the existing systems. Various applications are given in Figures 13 to 16.

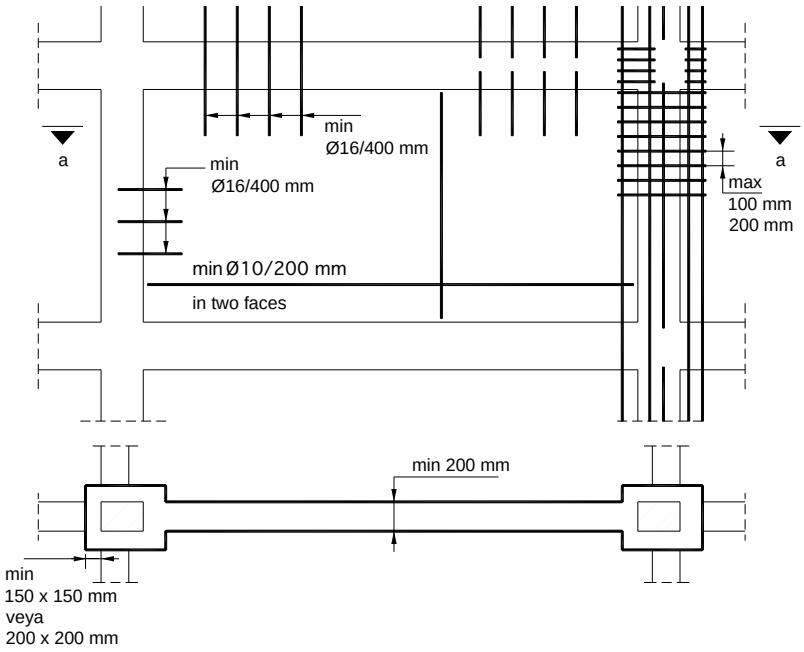

Fig. 11: Co-axial shear wall

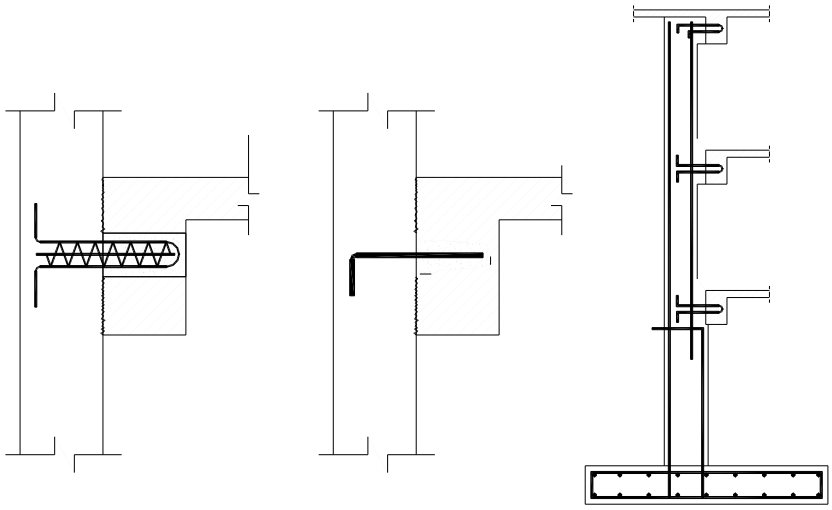

Fig. 12: Added external shear wall

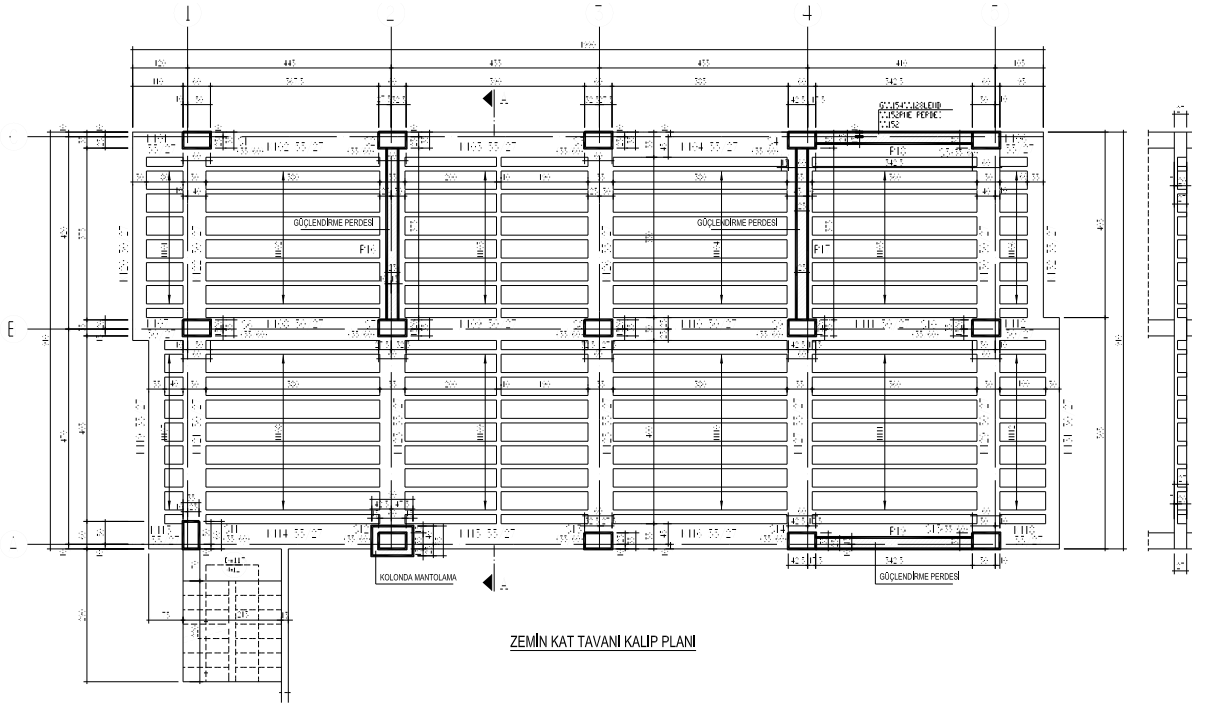

Fig. 13: Strengthening of the system by shear walls

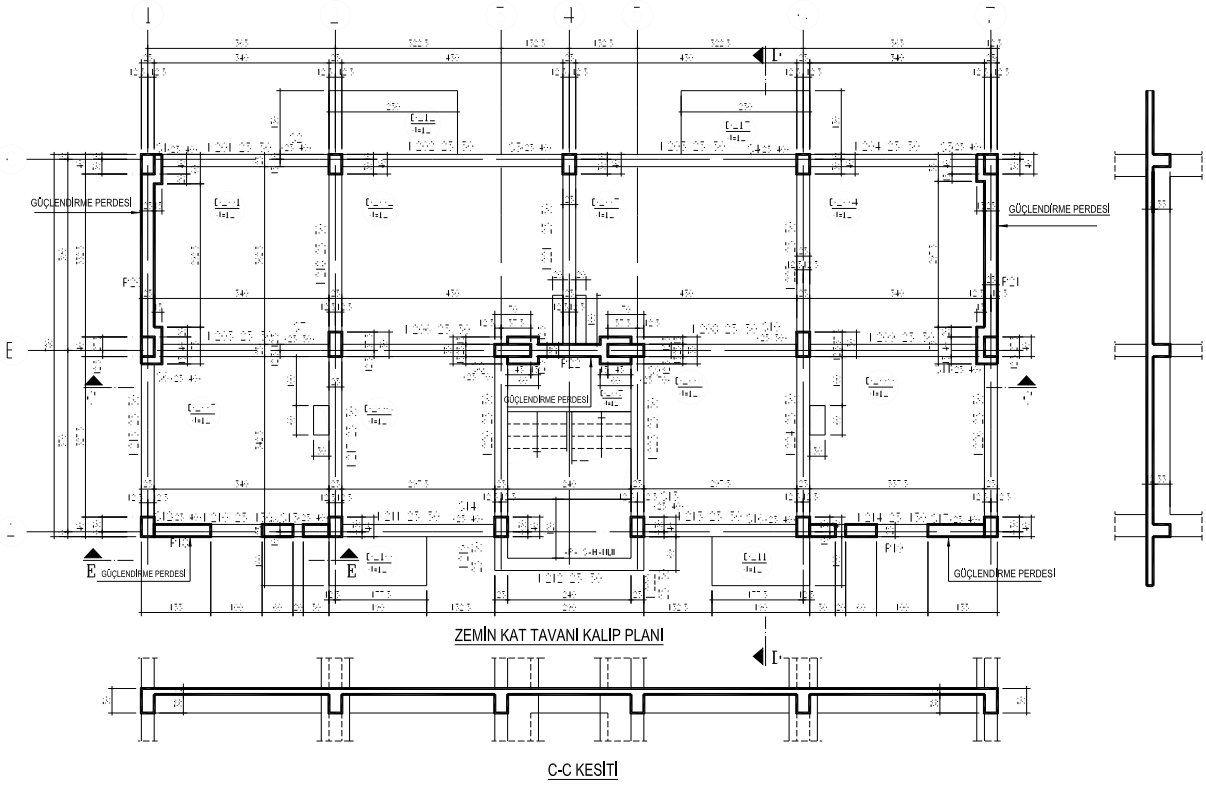

Fig. 14: Strengthening of the system by shear walls

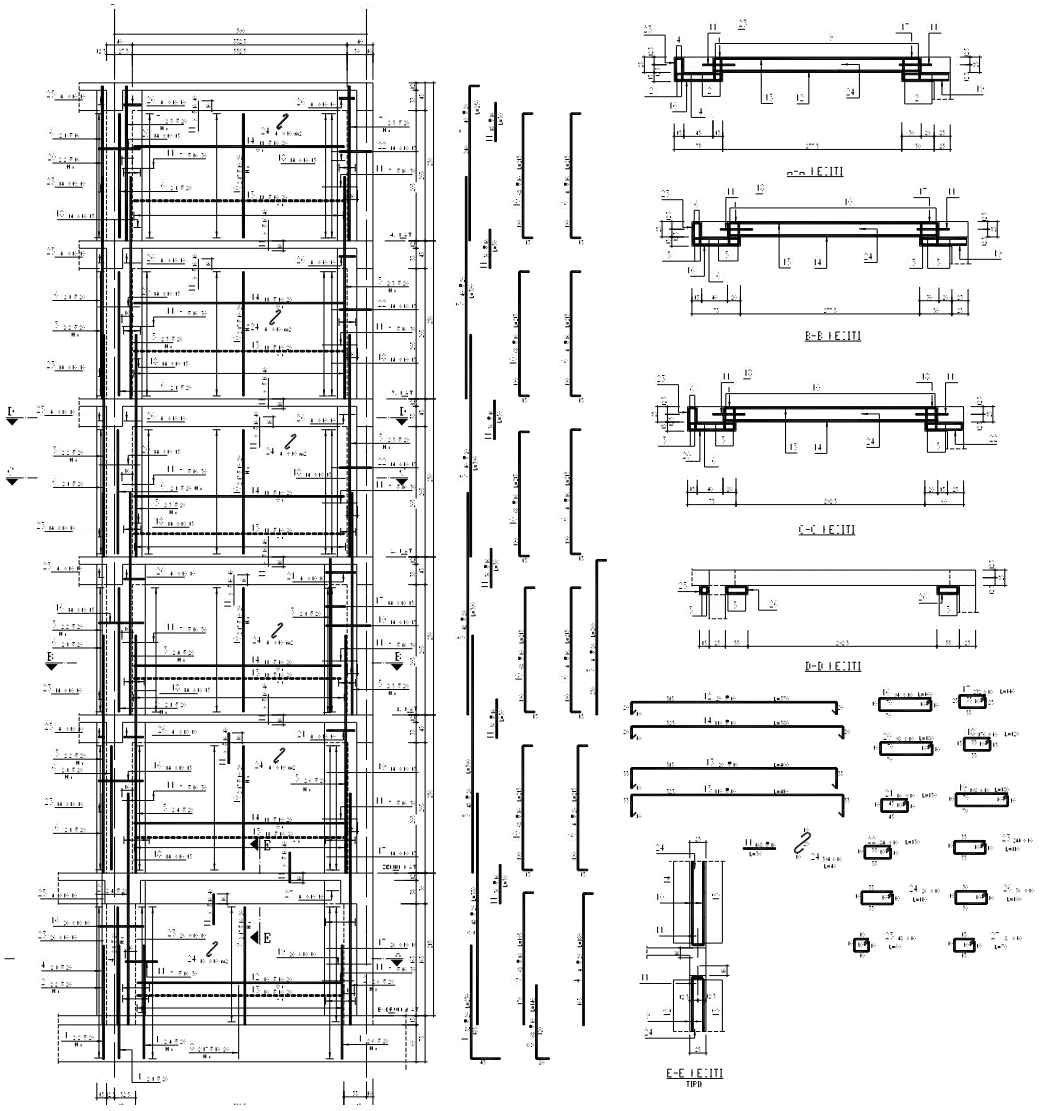

Fig. 15: Details of a shear wall added for strengthening

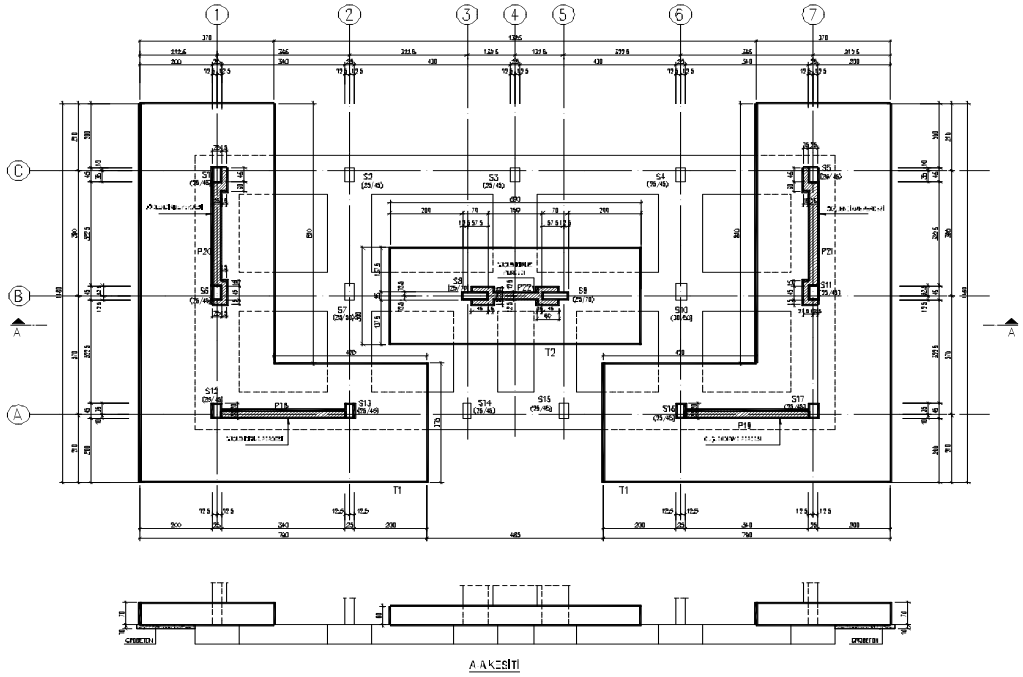

Fig. 16: Foundation layout for the new shear walls

5. Conclusions

The author would like to raise the following conclusions for further discussion:

a. Seismic evaluation of the existing structures is a complex task. Decision and preparation for strengthening is not a mathematical problem having a straightforward unique solution.
b. Seismic strengthening of a building that has a low level of seismic safety is not always a feasible solution.
c. Use of sophisticated evaluation and strengthening procedures is reasonable, when the level of knowledge for the structural system is relatively high. When a building has various simple deficiencies, simple evaluation and strengthening techniques are recommended.
d. Use of advanced technology materials is only recommended, when concrete quality in the existing buildings is relatively good.
e. When design and construction of new buildings conform to the Code, the problem of the existence substandard buildings will be solved in the long run, or at least the problem will not increase. The cost of strengthening of an existing building is much higher than the cost of additional design and construction measures necessary to render a new structure seismically safe.
f. In Turkey certain building types, such as, improperly detailed concrete frame buildings in metropolitan areas and unreinforced masonry buildings in rural areas, present high seismic risk. Since there are in Turkey a large number of buildings in need of strengthening, the problem cannot be solved by maintaining the required safety level high and by concluding that many of them have to be strengthened. It seems reasonable that relatively lower safety levels should be defined in the Code and accepted by the occupants of buildings, if they cannot afford higher safety levels. For this reason consideration should focus on existing buildings having very low seismic safety.

References

Bayülke, N. (1999). Repair and strengthening of earthquake damaged buildings (in Turkish), Chamber of Civil Engineers, Izmir.

Celep, Z. and Kumbasar, N. (2005). Introduction to earthquake engineering and earthquake resistant design of building (in Turkish), Beta Publications. Istanbul.

Federal Emergency Management Agency (2000) FEMA-356: Prestandard and commentary for seismic rehabilitation of buildings, Washington, D.C.

Penelis, G.G. and Kappos, A.J. 1997. Eartquake-resistant concrete structures, E&FN Spon, London.

Turkish Ministry of Public Works and Settlement (1998) Turkish seismic code, Ankara.

Turkish Ministry of Public Works and Settlement (2005) Turkish seismic code (Draft), Ankara.

FRP strengthening of RC columns (shear, confinement and lap splices)

Alper Ilki
Istanbul Technical University, Turkey

1 Introduction

In Turkey, many existing structures are characterized by various deficiencies of earthquake resistance. Inadequate lateral strength and stiffness, as well as inadequate ductility, are among the most common deficiencies. In order to reduce losses due to seismic events, many existing structures are in urgent need of retrofit. However, in many cases, there are various obstacles for retrofitting. Among these obstacles, financial problems, social problems (disagreement between residents), downtime and disturbance to the occupants are the most common. The retrofit strategy should take into account all these difficulties, as well as engineering decisions considering the situation of existing buildings. The majority of the existing buildings in Turkey are reinforced concrete structures, on which emphasis is placed in this contribution.

Retrofitting may basically follow one of the two main approaches; system upgrade and/or member retrofit. In general, system upgrading includes addition of new shear walls to the building and consequently reduction of seismic demand in existing members, while member retrofit includes individual retrofitting of existing members. Generally, when the structure is very weak in many aspects, system upgrade is preferred; when certain structural members are deficient, the member retrofit approach is followed. Although, in general, the system retrofitting approach seems more rational for most of existing structures in Turkey, due to a great number of deficiencies that those buildings possess, the necessity of a costly foundation retrofit is a significant disadvantage of this approach. The foundation retrofit may not be necessary, or may be much less costly when the alternative approach; namely the member retrofit strategy, is preferred. It should be noted that in many cases, the most appropriate approach may be to appply system upgrade and member retrofit together.

Columns are vitally important structural members for sustaining vertical and lateral loads, thus preventing collapse, during earthquakes. Retrofit of deficient columns can be carried out using different techniques depending on the type of deficiency. The most common column retrofitting technique in Turkey is reinforced concrete jacketing, followed by retrofitting with steel members, (Fig. 1). These conventional techniques are labour intensive, while material costs are not high. However, application of these techniques is difficult and causes significant disturbance to the occupants. External confinement of this type of structural members with high strength fibre reinforced polymer (FRP) composite sheets can significantly enhance the shear strength, the axial strength and the deformability of the members. Compared to conventional retrofitting techniques, the lower density, the higher tensile strength and modulus, the durability and easy construction are the advantages of FRP retrofitting. Particularly, when there is a time limitation for the retrofitting and/or access to the members to be strengthened is limited, FRP retrofitting may be preferable. Due to these advantages, the use of FRP composites in concrete structures has been increasing rapidly in recent years.

Considerig the increased number of applications, the draft new version of Turkish Earthquake Resistant Design Code (2005), covers column retrofitting using FRP composites. In this code, the main contributions that FRP composites can provide are defined as shear strength enhancement, axial strength enhancement, ductility enhancement and improvement of inadequate lap splices of ribbed (deformed) bars. There are also other codes, draft codes

and/or guidelines published in different countries, that include FRP retrofit of structural members, such as Eurocode 8 Part 3 (2005), the Technical Guide reported by ACI Committee 440 (2001), the *fib* bulletin 14 (*fib* 2001) and CSA S806-02 (2002): Design and Construction of Building Components with Fibre-Reinforced Polymers.

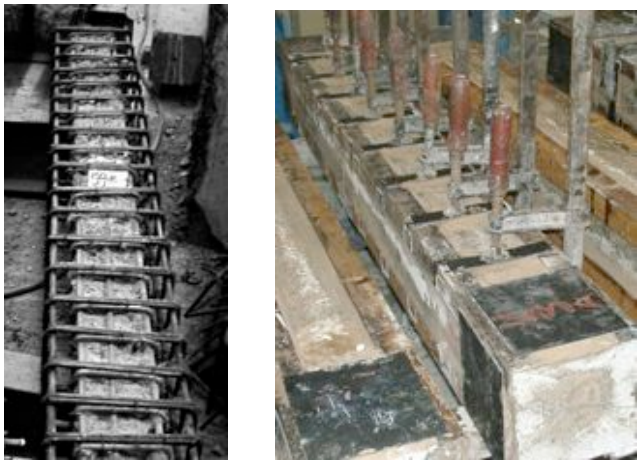

Fig. 1: Conventional retrofitting application examples from Istanbul Technical University Structures and Earthquake Engineering Laboratory

2 Shear strength of columns

This Section presents guidance on the calculation of the shear strength of a column, retrofitted with FRP shear reinforcement. Shear strengthening of reinforced concrete columns may be necessary when the columns are found to be deficient in shear, or when their shear capacities are below their flexural capacities.

The shear strengths of circular and rectangular columns can be enhanced by FRP composites with fibres oriented essentially perpendicular to the member axis (Fig. 2). Increasing the shear strength can result in flexural failures, which are relatively more ductile, compared to shear failures. The additional shear strength that can be provided by the FRP system is based on different factors, like the geometry of the column, the concrete strength and wrapping application.

Fig. 2: FRP wrapping of a column for shear strength enhancement

In design code approaches, the shear strength of a column strengthened by FRP composite with fibre oriented perpendicular to members' axis is usually determined by Eq. (1),

$$V_r = V_c + V_w + V_f \tag{1}$$

where V_c is the contribution of concrete, V_w is the contribution of steel stirrups and V_f is the contribution of FRP. The contribution of FRP is found by the truss analogy, similarly to the determination of the contribution of steel shear reinforcement. The shear capacity should not exceed a certain limit, to prevent diagonal compression failure in the column. In the TS500-Requirements for Design and Construction of Reinforced Concrete Structures (2000) this value is given as:

$$V_r \le 0.22 f_{cd} b_w d \tag{2}$$

where f_{cd} is the design compressive strength of concrete, and b_w and d are the width and effective depth of the column section.

The contributions of concrete and steel stirrups can be calculated according to TS500-Requirements for Design and Construction of Reinforced Concrete Structures (2000) as:

$$V_c = 0.8 V_{cr} \tag{3}$$

$$V_{cr} = 0.65 f_{ctd} b_w d \left(1 + \gamma \frac{N_d}{A_c}\right) \qquad \text{(N, mm)} \tag{4}$$

$$V_w = \frac{A_{sw}}{s} f_{ywd} d \tag{5}$$

where V_{cr} is the shear force causing diagonal cracking, f_{ctd} is the design tensile strength of concrete and coefficient γ is equal to 0.07 in the case of compression and to -0.03 in the case of tension. N_d is the design axial load of the member, to be considered positive for compression, and A_c is the gross cross-sectional area. In Eq. (5), A_{sw} is the effective cross-sectional area of stirrups, s is their spacing and f_{ywd} is the design yield strength of stirrups.

In the case of FRP wrapping in the form of discrete strips with width w_f and centre-to-centre spacing s_f, the contribution FRP to shear strength can be determined via Eq. (6).

$$V_f = \frac{2 n_f t_f w_f E_f \varepsilon_f d}{s_f} \tag{6}$$

In this equation, n_f is the number of FRP plies on each side, t_f is the effective thickness of one ply of FRP, and E_f and ε_f are the elastic modulus and effective ultimate tensile strain of FRP, respecitvely. In the application with discrete strips, the width and spacing of the strips should fullfil the requirement given by Eq. (7).

$$s_f \le w_f + \frac{d}{4} \tag{7}$$

In the case of wrapping FRP continuously through the height of the column, since w_f and s_f are equal to each other, Eq. (6) will be be simplified as given by Eq. (8).

$$V_f = 2n_f t_f E_f \varepsilon_f d \quad (8)$$

For reinforced concrete columns completely wrapped with FRP, loss of aggregate interlock of the concrete has been observed to occur at fibre strains less than the ultimate fibre strain (ACI Committee 440). Shear failure occurs very suddenly and in a brittle fashion. Therefore, to avoid sudden collapse of a structure by shear failure, the most important variable to control is the deformation of the FRP shear reinforcement. For this purpose, maximum ε_f values are defined. In the draft version of new Turkish Earthquake Resistant Design Code (2005), the maximum ε_f values are defined as,

$$\varepsilon_f = \min(0.004, 0.50\varepsilon_{fu}) \quad (9)$$

where ε_{fu} is the characteristic failure strain of FRP.

For rectangular sections with shear capacity enhancement provided by transverse FRP composite material, section corners should be rounded before placing composite material. The necessary minimum radius given by different sources vary; this value is given as 30 mm by the draft version of new Turkish Earthquake Resistant Design Code (2005). For both circular and rectangular sections, the draft version of new Turkish Earthquake Resistant Design Code (2005) requires at least 200 mm overlap length at the end of wrapping.

The draft new Turkish Earthquake Resistant Design Code (2005) allows shear strength enhancement through FRP only if all four sides of the column are fully wrapped with FRP composites. Complete or strip type wrapping schemes are illustrated in Fig. 3.

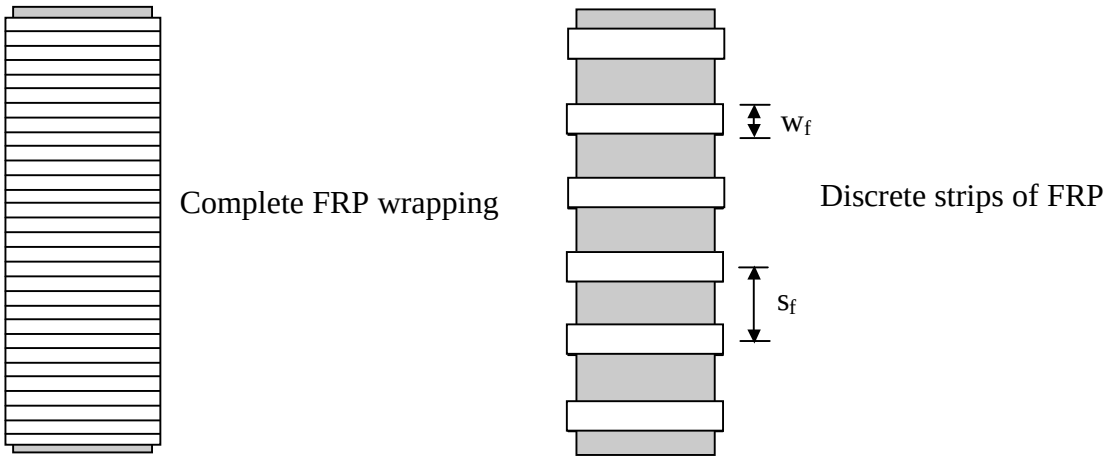

Fig. 3: FRP wrapping schemes for reinforced concrete columns

Fig. 4: Damaged short columns due to insufficient shear strength (1999 earthquakes in Duzce and Kocaeli)

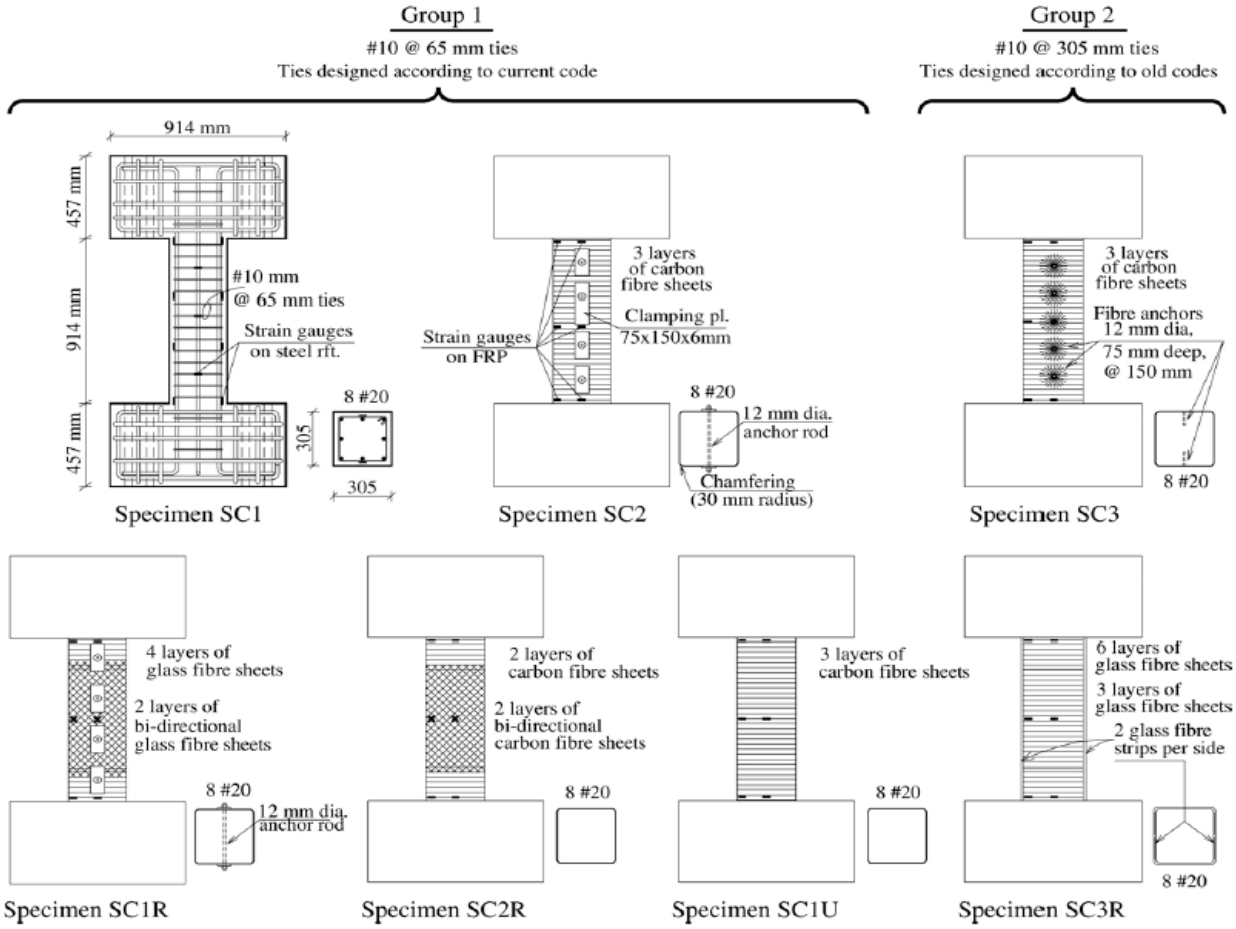

Fig. 5: Specimens retrofitted in Galal(2002) by FRP wrapping, for shear strength enhancement

In the recent earthquakes in Turkey many columns failed in a brittle manner due to insufficient transverse reinforcement. Damage to short columns was quite common (Fig. 4).

Various researchers tested different types of specimens for examining the contribution of FRP retrofitting systems to the shear capacity of the columns. A recent work by Galal (2002) and Galal et. al (2005) is summarized below. The basic purpose of that work was to demonstrate experimentally that it is possible to strengthen the shear resistance of short columns so that a flexural failure occurs by developing plastic hinges at both ends of the column. The specimens tested are shown in Fig. 5. They were tested under cyclic lateral loading and constant axial load. The test setup can be seen in Fig. 6, together with the load-lateral displacement relationships of the tested specimens. Fig. 6 shows the envelopes of hysteretic load-displacement relationships.

As can be seen in Fig. 6, significant improvement was obtained in the performance of the specimens retrofitted with FRP composites. Galal et. al (2005) concluded that anchoring the FRP jacket to the concrete cross-section of short column subjected to lateral cyclic displacements increased the column's shear strength and energy dissipation capacities. They also pointed out that the most appropriate strengthening technique for short columns was found to be the use of anchored carbon FRP jackets over the fullmheight of the column and the additional confinement of the end flexural hinge zones using carbon FRP sheets with unidirectional fibres in the hoop direction.

As can be seen in Fig. 6, significant improvement was obtained in the performance of the specimens retrofitted with FRP composites. Galal (2002) and Galal et. al (2005) concluded that anchoring the FRP jacket to the concrete cross-section of short column subjected to lateral cyclic displacements increased the column's shear strength and energy dissipation

capacities. They also pointed out that the most appropriate strengthening technique for short columns was found to be the use of anchored carbon FRP jackets over the fullmheight of the column and the additional confinement of the end flexural hinge zones using carbon FRP sheets with unidirectional fibres in the hoop direction.

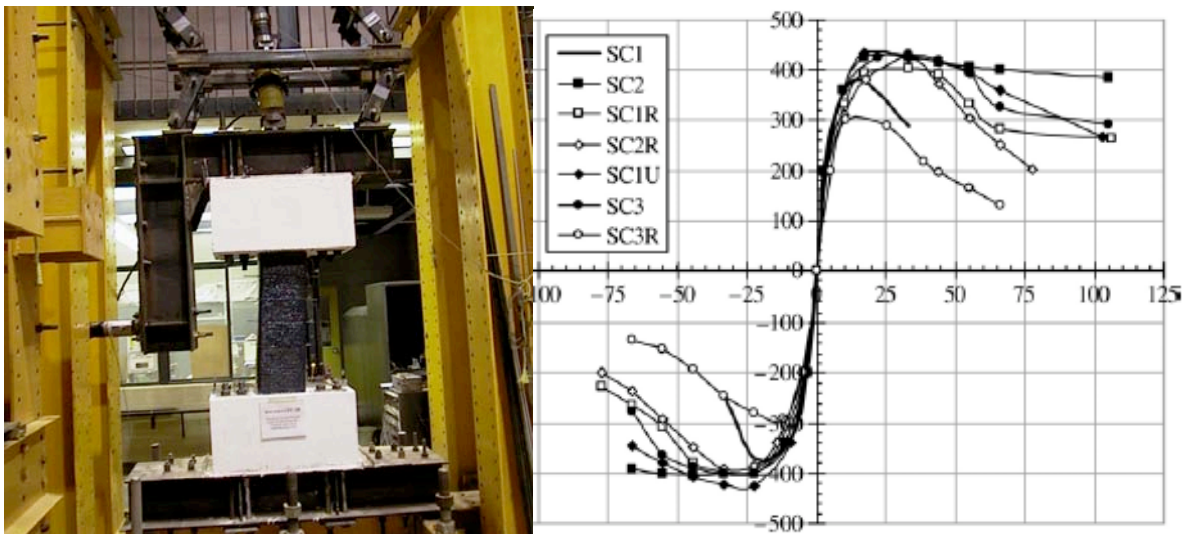

Fig. 6: Test setup and force (kN)-displacement (mm) results of Galal (2002)

Fig. 7: Failure of beam-column joints

3 Shear strength of beam-column joints

Many structures experienced shear failure of beam-column joints during recent earthquakes in Turkey (Fig. 7). The main reasons of this type of failure were inadequate transverse reinforcement, low quality of concrete and improper reinforcement detailing. Although rehabilitation is needed to improve the seismic performance of joints, often joint retrofitting is very difficult, due to the presence of slabs and transverse beams.

Recently experimental work has been carried out by Gergely et. al (2000), Ghobarah and Said (2001, 2002), Said (2001), Tsonos and Stylianidis (2002) and Antonopoulos and Triantafillou (2003) on the retrofit of beam-column joints using FRP composites. According to these studies, the shear resistance of joints was improved; the important role of mechanical

anchorage in limiting premature debonding was observed. However, these studies were carried out on plane members, which do not reflect most of the existing beam-column joints in actual buildings. The specimens tested by Ghobarah and Said (2002) and their test setup are shown in Fig. 8. The list of the specimens that they tested and the envelopes of load-displacement ductility factor relationships are given in Table 1 and Fig. 9, respectively. As seen in Fig. 9, significant improvement can be obtained in the shear performance of beam-column joints retrofitted with FRP composites, when proper details are applied.

Tsonos and Stylianidis (2002) concluded that FRP jacketing of beam-column joints was a feasible strengthening technique, but concrete jacketing was more effective. Since the experience on the seismic behaviour of beam-column joints retrofitted with FRP composite systems is currently limited, no recommendations or rules are included in codes, draft codes and/or guidelines on the FRP retrofit of beam-column joints.

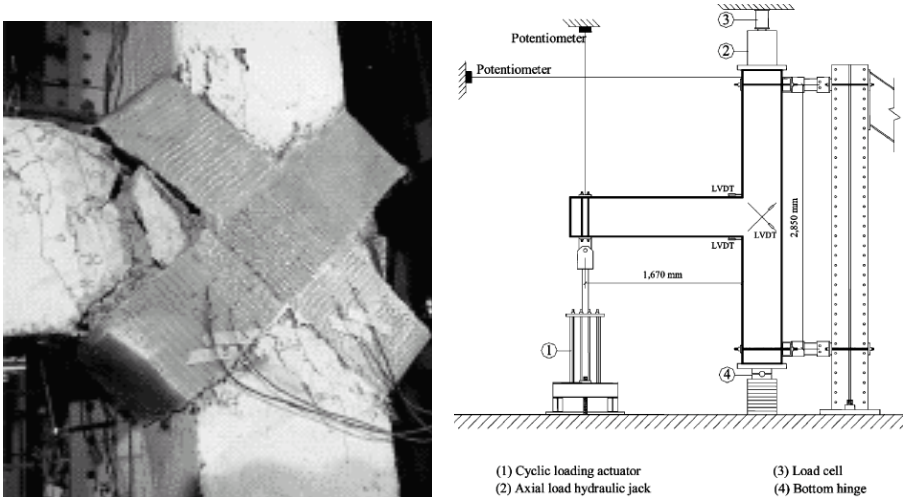

Fig. 8: Beam-column joint retrofitting and test setup (Ghobarah and Said 2001, Said 2001)

Specimen	Testing conditions and retrofitting schemes using GFRP
T1	Control specimen (column axial load 600 kN).
T2	Control specimen (column axial load 300 kN).
T1R	Specimen T1 repaired after control test, then retrofitted with one bi-directional "U" shaped GFRP sheet, of the same height as the joint with added cover plates and anchors through the joint.
T2R	Specimen T2 repaired after control test, then retrofitted with two "U" shaped GFRP layers extending above and below the joint with added cover plates and anchors through the joint.
T4	Specimen retrofitted using one bi-directional "U" shaped GFRP sheet, of the same height as the joint. Similar to T1R but without cover plates and anchors through the joint.
T9	Retrofitted with three diagonal GFRP layers.

Table 1: List of the beam-column joint specimens tested by Ghobarah and Said (2002)

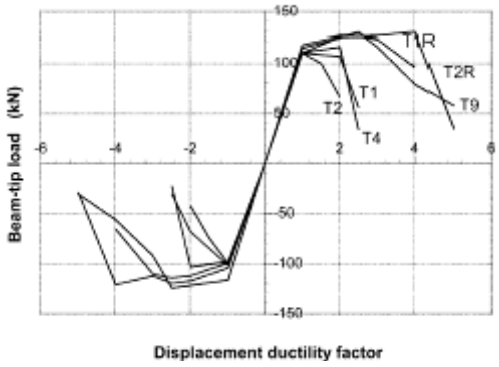

Fig. 9: Envelope curves for load-displacement ductility factor relationships (Said 2001)

4 Shear strength of shear walls

The available information on seismic retrofitting of concrete shear walls with FRP composite systems is very limited. In a recent work by Antoniades et. al (2005), it was reported that FRP reinforcement increased both the flexural and shear strength of wall specimens constructued at a scale of 1:2.5 and an aspect ratio of 1.5 (height/length). They also mentioned that a key parameter on the performance of FRP-retrofitted shear walls was the way of anchoring carbon FRP strips.

5 Confinement action

By wrapping FRP composites around columns, a passive lateral confinement pressure can be provided. Due to presence of passive lateral pressure, the uniaxial stress state may be transformed into triaxial stress state, when the member is under additional stresses. Consequently, as in the case of internal transverse reinforcement used for confinement of concrete, externally bonded transverse FRP composites provide enhancement in compressive strength and ductility of structural members. According to Fukuyama and Sugano (2000), the repair and seismic strengthening by continuous fibre sheet wrapping was first developed in Japan, where research was first carried out in 1979. Fardis and Khalili (1982), whose study is among the initial works on FRP confined concrete, stated that, excellent strength and ductility characteristics were obtained on FRP encased concrete cylinders in axial compression and of rectangular FRP-encased beams in bending.

The enhancement in the behaviour of reinforced concrete columns externally jacketed with FRP can be examined mainly for two cases in terms of confinement: behaviour under axial stresses and behaviour under combined effect of axial load and flexure. It may be noted that the uniaxial stress-strain behaviour of FRP-jacketed concrete members under axial compressive loads can be used for the stress-strain relationship of the compression zone of the reinforced concrete members subjected to both axial load and flexure. So, the information obtained at the end of the uniaxial compression tests on FRP jacketed concrete is useful for analyzing the flexural behaviour of FRP-jacketed concrete columns.

5.1 Axial behaviour

FRP composites may be bonded to the external surface of concrete columns with the fibres running essentially perpendicular to the longitudinal axis of the member, to enhance the axial load capacity of the column. The FRP composite system should be wrapped completely for axial strength enhancement. Axial strength enhancement provided by FRP composite wrapping is relatively more effective in circular than in rectangular sections. Since the efficiency of FRP wrapping reduces with increasing cross-sectional aspect ratio of the column, to make use of ductility enhancement by FRP jacketing, various sources limit the cross-sectional aspect ratio of members to a certain value. In the draft new Turkish Earthquake Resistant Design Code (2005), the cross-sectional aspect ratio is limited to 2.0 for rectangular sections. For the same purpose, for elliptical sections, the maximum ratio of the longer dimension to the shorter is limited to 3.0. For rectangular sections with axial strength enhancement provided by transverse FRP composite material, section corners should be rounded before placing the composite material. The minimum radius given by different sources varies; this value is given as 30 mm by the draft new Turkish Earthquake Resistant Design Code (2005). For both circular and rectangular sections, this draft Code requires at

least 200 mm overlap length at the end of wrapping. It should be noted that the axial strength enhancement provided by FRP wrapping decreases with increasing cross-sectional dimensions of columns.

In Fig. 10, the free body diagram of a confined circular cross-section is given. In this figure, f_l is the lateral stress acting on the concrete due to confinement, D is the diameter of the cross-section and t_f is the thickness of the wrap. The F_l, resultant lateral force applied on concrete, can be determined by Eq. (10) for unit height of the member.

$$F_l = f_l D \tag{10}$$

The tensile force of the wrapping material for unit height, F_j, can be determined from Eq. (11), where n_f is the number of FRP plies and f_j is the tensile stress of the wrapping material. Observations during compression tests of FRP confined members show that all failures are due to rupture of CFRP composite sheets. Therefore, the maximum lateral confinement stress that will be achieved just before failure can be obtained by considering the equilibrium condition for F_l and F_j and assuming that f_j is equal to the fracture strength of the wrapping material, f_t :

$$F_j = 2 n_f t_f f_j \tag{11}$$

$$f_l = \frac{2 n_f t_f f_t}{D} \tag{12}$$

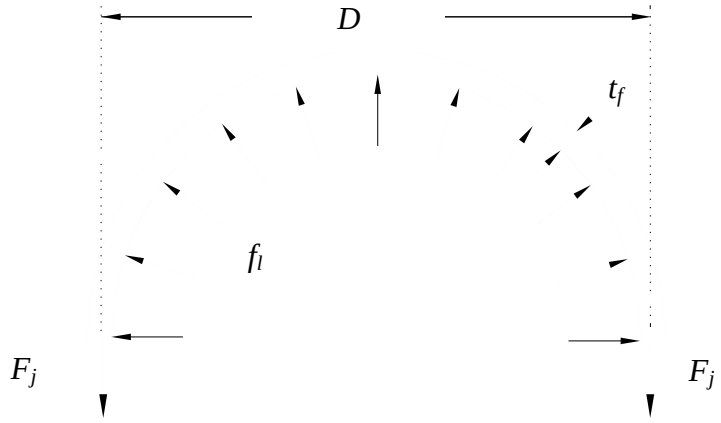

Fig. 10: Free body diagram of a FRP confined circular cross-section

The experimental results suggest that, the compressive strength of the confined concrete is influenced by the unconfined concrete strength and the maximum lateral stress that can be applied by the confinement mechanism. Richart et al. (1929) proposed the following equation for the compressive strength of confined concrete, on the basis of the experimental data:

$$f_{cc} = \bar{f}_{ck} + k_1 f_l \tag{13}$$

where f_{cc} and $\bar{f}_{ck}$ are the confined and unconfined concrete strengths, respectively, and k_1 is the confinement effectiveness coefficient that Richart et al. (1929) assumed as equal to 4.1. This equation became a basis for many studies, but has also been is revised by several researchers. While k_1 was considered to be a constant number in the past, recently it is assumed to be a function of lateral stress and of unconfined concrete compressive strength, (Mander et al. 1988, Toutanji 1999, Saatcioglu and Razvi 1992). Mostly various functions of the ratio of lateral stress to unconfined concrete strength are considered for k_1. Consequently,

dimensionless expressions could be obtained for confined concrete strength. Although there is a variety of equations for the compressive strength and the corresponding axial strain of concrete jacketed with FRP composites in the transverse direction, in the draft new Turkish Earthquake Resistant Design Code, the following equations are given, based on experimental works carried out by Ilki et. al (2002, 2003, 2004).

$$f_{cc} = \bar{f}_{ck}\left[1 + 2.4\left(\frac{f_l}{\bar{f}_{ck}}\right)\right] \geq 1.2\,\bar{f}_{ck} \tag{14}$$

$$\varepsilon_{cc} = 0.002\left[1 + 15\left(\frac{f_l}{\bar{f}_{ck}}\right)^{0.75}\right] \tag{15}$$

The lateral confinement pressure f_l can be calculated using Eq. (16). In this equation E_f is the tensile modulus of FRP, while the volumetric ratio of FRP jacket can be calculated using Eq. (17) and (18) for circular and rectangular sections, respectively. The confinement effectiveness coefficient κ_a can be calculated using Eq. (19) and Fig. 11. The effective tensile strain of the FRP, ε_f, can be calculated through Eq. (20), where ε_{fu} is the characteristic failure strain of FRP. In Eq. (19) r is the corner radius for rectangular sections, which should be at least 30 mm.

$$f_l = \frac{\kappa_a \rho_f \varepsilon_f E_f}{2} \tag{16}$$

$$\rho_f = \frac{4 n_f t_f}{D} \tag{17}$$

$$\rho_f = \frac{2 n_f t_f (b+h)}{bh} \qquad \text{(b: width, h: depth of the cross-section)} \tag{18}$$

$$\kappa_a = \begin{cases} 1 & \textit{Circular} \\ \left(\dfrac{b}{h}\right) & \textit{Elliptical} \\ 1 - \dfrac{(b-2r)^2 + (h-2r)^2}{3bh} & \text{Re}\,c\,\tan\,\textit{gular} \end{cases} \tag{19}$$

$$\varepsilon_f = \min(0.004, 0.50\varepsilon_{fu}) \tag{20}$$

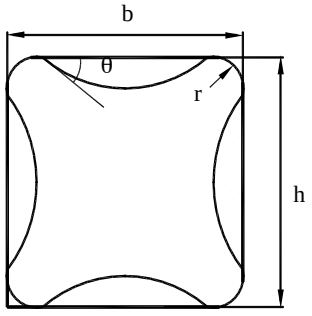

Fig. 11: Effectively confined cross-section

The appearance after the test of a rectangular specimen tested by Ilki et. al (2004) is

shown in Fig. 12. For demonstrating the effects of external FRP jacketing on the axial stress-strain relationships of concrete, experimentally obtained axial stress-axial strain and axial stress-transverse strain relationships of speciemens with circular sections tested by Ilki and Kumbasar (2002) are presented in Fig. 13. In this figure, stress-strain relationships of specimens jacketed with 1, 3 or 5 plies of carbon FRP sheets are presented. As seen in this figure, there is a significant enhancement in deformability and strength due to the FRP jacket.

Fig. 12: FRP confined specimens after testing under axial stresses

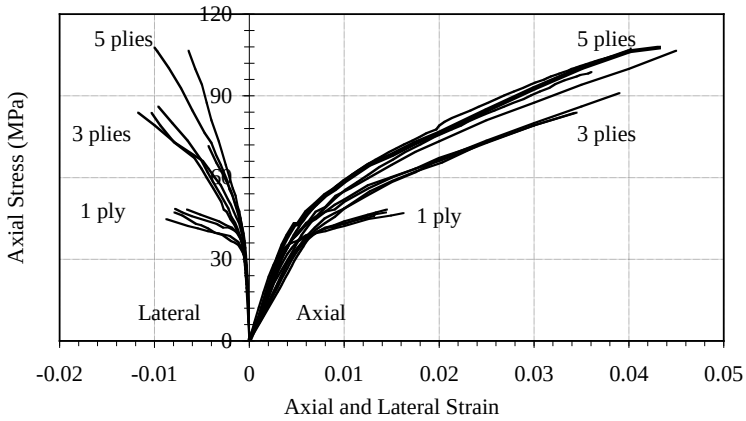

Fig. 13: Axial stress-axial strain and axial stress-lateral strain relationships for carbon FRP jacketed specimens with circular cross-section

5.2 Flexural behaviour

Many structures experienced severe damage due to inadequate ductility under the combined effects of axial load and flexure during the 1999 earthquakes in Turkey, (Fig. 14). In general the reason of insufficient ductility was lack of adequate transverse reinforcement and poor detailing.

As mentioned above, when such concrete columns are confined with external FRP composites in the transverse direction, the stress-strain behaviour is enhanced significantly in terms of strength and particularly ductility. Consequently, moment-curvature relationships of such confined members demonstrate slight enhancement in flexural strength and significant enhancement in ductility. In a recent study by Demir et. al (2005) the moment-curvature relationships of FRP confined columns are obtained analytically and compared with experimental results. Analytical and experimental results, in quite good agreement with each other, demonstrate significant enhancement of the behaviour (Figs. 15, 16).

Fig. 14: Failure of a column in Adapazari due to inadequate detailing of transverse bars

Column	f'_c (MPa)	n	f'_l (MPa)	Plies	Column	f'_c (MPa)	n	f'_l (MPa)	Plies
SC-20-40-0	20	0.40	-	0	RC-20-40-0	20	0.40	-	0
SC-10-40-1	10	0.40	1.11	1	RC-10-40-1	10	0.40	0.77	1
SC-20-40-1	20	0.40	1.11	1	RC-20-40-1	20	0.40	0.77	1
SC-30-40-1	30	0.40	1.11	1	RC-30-40-1	30	0.40	0.77	1
SC-20-40-2	20	0.40	2.21	2	RC-20-40-2	20	0.40	1.55	2
SC-20-40-3	20	0.40	3.32	3	RC-20-40-3	20	0.40	2.32	3
SC-20-20-1	20	0.20	1.11	1	RC-20-20-1	20	0.20	0.77	1
SC-20-60-1	10	0.60	1.11	1	RC-20-60-1	10	0.60	0.77	1

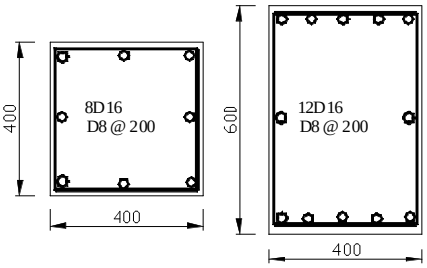

(f'_c: unconfined concrete strength, f'_l: maximum lateral stress as defined by Eq. (16), n: ratio of axial load to axial capacity)

Fig. 15: Details of the columns analysed by Demir et. al (2005)

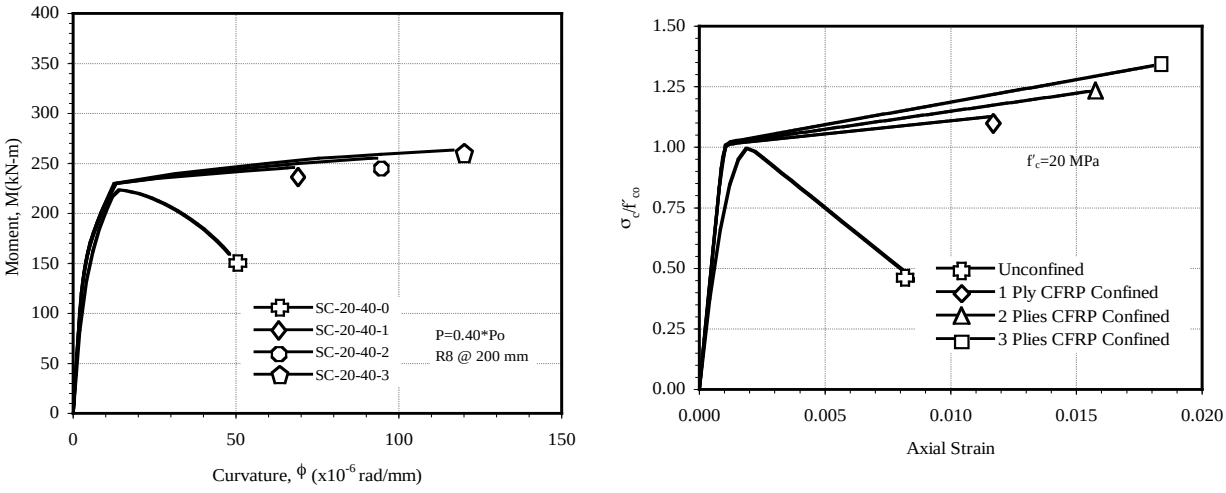

Fig. 16: Analytical moment-curvature relationships obtained by Demir et. al (2005)

Ilki et. al (2005) analyzed the nonlinear response of a typical six storey reinforced concrete frame building, whose columns were retrofitted by external carbon FRP jackets of one ply. The plan of the building is shown in Fig. 17 and the pushover curves before and after retrofitting are presented in Fig. 18. The significant enhancement in the behaviour is due to enhanced ductility under flexural effects provided by FRP jackets.

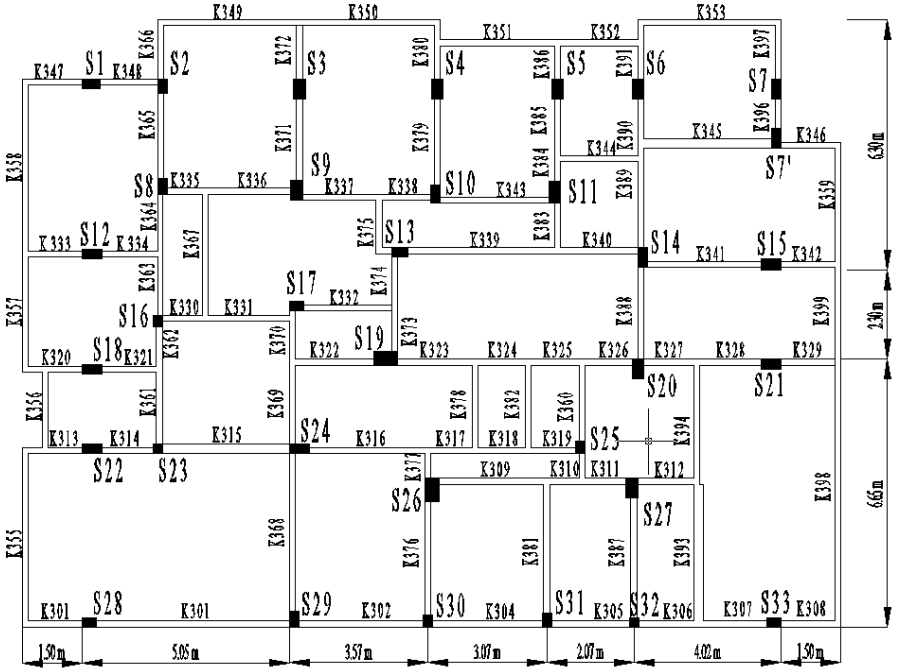

Fig. 17: Typical floor plan of the building analysed by Ilki et. al (2005) before and after retrofitting the columns with FRP wrapping

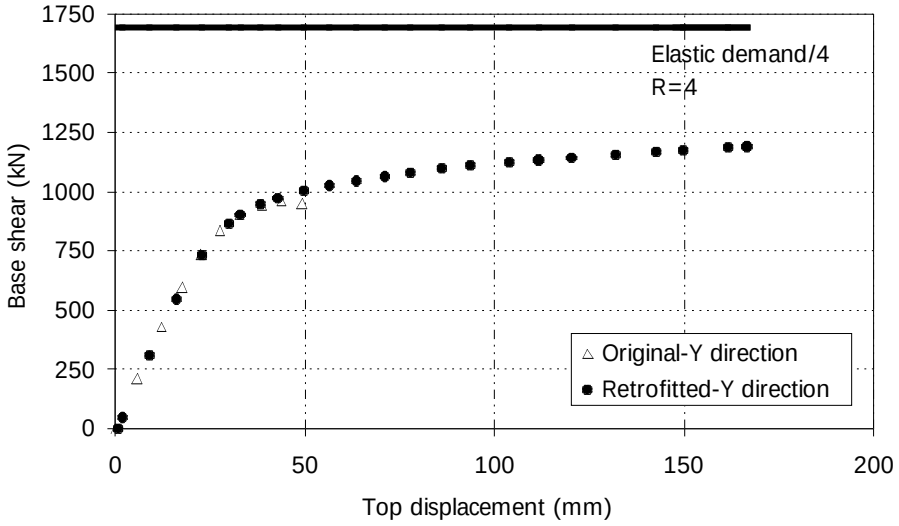

Fig. 18: Pushover curves before and after retrofitting (Ilki et. al 2005)

Specimen	**General explanation**	**Retrofit detail**	**Age (days)**	**f_{cj} (MPa)**	**f_{coj} (MPa)**	**ν**
C-O-1	Original-continuous reinforcement	-	51	10.61	9.02	0.47
R-C-C-3	Retrofitted-continuous reinforcement	3 plies of CFRP	164	13.41*	11.40	0.37
R-C-C-6	Retrofitted-continuous reinforcement	6 plies of CFRP	192	13.41*	11.40	0.37
R-R-C-C-6	C-O-1, after repair and retrofit	6 plies of CFRP	216	13.41*	11.40	0.37

* 180 days strength

Table 2: List of specimens tested by Ilki et. al (2004)

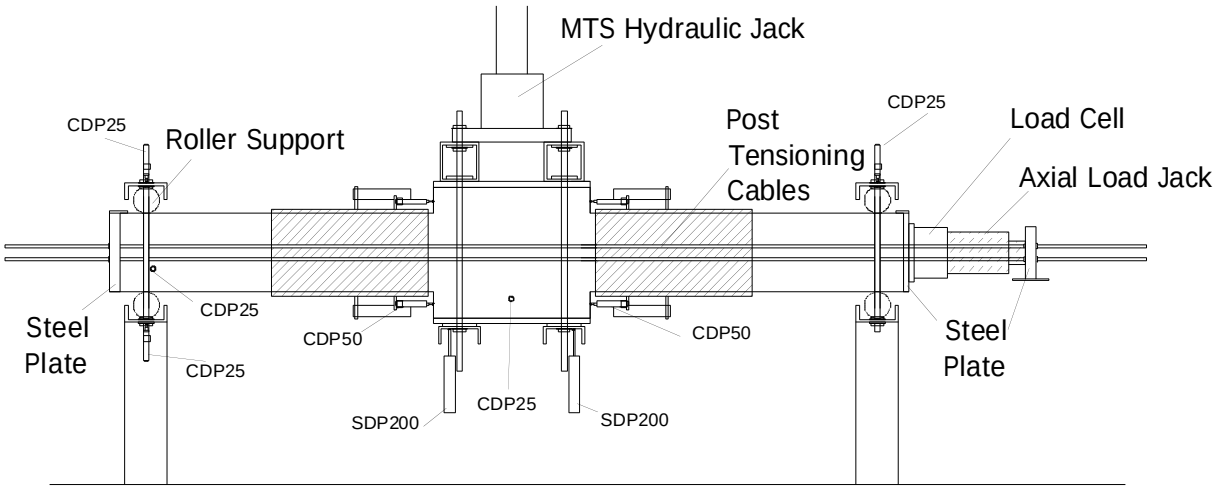

Fig. 19: Test setup (Ilki et. al 2004)

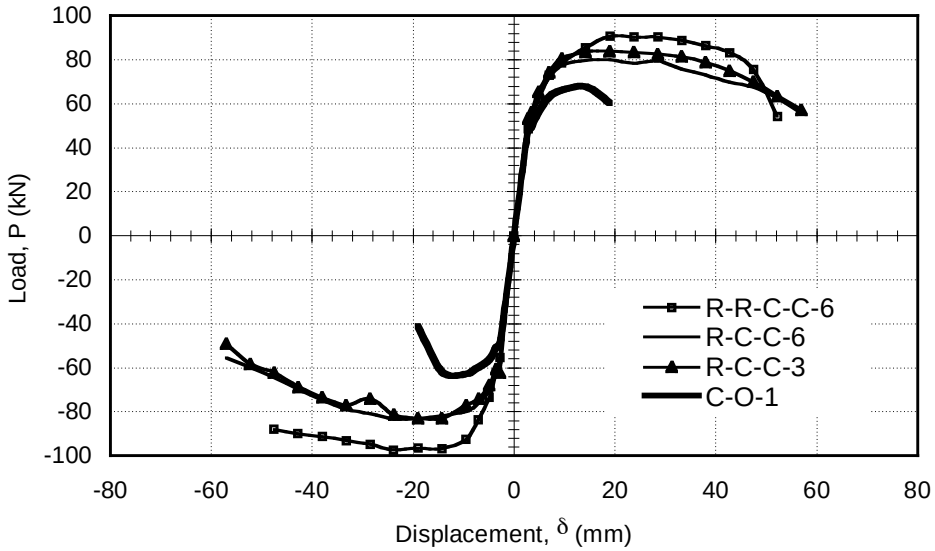

Fig. 20: Envelopes of load-displacement relationships (Ilki et. al 2004)

Ilki et. al (2004) examined the behaviour of non-ductile columns retrofitted by carbon FRP jackets. The experimental work, conducted at the Istanbul Technical University (ITU) Structures and Earthquake Engineering Laboratory, comprised testing of 4 specimens with 200mm×300mm cross section under constant axial and reversed cyclic lateral loading. All specimens were constructed with inadequate transverse reinforcement and low quality concrete, like many existing structures in Turkey (concrete strength of the members at the day of testing was around 10 MPa). Smooth (plain) bars were used for both longitudinal and transverse reinforcement, to represent most of the existing structures built in the 1970s and 1980s. One specimen was tested as a reference specimen, while the others were tested after being retrofitted by different thicknesses of transverse CFRP jackets. All specimens were reinforced so that shear failure would be avoided. The spacing of transverse reinforcement in the confined zones of columns was 200 mm, while in the other regions it was 100 mm. With this detail it was guaranteed that the damage would occur in the confined zones. For retrofitting, confined zones were wrapped by carbon FRP sheets. The purpose of retrofitting was to obtain ductile behaviour by providing confinement and preventing buckling of longitudinal bars. For repair of pre-damaged specimens, damaged zones were filled with repair mortar with compressive strength of 50 MPa, after removing all loose and damaged

concrete. For retrofitting, confined zones were jacketed externally by unidirectional carbon FRP sheets in transverse direction with 0-degree orientation, 7 days after repair. The test setup and specimen details can be seen in Fig. 19 and in Table 2, respectively. It should be noted that in Table 2, f_{cj} and f_{coj} are standard cylinder strength and concrete strength of the member at testing, and ν is the dimensionless axial load determined by the ratio of axial load to axial capacity. f'_{coj} values are determined as 85% of the corresponding f'_{cj} values. Test results are outlined in Fig. 20. As seen in this figure, both ductility and strength are enhanced significantly due to FRP jacketing of potential plastic hinging regions. FRP jackets prevented premature strength loss, by providing sufficient confinement that helped to prevent buckling of longitudinal bars. Pre-damage of specimen R-R-C-C-6 did not have a significant adverse effect on the performance.

In the draft new Turkish Earthquake Resistant Design Code (2005), ductility enhancement by externally bonded FRP jackets under flexural effects is are considered in two different ways, depending on the structural analysis type.

In the case of linear analysis of an existing or retrofitted structure, the engineer needs to decide whether the columns are confined or not, in order to determine the value of the factor R or q (behaviour factor, in Eurocode 8 terminology) that is used for the reduction of elastic internal force demands. In the case of confined columns, larger R or q values are accepted for a certain performance level, compared to unconfined columns. Assuming that a compressive strain in the extreme compression fibre of a column section equal to 0.018 is sufficient for ductile behaviour, then if the thickness used for the external FRP jacket is sufficient to provide an ε_{cc} value of 0.018 by using Eq. (15) above, then the column is assumed to be confined. Consequently, the structural engineer is allowed to use the relatively larger R or q reduction factors given for the confined columns.

In the case of nonlinear analysis of an existing or retrofitted structure, the structural engineer needs moment-curvature relationships of potential plastic hinge regions of concrete members. For that purpose, a simplified stress-strain relationship for FRP confined concrete is recommended in the draft new Turkish Earthquake Resistant Design Code (2005). This bilinear stress-strain relationship is defined with an inflection point corresponding to 0.002 axial compressive strain and $\bar{f}_{ck}$ axial stress and a final point corresponding to ε_{cc} and f_{cc} determined by Eqs. (14) and (15). This relationship is schematically shown in Fig. 21.

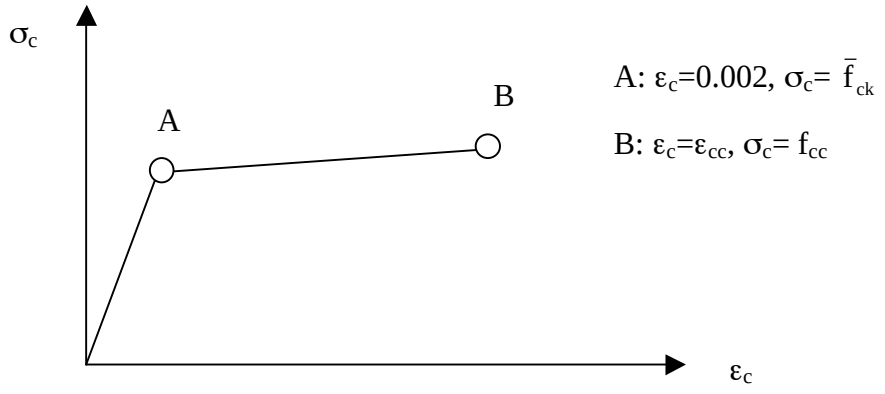

Fig. 21: Simplified stress-strain relationship for FRP confined concrete

6 Clamping of lap splices

Recent earthquakes in Turkey have shown that one of the major causes of severe damage of existing concrete structures is inadeqaute lap splices of longitudinal reinforcement either at the connections of the foundation to the first storey columns or between storeys, Fig. 22. The

reasons of this common problem are low concrete strength, use of smooth (plain) bars even without hooks, inadequate lap splice length, insufficient transverse reinforcement, insufficient concrete cover and inadequate preparation of the concrete surfaces before casting upper storey columns. Unfortunately, in many cases, all these deficiencies exist together.

Fig. 22: Damage due to lap splice deficiency in Kaynasli (Duzce earthquake 1999)

Specimen	**General explanation**	**Retrofit detail**	**Age (days)**	**f_{cj} (MPa)**	**f_{coj} (MPa)**	**ν**
LS-O-1	Original-lap spliced	-	58	11.03	9.38	0.45
R-LS-C-3	Retrofitted-lap spliced	3 plies of CFRP	170	13.41*	11.40	0.37
R-LS-C-6	Retrofitted-lap spliced	6 plies of CFRP	181	13.41*	11.40	0.37
R-R-LS-C-6	LS-O-1, after repair and retrofit	6 plies of CFRP	232	13.41*	11.40	0.37

Table 3: List of specimens with lap splice deficiency tested by Ilki et. al (2004)

Ilki et. al (2004) examined the behaviour of non-ductile columns with lap splice deficiency retrofitted by FRP jackets. Experimental work, conducted at the ITU Structures and Earthquake Engineering Laboratory, comprised four specimens with 200mm×300mm cross section tested under constant axial and cyclic lateral loads. All specimens were constructed with inadequate transverse reinforcement and low quality concrete, like many existing structures in Turkey (concrete strength at testing day was around 10 MPa). Smooth (plain) bars were used for both longitudinal and transverse reinforcement, to represent most of the existing structures built in the 1970s and 1980s. Longitudinal reinforcing bars had lap-splices of 40-bar diameters, whereas the lap lengths should had been around 80-bar diameters, in view of the yield strength and the type of the reinforcing bars and the concrete quality. One specimen was tested as a reference, while the others were tested after retrofitting with different thicknesses of transverse carbon FRP jackets. All specimens were reinforced so that shear failure would be avoided. The spacing of transverse reinforcement in the confined zones of columns was 200 mm, while in the rest it was 100 mm. With this detail it was guaranteed that damage would occur in the confined zones. Reinforcement details can be seen in Fig. 23 and specimen details in Table 3 (the test setup was same as in Fig. 19). Test results are outlined in Fig. 24. As seen in this figure, both ductility and strength are enhanced slightly due to FRP jacketing of potential plastic hinging regions. Although not reflected in these

envelope curves, significant pinching of the load-displacement hysteresis curves were oberved, due to bond-slippage of longitudinal bars giving relatively little energy dissipation.

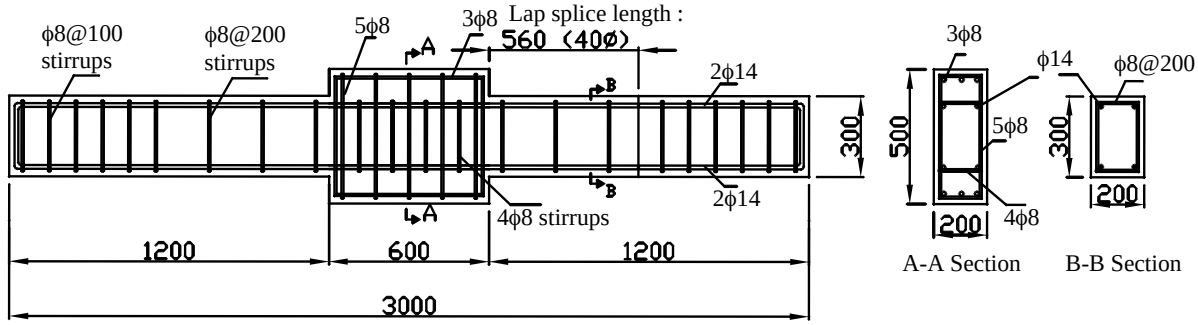

Fig. 23: Reinforcing details for the specimens with lap splice deficiency tested by Ilki et. al (2004)

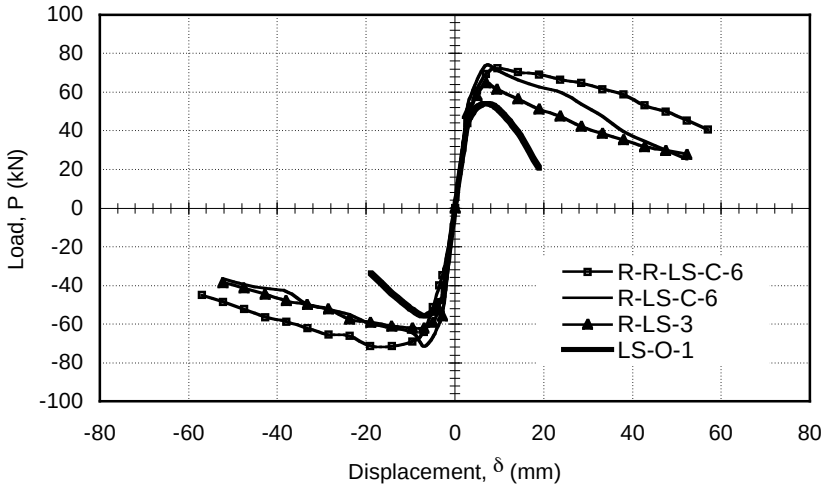

Fig. 24: Envelopes of load-displacement relationships of the specimens with lap splice deficiency (Ilki et. al 2004)

Bousias et. al (2004) investigated the effectiveness of carbon FRP wrapping as a seismic retrofit measure of rectangular columns with poor detailing, and in particular with lap splicing of bars at floor levels. 12 cantilever columns with smooth bars and hooked ends and another 12 specimens with ribbed bars and straight ends, with or without carbon FRP wrapping , were cyclically tested to failure, (Fig. 25). Other test parameters were lap splice length, thickness of FRP jacket and length of the member over which FRP wrapping wis applied. In unretrofitted columns with smooth bars and hooked ends, the low deformation capacity does not depend on lapping length, if it is at least equal to 15 bar diameters. Unlike what happens for smooth bars with hooked ends, unretrofitted columns with straight ribbed bars lose deformation capacity when lap splice length decreases below 45 bar diameters. In columns with smooth bars and hooked ends, no systematic effect of the number of layers and the length of application of the FRP, or even of the lapping, on the force and cyclic deformation capacity and the rate of strength degradation was found. However, a decrease in lapping seems to reduce energy dissipation in the retrofitted columns. In retrofitted columns with straight ribbed bars, five carbon FRP layers were more effective than two layers. However, the improvement in effectiveness was not commensurate to the number of carbon FRP layers. It seems there is a limit to what FRP wrapping can do: if the lapping of straight ribbed bars is as short as 15 bar diameters, its adverse effects on force capacity and energy dissipation can not be fully removed by FRP wrapping.

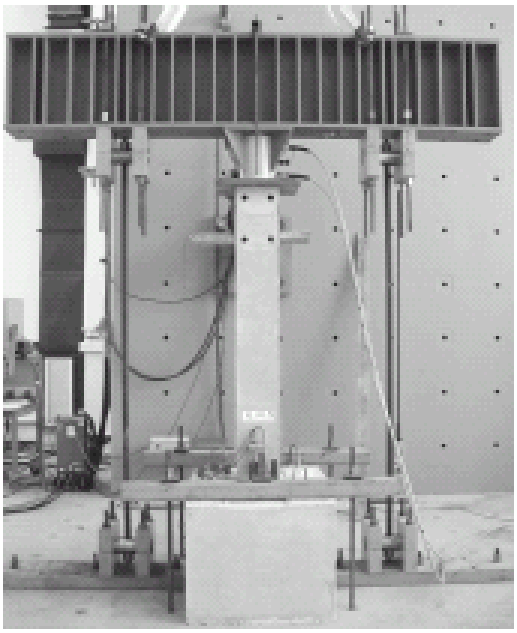

Fig. 25: Test setup (Bousias et. al 2004)

In the draft new Turkish Earthquake Resistant Design Code (2005), it is permitted to overcome the lap splice deficiency problem by using adequate amount of FRP composite sheets externally bonded on the columns in the transverse direction. However, since there is not enough information for the case of smooth (plain) bars, this enhancement in the lap splice behaviour provided by FRP composites can be taken into account only when the longitudinal reinforcement consists of deformed bars. In addition, to obtain enhancement in the behaviour of lap spliced columns, the cross-sectional aspect ratio should be at most equal to 2. The thickness of FRP required in the case of insufficient lap splices can be determined from Eqs. (21) and (22) according to the draft code. These equations are based on the studies carried out by Seible et. al (1997). Similar equations are given by the Eurocode 8 Part 3 (2005).

$$t_f = \chi_a \frac{500 b_w (f_k - f_{hs})}{E_f} \tag{21}$$

$$f_k = \frac{A_s \bar{f}_{yk}}{\left(\frac{p}{2n} + 2(\phi + d')\right) L_s} \tag{22}$$

In these equations, f_k is the lateral pressure to be provided by the FRP jacket over the lap splice length L_s. In Eq. (21), b_w is the section width and f_{hs} is the clamping stress provided by the internal transverse reinforcement corresponding to a 0.001 tensile strain. χ_a is the confinement effectiveness coefficient, to be calculated from Eq. (19). In Eq. (22) A_s is the total area of each spliced bar, $\bar{f}_{yk}$ is the yield strength of longitudinal bars, p is the perimeter line in the column cross-section along the inside of longitudinal steel, n is the number of spliced bars along the perimeter p, ϕ is the largest diameter of longitudinal steel bars and d' is the thickness of the concrete cover.

References

Antoniades, K.K., Salonikios, T.N. and Kappos, A.J. (2005). Tests on seismically damaged reinforced concrete walls repaired and strengthened using fibre-reinforced polymers, J. of Comp. for Const., Vol. 9, No. 3, pp. 236-246.

Antonopoulos, C.P., Triantafillou, T.C. (2003). Experimental investigation of FRP-strengthened RC beam-column joints, J. of Comp. for Const., Vol. 7, No. 1, pp. 39-49.

Bousias, S., Spathis, A-L., and Fardis, M.N. (2004). Seismic retrofitting of columns with lap-splices through CFRP jackets, Proc. of 13th World Conf. on Earthquake Engineering, Vancouver.

CEN (2005) European Standard EN1998-3:2005 Eurocode 8: Design of sturctures for Earthquake Resistance - Part 3, Assessment and retrofitting of buildings. Brussels.

CSA (2002) Design and construction of building components with fibre-reinforced polymers, S806-02, Canadian Standards Association.

Demir, C., Ilki, A. and Kumbasar, N. (2005). Moment-curvature relationships for columns jacketed with FRP composites, Proc. of *fib* Symposium "Keep Concrete Attractive", Budapest.

Fardis, M.N. and Khalili, H. (1982). FRP-encased concrete as a structural material, Magazine of Concrete Research, Vol. 34, No. 121, pp.191-202.

fib Bulletin 14 (2001) Externally bonded FRP reinforcement for RC structures, *fib*, Lausanne.

Fukuyama, H. and Sugano, S. (2000). Japanese seismic rehabilitation of concrete buildings after the Hyogoken-Nanbu earthquake, Cement and Concrete Composites, Vol. 22, pp. 59-79.

Galal, K. (2002). Modeling and rehabilitation of nonductile spatial RC columns. Ph.D. Thesis, McMaster University, Hamilton, Canada.

Galal, K., Arafa, A. and Ghobarah, A. (2005). Retrofit of RC square short columns, Engineering Structures, Vol. 27, pp. 801-813.

Gergely, J., Pantelides, C.P. and Reaveley, L.D. (2000). Shear strengthening of RC T joints using CFRP composites, J. of Comp. for Const., Vol. 4, No. 2, pp. 56-64.

Ghobarah, A. and Said, A. (2001). Seismic rehabilitation of beam-column joints using FRP laminates, J. Earthquake Engineering, Vol. 5, No. 1, pp. 113-129.

Ghobarah, A. and Said, A. (2002). Shear strengthening of beam-column joints, Engineering Structures, Vol. 24, pp. 881-888.

Guide for the design and construction of externally bonded FRP systems for strengthening concrete structures, ACI Committee 440, Oct. (2001).

Ilki, A. and Kumbasar, N. (2002). Behaviour of damaged and undamaged concrete strengthened by carbon fibre composite sheets, Structural Engineering and Mechanics, Vol. 13, No. 1, pp. 790.

Ilki, A. and Kumbasar, N. (2003). Compressive behaviour carbon fibre composite jacketed concrete with circular and non-circular cross-sections, J. Earthquake Engineering, Vol. 7, No. 3, pp. 381-406.

Ilki, A., Kumbasar, N. and Koc, V. (2004). Low strength concrete members externally confined with FRP sheets, Structural Engineering and Mechanics, Vol. 18, No. 2, pp. 167-194.

Ilki, A., Tezcan, A., Koc, V. and Kumbasar, N. (2004). Seismic retrofit of non-ductile rectangular reinforced concrete columns by CFRP jacketing, Proc. of 13th World Conf. On Earthquake Engineering, Vancouver.

Ilki, A., Darilmaz, K., Demir, C., Bedirhanoglu, I., and Kumbasar, N. (2005). Non-linear seismic analysis of a reinforced concrete building with FRP jacketed columns, Proc. of *fib* Symposium "Keep Concrete Attractive", Budapest.

ISIS, An introduction to FRP strengthening of concrete structures, ISIS, Educational Module 4, Canada.

Mander, J.B., Priestley, M.J.N., and Park, R. (1988). Theoretical stress-strain model for confined concrete, ASCE J. of Structural Div., Vol. 114, No. 8, pp. 1804-1826.

Richart, F.E., Brandtzaeg, A. and Brown, R.L. (1929). The failure of plain and spirally reinforced concrete in compression, Bulletin 190, Univ. of Illinois, Engineering Experimental Station, Champaign, Ill.

Saatcioglu, M. and Razvi, S.R. (1992). Strength and ductility of confined concrete, ASCE Structural Journal, Vol. 118, No. 6, pp. 1590-1607.

Said A. (2001) Seismic rehabilitation of beam-column joints using advanced composite materials. M.Eng. Thesis, McMaster University, Hamilton, Canada.

Seible, F., Priestley, M.J.N., Hegemier, G.A. and Innamorato, D. (1997). Seismic retrofit of RC columns with continuous carbon fibre jackets, ASCE Journal of Composites for Construction, Vol. 1, No. 2, pp. 52-62.

Teng, J.G. and Lam, L. (2002). Compressive behaviour of carbon fibre reinforced polymer-confined concrete in elliptical columns, J. of Struct. Eng., Vol. 128, No. 12, pp. 1531543.

Teng, J.G., Lam, L. and Chen, J.F. (2004). Shear strengthening of rc beams with FRP composites, Prog. Struct. Engng Mater., Vol. 6, pp. 173-184.

Toutanji, H.A. (1999). Stress-strain characteristics of concrete columns externally confined with advanced fibre composite sheets, ACI Materials Journal, Vol. 96, No. 3, pp. 397-404.

Tsonos, A.G. and Stylianidis, K. (2002). Seismic retrofit of beam-to-column joints with high-strength fibre jackets, European Earthquake Engineering, Vol. 16, No. 2, pp. 56-72.

Turkish Ministry of Public Works and Settlement (2005) Draft Turkish Earthquake Resistant Design Code, Ankara.

Turkish Standards Institute (2000) TS500, Requirements for Design and Construction of Reinforced Concrete Structures, Ankara.

Seismic retrofitting of RC beam-column joints using FRP

Khalid M. Mosalam
University of California, Berkeley, USA

1 Introduction[1]

Many existing reinforced concrete (RC) buildings have deficient beam-column joints. Pre 1970 codes, governing design and construction did not require ties in the joint area. In addition, beam bottom reinforcement is typically anchored only 150 mm into the joint region. This is practiced on the assumption that under gravity load, the beam is subjected to negative moment at the joint to the column and therefore the bottom reinforcement is in compression. However, when subjected to lateral load, the beam-column joints may fail in shear and/or bond-slip of the beam bottom reinforcement, which is in tension. Due to these deficiencies, the joint may experience shear or bond-slip failure modes. These brittle types of failure will significantly reduce the overall ductility of the structure and may lead to excessive lateral deformation of multistorey RC building subjected to strong earthquake loading.

Exterior beam-column joints are more vulnerable than interior joints, which are partially confined by beams attached to four sides of the joint and contribute to the core confinement. Accordingly, there are some differences between the shear behaviour of interior and exterior joints when subjected to earthquake ground motion due to joint confinement by beams. However, the bond-slip mode of failure of exterior and interior joints is similar. To reduce the seismic hazard, it is necessary to apply practical and economical rehabilitation techniques and to upgrade the shear resistance of beam-column joints and to improve the anchorage of the beam bottom reinforcement. The objective of the beam-column joint rehabilitation is to strengthen the shear and bond-slip resistance in order to eliminate these types of brittle failures and instead ductile flexural hinging in the beam will take place.

This chapter focuses on modeling deficient beam-column joint regions. First, observations from recent earthquakes in Turkey are discussed focusing on the damages observed in beam-column joint regions of deficiently detailed RC buildings. Motivated by these observations, a detailed computational model to represent the shear deformation and bond-slip in beam-column joint regions is discussed. This model can be used in modeling RC beam-column joints in static (pushover) or dynamic (time history) nonlinear frame analysis to take into account the additional lateral deformation due to rotations of the joint region caused by shear deformation and/or bond slip of the beam longitudinal reinforcement. Subsequently, experimental studies on fiber-reinforced polymer (FRP) retrofit of beam-column joints is discussed followed by design procedures of this retrofit technique of deficient buildings.

2 Observations from recent earthquakes in Turkey

During recent earthquake events such as August, 17, 1999 Kocaeli (Turkey) earthquake, it was observed that beam-column joint failures contributed to the severe damage and collapse of many RC buildings [Sezen et al., 2000 and 2003]. Description of the state-of-practice for building seismic design and construction in Turkey, and comparison between the US and

[1] Part of this chapter is based on a draft document prepared for ACI 440 with important contributions from Professor Ahmed Ghobarah, McMaster University and Professor Ayman Mosallam, University of California, Irvine.

Turkish codes can be found in [Sezen et al., 2000 and 2003]. Moreover, these references include evaluations of the performance of RC frame and wall buildings and their components during 1999 Kocaeli earthquake. This section is a summary of the performance of beam-column joints during this earthquake based on the findings in [Sezen et al., 2000 and 2003].

Typical details for an existing column and beam reinforcing bars are shown in Figure 1. Bent-up bars are shown in the typical beam section. Corner column bar are spliced above the floor slab with lap lengths of 40 to 70 bar diameters. Side-face column reinforcing bars are either spliced per corner bar in the upper storey or terminated above the joint with 180-degree hooks as shown Figure 1. No additional transverse reinforcement for the purpose of confinement is provided in the beam hinge, beam-column joint, or splice regions.

One type of beam damage is shown in Figure 2 where the shown building suffered a partial storey collapse because the fault ruptured beneath the building. The beams shown were forced to accommodate the partial collapse and were badly damaged at the beam-column joint due to slip of the smooth longitudinal beam reinforcing bars. In many cases, beam bottom reinforcing bars were inadequately anchored through the beam-column joint.

Damage to beam-column joints is shown in Figure 3 where much of the framing is essentially intact but many of the beam-column joints were heavily damaged. A detailed view of one of the damaged joints is also shown in Figure 3. Apparently, beam reinforcing bars anchorage in the joint is inadequate and no transverse ties are present in the joint region.

The photograph of a building in Figure 4 that was under construction in Adapazari, Turkey at the time of the earthquake shows severe damage in the beam-column joints. However, the horizontal transverse ties maintained the integrity of the joints.

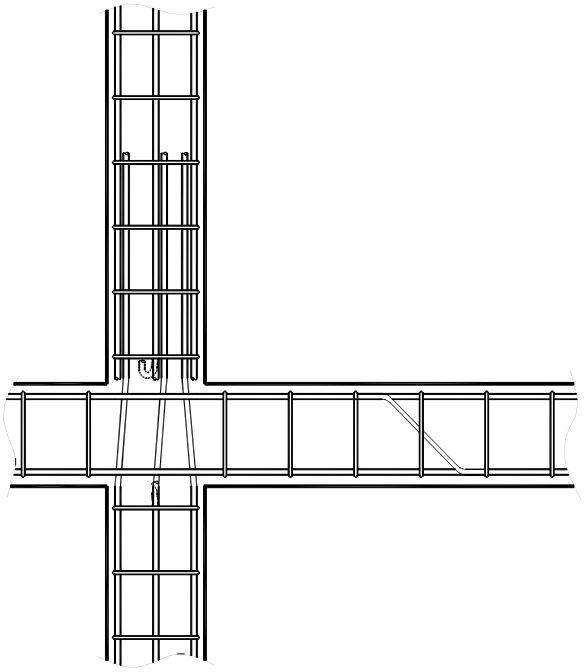

Fig. 1: Typical beam and column reinforcing bar details in the damaged RC buildings during 1999 Kocaeli earthquake [Sezen et al., 2000]

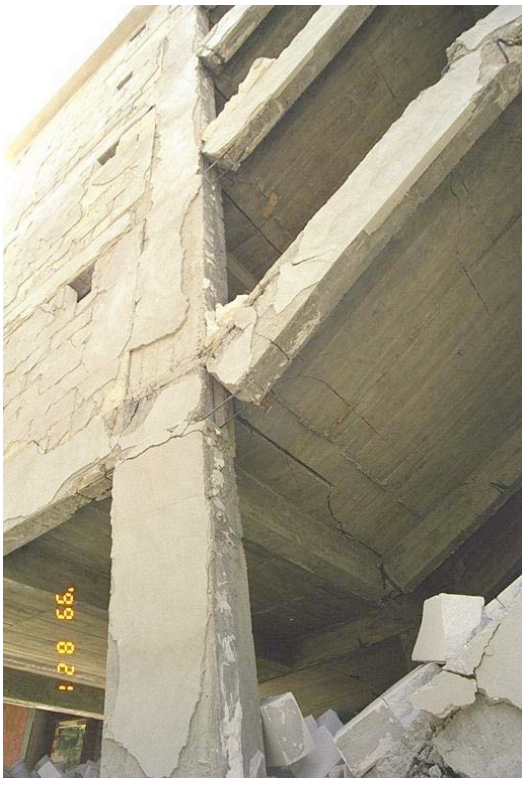

Fig. 2: Damage to non-ductile RC beam during 1999 Kocaeli earthquake [Sezen et al., 2000]

a) Building overview b) Detailed view of beam-column joint damage

Fig. 3: Building collapse due to failure of beam-column joints in 1999 Kocaeli earthquake [Sezen et al., 2000]

Fig. 4: Damage to a new RC moment-frame beam-column joints in 1999 Kocaeli earthquake [Sezen et al., 2000]

Much has been written in the aftermath of 1999 Kocaeli earthquake about the poor quality of residential and commercial construction in the epicentral region. The detailing and quality of the residential construction, perhaps most of it not rigorously engineered, was poor by modern US and Turkish standards. Both poor construction practices and the continued use of non-ductile seismic detailing were the primary reasons for most of the building collapses. Shear reinforcement was lacking in most damaged columns. In contrast with the code design provisions, common use of 90^0 hooks for transverse reinforcement reduced the lateral strength and confinement of columns. Short columns, poor detailing in beam-column joints, strong-beam weak-columns, and use of inconsistent unreinforced masonry infill walls were among other reasons for the widespread destruction in the region affected by the earthquake.

3 Modeling RC beam-column joints

3.1 General

Adequately detailed beam-column joint mobilizes two self-equilibrating mechanisms of shear transfer, namely the truss mechanism, Figure 5, and the diagonal compression strut, Figure 6 [Naito et al., 2001]. The former assumes proper bond characteristics between the joint reinforcement and the surrounding concrete. However, the latter is the principal mechanism after bond deterioration.

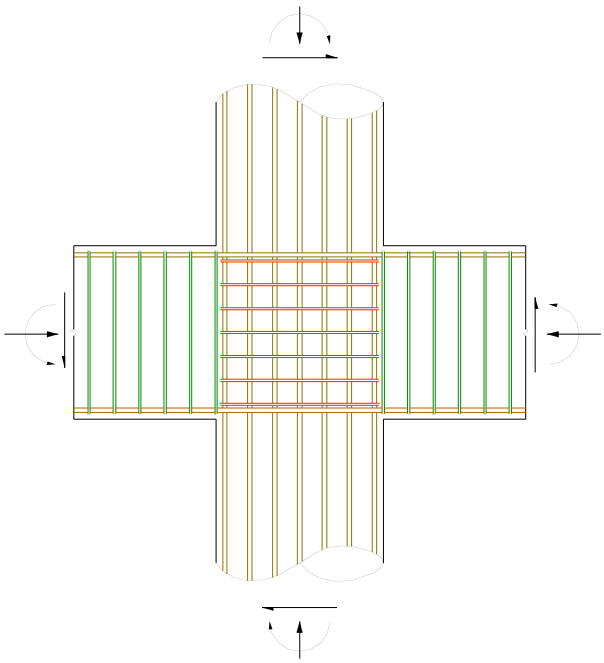

Fig. 5: Adequately detailed RC beam-column joint [Naito et al., 2001]

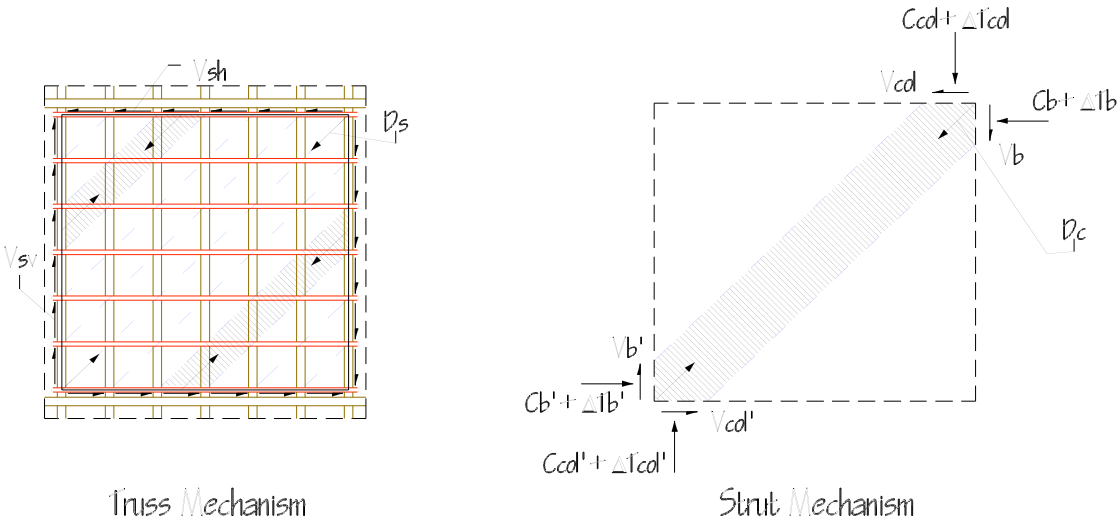

Fig. 6: Load transfer mechanisms of adequately detailed RC beam-column joint [Naito et al., 2001]

3.2 Shear deformation

In this section a summary of the model proposed in [Biddah and Ghobarah, 1999] is

provided. The model is a two-dimensional (2D) panel representation of the joint in the loading direction and subjected to biaxial normal stresses and in-plane shear stresses. The model utilizes the softening truss model theory described in [Hsu, 1993]. This model satisfies:

- Equilibrium of stress resultants
- Compatibility of deformations, and
- Constitutive laws of concrete (accounting for softening of the concrete in compression caused by cracking due to tension in the perpendicular direction) and reinforcement (assumed linear elastic). Amongst many constitutive laws for concrete relating the average principal tensile stress, f_{c1}, to the principal tensile strain, ε_1, the one illustrated in Figure 7 can be adopted. The main assumption is that principal strain directions coincide with the principal stress directions which is not the case after cracking2. However, the difference is within $\pm 10^0$ [Vecchio and Collins, 1986].

Vecchio and Collins (1982) tested RC panels under biaxial stresses including pure shear and determined the principal compressive stress in the concrete, f_{c2}, as a function of the principal compressive strain, ε_2, and the coexisting principal tensile strain, ε_1 [Collins and Mitchell, 1991]. The suggested function is

$$f_{c2} = f_{c2\max}\left[2\left(\varepsilon_2/\varepsilon'_c\right) - \left(\varepsilon_2/\varepsilon'_c\right)^2\right] \quad (1)$$

$$f_{c2\max}/f'_c = 1/\left(0.8 + 170\varepsilon_1\right) \le 1.0 \quad (2)$$

where ε'_c is the strain at ultimate compressive strength and typically taken as 0.002.

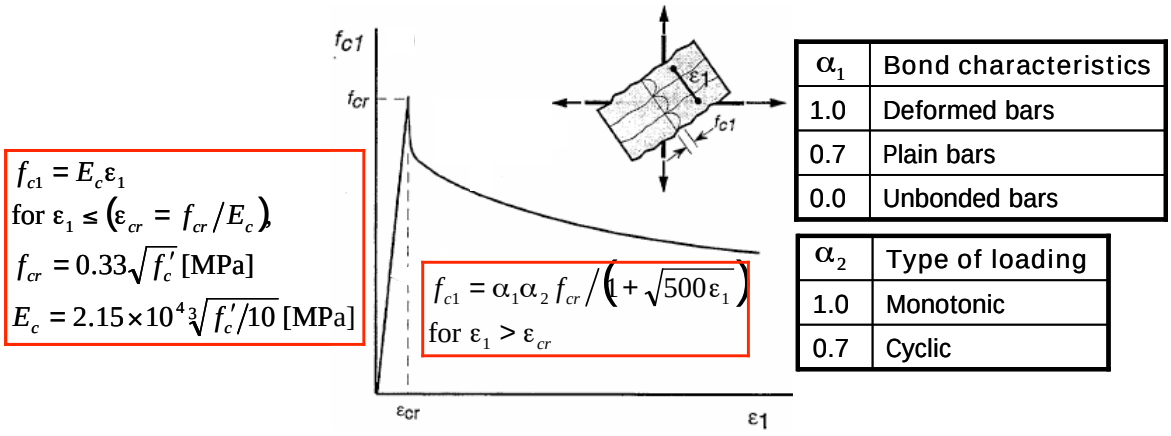

α_1	Bond characteristics
1.0	Deformed bars
0.7	Plain bars
0.0	Unbonded bars

α_2	Type of loading
1.0	Monotonic
0.7	Cyclic

Fig. 7: Concrete constitutive law in tension

At high shear forces, the two sets of stresses at a crack and between cracks must be statically equivalent. Accordingly, transmitting tension across cracks, f_{c1}, will require local shear stress, v_{ci}, on the crack surface. Therefore,

$$f_{c1} = v_{ci}\tan\theta + \frac{A_v}{b_w s}\left(f_{vy} - f_v\right) \quad (3)$$

where θ is the angle of inclination of the diagonal cracks with the horizontal, A_v is the total cross-sectional area of the transverse vertical reinforcement within one horizontal spacing s, b_w is the width of the web of the concrete cross-section, and f_v is the stress in the transverse

reinforcement between the diagonal cracks. This transverse reinforcement is assumed to yield, i.e. $f_v = f_{vy}$, at the diagonal crack location where f_{vy} is the yield strength of the transverse reinforcement. Based on experiments by Walraven (1981), Vecchio and Collins (1986) suggested the following limiting value:

$$v_{ci} = \frac{0.18\sqrt{f_c'}}{0.3 + [24w/(a+16)]} \text{ [MPa]} \quad (4)$$

where $w = \varepsilon_1 s_{m\theta}$ is the inclined crack width in [mm] of cracks at average spacing of $s_{m\theta}$, and a is the maximum aggregate size in [mm]. The average inclined crack spacing depends on the crack control characteristics of the reinforcement in both horizontal and vertical directions and the inclination of the cracks [Biddah and Ghobarah, 1999]. This is illustrated by the following procedure:

- A code designed joint with width b_j must include cross-sectional area of tie bars, say $A_{tie} = \frac{0.06\sqrt{f_c'}}{f_y} b_j S$ [MPa] according to the [CSA, 1994], within a vertical spacing S.
- If the cross-sectional area of the ties in an existing joint, $A_{tie,existing} \geq A_{tie}$, then $s_{m\theta} = 300$ mm, otherwise,

$$s_{m\theta} = 1 \Big/ \left(\frac{\sin\theta}{S_{mx}} + \frac{\cos\theta}{S_{my}} \right) \quad (5)$$

where S_{mx} and S_{my} are the average crack spacing that would result if the element was subjected to horizontal and vertical tension, respectively. This fictitious crack spacing can be determined as follows:

- Given the area of the horizontal joint reinforcement A_{sx} within one vertical spacing S_y, and knowing the beam depth d_{beam}:

  If $A_{sx} < 0.004 b_j S_y$, then $s_{mx} = 0.9 d_{beam}$, otherwise $s_{mx} = S_y$ (6)

- Given the area of the vertical joint reinforcement A_{sy} within one horizontal spacing S_x, and knowing the column depth d_{column}:

  If $A_{sy} < 0.004 b_j S_x$, then $s_{my} = 0.9 d_{column}$, otherwise $s_{my} = S_x$ (7)

The previously discussed model for shear deformation of beam-column joints, based on the softening truss approach, targets the development of shear stress-shear strain, $\tau - \gamma$, relationship of the panel element representing a beam-column joint. Note that a program such as Membrane-2000, refer to http://www.ecf.utoronto.ca/~bentz/m2k.htm, can be easily used for this purpose. For practical application in frame analysis, this $\tau - \gamma$ relationship is represented by a rotational spring with a predefined moment-rotation, $M - \theta$, relationship defining the characteristics of an added *rotational spring* in the computational model for frame analysis, Figure 8. This $M - \theta$ relationship can be monotonic as maybe needed for pushover analysis or cyclic as maybe needed in the more sophisticated nonlinear time history analysis. In that regard the rotation, θ, representing the change in the angle between the connected beams and columns, not to be confused with the inclination of the diagonal cracking as discussed above, is directly related to the shear deformation, γ. On the other hand, the total moment, $\sum M_b$, to be transferred from the beams to the columns through the beam-column joint is determined from equilibrium as demonstrated by Figure 9 and from the following derivation.

$$M = V_b L_b = V_{col} L_c \Rightarrow V_b = M/L_b, \quad V_{col} = M/L_c$$

$$M_b = V_b\left[(L_b - h_c)/2\right] \Rightarrow 2M_b = M\left(1 - h_c/L_b\right)$$

$$T_b + C_b = 2M_b / jd$$

$$V_{col} = \frac{2M_b}{L_c\left(1 - h_c/L_b\right)}$$

$$V_{jh} = T_b + C_b - V_{col} = 2M_b\left[\frac{1}{jd} - \frac{1}{L_c\left(1 - h_c/L_b\right)}\right]$$

$$\Rightarrow \sum M_b = 2M_b = \frac{V_{jh}}{\left[\frac{1}{jd} - \frac{1}{L_c\left(1 - h_c/L_b\right)}\right]} \qquad (8)$$

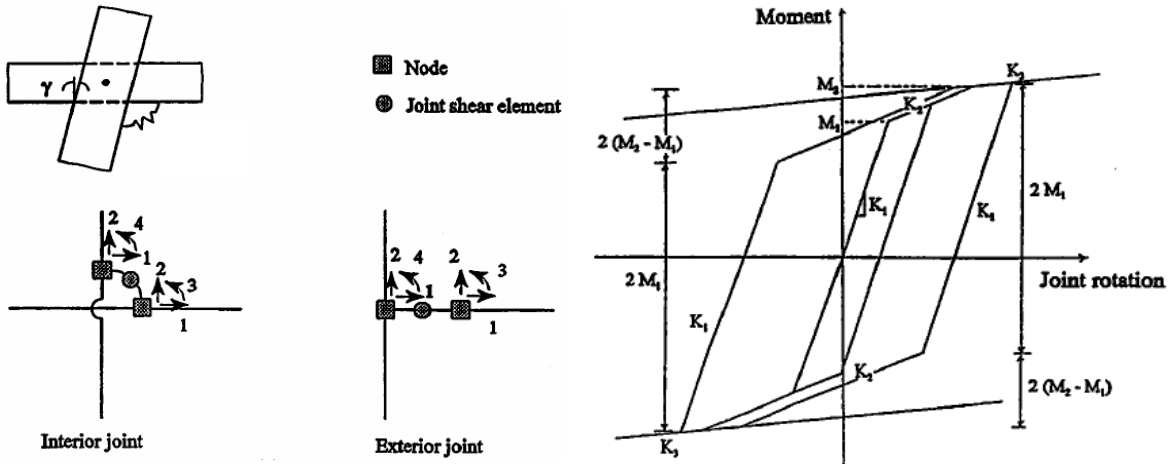

Fig. 8: Idealization of joint shear in frame analysis together with a possible hysteretic model for moment-rotation of shear spring [Biddah, 1997]

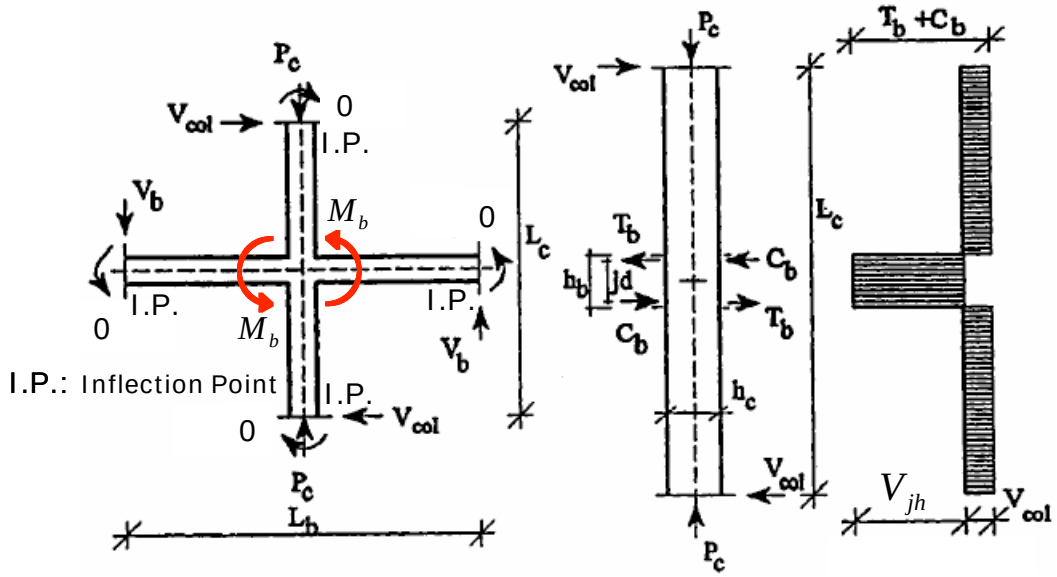

Fig. 9: Equilibrium of interior beam-column joint [Biddah, 1997]

3.3 Slip deformation

This section summarizes the model proposed in [Biddah and Ghobarah, 1999] for additional rotations caused by the anchorage slip of the reinforcing bars from the beam-

column joints. These additional rotations can significantly contribute to the total inelastic deformations of RC multistorey frames subjected to strong earthquake motions. The model starts by defining the additional bilinear $M-\theta$ relationship shown in Figure 10.

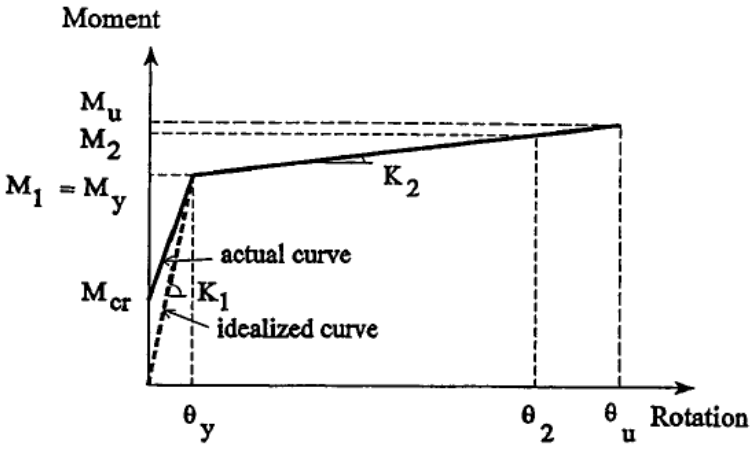

Fig. 10: Model for moment-rotation of bond-slip spring under monotonic loading [Biddah, 1997]

The slip, Δ_s, at the beam-column interface is obtained by integrating the steel strain (neglecting the concrete strain) distribution over the length, L_s, shown in Figure 11. Before yielding, i.e. $\varepsilon_s \le \varepsilon_y$, the uniform concrete bond stress can be expressed by:

$$f_b = 600\varepsilon_s\sqrt{f_c'}\ [\text{MPa}] \tag{9}$$

From the above equation, Figure 12, and assuming linear stress–strain relationship of steel, i.e. $f_s = \varepsilon_s E_s$ where E_s is Young's modulus of steel, one obtains

$$L_s = \frac{d_b E_s}{2400\sqrt{f_c'}} \tag{10}$$

$$\Delta_s = \frac{1}{2}L_s\varepsilon_s = \frac{d_b f_s}{4800\sqrt{f_c'}} \tag{11}$$

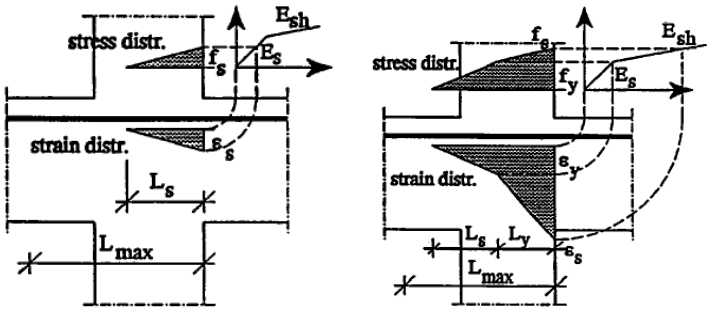

a) before yielding, $\varepsilon_s \le \varepsilon_y$ b) after yielding, $\varepsilon_s > \varepsilon_y$

Fig. 11: Strain and stress distribution in the joint model for bond slip of tension longitudinal bars of the beam [Biddah, 1997]

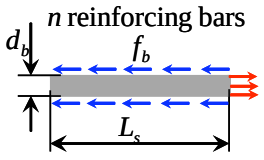

$$\text{Equilibrium}: n\pi d_b f_b L_s = n\pi\frac{d_b^2}{4} f_s \Rightarrow L_s = \frac{d_b f_s}{4 f_b}$$

Fig. 12: Equilibrium of a bar segment subjected to uniform bond stress

After yielding, i.e. $\varepsilon_s > \varepsilon_y$, the slope of the bilinear $M-\theta$ relationship, Figure 10, depends on the following factors:

- The strain hardening characteristics of the reinforcing bars,
- The thickness of the concrete cover relative to the dimensions of the cross-section confined by the transverse steel,
- The amount of transverse steel,
- The size of the yield region,
- The penetration of yielding into the beam-column joint … etc.

The yield development length, L_y as shown in Figure 11b, can be determined as follows:

$$L_y\,[\text{mm}] = \begin{cases} 2000\chi - 2000 & \text{for } 1 < \chi \le 1.05 \\ 500\chi - 425 & \text{for } \chi > 1.05 \end{cases}, \quad \chi = \frac{f_s}{f_y} \le \frac{f_u}{f_y} \tag{12}$$

where f_u is the ultimate strength of the reinforcing bars. Therefore,

$$\Delta_s = \frac{1}{2}L_s\varepsilon_y + L_y\varepsilon_y + \frac{1}{2}L_y(\varepsilon_s - \varepsilon_y) = (L_s + 2L_y)\frac{\varepsilon_y}{2} + \frac{1}{2}L_y\frac{f_s - f_y}{E_{sh}}$$

$$\Delta_s = \frac{L_s + 2L_y}{E_s}\frac{f_y}{2} + (\chi f_y - f_y)\frac{L_y}{2E_{sh}}$$

$$\Delta_s = \left[\frac{L_s + 2L_y}{E_s} + (\chi - 1)\frac{L_y}{E_{sh}}\right]\frac{f_y}{2} \tag{13}$$

where E_{sh} is the slope of the strain hardening branch of the stress-strain relationship of steel assuming no plastic flow where strain hardening immediately follows the onset of yielding. The upper limits on the length of the slip region $(L_s + L_y)$, i.e. $L_{\max} \ge (L_s + L_y)$, and of the yield development length (L_y), i.e. $L_{y\max} \ge L_y$, are defined in Figure 13 [Morita and Kaku, 1984].

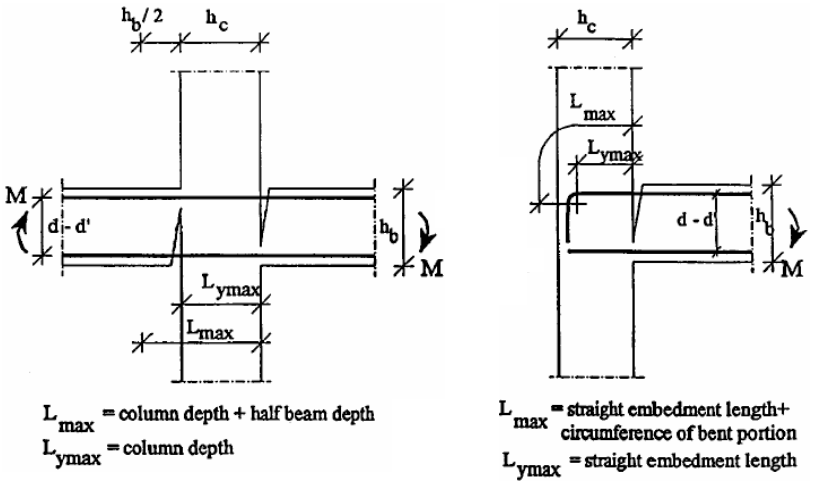

a) Interior joint b) Exterior joint

Fig. 13: Definition of upper limit lengths for the slip region and yield development in beam-column joints [Biddah, 1997]

3.3.1 Yielding before slippage $(L_s \le L_{\max})$

The stiffness before yielding, K_1, Figure 10, is determined from:

$$K_1 = \frac{M_y}{\theta_y} = \frac{A_s f_y (d-d')}{\Delta_y/(d-d')} = \frac{n\pi \frac{d_b^2}{4} f_y (d-d')^2}{\frac{d_b f_y}{4800\sqrt{f_c'}}} = 1200 n\pi d_b (d-d')^2 \sqrt{f_c'} \quad (14)$$

where $\theta_y = \Delta_y/(d-d')$ and Δ_y are the rotation and bar slippage at yielding, respectively, $(d-d')$ is the effective depth of the beam, and d_b and n are the bar diameter and number of tensile reinforcing bars in the beam, respectively.

After yielding, the stiffness, K_2, Figure 10, is assumed a function of χ defined in Eq. (12). With reference to Figure 10 and letting $L_y = L_{y\max}$ and $\chi_2 = f_{s2}/f_y = M_2/M_y \le f_u/f_y$ at point 2, then

$$K_2 = \frac{M_2 - M_y}{\theta_2 - \theta_y} = \frac{(\chi_2 - 1) A_s f_y (d-d')}{(\Delta_2 - \Delta_y)/(d-d')} = \frac{(\chi_2 - 1) n\pi \frac{d_b^2}{4} f_y (d-d')^2}{\left[\frac{L_s + 2L_{y\max}}{E_s} + (\chi_2 - 1)\frac{L_{y\max}}{E_{sh}}\right]\frac{f_y}{2} - \frac{L_s f_y}{2E_s}}$$

$$K_2 = \frac{(\chi_2 - 1) n\pi d_b^2 (d-d')^2 E_s}{2L_{y\max}[2 + (\chi_2 - 1)/\zeta]} \quad (15)$$

where $\zeta = E_{sh}/E_s$.

If $L_s + L_{y\max} > L_{\max}$, then in the above derivation, $L_y = L_{\max} - L_s$ at point 2. Accordingly,

$$K_2 = \frac{(\chi_2 - 1) n\pi d_b^2 (d-d')^2 E_s}{2(L_{\max} - L_s) L_{y\max}[2 + (\chi_2 - 1)/\zeta]} \quad (16)$$

3.3.2 Pullout before yielding $(L_s > L_{\max})$

In this case $(K_2 = 0)$,

$$M_1 = n\pi \frac{d_b^2}{4} f_s (d-d') = n\pi \frac{d_b^2}{4} f_y \left(\frac{L_{\max}}{L_s}\right)(d-d') \quad (17)$$

$$\theta_1 = \frac{\Delta_1}{(d-d')} = \frac{1}{2}\varepsilon_s L_{\max}\frac{1}{(d-d')} = \frac{1}{2}\left(\varepsilon_y \frac{L_{\max}}{L_s}\right) L_{\max}\frac{1}{(d-d')} = \frac{1}{2}\frac{f_y}{E_s}\frac{L_{\max}^2}{L_s}\frac{1}{(d-d')} \quad (18$$

$$K_1 = \frac{M_1}{\theta_1} = \frac{n\pi d_b^2 E_s (d-d')^2}{2L_{\max}} \quad (19)$$

3.3.3 Joint macro-element

In addition to the shear deformation represented by a rotational spring in Figure 8, another rotational spring can be added to represent the reinforcing bars bond-slip, Figure 14. In this case a hysteretic behavioural model can be adopted to account for stiffness degradation, strength deterioration as well as pinching (Figure 14). Refer to [Biddah and Ghobarah, 1999] for further discussion about experimental validation of the beam-column joint model and how to account for confining effect of transverse beams and slab contribution to the joint shear resistance. The model was also used in nonlinear time history analyses of 3 and 9 storey non-ductile buildings [Ghobarah and Biddah, 1999]. The analyses were conducted for the buildings with and without retrofit using corrugated steel jackets of the columns and joints and using external steel angles and straps to rehabilitate the discontinuity of the beam bottom reinforcement.

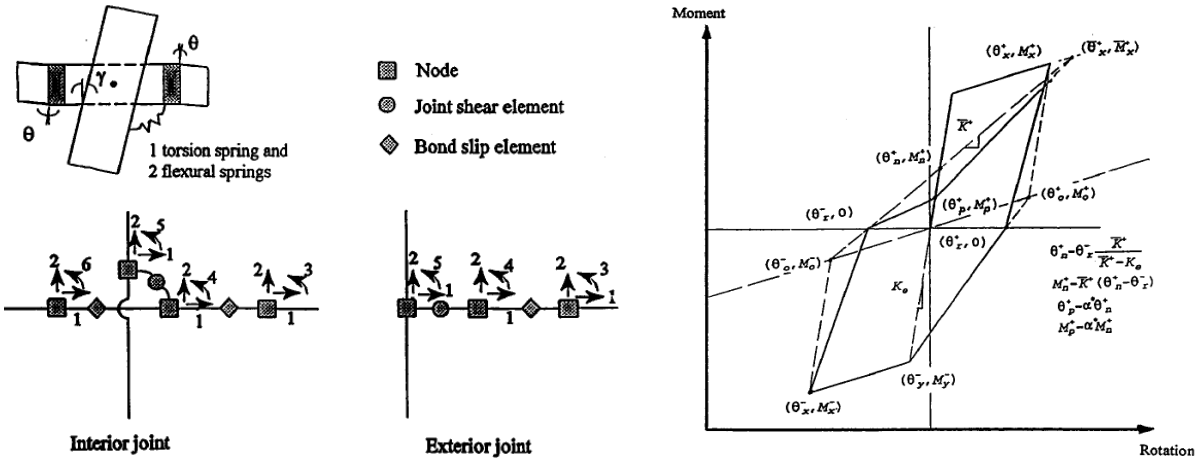

Fig. 14: Idealization of joint shear and bond-slip in RC frame analysis and hysteretic model for moment-rotation of bond-slip spring accounting for pinching [Biddah, 1997]

4 Experimental investigation of FRP retrofitting of RC beam-column joints

4.1 General

Several retrofitting techniques for RC beam-column joints to enhance the shear resistance have been proposed and reported in the technical literature with much attention during the last two decades. Recent studies on the effect of shear and bond-slip rehabilitation on the behaviour of RC frame have shown significant improvement in the overall frame ductility [Ghobarah and Youssef, 1999].

Concrete jacketing is one of the most common techniques [Corazo and Durrani, 1989, Alcocer and Jirsa, 1993]. Unfortunately, concrete jacketing suffers from disadvantages such as:

- Application is complex,
- It is an intrusive technique, and
- It is labor intensive and costly.

Therefore, concrete jacketing is not very popular for strengthening beam-column joints.

Another beam-column strengthening technique is based on attaching external flat or corrugated steel sheets or plates to the joint face using non-shrink grout or steel anchors and rods. An interior beam-column joint was rehabilitated and tested under simulated earthquake loads [Estrada, 1990]. Steel plates were anchored to the beam bottom face at each side of the joint and connected together using threaded steel rods driven through the column. The idea is to replace the effect of inadequately anchored steel bars with equivalent steel plates. On the other hand, steel plate jacketing was used to enhance the joint shear strength. Test results showed that joint jacketing was ineffective in improving the joint shear strength due to the slippage of the steel plates. The specimen reached a drift of 4% without significant deterioration in strength. Flat steel plates were used to confine the joint in an attempt to prevent spalling of concrete and to maintain the concrete integrity [Beres et al., 1992a, b]. Steel channels were attached to the beam bottom face to prevent the slip of the bars. This scheme was found to be efficient in preventing the bars slippage, increasing the joint shear strength and reducing the rate of strength deterioration. Ghobarah et al. (1996) used corrugated steel sheet jacketing for joint confinement, leaving a gap between the concrete and the jacket to be filled with grout. The shear strength of the rehabilitated joints was increased

and the failure mode became flexural hinging in the beam [Biddah et al., 1997]. However, the corrosion potential and the need to fire proof the added steel elements pose a challenge to the widespread application of this technique.

One of the effective materials for deficient RC beam-column joint retrofit is the FRP composites as it offers several advantages including:

- Fast and simple application with minimum disruption to occupants,
- Less need for costly labor, and
- Material is corrosion resistant and eventually cost effective.

Retrofitting schemes using FRP jackets were developed and tested by several researchers such as [Mosallam, 2000; Pantelides et al., 2000; Gergely et al., 2000; Prota et al., 2001; Ghobarah and Said, 2001 and 2002; Clyde and Pantelides, 2002; El-Amoury and Ghobarah, 2002; Antonopoulos and Triantafillou, 2003; Ghobarah and El-Amoury, 2005]. Some of these experimental research activities are discussed in the following section.

4.2 FRP retrofit of RC beam-column joints

Carbon fiber-epoxy reinforced polymer (CFRP) material was used to retrofit an external beam-column joint in shear [Pantelides et al., 2000]. The retrofitted specimen was wrapped with multiple layers of CFRP laminates. The joint shear capacity was increased by 25% and the specimens reached 5% drift. Significant improvements in the strength, stiffness and ductility of the retrofitted joints were also achieved.

Glass fiber-epoxy reinforced polymer (GFRP) material was used to retrofit external beam-column joints [Ghobarah and Said, 2001 and 2002]. Two joints were tested as control specimens with different column axial load (10% and 20% of the column axial capacity). The control specimens were tested and then repaired and re-tested. Two other specimens were rehabilitated and tested. The behaviour of the rehabilitated specimens was significantly improved over the as-built specimens; refer to Figures 15 and 16. The brittle shear failure of the beam-column joint was eliminated and instead ductile flexural hinging of the beam occurred. The joints tested in this research program were designed with deficient shear strength but with adequate positive reinforcement anchoring in the joint, i.e. bond-slip failure was not included in the rehabilitation scheme, Figure 15. The shown repaired joint was wrapped with U-shaped GFRP laminates. The ends of the composite laminates were tied together using two steel plates and four steel tie rods through the joint, Figure 16b. On the other hand, the shown retrofitted specimen was wrapped with three-diagonal GFRP laminates, Figure 16c.

Ghobarah and El-Amoury (2005) investigated the CFRP retrofit of external beam column joints with bond slip deficiency due to improper anchorage of beam bottom reinforcement, Figure 17a. The retrofit provided systems to transmit the tensile forces of the bars to the concrete, Figures 17b and 17c. T-B12 failed due to complete de-bonding of the composite sheets from the beam and column faces where the steel angle was inadequate to force the crack to form at the toe of the angle rather than at the beam-column interface. On the other hand, T-B11 failed due to ductile flexure hinging in the beam. Refer to Figure 18 for comparison between the beam tip force-displacement envelopes of the three joints shown in Figure 17.

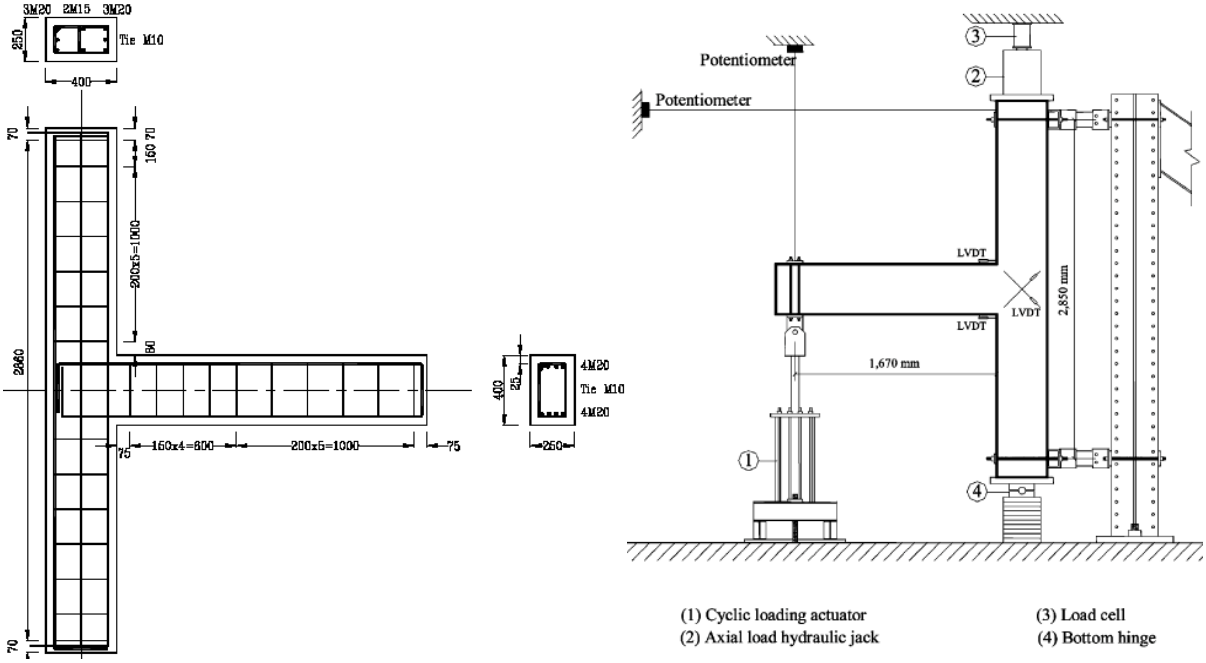

a) Joint with shear deficiency

b) Test setup

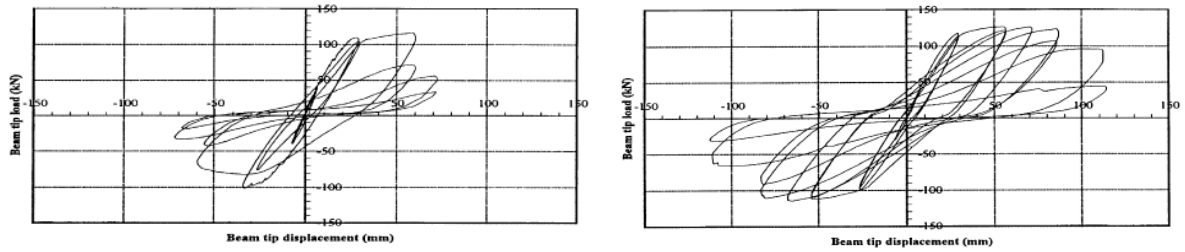

c) As-built specimen

d) GFRP repaired specimen

Fig.15: Tests of external beam-column joints with shear deficiency [Ghobarah and Said, 2001]

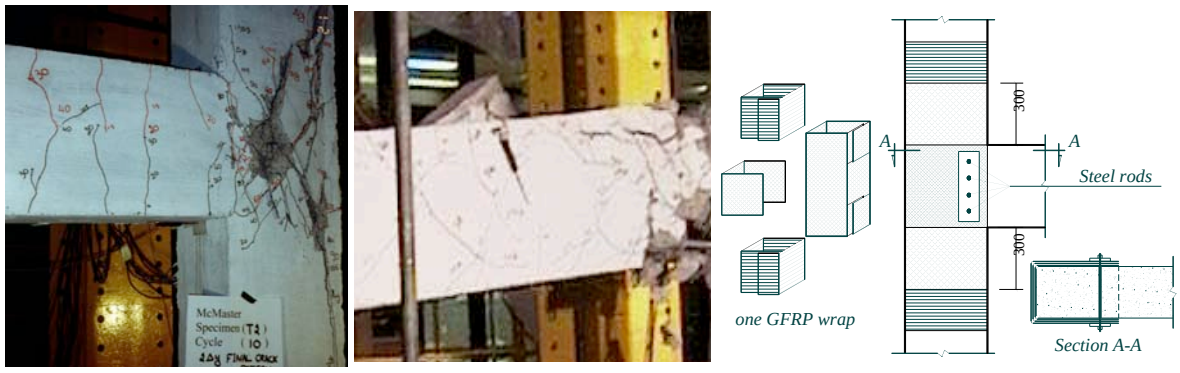

a) As-built specimen

b) GFRP repaired specimen

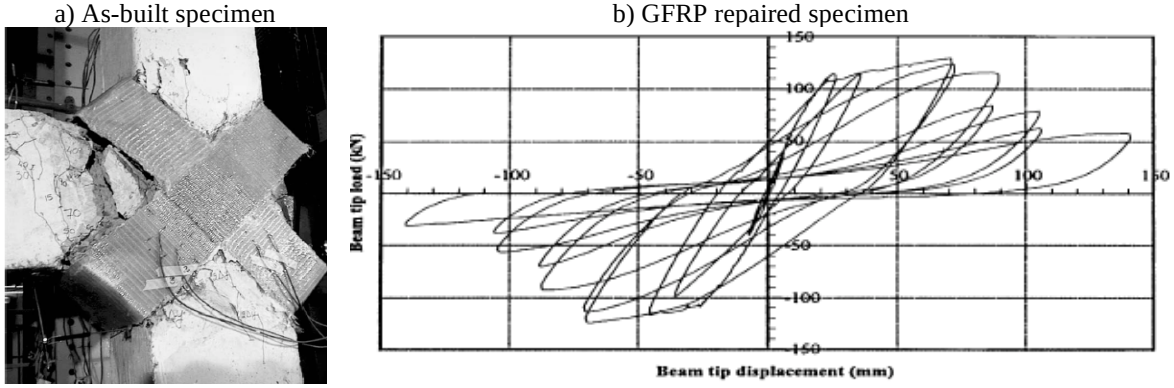

c) GFRP retrofitted specimen

Fig. 16: Repair and retrofit of external beam-column joints with shear deficiency [Said, 2001]

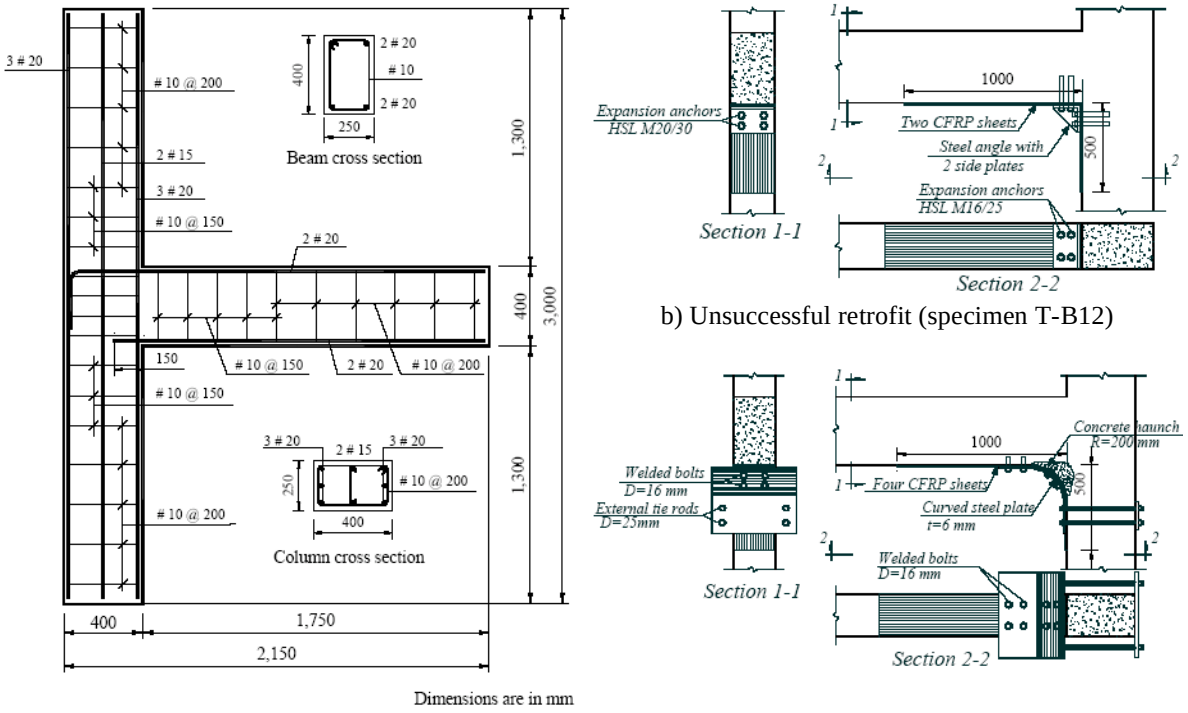

a) Joint with anchorage deficiency (T-B10)

b) Unsuccessful retrofit (specimen T-B12)

c) Successful retrofit (specimen T-B11)

Fig. 17: CFRP retrofitting of external beam-column joints with anchorage deficiency [El-Amoury, 2004]

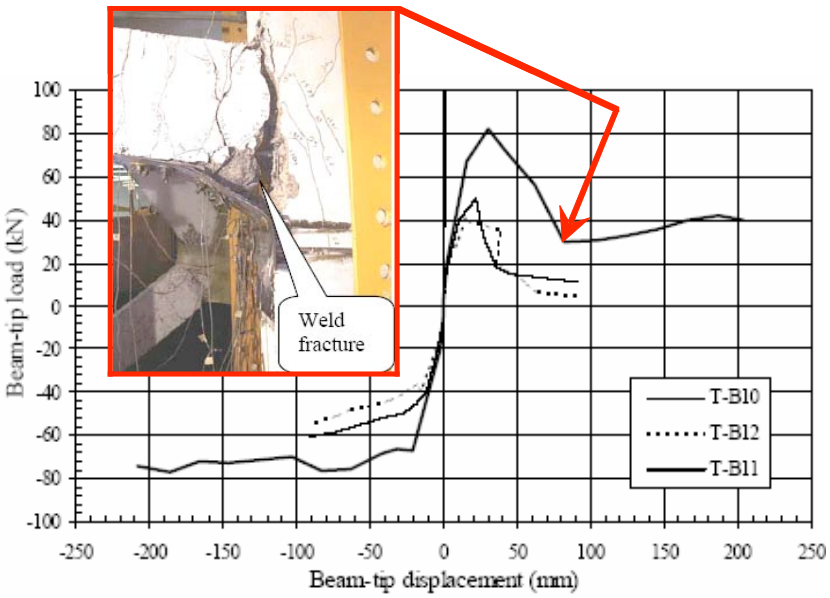

Fig. 18: Comparison of hysteretic envelopes of anchorage deficient external joints [El-Amoury, 2004]

The experimental program in [Ghobarah and El-Amoury, 2005] also investigated the CFRP/GFRP retrofit of external beam column joints with both joint shear and bond slip deficiencies, Figure 19a. Two retrofit systems were investigated as illustrated in Figs. 19b and 19c. T-SB8 failed due to de-lamination of the new concrete causing malfunctioning of the installed threaded rods leading to bond-slip failure of the beam bottom reinforcement. On the other hand, T-SB7 experienced fracturing of the top tie rod near the end of the test with excellent behaviour of the joint jacket without de-bonding of the GFRP laminates. It was clear that the tying mechanism of the bottom bars of T-SB7 was effective in preventing the pullout

of the bottom bars and effectively upgrading the specimen. Refer to Figure 20 for comparison between the beam tip force-displacement envelopes of the three joints shown in Figure 19. It is to be noted that specimen T-SB3 (designated T0 in [El-Amoury and Ghobarah, 2002]) was also retrofitted using two other schemes with GFRP only in [El-Amoury and Ghobarah, 2002] as illustrated in Figure 21 with the results shown in Figure 22. In this case, lower strength was achieved compared with that of Figure 20.

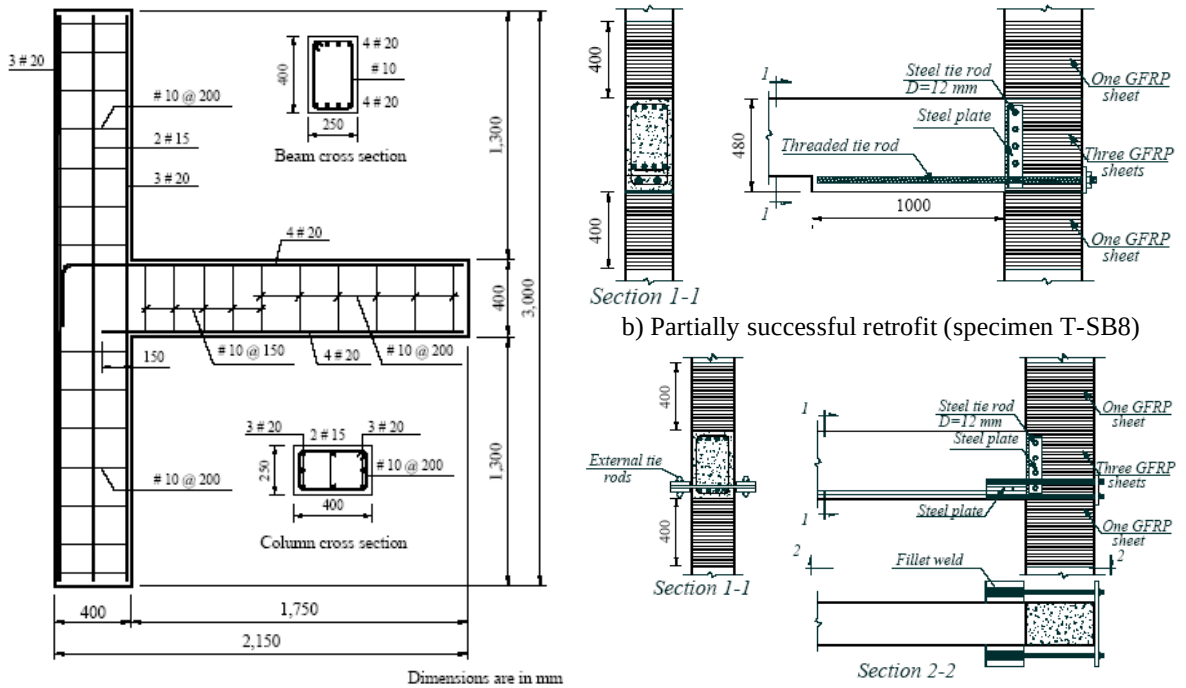

a) Shear and anchorage deficient joint (T-SB3)

b) Partially successful retrofit (specimen T-SB8)

c) Successful retrofit (specimen T-SB7)

Fig. 19: CFRP/GFRP retrofit of deficient external beam-column joints [El-Amoury, 2004]

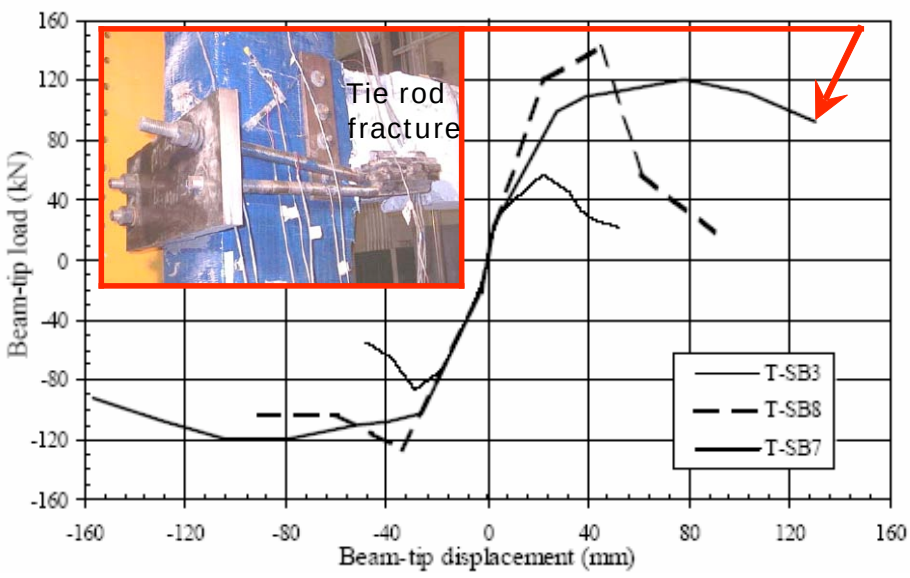

Fig. 20: Comparison of hysteretic envelopes of deficient external joints [El-Amoury, 2004]

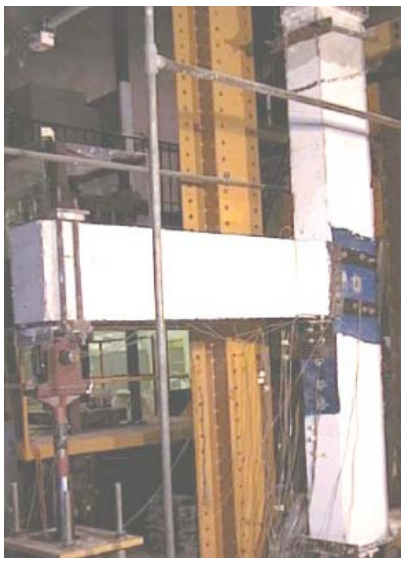

a) Specimen TR1 (4 unidirectional GFRP sheets extending 1000 mm on the underside of beam and 500 mm along column with corner steel angle connected to column with 4 Hilti adhesive anchors)

b) Specimen TR2 (8 GFRP sheets on the underside of the beam and column with corner steel angle 500x225x225x8 mm connected to beam with 8 steel bolts 20 mm dia and sandwiching column with 500x200x25 mm back steel plate using 4 steel rods 25 mm dia. 3 mm thick U-shaped steel plates are used in beam and 2 steel plates 320x100x12 mm with 4 steel rods 12 mm dia. are used in column)

Fig. 21: GFRP retrofit of deficient external beam-column joints in [El-Amoury and Ghobarah, 2002] [Courtesy. A. Ghobarah]

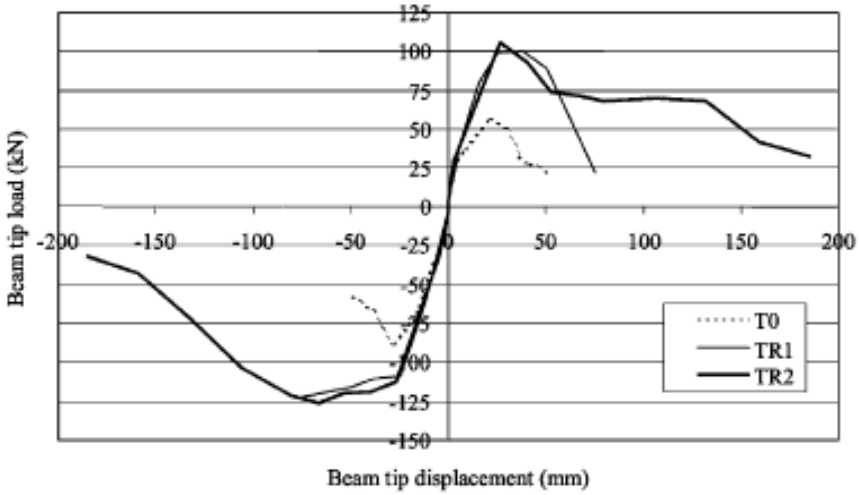

Fig. 22: Comparison of hysteretic envelopes of deficient external joints [El-Amoury, 2004]

Limited experimental research was conducted on RC beam-column joints retrofitted using composite rods to strengthen the column flexural strength and composite laminates to strengthen the joint shear [Prota et al., 2001]. Antonopoulos and Triantafillou (2003) conducted an experimental study using carbon/epoxy and E-glass/epoxy retrofitted beam-column joints subjected to simulated seismic loading. The results highlighted the importance of using mechanical anchors to prevent premature de-bonding of composite laminates. The experimental results also provided important information on the impact of different design parameters including:

- FRP area fraction,
- Distribution of FRP laminates between the beam and the column,

- Column axial load,
- Internal joint steel reinforcements,
- Damage initiation,
- Type of composite system (carbon/epoxy vs. E-glass/epoxy and wet lay-up vs. procured composite systems), and
- Effect of the existence of transverse beam(s).

Although several tests were conducted on exterior beam-column joints retrofitted with FRP, very limited tests are available on interior beam-column joints retrofitted with FRP. One of such rare studies is the one conducted by Mosallam (2000) where he used composite overlays to strengthen simple models of interior beam-column joints and recorded increases in the strength, the stiffness, and the ductility of the repaired as well as the retrofitted specimens compared with the as-built specimens. However, these specimens were not representative of true shear-critical behaviour, but they behaved more like column-type elements subjected to bending without axial force.

5 Design of FRP retrofit system of RC beam-column joints

The design approach is based on providing FRP reinforcement to replace the deficiency in the required joint shear reinforcement or the inadequately anchored steel reinforcement. This section describes a two step design for flexure and shear. The exposition is based on the proposed design procedure of retrofitting external beam-column joints with GFRP laminates discussed in [El-Amoury and Ghobarah, 2002].

5.1 Flexure

The FRP composites are used to replace the inadequately anchored bottom steel bars of the beam. In this design, the composite laminates are provided to develop the same moment capacity of a beam section that is reinforced with well-anchored longitudinal bars. This moment limit is imposed on the flexural strengthening system to avoid creating a beam that is stronger than the column.

5.1.1 The beam flexural moment

The moment capacity of the beam section is determined taking into account the over-strength of the reinforcing steel. The tensile force in the steel is calculated using the actual yield strength as follows:

$$T_s = 1.25 f_y A_s \tag{20}$$

where T_s is the tension force in the bottom steel bars, f_y is the nominal yield strength of the steel, and A_s is the cross-sectional area of the tension steel reinforcing bars.

The concrete compression block depth, a, can be calculated using the well-known force equilibrium expression

$$T_s = C_c + C_s = \alpha_1 f_c' a b + A_s' E_s \varepsilon_s' \tag{21}$$

where C_c is the compression force in concrete, C_s is the compression force in the compression reinforcement, $\alpha_1 = 0.85 - 0.0015 f_c' \geq 0.67$ is equivalent compression block reduction factor (according to [CSA, 1994]), f_c' is the concrete compressive strength, b is

the beam width, A_s' is the area of the compression steel, E_s is the modulus of elasticity of the steel, and $\varepsilon_s' \le f_y/E_s$ is the strain in the compression steel assumed to remain elastic.

The resisting positive moment of the section at the face of the column, M_r, is

$$M_r = C_c(d - a/2) + C_s(d - d') \tag{22}$$

where d is the effective beam depth, and d' is the concrete cover of the compression steel.

5.1.2 Required number of FRP laminates

The design objective is to achieve the same flexural capacity of the beam section with adequately anchored steel bars. In this design procedure, three assumptions are made:

- Strain compatibility between different materials is assumed.
- The ultimate concrete strain in compression is taken as 0.0035.
- The contribution of the inadequately anchored steel bars is ignored.

The tensile force developed in the composite laminate can be estimated as,

$$T_{frp} = \varepsilon_{frp} E_{frp} A_{frp} \tag{23}$$

where ε_{frp} is the strain developed in the FRP laminates, which should be less than the ultimate strain, and can be derived from the geometry, as shown in Figure 23, E_{frp} is the modulus of elasticity of the FRP; and A_{frp} is the cross-sectional area of the FRP laminates.

The depth of the concrete compression block a can be calculated from the moment equilibrium equation

$$M_r = \alpha_1 f_c' a b(t - a/2) + A_s' E_s \varepsilon_s' (t - d') \tag{24}$$

where t is the total depth of the concrete cross-section, Figure 23.

The strain in the laminates can be written as,

$$\varepsilon_{frp} = \varepsilon_c' [(t - c)/c] \tag{25}$$

where ε_c' is the compression strain in concrete, and c is the location of the neutral axis from the extreme concrete compression fibers.

The force equilibrium of the section can be written as,

$$T_{frp} = C_c + C_s \tag{26}$$

$$T_{frp} = \varepsilon_{frp} E_{frp} n_{frp} t_{frp} b \tag{27}$$

where n_{frp} is the number of FRP laminates with t_{frp} thickness each to be determined.

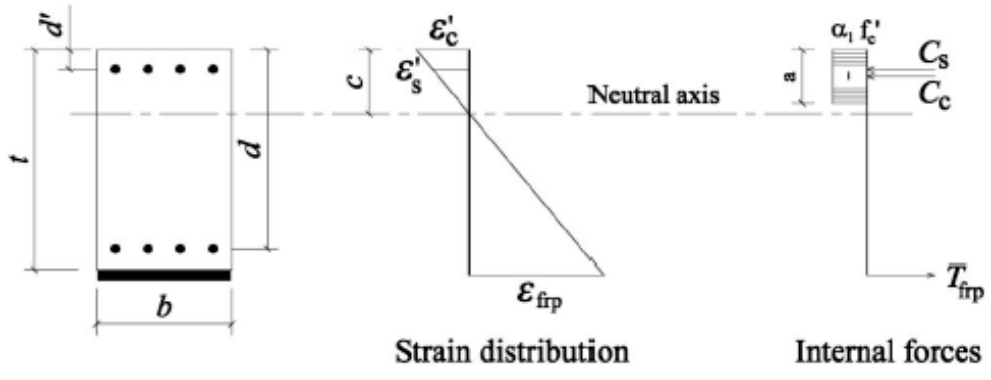

Fig. 23: Determination of the required number of FRP laminates

5.2 Joint shear

The behaviour of RC beam-column joints was discussed by Park and Paulay (1975). For external joints, the developed shear forces in the joint can be obtained from the equilibrium conditions as follows,

$$V_j = T_b - V_{col} \tag{28}$$

where V_j is the developed joint shear force, $T_b = T_s$ (from Eq. (20)) is the tension force in the beam steel bars and V_{col} is the column shear force. Due to the applied joint shear, diagonal tensile and compressive stresses are created in the joint. If the ultimate capacity of the adjoining members is developed, extensive diagonal cracking will occur. Moreover, cyclic loading causes repeated opening and closing of cracks that lead to disintegration of the concrete, deterioration of aggregate interlocking, degradation of concrete shear strength and hence results in joint shear failure.

The developed joint shear force is calculated according to [Park and Paulay, 1975] as follows,

$$V_j = 1.25 f_y A_s - V_{col} \tag{29}$$

The total shear resistance consists of the concrete resistance, V_c, the resistance of the ties, V_s, and the resistance provided by the composite laminates, V_{frp}, i.e.,

$$V_j = V_c + V_s + V_{frp} \tag{30}$$

The concrete shear resistance can be estimated using ACI 352 (1976) provision to be:

$$V_c = 0.3\sqrt{f_c'(1 + 0.3 f_{col})}\, b_j d_j \tag{31}$$

where f_{col} is the axial stress applied to the column, b_j is the joint width, and d_j is the joint effective depth. For the case of no ties provided in the joint, V_s is taken to be zero. On the other hand, the laminates contribution, with total cross-sectional area, A_{frp}, is estimated to be:

$$V_{frp} = A_{frp} \varepsilon_{frp} E_{frp} \tag{32}$$

From Eq. (32), the cross-sectional area of the FRP laminates, A_{frp}, can be determined.

It is important to anchor the free edge of the FRP laminates at the beam-column interface as shown in Figure 16b to provide confinement to the joint and prevent de-bonding of the FRP. Steel or polymeric composite anchors may be used for this purpose.

5.3 Numerical example

Consider an external beam-column joint where the beam and column concrete cross-sections are 250×400 mm with concrete cover $d' = 45$ mm. The top and bottom longitudinal reinforcement of the beam are four 20 mm bars and the transverse steel is 10 mm spaced at 150 mm. The column reinforcement is six 20 mm diameter bars plus two 15 mm diameter bars as longitudinal reinforcement and 10 mm diameter ties spaced at 200 mm. The nominal concrete and steel strengths are 40 and 400 MPa, respectively. The column axial load is 600 kN. The beam length is 1.75 m and the column lengths above and below the joint are 1.3 mm. The load is applied at the tip of the beam. This example represents the specimen tested in [Ghobarah and El-Amoury, 2005], designated T-SB3 and depicted in Figure 19a. The candidate GFRP systems have the properties summarized in Table 1.

GFRP system	Tensile strength in 0^0 direction [MPa]	Elongation at break [%]	Tensile modulus [GPa]	Thickness [mm]
$\pm 45^0$ Bidirectional	279	1.5	19	0.864
Unidirectional	1700	2.0	71	0.353

*Table 1: GFRP systems used for the numerical example [*El-Amoury and Ghobarah, 2002*]*

In the case of as-built joint, Eq. (20) gives the tension force in the steel bars to be: $T_s = 600.00\,\text{kN}$, and Eq. (21) gives the depth of the concrete block to be $a = 61.00\,\text{mm}$. The resisting moment capacity given by Eq. (22) is $M_r = 187.32\,\text{kN.m.}$

For the retrofitted beam-column joint, using the same resisting moment capacity, $M_r = 187.32\,\text{kN.m.}$, Eq. (24) gives the depth of the concrete block to be: $a = 55.95\,\text{mm}$. Eqs. (25) to (27) and using $\varepsilon_c' = 0.35\%$ give the strain in the laminate $\varepsilon_{frp} = 1.89\% < 2.00\%$ with the number of E-glass/epoxy (GFRP) unidirectional plies $n_{frp} = 4.35$ layers. Alternatively, to reduce the number of layers, a higher strength and modulus composites such as carbon/epoxy composites can be used.

For the retrofitted beam-column joint, the beam shear force is obtained by dividing the nominal moment capacity by the clear beam length, which is equal 1,670 mm, i.e. $V_{beam} = 187.32/1.67 = 112.17\,\text{kN}$. Accordingly, the column shear force is obtained by dividing the beam moment calculated at the joint center by the column shear arm, which is equal to 2,850 mm, i.e. $V_{col} = [112.17 \times (1.67 + 0.20)]/2.85 = 73.60\,\text{kN}$. Eq. (28) gives the total joint shear as $V_j = 526.40\,\text{kN}$. The column axial stress is determined such that $f_{col} = (600 \times 1000)/(400 \times 250) = 6.00\,\text{MPa}$. Accordingly, Eq. (31), using $b_j = 250.00\,\text{mm}$ and $d_j = 400.00 - 45.00 = 355.00\,\text{mm}$, gives $V_c = 276.06\,\text{kN}$. From Eq. (30) and for $V_s = 0.00$ due to absence of transverse ties in the joint region, the required shear resistance contributed by the FRP composites is $V_{frp} = 250.34\,\text{kN}$. The provided shear strength using one bidirectional and one unidirectional layers can be estimated from Eq. (32), assuming that both laminates will reach the same strain level of 1.0%, which is equal to $2/3$ the smallest maximum strains of the two composite laminate types, refer to Table 1 for the material properties of the used U-shaped, i.e. 2 sides, laminates. This provides shear resistance of $V_r = 2 \times 0.01 \times (19 \times 0.864 + 71 \times 0.353) \times (400 - 45) = 294.50\,\text{kN}$ which is greater than the required composites resistance V_{frp}.

5.4 Final remarks on the design of FRP retrofit systems of deficient RC beam-column joints

The following is a list of some remarks related to the design procedure discussed in the previous section making use of the findings and observations from the different experimental studies outlined above:

- The composite laminate is expected to de-bond from the concrete surface when it reaches a strain of 0.004, which is approximately 25% of the composites ultimate strain.
- Using U-shaped steel plates to restrain the FRP laminates that are attached to the beam bottom face, refer to Figure 21b, eliminates de-bonding of the FRP from the concrete surface of the underside of the beam. The FRP may reach a strain that is approximately 1/3 of its ultimate strain in both tension and compression without failure. Accordingly, the retrofitted joint is expected to achieve higher strength and to dissipate multiples of

the energy dissipated by the as built deficient joint.

- Retrofitting of the beam near the joint should be avoided whereas confining the column potential plastic hinge region is crucial.
- Based on experimental data, the steel or composites anchors, refer to Figure 16b, represent an efficient technique in confining the joint region and in preventing de-bonding of the composite laminates.

6 FRP retrofit of RC frames

The previous sections dealt with the evaluation and retrofit of RC beam-column joints using FRP jacketing. The natural subsequent step is to attempt to answer two important questions namely,

- How do FRP jacketing compare with other retrofit system as far as the structural system response is concerned?
- How can one select location of joints to retrofit with FRP jacketing in a structural system? and what are the implications of this selection on the system response?

A study documented in [El-Amoury and Ghobarah, 2005] attempted to answer the first question where the seismic responses of two RC frames (9-strory and 18-storey office buildings designed according to the 1960's code provisions) were examined. Two retrofit techniques were considered. The first is FRP jacketing to enhance the beam-column joint shear strength and ductility. The second is steel X-bracing installed in the middle bay of the frames along their height. It was found that FRP jacketing eliminated the brittle failure modes without significant change in the structural response. On the other hand, steel bracing significantly contributed to the structural stiffness and reduced the frame lateral deflection and inter-storey drift.

A study documented in [Ghobarah and Arafa, 2005] attempted to answer the second question where the lateral load carrying capacity of four frames with different heights were assessed and two retrofit strategies were applied to the frames. In the first retrofit strategy, jacketing of all beam-column joints using FRP was conducted. In the second retrofit strategy, selective retrofit of specific beam-column joints was conducted. The selective retrofit with FRP jacketing of the beam-column joints reduced drift and damage due to its reduction of shear deformation and opening of joint cracks. Moreover, the effectiveness of the selective retrofit strategy increased as the building height increased.

The above studies on system response rely heavily on complete understanding of the role of the retrofit method, e.g. FRP jacketing, in improving the structural behaviour of the retrofitted element, i.e. RC beam-column joint in the present study. Reliable models as the one described in section 3 for as-built and retrofitted elements are essential to incorporate in the analysis of the as-built and the retrofitted systems. This fact is demonstrated in [Ghobarah and Biddah, 1999] for 3-storey and 9-storey frames analyzed with the assumption of rigid joints and with the inclusion of the joint model described in section 3. It was concluded that the rigid joint assumption, as customary conducted in structural analysis of multistorey frames, is inappropriate when assessing the behaviour of existing non-ductile RC structures, refer to Figures 24 and 25.

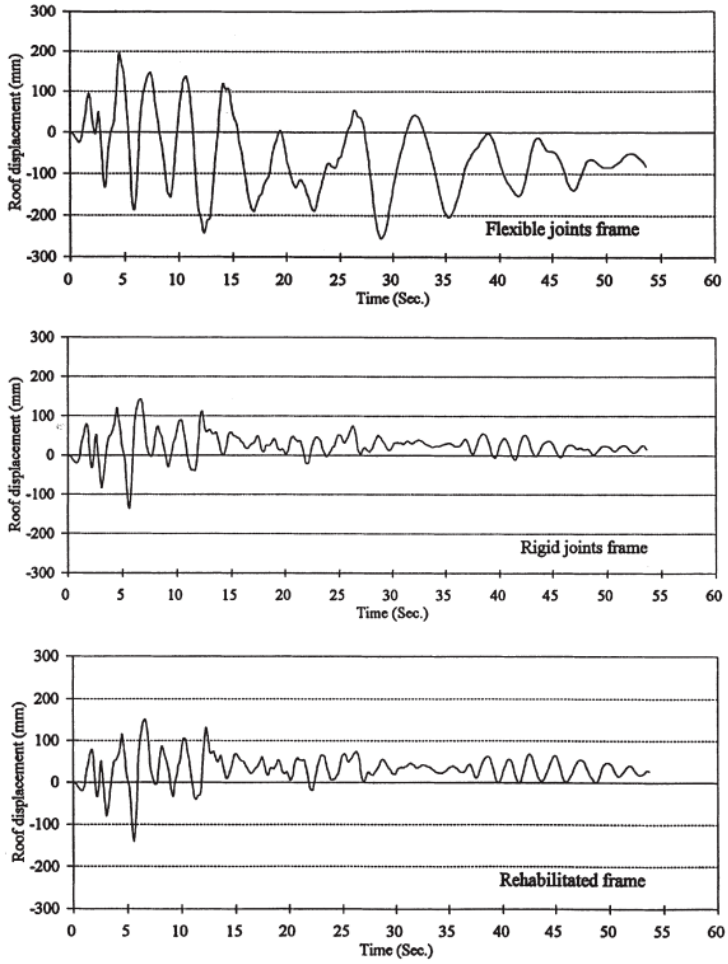

Fig. 24: Roof displacement time histories of a non-ductile 9-storey frames [as-built (top two plots) and FRP jacketing of beam-column joints (bottom plot)] due to El-Centro record scaled to PGA=0.3g [Biddah, 1997]

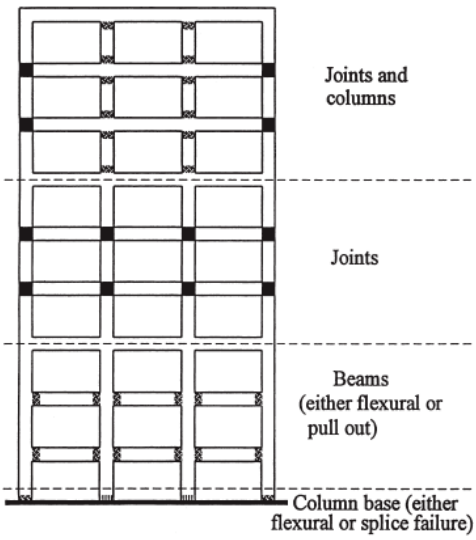

Fig. 25: General pattern of damage in as-built non-ductile frames [Biddah, 1997]

References

ACI 352 recommendation for design of beam-column joints in monolithic reinforced concrete structures (1976) *American Concrete Institute*, Detroit, Michigan.

Alcocer, S.M. and Jirsa, J.O. (1993) Strength of reinforced concrete frame connections rehabilitated by jacketing, *ACI Structural Journal*, 90(3): 249-261.

Antonopoulos, C. P., and Triantafillou T.C. (2003) Experimental investigation of FRP-strengthened RC beam-column joints, *J. of Composites for Construction, ASCE*, 7(1): 39-49.

Beres, A., El-Borgi, S., White, R.N. and Gergely, P. (1992a) Experimental results of repaired and retrofitted beam-column joint tests in lightly reinforced concrete frame buildings, Report No. NCEER-92-25, *National Center for Earthquake Engineering Research*, State University of New York at Buffalo, NY.

Beres, A., White, R.N. and Gergely, P. (1992b) Seismic performance of interior and exterior beam-to-column reinforced concrete frame buildings, detailed experimental results, Report No. 92-06, *Department of Structural Engineering*, Cornell University, Ithaca, NY.

Biddah, A. (1997) Seismic behaviour of existing and rehabilitated reinforced concrete frame

connections, *Ph. D. thesis*, McMaster University, Canada, 326 pp.

Biddah, A and Ghobarah, A. (1999) Modelling of shear deformation and bond slip in reinforced concrete joints, *Structural Engineering and Mechanics*, 7(4): 413-432.

Biddah, A, Ghobarah, A. and Aziz, T.S. (1997) Upgrading of non-ductile reinforced concrete frame connections, *J. of Structural Engineering*, ASCE, 123(8):1001-1010.

Clyde, C. and Pantelides, C.P. (2002) Seismic evaluation and rehabilitation of R/C exterior building joints, *Proc. Seventh U.S. National Conference on Earthquake Engineering*, EERI, July 21-25, Boston, Massachusetts.

Collins, M.P. and Mitchell, D. (1991) *Prestressed concrete structures*, Prentice-Hall Inc., Englewood Cliffs, N.J., 766 pp.

Corazo, M. and Durrani, A.J. (1989) Repair and strengthening of beam-to-column connections subjected to earthquake loading, NCEER-89-13, *National Center for Earthquake Engineering Research*, State University of New York at Buffalo, NY.

CSA A23.3-94, (1994) Design of concrete structure, Rexdale, Ontario, *Canadian Standards Association*, pp. 209.

El-Amoury, T. and Ghobarah, A. (2002) Seismic rehabilitation of beam-column joints using GFRP sheets, *Engineering Structures*, 24: 1397-1407.

El-Amoury, T. (2004) Seismic rehabilitation of concrete frame beam-column joints, *Ph. D. Thesis*, McMaster University, Hamilton, Canada, 351 pp.

El-Amoury, T. and Ghobarah, A. (2005) Retrofit of RC frames using FRP jacketing or steel bracing, *J. of Seismology and Earthquake Engineering*, 7(2).

El-Amoury, T. and Ghobarah, A. (2002) Seismic rehabilitation of beam-column joints using GFRP sheets, *Engineering Structures*, 24: 1397-1407.

Estrada, J.I. (1990) Use of steel elements to strengthen a reinforced concrete building, M.Sc. Thesis, University of Texas at Austin, pp. 65.

Gergely, J., Pantelides, C.P. and Reaveley, L.D. (2000) Shear strengthening of RC T-Joints using CFRP composites. *J. of Composites for Construction, ASCE*, 4(2): 56-64.

Ghobarah, A. and Biddah, A. (1999) Dynamic analysis of reinforced concrete frames including joint shear deformation, *Engineering Structures*, 21: 971-987.

Ghobarah, A. and Youssef, M. (1999) Response of an existing RC building including concrete crushing and bond slip effects, *8th Canadian Conference on Earthquake Engineering*, Vancouver, BC, 427-432.

Ghobarah, A., Aziz, T. S. and Biddah, A. (1996) Seismic rehabilitation of reinforced concrete beam-column connections, *Earthquake Spectra*, 12(4): 761-780.

Ghobarah, A. and Said, A. (2001) Seismic rehabilitation of beam-column joints using FRP laminates, *J. of Earthquake Engineering*, 5(1): 113-129.

Ghobarah, A. and Said, A. (2002) Shear strengthening of beam-column joints, *Engineering Structures*, 24: 881-888.

Ghobarah, A. and El-Amoury, T. (2005) Seismic rehabilitation of deficient exterior concrete frame joints, *J. of Composites for Construction, ASCE*, 9(5): 408-416.

Ghobarah, A. and Arafa, A. (2005) Selective rehabilitation of RC frame joints using FRP jackets, *European Earthquake Engineering Journal*, XIX(1).

Hsu, T. (1993) *Unified theory of reinforced concrete*, CRC Press.

Morita, S. and Kaku, T. (1984) Slippage of reinforcement in beam-column joint of reinforced concrete frame, *8th World Conference on Earthquake Engineering*, San Francisco, pp. 477-484.

Mosallam, A.S. (2000) Strength and ductility of reinforced concrete moment frame connections strengthened with quasi-isotropic laminates, *Composites Part B: Engineering*, 31: 481-497.

Naito, C.J., Moehle, J.P., and Mosalam, K.M. (2001) Experimental and Computational Evaluation of Reinforced Concrete Bridge Beam-Column Connections for Seismic Performance, PEER 2001/08, *Pacific Earthquake Engineering Research Center*, University of California, Berkeley, CA.

Pantelides, C., Clyde, C. and Dreaveley, L. (2000) Rehabilitation of R/C building joints with FRP composites, *12th World Conference on Earthquake Engineering*, Auckland, New Zealand, Paper No. 2306.

Park, R. and Paulay, T. (1975) *Reinforced concrete structures*, John Wiley & Sons, N.Y.

Prota, A., Nanni, A., Manfredi, G. and Cosenza, E. (2001) Seismic upgrade of beam-column joints with FRP reinforcement, *Proc. 5th Non-Metallic Reinforcement for Concrete Structures (FRPRCS5)*, Cambridge, UK, 1, paper No 339, pp. 10.

Said, A. (2001) Seismic rehabilitation of beam-column joints using advanced composite materials, *M. Eng. Thesis*, McMaster University, Hamilton, Canada.

Sezen, H., Elwood, K, Whittaker, A., Mosalam, K.M., Wallace, J., and Stanton, J. (2000) Structural engineering reconnaissance of the August 17, 1999, Kocaeli (Izmit), Turkey, earthquake, PEER 2000/09, *Pacific Earthquake Engineering Research Center*, University of California, Berkeley, CA.

Sezen, H., Whittaker, A.S., Elwood, K.J., and Mosalam K.M. (2003) Performance of reinforced concrete buildings during the August 17, 1999 Kocaeli, Turkey earthquake and seismic design and construction practice in Turkey, *Engineering Structures*, 25: 103-114.

Vecchio, F.J. and Collins, M.P. (1986) The modified compression field theory for reinforced concrete elements subjected to shear, *ACI Journal*, 83(2): 216-231.

Vecchio, F.J. and Collins, M.P. (1982) The response of reinforced concrete to in-plane shear and normal stresses, Pub. 82.03, *Department of Civil Engineering*, University of Toronto, 332 pp.

Walraven, J.C. (1981) Fundamental analysis of aggregate interlock. *J. Structural Division, ASCE*, 107(ST11): pp. 2245-2270.

Analysis of infilled reinforced concrete frames strengthened with FRPs

Guney Özcebe (lead author), Barış Binici, Ugur Ersoy, Tugrul Tankut
Middle East Technical University, Ankara, Turkey
Sevket Özden
Kocaeli University, Turkey
Faruk Karadogan, Ercan Yüksel, Alper Ilki
Istanbul Technical University, Turkey

1 Introduction

A re-evaluation of structural damage observed in the aftermath of the earthquakes of the last decade has revealed that the causes of earthquake damage in Turkey can be classified into four groups (Aschheim M. et al, 2000), Ozcebe et al, 2004). These are:

- *Structural System:* Apart from masonry construction and rural dwellings, most of the residential buildings in Turkey are R/C frame structures having inadequate lateral stiffness. Discontinuities in plan and elevation, soft and weak ground floors, strong beams-weak columns and short columns are very common in such frame buildings.
- *Detailing:* Detailing errors and inadequate detailing of the reinforcement result in considerable seismic damage in Turkey. Usually the ends of columns and beams are not properly confined, ties with 90° hooks are generally used, there are no ties in beam-column joints, and column longitudinal bars are lap spliced at floor levels.
- *Construction:* Until very recently most residential buildings in Turkey were built with practically no inspection. As a result, dimensions and reinforcement of members in the built structure could be different from those on the design drawings. Poor concrete quality is also very common in residential buildings.
- *Soil:* Soil has not been one of the main causes of seismic damage until the August 17 1999 Marmara earthquake. In the Marmara earthquake liquefaction and bearing failure of soil caused extensive building damage in the city of Adapazari.

Therefore, in order to make sound interventions toward structural rehabilitation of existing buildings (damaged or undamaged) the engineer should perform a thorough assessment of the existing building by considering the facts listed above and should have special expertise both at the design and construction stages.

The current approaches in the seismic rehabilitation of structures have been based on the accumulated knowledge and experience gained from experimental research and field applications in the past thirty years. In the following paragraphs the general approach for the structural rehabilitation will be summarized and then a special retrofitting technique for the seismic strengthening of existing buildings by using CFRP sheets will be introduced.

2 Steps towards seismic strengthening of R/C frames

2.1 Assessment

This step is not in the scope of the current lecture, however; it is an essential part of the rehabilitation process. Before making the rehabilitation intervention, the structure under

construction should be carefully studied to assess its current status. This requires a series of investigations on the actual structure, which is then followed by a series of analyses to assess its current performance level. In the next step the designer should decide on the type of intervention, which will be the most suitable for the structure under investigation.

The investigation on the actual structure includes:

- Determination of the age of the structure,
- determination of the floor layout (architectural and structural),
- determination of member sizes,
- determination of material properties,
- determination of reinforcement details,
- reporting the current status of the building, including the current damage state (especially important if the investigation is made after the earthquake), corrosion etc.

The data collected from the site shall be used for the detailed seismic performance evaluation of the building under investigation. This investigation will lead to the identification of all weaknesses and deficiencies in the structural system and therefore would help to decide on the type of retrofitting intervention required. While performing these activities, the basic principles, rules and procedures set by the current codes and/or guidelines should be followed.

2.2 Rehabilitation philosophy

A rational rehabilitation philosophy should address the common potential weaknesses of existing reinforced concrete buildings in Turkey, which include:

- Inadequate lateral stiffness,
- irregularities in the frame system both in plan and elevation,
- inadequate reinforcement detailing,
- features, which would lead to undesirable seismic behaviour, such as weak ground floors, short columns and strong beam – weak column applications.

In Turkey most of the buildings the lateral-load resisting system consists of frames, which have irregularities and weaknesses. In addition, these frames cannot be classified as ductile frames and their drift demands are high. A design philosophy which considers these facts would therefore be a realistic one. One such approach, which is called “system behaviour improvement”, is based on providing a new lateral-load resisting system to the existing structure. This load resisting system consists of introducing RC structural walls in both directions, formed by filling selected bays of frames with reinforced concrete infills, properly connected to the frame members. The existing frames are used mainly to resist the gravity loads.

The other alternative would be to rehabilitate the existing frames and use them as the main lateral-load resisting system. It should be kept in mind that, considering the weaknesses of the existing building stock of Turkey; such an approach may lead to unfeasible solutions, because it would require strengthening of all beams and columns. Even if all these members are strengthened, the frame structure could still suffer damage due to local weaknesses and interstory drift limits may not be satisfied. For this reason, the system behaviour improvement by adding structural walls (infilled frames) has been the basic repair/rehabilitation philosophy in the post quake seismic rehabilitation projects carried out after the Erzincan (1992), Dinar (1995) and Ceyhan (1998) earthquakes.

On the other hand, surveys made in several cities in Turkey indicated that the number of seismically deficient reinforced concrete structures is tremendously high (Bogazici University, 2003). Although strengthening of RC frames by introducing RC infills to selected frame bays in both directions proved to be an effective, practical and economical seismic rehabilitation technique; the construction work involved is tremendously demanding.

Furthermore, this procedure requires evacuation of the building for several months; therefore its applicability in the rehabilitation of the existing structures, which are currently in use, is neither feasible nor practical. In order to overcome these shortcomings, alternative retrofit schemes are needed.

These observations forced the researchers to work on developing rapid and effective rehabilitation techniques. In a similar attempt a research project, which was carried out and recently completed in the leadership of the Middle East Technical University (METU) addressed this issue. The main idea was to develop strengthening methods which would not require evacuation of the building. It was intended to convert the non-load bearing existing masonry walls and partitions into structural elements which would form a new lateral load resisting system by strengthening them with CFRP fabrics and integrating them with the existing structural system. Thus the rehabilitated structure would have adequate lateral stiffness and lateral load carrying capacity.

In this chapter, the details of this experimental study will be briefly introduced and the analytical models developed for the redesign calculations will be introduced.

3 Experimental studies

3.1 Summary

A comprehensive experimental study was initiated under the leadership of the Middle East Technical University Structural Mechanics Laboratory (METU), which aimed to develop rapid and user friendly techniques for the retrofit of the existing RC frames in Turkey (NATO, 2003). In this study, it was intended to convert the non-load bearing existing masonry walls and partitions into structural elements, which would form a new lateral load resisting system, by strengthening them with CFRP fabrics and integrating them with the existing structural system.

This joint effort was carried out in four national institutions along with the contributions of institution from abroad. These laboratories are namely:

- Middle East Technical University (METU), Ankara, Turkey
- Kocaeli University-Bogazici University (KU-BU), Kocaeli-Istanbul, Turkey
- Istanbul Technical University, Istanbul, (ITU)

In METU a total of 7, 1/3 scaled 2-storey 1-bay reinforced concrete frames were tested. The frame of the test specimens was detailed to include the common deficiencies (excluding lap splice problem) of the structures in Turkey. All together seven specimens were tested. The arrangement of the CFRP layers, the amount of CFRP used, the anchorage of CFRP fabric to the wall and the frame elements were the major parameters investigated. These tests indicated that CFRP strips properly infilled to the infill and the frame members improved the seismic behaviour and increased the lateral strength significantly (Ozcebe et al, 2003).

In KU-BU an experimental work, parallel to the one carried out at METU, was conducted. A total of 5 similar test specimens were tested. These tests addressed the lap splice problem that is commonly encountered in the existing structures in Turkey. At the end of these experimental series further CFRP detailing reducing the adverse effect of improper lap splicing were developed (Akgüzel, 2003).

In ITU, the design details developed in the pioneering work described above were tested on larger scale specimens. The ITU specimens were 1/2 scaled 2-storey 1-bay RC frames. The test parameters considered were the same as METU and KU-BU series (Yuksel et al, 2005).

In the following sections a comprehensive summary of these test series are given.

3.2 Two-storey one-bay RC frame tests

3.2.1 METU Tests (Ozcebe et al, 2003)

Seven geometrically identical, one-bay, two-storey RC frames with common structural deficiencies observed in the Turkish practice were constructed. The test specimen was a 1/3 scale model of a non-ductile frame having weak columns and strong beams. Insufficient confinement was provided at column and beam ends and no confinement was provided at beam-column joints. The ties used in beams and columns of the test specimens had 90 degree hooks at their free ends. Furthermore, the beam reinforcement was detailed considering gravity loads only. This led to inadequate anchorage of the beam bottom reinforcement. All frames had lapped splices in second storey column longitudinal bars, made at the column base. Although the lap splice length was conforming to the Turkish Seismic Design Code (Turkish Ministry of Public Works and Settlement, 1998) (40 bar diameters), the transverse reinforcement provided in this region did not comply with the code requirements. Figure 1 presents the dimensions and the reinforcement details of the R/C frames. Upon the construction of the R/C frames, the hollow clay tile infills were constructed and plastered by a professional mason.

Prior to the test, six of the seven specimens were strengthened with one-directional CFRP sheets. One of the infilled specimens (SP-1) was not strengthened and served as a reference specimen.

The infill of Specimen SP-2 was strengthened by covering both faces of the infills with two orthogonal layers of CFRP. This type of CFRP application which fully covers the infill was designated as, “Blanket Type”. The CFRP sheets did not extend to the frame members and were not connected to these members. The CFRP sheets were bonded to the infills by using a special adhesive as recommended by the manufacturer.

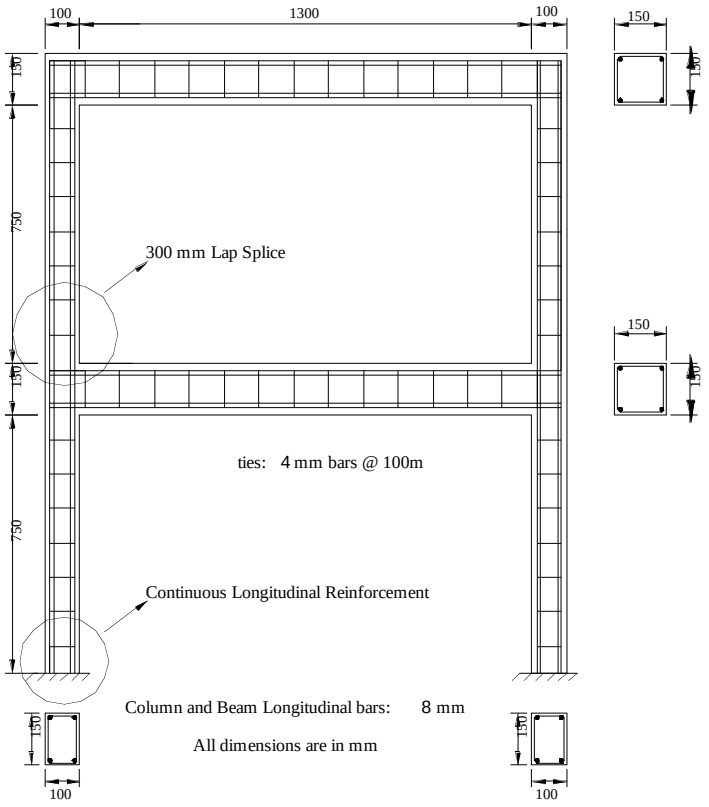

Fig. 1: Geometry and the reinforcement details of the test frames

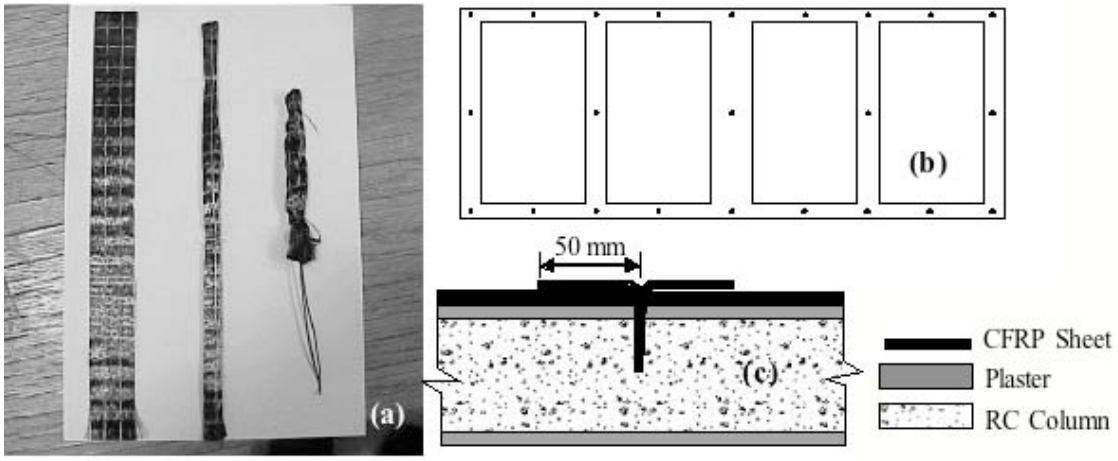

Fig. 2: (a) Anchor dowels, (b) location and (c) configuration of anchor dowels for Specimen SP-3

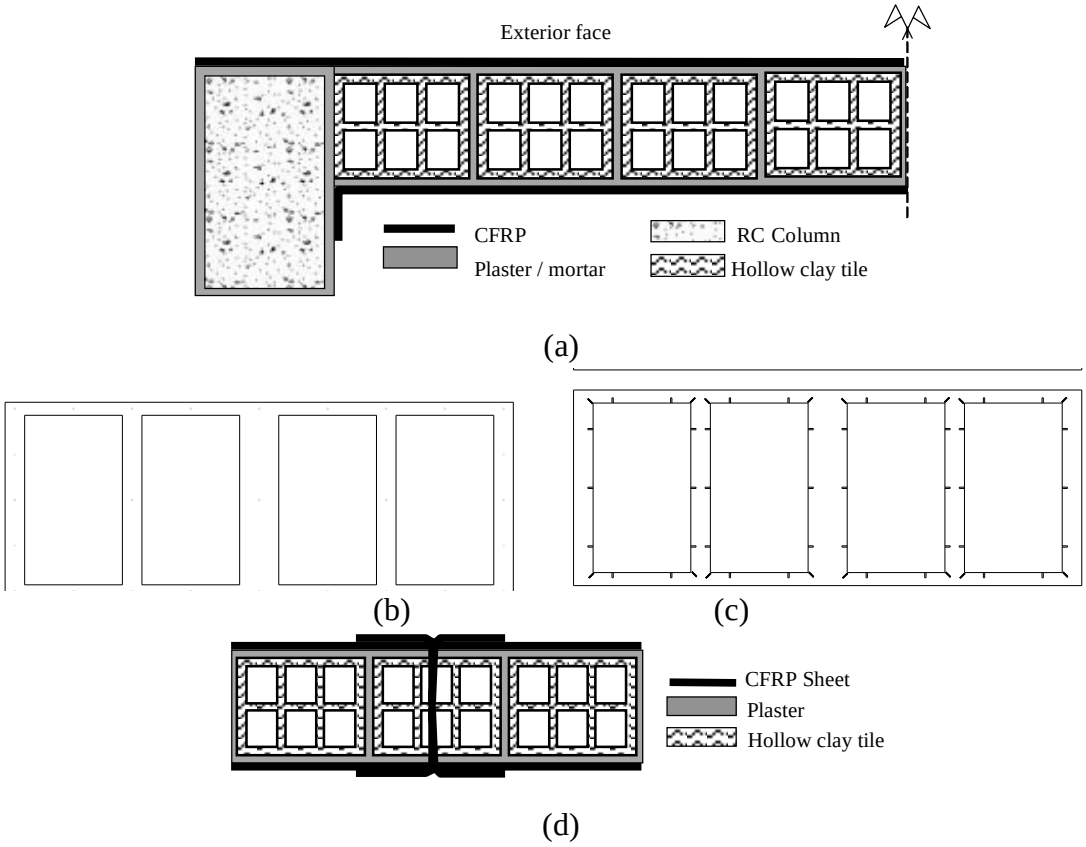

Fig. 3: (a) CFRP pattern and, anchor dowels on the (b) exterior face; (c) interior face; (d) the infill of the Specimen SP4

In Specimen SP-3 only the exterior face of the infill was fully covered by two orthogonal CFRP sheets (blanket type) which were also extended to the frame members. The CFRP sheets were bonded to the infill as in Specimen SP-2. The CFRP sheets were anchored to the frame members using special anchors developed. These anchors were made by rolling the CFRP sheets. The rolled CFRP anchors were folded and tied to a guide wire having a diameter of 1 mm, Figure 2a. Holes having a depth of 50 mm and a diameter of 10 mm were drilled into the frame members. After placing the CFRP sheets on the specimen, the drilled holes were filled with epoxy and the anchors were implanted in these holes by using the guide wires. The fibres of the anchors outside the holes were pierced using a knife and then these fibres were bonded to the CFRP sheets. Number, location and configuration of the anchors for

specimen SP-3 are shown in Figures 2b and 2c.

In SP-4, both sides of the specimen were fully covered by two orthogonal layers of CFRP. The CFRP sheets on the exterior face were extended and anchored to the frame members. On the interior face, the CFRP sheets were bent and anchored to the beam and column face as shown in Figure 3a. The anchor dowels used in SP-3 contributed to the behaviour of the specimen significantly. However, it was observed that, the number of the dowels used in SP-3 was insufficient. Thus, the number of dowels used was increased in SP-4, Figures 3b and 3c. In Specimen SP-4, CFRP sheets covering the two faces of the infill were connected to each other by using CFRP anchors. Holes were drilled through the infill to place these anchors as shown in Figure 3d.

Since a premature failure was observed in testing SP-3 due to the presence of lapped splices in column longitudinal bars at the second floor level, the lapped regions in SP-4 were confined by wrapping CFRP sheets extending along the lap length. The confinement was provided to prevent a premature local failure resulting from lapped splices was eliminated.

The CFRP strengthening in Specimen SP-4 resulted in significant strength increase as compared to the reference specimen SP-1. However the amount of CFRP used in this specimen would make this type of strengthening uneconomical for practical use. Therefore in Specimen SP-5 it was decided to use CFRP strips placed in two diagonal directions instead of fully covering the infill. This type of strengthening was called, “Strut Type”. The width of the strips used as diagonals was 200 mm. The configuration of the CFRP strips and the anchor dowels used are shown in Figure 4. The lapped spliced region of this specimen was also confined with CFRP sheets similar to SP-4.

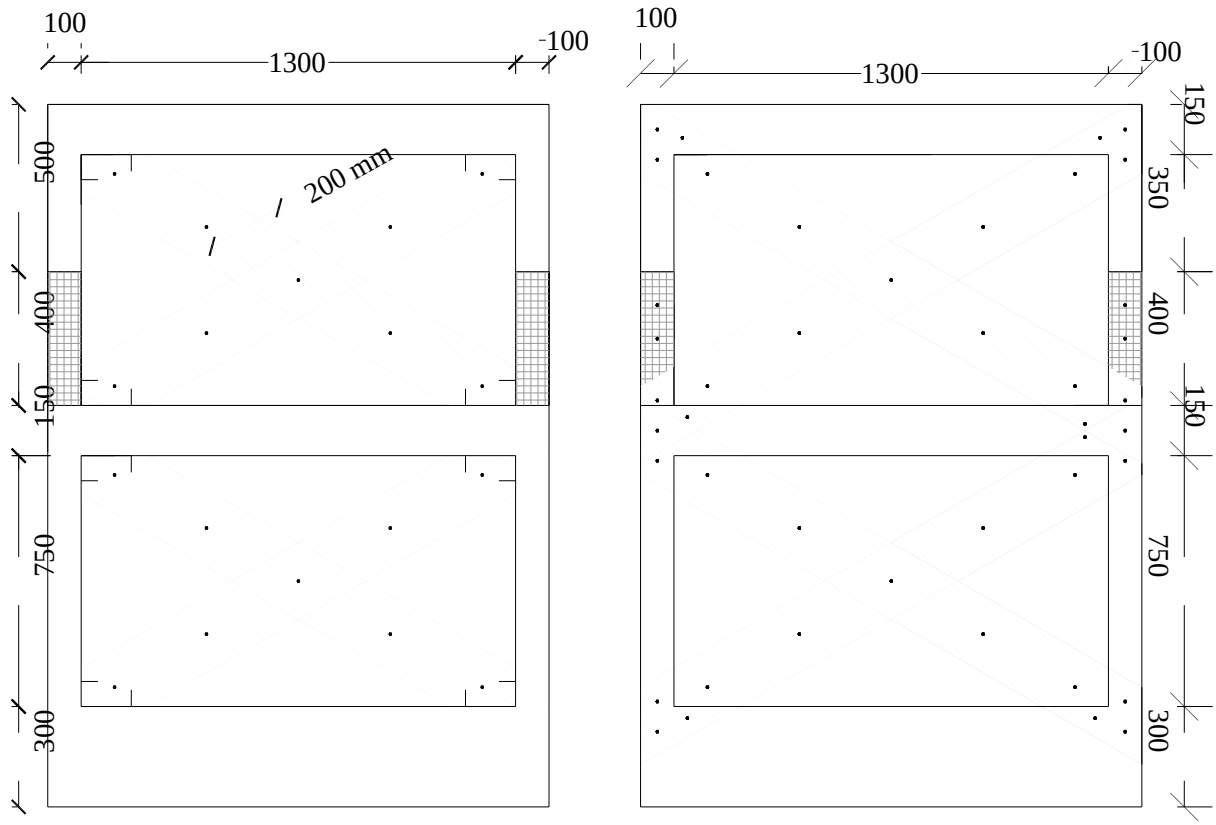

(a) Interior face (a) Exterior face

Fig. 4: CFRP arrangement and location of the anchor dowels in Specimen SP-5 (dimensions are in mm)

Dimensions are in mm

The CFRP detailing used in SP-5 resulted in a significant increase in lateral load capacity and energy dissipation capacity. The failure of SP-5 was initiated by delamination of CFRP

strips at the foundation level. Yielding of longitudinal reinforcement and crushing of concrete were also observed at this region. To prevent this local failure, in Specimen SP-6 the bottom of the first storey columns were also confined using two layers of CFRP. The length of this confined zone at the base was 150 mm. The configuration of diagonal CFRP strips and the number and location of anchors in this specimen were identical with those of SP-5.

In SP-6, shear failure in the first storey beam-column joints was observed. This failure was due to the sudden failure of the anchors used in these regions. Specimen SP-6 reached its capacity when shear cracks at beam-column joints widened following the failure of anchors at this region. To overcome this type of failure, the size of anchors used on the first storey beam-column joints were increased in Specimen SP-7. The properties of the test specimens are summarized in Table 1.

			SPECIMEN						
			SP-1	SP-2	SP-3	SP-4	SP-5	SP-6	SP-7
Longitudinal Reinf. (8 mm bars)		Yield Strength, (MPa)	388	388	388	388	388	388	388
		Ultimate Strength, (MPa)	532	532	532	532	532	532	532
Transvers Reinf. (4 mm bars)		Yield Strength, (MPa)	279	279	279	279	279	279	279
		Ultimate Strength, (MPa)	398	398	398	398	398	398	398
Number of Bars		Beams and Columns	4	4	4	4	4	4	4
		Foundation Beam	6	6	6	6	6	6	6
Detailing of Transverse Reinf.		Spacing (mm)	100	100	100	100	100	100	100
		Hook Angle (º)	90	90	90	90	90	90	90
Compressive Strength of Concrete, (MPa)			19.5	15.3	12.9	17.4	12.0	14.7	17.5
Compressive Strength of Mortar, (MPa)			4.3	4.3	3.1	2.9	4.1	4.2	4.3
CFRP	Infill	Application Side	None	Both	Ext.	Both	Both	Both	Both
		Type	-	Blanket	Blanket	Blanket	Strut	Strut	Strut
		Anchors	No	No	Yes	Yes	Yes	Yes	Yes
	RC Frame	Application Side	None	None	Ext.	Ext.	Ext.	Ext.	Ext.
		Anchors	No	No	Yes	Yes	Yes	Yes	Yes

Table 1: Properties of the test specimens

3.2.1.1 Test set-up and instrumentation

The loading system and the test specimen are shown in Figure 5. The test set-up is similar to one which was developed by Smith (1968). Twin specimens with a common foundation beam were constructed and laid upon the steel plates resting on the ball bearings. The foundation beam was properly constructed and heavily reinforced to prevent the local failures.

The specimens were tested under reversed cyclic loading. The lateral load was applied through the foundation beam. Hence, the reaction forces at each end of the twin specimens become the lateral forces applied at the second storey level. Axial load was applied to the columns by prestressing tendons as shown in Figure 5. The level of applied axial load on each column was about 25% of the nominal axial load capacity of the frame columns, $0.25N_o$.

Test specimens were instrumented to measure the applied loads, lateral displacements, rotations of the foundation beam and diagonal strains on the infill. Figure 6 shows the instrumentation.

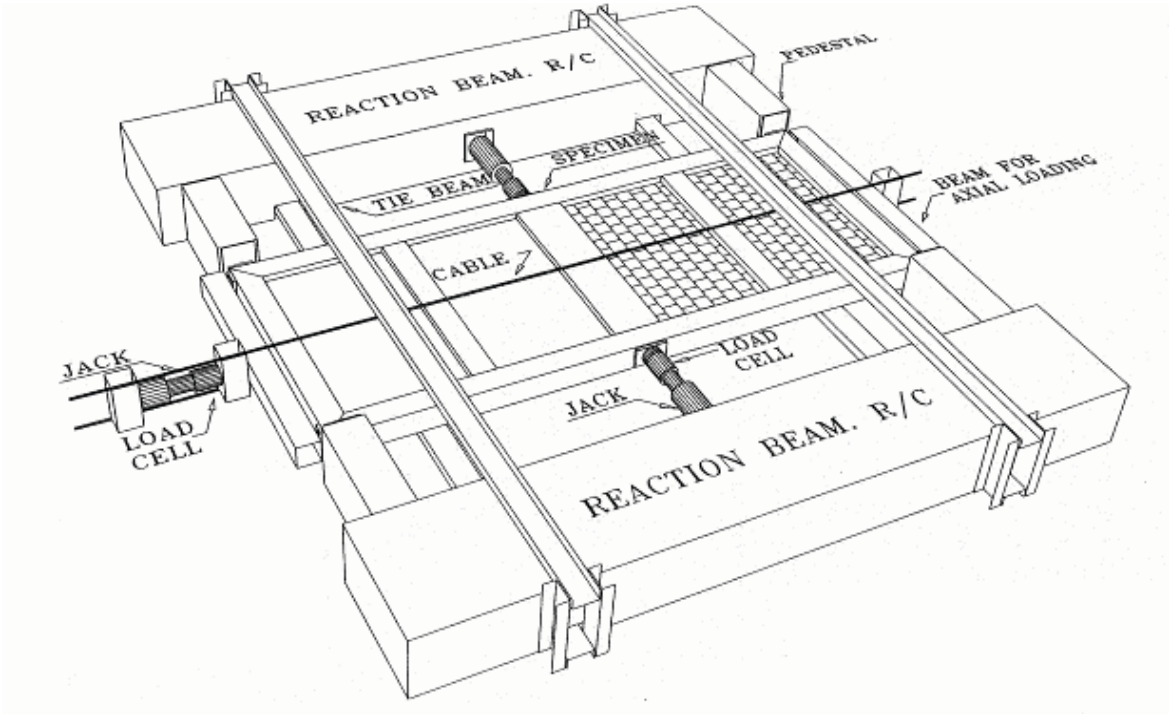

Fig. 5: Test Set-Up

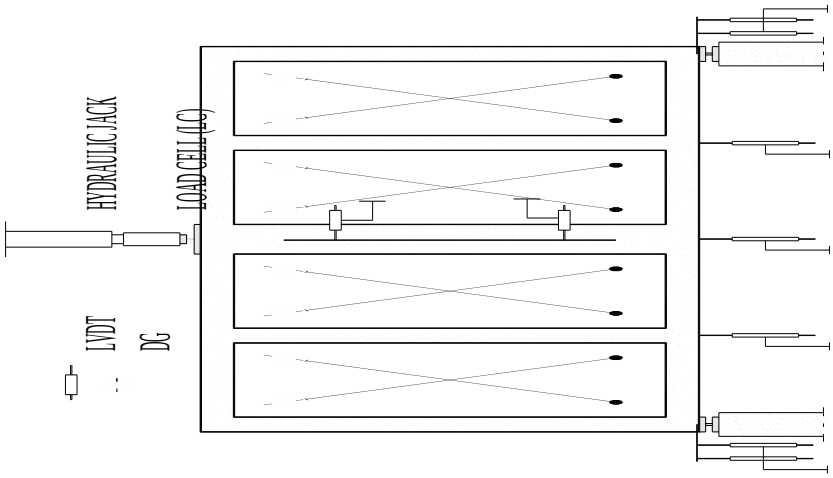

Fig. 6: Instrumentation

Lateral displacements and support settlements were measured by means of linear variable differential transducers (LVDT) which were mounted at each storey and at the foundation beam levels. Two additional LVDTs were attached to the foundation beam to measure rotations. The infills were further instrumented with electrical dial gages (DG) placed diagonally to monitor the shear deformations. After each test, storey displacements were calculated by making corrections considering both support settlements and rigid body rotations. Since each specimen is made up of two specimens, experimental results were presented only for the specimen where failure was observed.

3.2.1.2 Behaviour of test specimens

The first specimen tested (SP-1) was an unstrengthened, hollow clay tile infilled reinforced concrete frame. This specimen was constructed with the most common deficiencies observed in practice and it served as the reference specimen of this test series. As expected, it

displayed a very poor behaviour with limited lateral load and displacement capacities. The maximum lateral load resisted by this specimen was 55 kN. The specimen failed due to crushing of the first storey beam column joint at the end of the seventh cycle.

Specimen SP-2 was strengthened by the application of two orthogonal CFRP sheets on each face of the infills. Since the CFRP sheets were neither extended nor anchored to the reinforced concrete frame members, delamination occurred at the early stages of the test. Therefore, no significant increase in the lateral load capacity was achieved as compared to specimen SP-1. Despite this unfavorable behaviour, the inelastic displacement capacity and energy dissipation capacity of SP-2 were considerably higher than those of SP-1. The specimen failed due to crushing of the first storey beam-column joints in the ninth cycle.

The exterior face of the masonry infills of the third specimen (SP-3) was fully covered by two orthogonal layers of CFRP sheets. Although, CFRP sheets were anchored to the frame members by special anchors, delamination of the CFRP layers on the second storey infill panel was observed at the early stages of the test. The failure of one anchor located at the mid-height of one of the second storey columns had triggered this phenomenon. No delamination was observed on the remaining three panels. The delamination which took place on one infill out of four was probably due to poor workmanship in placing the anchors. This specimen resisted a maximum shear force of V = 65.4 kN. Although this level of lateral resistance was slightly higher than the one experienced by specimen SP-1, the strength increase was only 20 percent and it was not sufficient to ensure the required safety. The ninth cycle marked the end of the test. At the end of this cycle, the second storey beam-column joints failed by crushing of concrete.

In SP-4, the CFRP sheets were applied on both faces of the masonry infills in two orthogonal directions (blanket type). The CFRP sheets were also extended to the frame members. Homemade CFRP anchors were used to fasten the CFRP sheets to the frame members and to the hollow clay tile infills. As a result of this strengthening scheme, a significant improvement of behaviour was achieved. The lateral load carrying capacity of SP-4 was almost 135 percent higher (V = 131.5 kN) than that of SP-1. This load level was achieved in the twentieth load cycle. At this load level CFRP buckled at the edge of the first storey joint and the previously observed cracks at the bottom of the first storey columns widened significantly. In the twenty-second cycle, the maximum load was 125 kN in the positive half cycle and 127 kN in the negative half cycle. At this load level, the anchors at the bottom of the first storey column failed and the CFRP was completely delaminated at the foundation level, which was then followed by crushing of concrete at the bottom of the first storey columns. In the last cycle (i.e. cycle 23), the maximum loads were 104 kN and 75 kN in the positive and negative half cycles, respectively. Longitudinal bars of the columns buckled at the foundation level. A tie at this level ruptured due to buckling of longitudinal bars.

The failure of SP-4 was a flexural failure and this specimen exhibited a far more ductile behaviour as compared to the reference specimen SP-1 and it dissipated nearly five times more energy than SP-1.

In the design of CFRP detailing of SP-5, the main aim was to obtain a similar response as that of the specimen SP-4 by using less amount of CFRP. For this purpose the CFRP strips were placed on the infills in a cross-bracing configuration. The strips were anchored to the infills and to the frame members. This strengthening pattern led to remarkable savings in the CFRP material. The amount of CFRP used in SP-5 was only one fourth of the CFRP used in SP-4. In spite of this reduction in the amount of CFRP used, SP-5 resisted a lateral load of 118.8 kN (113 percent increase as compared to SP-1). The lateral load capacity of SP-5 was about 11 percent less than that of SP-4. Moreover, the energy dissipation characteristics of specimens SP-4 and SP-5 were very similar.

The failure of Specimen SP-5 was triggered by buckling of the CFRP material in the

compression strut. This phenomenon was then followed by failure of the anchor dowels at the foundation level. In the twentieth cycle, plastic hinges at the bottom of the first storey columns were fully developed and the specimen failed due to crushing of concrete in these regions.

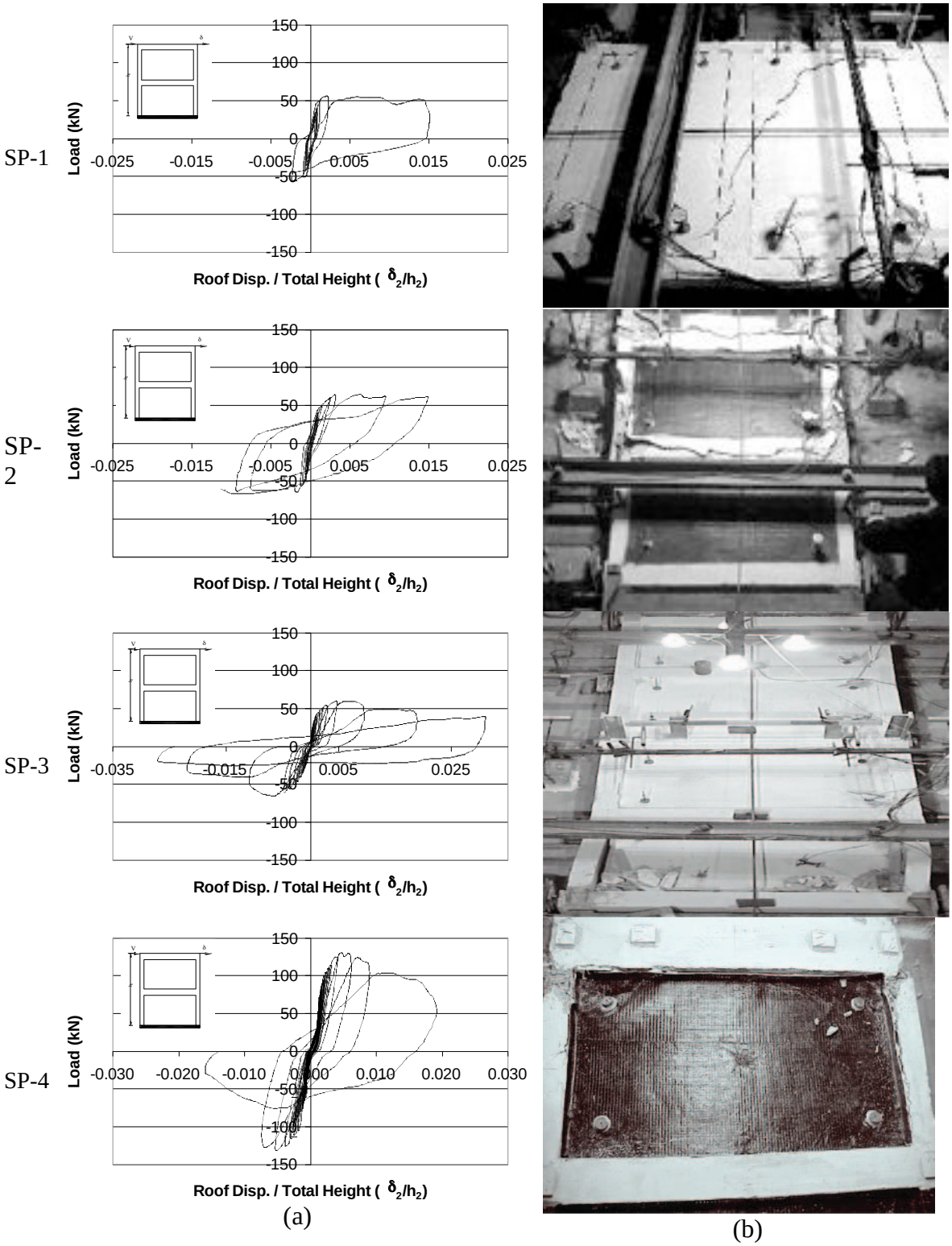

Fig. 7: (a) Lateral load vs. roof drift ratio hysteretic relationships for all test specimens; (b) specimens at the end of the test.

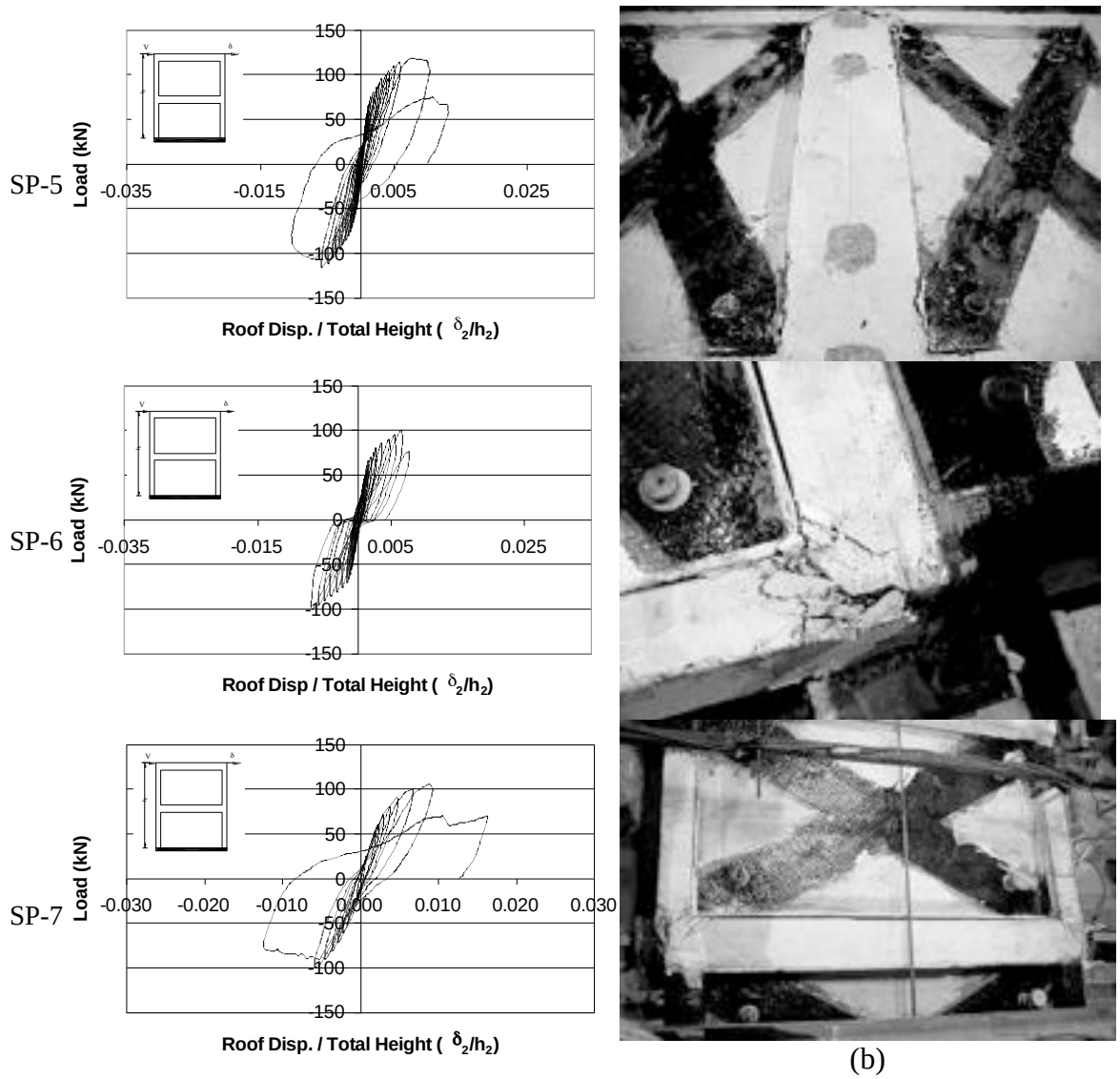

Fig. 7: (cont'd) – (a) Lateral load versus roof drift ratio hysteretic relationships for all test specimens; (b) Specimens at the end of the test.

The strengthening pattern used in SP-5 was economically feasible and resulted in a considerable improvement in the behaviour and strength of the frame. For this reason it was considered as being satisfactory and the strengthening patterns used in the remaining two specimens were slight modifications of this pattern. In SP-6 the only difference was the confinement of the plastic hinge zones at the base of the first storey columns by CFRP. This modification did not improve the behaviour and the strength of the specimen. While in the fifteenth cycle when the lateral load was 100 kN, the anchors of the tensile strut failed suddenly and the tensile load carried by this strut was released. As a result of redistribution of forces within the system, the load on the compressive strut increased significantly, which led to a sudden and brittle shear failure in the first storey beam-column joint.

To prevent the shear failure observed in the first storey beam-column joints of SP-6, these zones were strengthened in SP-7 by increasing the size of anchors. However, this modification did not improve the behaviour of this specimen. The testing was stopped when the first storey beam-column joints of the specimen failed in shear. In general, specimens SP-6 and SP-7 displayed similar strength, ductility and energy dissipating characteristics.

The experimental hysteretic load-deflection relationships of the test specimens and their views at the end of the tests are presented in Figure 7.

The envelope curves for all the specimens tested are presented in Figure 8. The test results are also summarized in Table 2. As can be seen in Figure 8 and Table 2, specimens SP-4 and SP-5 displayed significantly superior behaviour as compared to the other specimens. Although, SP-4 behaved better than SP-5, the amount of CFRP used in that specimen was not economical at all. Thus, it can be stated that, the CFRP detailing used in SP-5 seems to be the most efficient strengthening scheme tested within the scope of this study as far as economy and the ease in application are concerned.

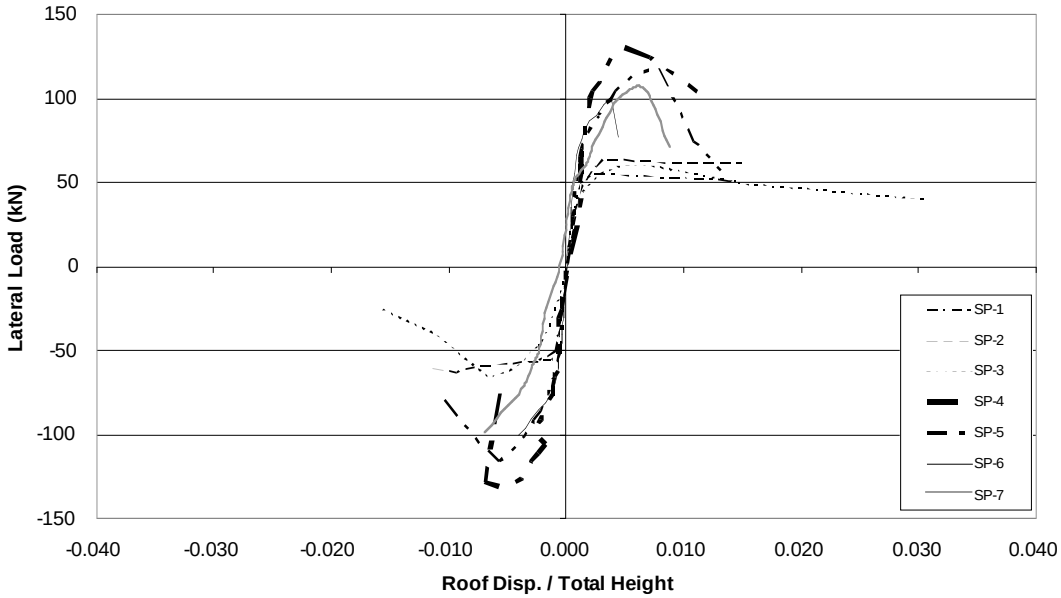

Fig.8 : Response Envelope Curves

Specimen	Max Lateral Load (kN)	Initial Stiffness (kN/m)	Total Energy Dissipation (kJ)
SP-1	55.8	29 660	2.5
SP-2	64.6	29 520	6.1
SP-3	65.4	21 820	8.7
SP-4	131.5	36 430	11.1
SP-5	118.8	39 604	7.8
SP-6	100.4	32 624	4.2
SP-7	105.7	24 392	4.0

Table 2: Summary of Test Results

3.2.1.3 Conclusions

Conclusions summarized below are based on seven 1/3 scale specimens tested. These conclusions should not be generalized without due judgment. Further experimental studies on larger scale, multi-bay specimens are needed. Such a testing program is being carried out at the METU Structural Mechanics Laboratory.

- Tests have revealed that converting masonry infills into structural walls is possible by strengthening such non-structural members by CFRP sheets and strips connected to of the frame members.
- Covering both faces of the infills by CFRP sheets anchored to the frame members (blanket type) increased the strength significantly. The lateral load capacity of SP-4

was more than twice that of the unstrengthened specimen (SP-1).

- Strengthening made using diagonal CFRP strips connected to the frame members seems to be a feasible and economical solution (SP-5). Although the amount of CFRP used in SP-5 was about ¼ of that of SP-4, the strength was only slightly less. The ratio of lateral strength of SP-5 was about twice that of the unstrengthened specimen SP-1.
- Test results indicated that the CFRP strengthening increased the energy dissipation capacity of the infilled frames significantly.
- During the tests on strengthened specimens, no damage was observed on the infill even at high interstory drift ratios (about 0.01).
- Among the common deficiencies observed in existing buildings, lapped splices in column longitudinal bars made at the column base seem to have the must adverse effect on behaviour. Tests indicated that wrapping the lapped region with CFRP strips eliminated this adverse effect.
- Observation made during the tests showed that the effectiveness of CFRP strengthening highly depends on the anchors which connect the CFRP to the frame members. Workmanship is extremely important in making and placing the CFRP anchors.
- A comparison the test results reported here with the test results on frames with reinforced concrete infills revealed that the behaviour of masonry infilled frames strengthened with CFRP is not as ductile as frames with reinforced concrete infills.

3.2.2 KU-BU Tests (Akgüzel, 2003)

The rehabilitation technique developed at METU established the basis of this experimental study. In METU tests, the lap splice problem encountered in the existing frame structures was not addressed. As it was pointed out by many post quake reconnaissance reports inadequately lap spliced regions of columns led to premature and nonductile failure of RC frames (Aschheim et al, 2000, Ozcebe et al, 2004). For this reason, it was decided that frames with inadequate lap splices in column longitudinal bars should also be studied. Five test specimens, namely U1 (bare frame), U2, U3, U4 and U5 (infilled frames), were designed to one-third scale one-bay, two-storey frames (Akgüzel, 2003). Reinforcement detail of the specimens is shown in Figure 1. The properties of the test specimens and materials are summarized in Table 3.

Specimen	Type	Col. Rein.	Beam Rein.	Lap Splice (mm)	f_c (MPa)	f_m (MPa)
U1	Bare	4ϕ8	6ϕ8	160	15.4	-
U2	Infilled	4ϕ8	6ϕ8	160	14.8	5.5
U3	Infilled	4ϕ8	6ϕ8	160	16.1	5.1
U4	Infilled	4ϕ8	6ϕ8	160	15.3	3.8
U5	Infilled	4ϕ8	6ϕ8	160	14.4	4.7
Material	Type	f_y (MPa)	f_u (MPa)	E (MPa)		
Steel	Stirrup	241	423	198,600		
	Long.	380	518	194,400		
CFRP		N/A	3,500	230,000		
Epoxy		N/A	30	3,800		

Table 3: The properties of the test specimens and materials

Lateral loading was applied with a displacement controlled 250 kN capacity hydraulic actuator. For the bare-frame test specimen, the horizontal cyclic loading was applied to the

second storey beam level only, while the load was divided into two by a steel spreader beam and applied both at the first and second storey levels for brick infilled specimens such that two thirds of the applied load goes to the upper storey level. To amplify the adverse effect of inadequate lap splicing on the frame response, the axial load applied on the frame columns was kept low at N/No=0.10. Specimens were tested under reversed cyclic loading. The magnitude of the applied lateral load is gradually increased in each load cycle until general yielding of the test specimen. At the onset of yielding, the specimen was subjected to displacement controlled load cycles. The amplitudes of these cycles were increased as the integer multiples of the yield displacement in both directions. Each test continued until the specimen experienced a significant loss of capacity.

As in the METU tests the specimens were instrumented to measure the lateral displacement at floor levels. Moreover, rotations at column ends and average diagonal strains on CFRP reinforced infill panels were steadily monitored throughout the tests. The applied lateral loading and the axial loading were also measured by the use of load cells.

The test setup used in the KU-BU tests is shown in Figure 9.

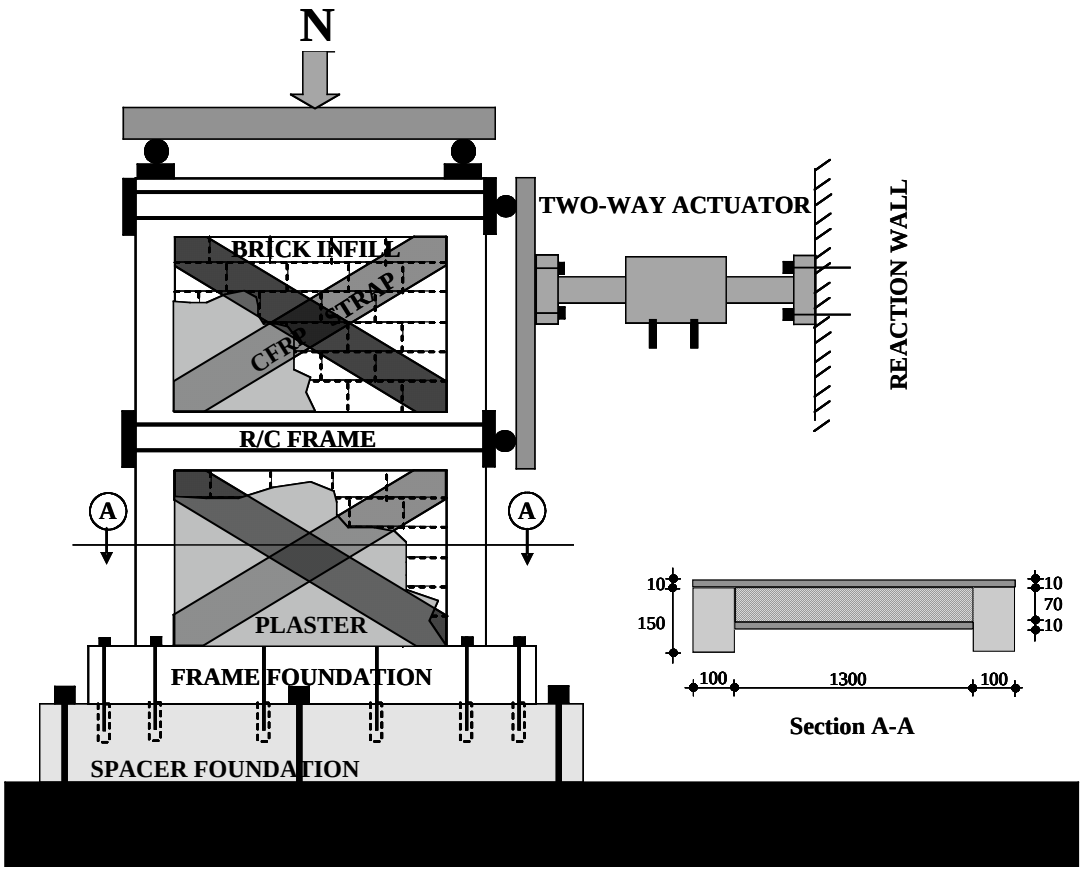

Fig. 9: The test setup used in KU-BU tests (Akgüzel, 2003)

3.2.2.1 Observed behaviour of test specimens

Specimen-U1 : First cracks observed at a load level of 7kN on the base of lower left column. In the 7th cycle (10kN) specimen reached its yielding capacity. After the drift level of 1.65% the lateral load capacity of the specimen stabilized under the increasing lateral displacements. The failure of the system was a typical frame failure. It turned into a mechanism by the formation of plastic hinges in beam-column joints and in the columns especially at the lap splice regions.

Specimen-U2 : First cracks observed at a load level of 40kN through the second storey brick wall. In the 8th cycle (55kN, 0.14% drift) specimen reached its yielding point. At a drift level of 0.34% sliding was observed between the first storey wall panel and beam. After the drift level of 0.55% crack propagation stabilized and separation of the infill panel into four parts completed. The failure mechanism can be identified as a combination of flexure, sliding and crushing of the infill panel at compression regions due to compression strut formation.

Specimen-U3 : Specimen-U3 was the first specimen strengthened by means of CFRP overlays applied as cross diagonal strut and placement of anchor dowels into the predetermined locations. Main idea was to investigate the behaviour of CFRP sheets and anchor dowels efficiency during the test. Moreover, separation and crushing of the infill from the frame along the compression struts as seen in Specimen-U2 necessitated the using of CFRP sheets as cross-overlays. First cracks observed at a load level of 35kN in the first and the second storey infill panels. In the 12th cycle (75 kN, 0.18% drift) specimen reached its yielding point. At a drift level of 0.31% delamination of CFRP overlay began to form at the frame foundation near both columns and sliding was observed between the beam and first storey infill panel. At a drift level of 0.65% separation of the first storey panel from the foundation, fracture of CFRP cross overlays and debonding of anchor dowels observed. In the following cycles, at drift level of 0.9%, the cross CFRP overlay sheets buckled and started to debond from the plaster as a result of compression and tension struts. Anchor dowels were failed by pull-out cone at the foundation level on both faces.

Specimen-U4 : Number and depth of the anchor dowels increased. In addition; rectangular CFRP flag sheets applied to each panel corner to prevent the crushing of brick due to the compression strut, additional anchor dowels were aligned in the same direction with cross-overlays. First cracks observed at a load level of 55kN on the first storey left columns just above the rectangular CFRP flag. In the 13th cycle (95kN, 0.2% drift) specimen reached its yielding point. At a drift level of 0.34% pre-formed cracks especially located on the bottom of the columns widened suddenly. Columns and the frame foundation separated completely. At further drift levels separation of frame base from foundation and rocking was more pronounced due to complete bond loss of anchor dowels and excessive slip deformation on the columns. Till the end of the test, specimen remained intact without any crushing of brick infill corner joints and delamination of CFRP from the concrete cover did not appear. Moreover no significant buckling or rupture of CFRP overlay was observed. However, it was revealed that depth of the anchor dowels was not sufficient. The problem of lap-splice in columns govern the capacity and post-failure behaviour.

Specimen-U5 : Strengthening process for Specimen U5 consisted of two phases. First phase was similiar to that of U4 except the increment in the depth of foundation level anchorage length up to 12cm. Extra anchor dowels at foundation level with increased anchoring depth together with continuity CFRP sheets along the column splice regions were used. To satisfy the required longitudinal reinforcement at foundation and 1st storey level additional CRFP sheets were bonded on the exterior faces of the columns. Afterwards, by wrapping around each column with one layer of CFRP sheet strengthening was finished. First cracks observed at a load level of 55 kN on the left column at the intersection region of the CFRP column wrap. In the 16th cycle at a load level of 95 kN debonding and peeling off was suddenly occurred on the cross overlay CFRP sheets and boundary separation between the columns and the brick infill wall transpired. In the 17th cycle (115 kN) specimen reached its yielding point. After the drift level of 1,39% sudden drop in load capacity observed due to the complete failure of CFRP overlay sheets by means of rupture through the sliding shear plane along the bed joints which is 300 mm above the foundation.

The strength envelops of the experimental hysteretic load-deflection relationships of the test specimens are presented in Figure 10. The photograph of Specimen U5 at the end of test is shown in Figure 11.

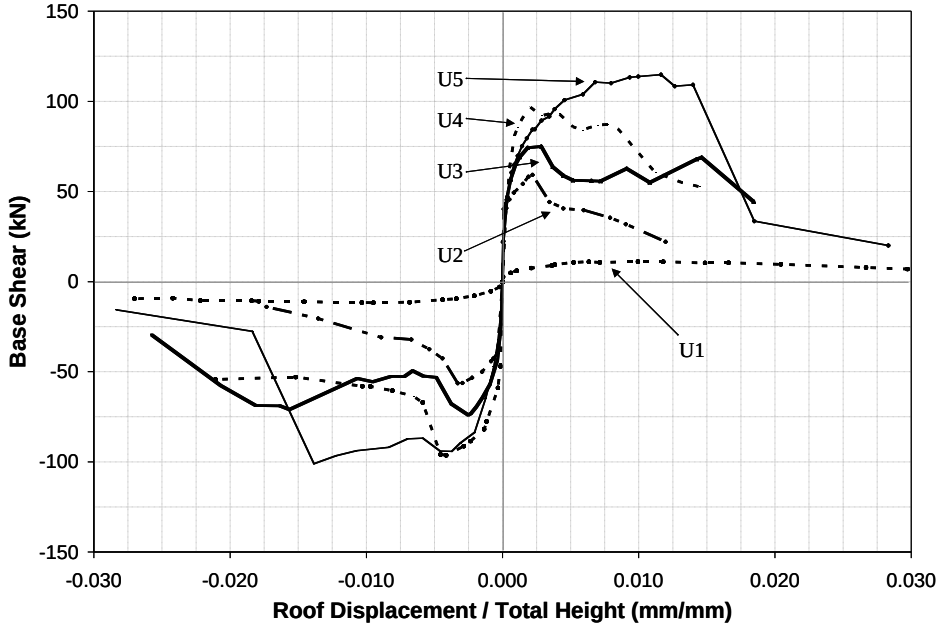

Fig 10: Response envelope of specimens

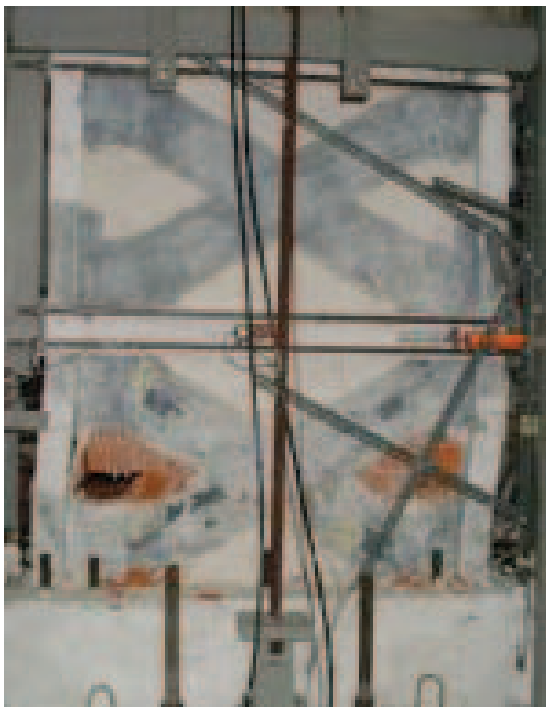

Fig. 11: Specimen U5 at the end of test

3.2.2.2 Conclusions

The proposed X-overlay CFRP reinforcement scheme with flag sheets and special anchorage details resulted in a significant enhancement in the response of the brick infilled r/c frame specimens under reversed cyclic loading. The strengthened specimens yielded a gradual and prolonged failure, a higher base shear, more energy dissipation and apparent post peak strength. However, stiffness enhancement of the specimens was critically low. The interstory drift limit values which are the constraints for rehabilitation of the existing

structures should be revised. What is critical here is, the reliance on a retrofit analysis and design which limits the storey drift to an amount which would prevent any major degradation of the masonry. Test results revealed that an interstory drift level of 0.35%˜0.50% may be a limiting value preventing the CFRP modified masonry from degradation.

3.2.3 ITU Tests (Yuksel et al, 2005)

The details developed in METU and KU-BU tests on 1/3 scale specimens are examined in ITU on 1/2 scale one-bay-two storey frames. A total of five frames were tested in this series. Figure 12. Some of the test specimens were constructed with continuous column rebars as in METU tests whereas the others had inadequate lap splices as KU-BU tests. The properties of the test specimens are given in Table 4.

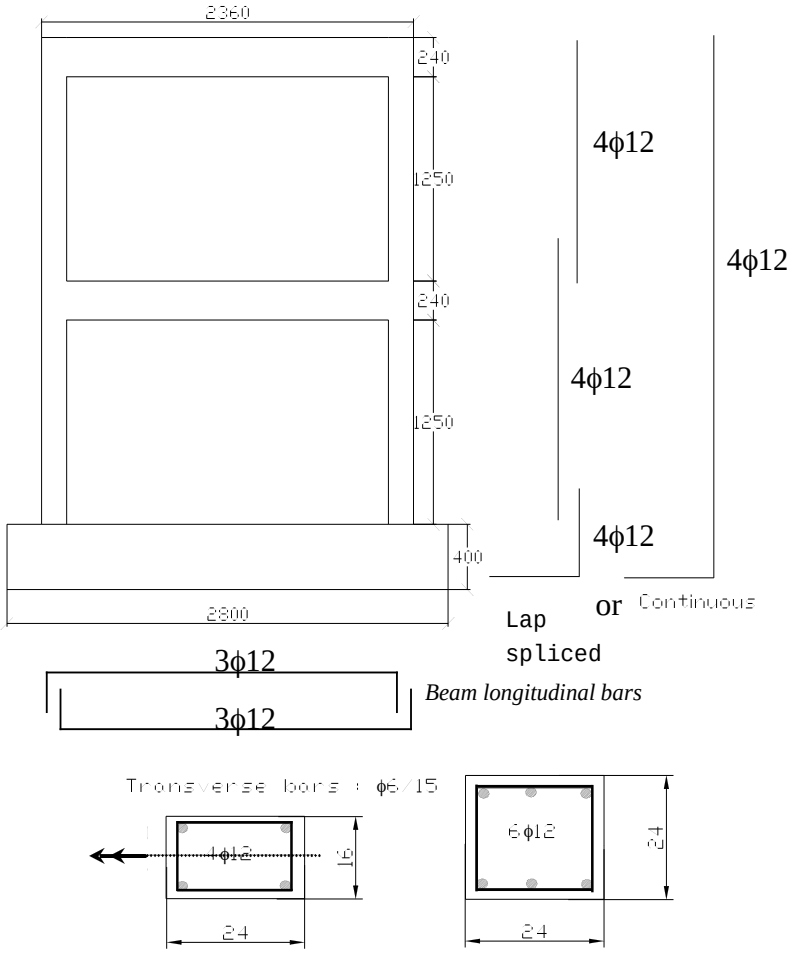

Fig.12: Dimensions and reinforcement of ITU specimens

Specimen	f_c (MPa)	Bare/Infill walls	Longitudinal reinforcement	Retrofit
BC-0-1-14	14	Bare	Continuous	-
BL-0-1-8.6	8.6	Bare	Lap spliced	-
IC-0-1-11	11	Plastered Infills	Continuous	-
IL-0-1-17	17	Plastered Infills	Lap spliced	-
IC-C1-1-10	10	Plastered Infills	Continuous	CFRP diagonals
IL-C1-1-8.6	8.6	Plastered Infills	Lap spliced	CFRP diagonals and confinement of lap spliced zones

Table 4: Properties of ITU specimens

Specimens were tested in vertical position. The level of constant axial load applied on the specimens was in the order of N/N_o=0.15. Specimens were tested under reversed cyclic lateral loading. The lateral load was applied at the second storey level.

All specimens were instrumented to measure the storey displacements, the column end rotations and the average diagonal strains developing in the panels. Figure 13 schematically shows the applied loading and the instrumentation of the test specimen. Figure 14 shows the basic elements of the applied retrofitting technique.

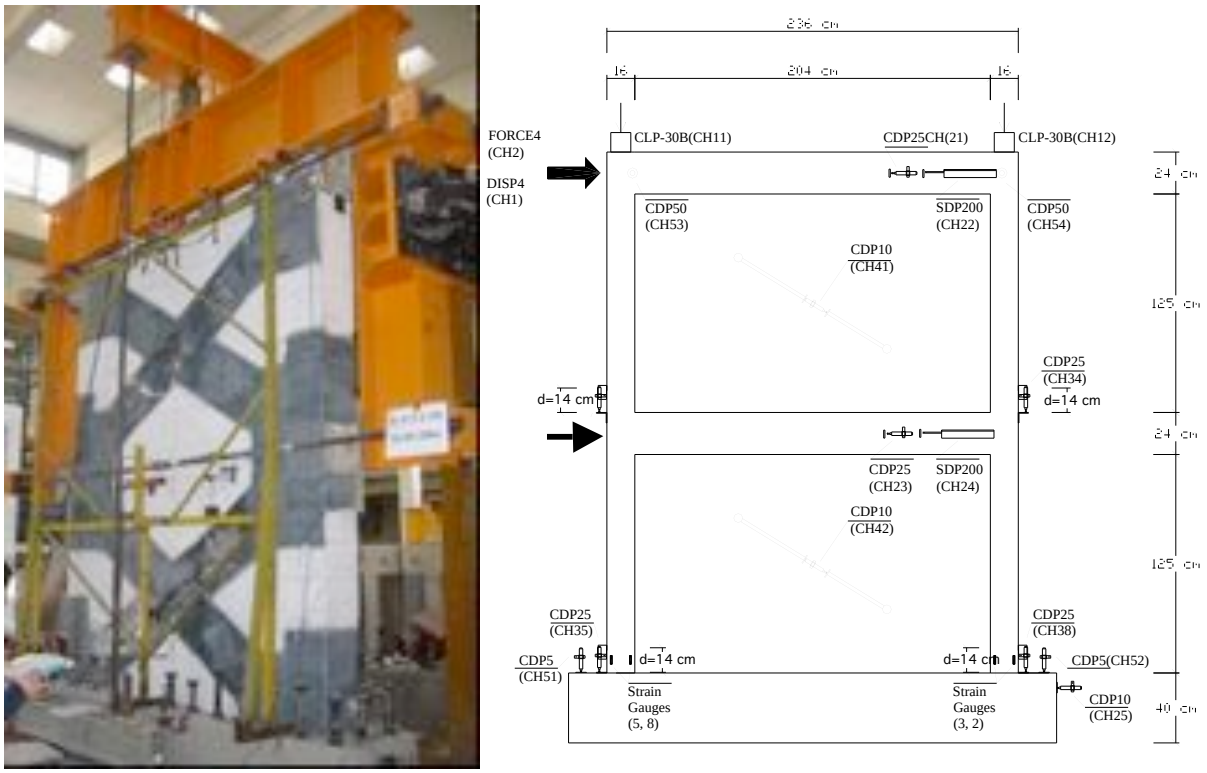

Fig. 13: Test setup and instrumentation

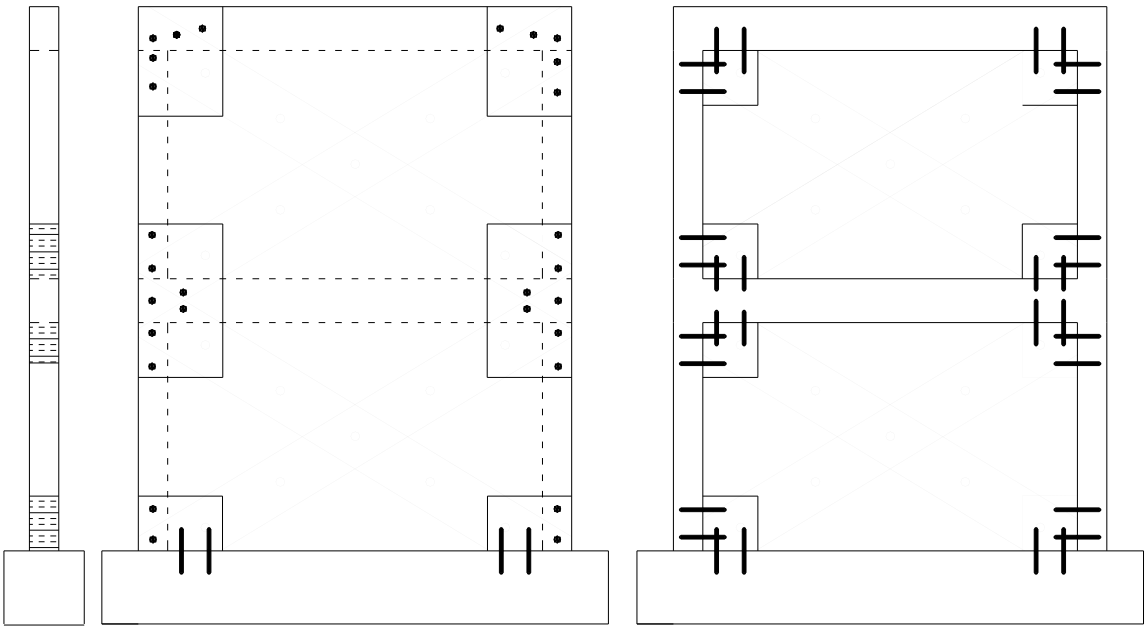

Fig. 14: The basic elements of the applied retrofitting technique.

3.2.3.1 Observed behaviour of test specimens

The experimental results showed that significant enhancement in strength and stiffness was obtained due to retrofit of infill walls with CFRP sheets. It should be noted that even the infill walls themselves are very effective for strength and stiffness enhancement. A comparison of load-displacement relationships for specimens BL-0-1-8.6, IL-0-1-17 and IL-C1-1-8.6 is presented in Figure 15 in the form of envelope curves. The damage observed in specimens BL-0-1-8.6, IL-0-1-17 and IL-C1-1-8.6 are presented in Figure 16.

3.2.3.2 Conclusions

The following conclusions apply for the test series, which was summarized in this section. It should be noted that these conclusions are derived based on limited test data, and more experimental and analytical work is needed for more general and reliable conclusions.

The infill walls contribute significantly to the lateral strength and stiffness of the reinforced concrete frames. By reinforcing the infill walls with CFRP composite sheets, the behaviour of the test specimens further improved in terms of strength, stiffness and the energy dissipation characteristics. In specimens with inadequate lap splices, confinement of lap splice regions of the columns with CFRP composite sheets in transverse direction delayed bond slip and significant energy dissipated through the hysteretic behaviour.

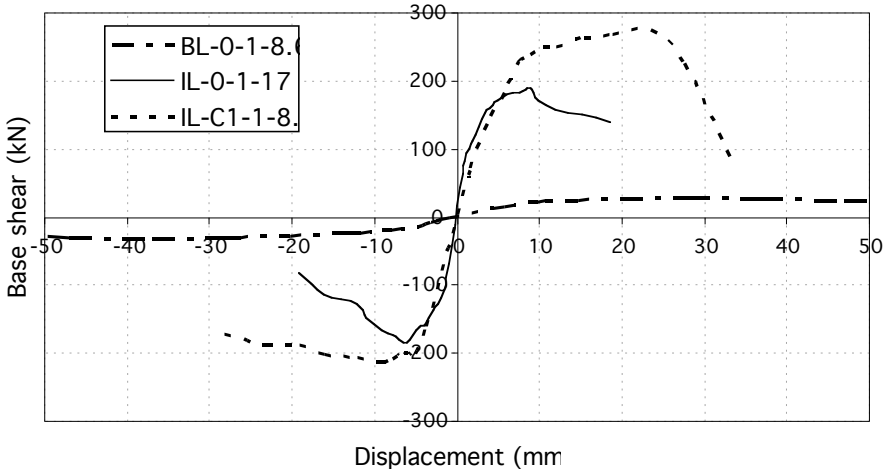

Fig. 15: Load-displacement envelopes of specimens BL-0-1-8.6, IL-0-1-17 and IL-C1-1-8.6

4 Analytical Models

4.1 Introduction

Fibre reinforced polymers have been used in strengthening infill and masonry walls in a number of studies (Valluzzi et al, 2002,-Hamoush et al, 2001). Both in plane and out-plane behaviour of strengthened walls have been investigated in these studies. Recently, a novel technique that makes use of fibre reinforced polymers (FRPs) in the upgrade of reinforced concrete frames with infill walls was developed (Ozcebe et al, 2003) as a part of a NATO sponsored extensive research project (NATO, 2003). The method is based on the premise of limiting inter-storey deformations using FRPs bonded on infill walls that are integrated to the boundary frame members. Quasi-static cyclic tests were performed on multi-bay multi storey

structures in order to experimentally validate the effectiveness of the FRP strengthening system (Ozcebe et al, 2003, Triantafillou, 1998, Yuksel et al, 2005). The proposed method was found to be attractive due to its speed and ease of application with little or no disturbance of the occupants. It is believed that this method can efficiently be used in the upgrade of existing reinforced concrete frames with infill walls, especially when the number of buildings that needs rapid rehabilitation measures is immense. An analytical model was developed at Middle East Technical University to analyze FRP retrofitted reinforced concrete frames with infill walls. This section briefly describes the developed model whose details can be found in (Binici and Ozcebe, 2005).

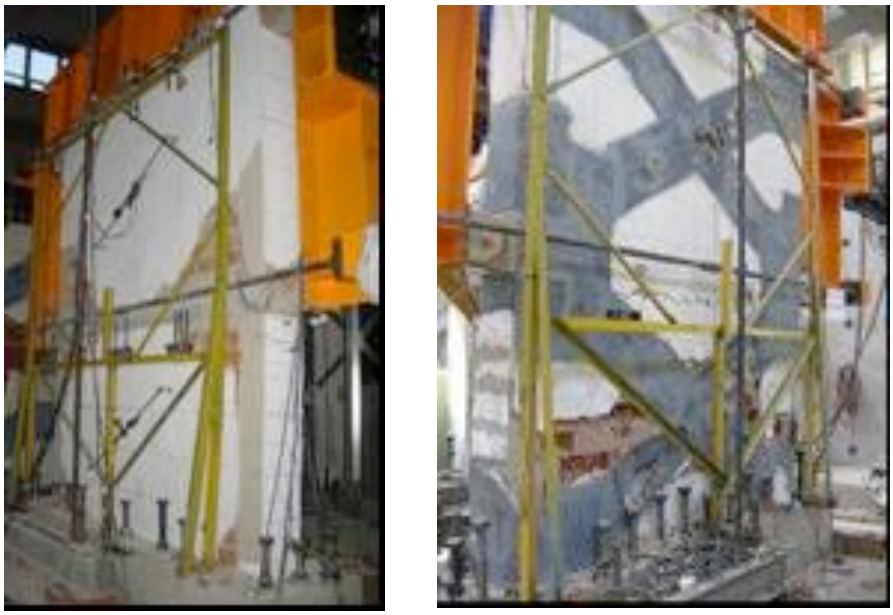

Fig. 16: Damages of specimens IL-0-1-17 and IL-C1-1-8.6

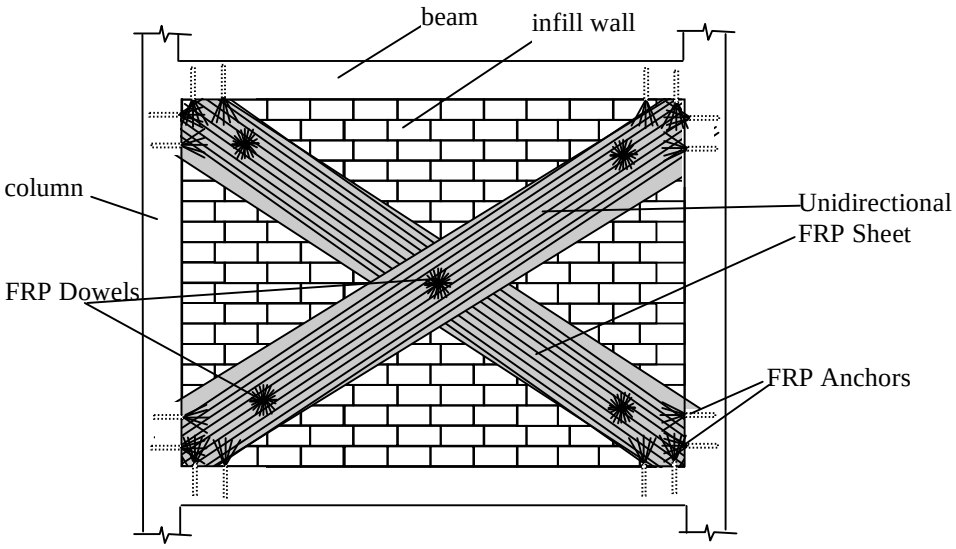

Fig. 17: FRP strengthening method for reinforced concrete frames with infill walls

4.2 Behaviour and Failure modes

When a reinforced concrete frame with infill walls is subjected to lateral deformations, the infill wall acts as a diagonal strut, while the separation of the infill occurs on the opposite side. The idea of the FRP retrofit scheme is to reduce inter-storey deformation demands by using FRPs to act as tension ties. In order to achieve this, diagonal FRPs bonded on the infill wall is tied to the framing members using FRP anchors as shown in Figure 17. In this way, a tension tie contributes to the load carrying capacity in addition to the strength provided by the compression strut formed along the infill diagonal. Special embedded fan type FRP anchors formed by rolling FRP sheets are connected in the corner region in order to achieve efficient use of FRP materials, while, to eliminate premature debonding of FRP from the plaster, surface anchor dowels are used along the thickness of the infill wall (Figure 17).

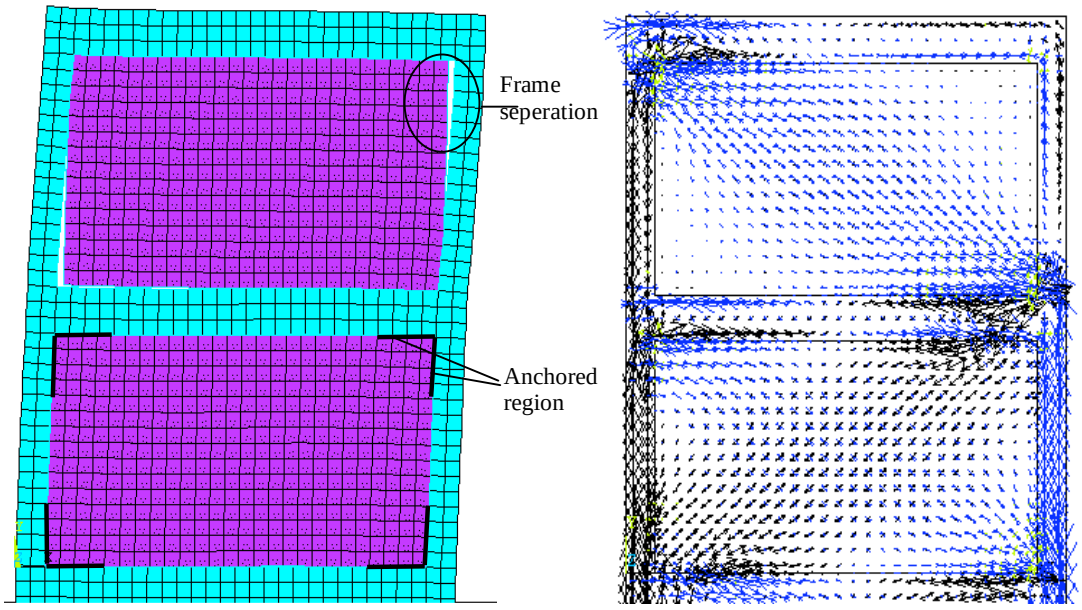

a) Deformed Shape b) Principal Stresses

Fig. 18: Finite element analysis results of a two-storey frame with anchors provided for the first-storey infill wall

To demonstrate the structural deformations and flow of stresses, a two storey frame is analyzed using plane stress elements available in ANSYS. The objective of this analysis is not to reproduce the complete inelastic behaviour of a retrofitted specimen. Instead, a qualitative picture of the deformations and flow of stresses is obtained to gain insight for a structural model. Concrete beams and columns are assigned isotropic elastic material properties whereas the infill wall is modeled with orthotropic elastic material properties to reflect the direction dependent behaviour of masonry. Frictional contact surface is used between the frame members and the infill wall to capture the separation of the infill from the boundary frame. Second storey infill wall represents the conventional infill behaviour whereas the first storey infill wall mimics the behaviour of an FRP strengthened infill wall. The connection of the infill wall elements are provided only at the nodes where FRP anchors are used for the first storey. Deformed shape of the analyzed frame is presented in Figure 18a. It can be observed that separation of the infill occurs in the second storey, whereas first storey infill wall acts an integral part of the frame due to the presence of FRP anchors. Principal stresses are shown in Figure 18b for the analyzed frame. The use of FRPs together with proper anchors in the first storey results in a tension tie limiting the inter-storey displacements in addition to the

resistance provided by the compression strut that forms due to bearing of boundary frame on the infill wall. The analysis results show that when FRPs are bonded to the infill wall and tied to the boundary frame, it acts as a tension tie whose width is similar to the width of the provided FRP sheet in the effectively anchored region.

Experiments conducted on FRP strengthened reinforced concrete frames (Ozcebe et al, 2003, Akgüzel, 2003, Yuksel et al, 2005) with infill walls revealed that there are two dominant failure modes, Figure 19. The first mode initiates with the failure of the FRP anchors in the form of a combined pull-out and slip failure. As soon as the anchors fail, the load carried by the FRP is transferred to the diagonal compression strut and failure of the infill wall occurs due to corner crushing. When three CFRP anchors with a depth of about five times the hole diameter is used per corner on each side of the infill, it has been observed that anchor failure occurs at an effective diagonal FRP strain of about 0.0026 (Smith, 1968). The second failure mode occurs because of FRP debonding from the infill wall surface. After FRP debonding, previously formed horizontal cracks start to open and when the tie action of FRP is lost, sliding shear failure of the infill wall occurs. The first failure mode is mainly due to insufficient anchor depth and can be avoided by increasing the depth and number of anchor dowels (Akgüzel, 2003). However, the second failure mode marks the limiting strength of the strengthened infill. Tests have shown that beyond a strain level of about 0.006, FRP debonding took place resulting in a sliding shear failure of the infill followed by a sudden drop of strength (Akgüzel, 2003). These observations obtained from the finite element analysis and experiments are used to develop structural models for the FRP strengthened RC frames with infill walls.

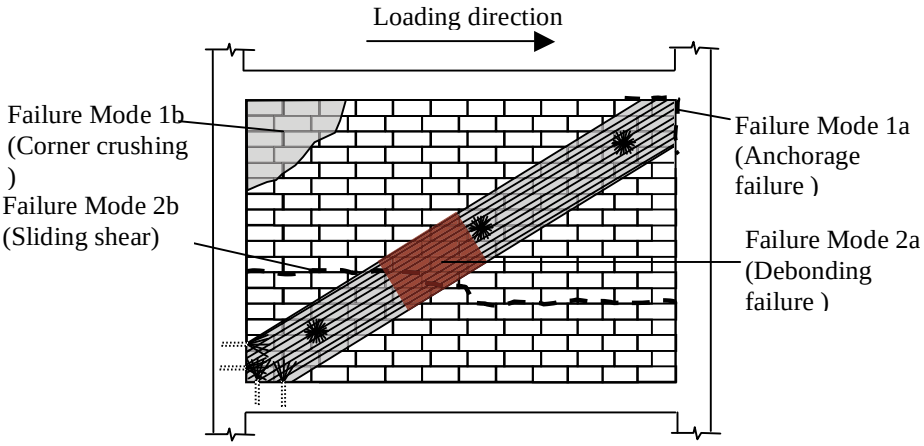

Fig. 9: Failure modes of FRP strengthened infill wall in a reinforced concrete frame

4.3 Analytical model

4.3.1 Frame Elements

Models using structural elements (frames, trusses, plates etc.) are computationally much more efficient compared to continuum models. Continuum models can provide more accurate information on local stresses and strains at the expense of additional computation time. However, structural models allow the analyses of a number of cases to conduct parametric and reliability studies. The analytical model of a strengthened frame proposed in this study is a structural one and is shown in Figure 20. Frame elements (beams and columns) are modeled using elastic elements with predefined plastic hinge regions at their ends. The cross sections of the plastic hinge regions are discretized into a number of fibres with appropriate uniaxial stress-strain behaviour for different materials. Unconfined concrete fibres are modeled using The Hognestad stress-strain curve (Scott et al, 1982) with a linear descending branch up to a

strain of 0.004 at zero stress. The modified Kent and Park model (Scott et al, 1982) is implemented for core concrete fibres confined with transverse reinforcement. Steel reinforcement is modeled with an elastic perfectly plastic material model. The advantage of fibre models is the consideration of axial load moment interaction during analysis and avoiding the need of performing sectional analysis separately. Plastic hinge length, which is the length of the region where inelastic action is expected, is taken equal to the depth of the member. Effective cracked stiffness equal to the 75% of the gross section properties and modulus of elasticity of concrete are used between the plastic hinge regions to model the elastic portion of the frame elements.

4.3.2 FRP ties

Infill wall strengthened using FRPs is modeled using a compression strut and a tension tie, Figure 20, which adequately represents the load transfer mechanism observed from the experiments and finite element analysis. A trilinear stress-strain response is proposed for the truss members to simulate the behaviour of the strengthened infill wall, Figure 21.

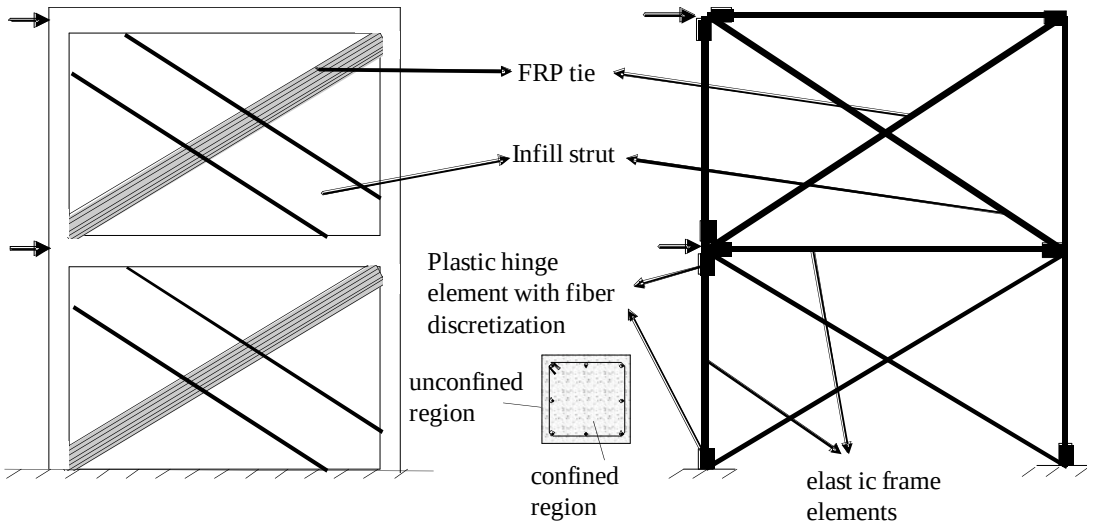

a) Strengthened frame a) Structural model

Fig. 20: Structural model of a two-storey frame strengthened with FRPs

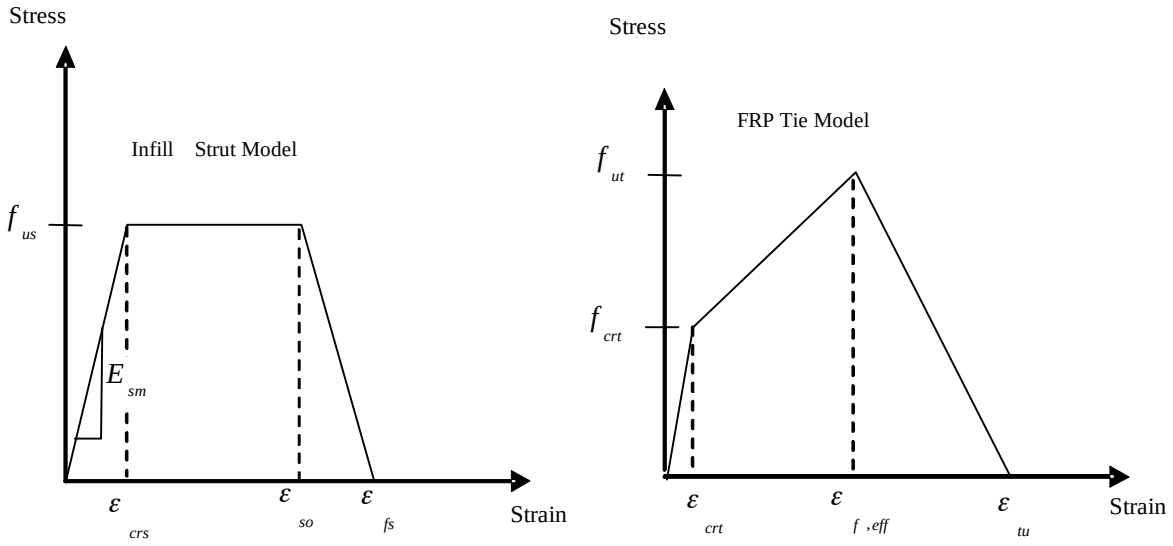

Fig. 21: Stress-strain behaviour of the infill strut and FRP tie

Experiments conducted on reinforced concrete frames with infill walls with and without plaster showed that presence of plaster on infill wall surface needs to taken into account for accurate estimation of stiffness and strength Marjani (1997). Therefore it assumed here that FRP, infill material and plaster on the infill wall surface contributes to the stiffness of the tension tie. The area of the composite tension tie is:

$$A_{tie} = w_f t_{tie} \tag{1}$$

where w_f is the width of the FRP provided and t_{tie} is given by:

$$t_{tie} = t_f + t_p + t_{in} \tag{2}$$

in which t_f, t_p, t_{in} are the thicknesses of FRP, infill and plaster, respectively. It is not unrealistic to assume that mortar used between the infill blocks is similar to the plaster used for exterior coating. Therefore cracking stress of the tie, f_{crt} can be found from:

$$f_{crt} = \frac{V_{crt}}{A_{tie}} \tag{3}$$

$$V_{crt} = f_{pt} w_f \left((t_{in} + t_p) + \frac{E_f}{E_m} t_f \right) \tag{4}$$

where f_{pt} is the tensile strength of the plaster, E_f and E_m are the moduli of elasticity of FRP and mortar, respectively. Eq. (4) assumes that cracking of plaster and mortar occurs simultaneously up to which the three-phase material behaves as a unit. The corresponding cracking strain, ε_{crt} is the cracking strain of the plaster which can be determined from uniaxial tension tests. Beyond cracking, contribution of mortar and plaster to load carrying capacity gradually decreases, Figure 21. Tensile capacity V_{ut}, and tensile strength, f_{ut}, can be computed from Eqs. (5) and (6) respectively, based on the capacity of the FRP at the effective strain obtained from experimental results, $\varepsilon_{f,eff}$, at which anchor failure or debonding initiates.

$$V_{ut} = \varepsilon_{f,eff} w_f t_f E_f \tag{5}$$

$$f_{ut} = \frac{V_{ut}}{A_{tie}} \tag{6}$$

The last definition required for the tension tie is the strain at which complete failure of FRP occurs (ε_{tu}). This strain limit controls descending portion of the global response. The preliminary analyses results showed that three times the effective strain ($\varepsilon_{f,eff}$) can be used to model the strength degradation beyond ultimate strength.

4.3.3 Infill struts

The strut stress-strain model is also a trilinear model with a perfectly plastic plateau and limited deformation capacity. The area of the composite strut, A_{str}, is computed by:

$$A_{st} = w_s t_{st} \tag{7}$$

where

$$t_{st} = t_p + t_{in} \tag{8}$$

$$w_s = \frac{(1-\alpha)\alpha\, h}{\cos\theta} \tag{9}$$

Eq. (9) is proposed by El-Dakhakhi et. al. (2003) to estimate the effective width of the strut, based on the work by Saneinejad and Hobbs (1995). In Eq. (9), h is the height of the infill wall, θ is the strut inclination angle and α is a dimensionless parameter to account for the frame infill contact length computed by:

$$\alpha = \sqrt{\frac{2(M_{pj} + 0.2M_{pc})}{h^2 t_{st} f_{mc}}} \tag{10}$$

in which M_{pj} is the minimum of the moment capacities of the column or the beam, M_{pc} is the moment capacity of the column and f_{mc} is the compressive strength of the infill plaster composite.

The ultimate strength of the diagonal compressive strut V_{us}, is computed based on the minimum of the two capacities, namely sliding shear, V_{ss}, and corner crushing, V_{cc}.

$$V_{us} = \min(V_{ss}, V_{cc}) \tag{11}$$

$$V_{ss} = f_{mv}\, L\, t_{st} \tag{12}$$

$$V_{cc} = 250\, t_{st}\, f_{mc} \tag{13}$$

and the ultimate strength, f_{us}, can be computed by:

$$f_{us} = \frac{V_{us}}{A_{st}} \tag{14}$$

In Eq. (12), f_{mv} is the shear strength of the mortar (or plaster) bed joint and *L* is the width of the infill wall. Eq. (13) is an empirical equation calibrated with test results and proposed by Flanagan and Bennett (1999) to predict corner crushing strength of infill walls. f_{mc} that appears in Eqs. (10) and (13) and the slope of the stress strain curve in Figure 21 (E_{sm}), can be obtained from uniaxial compression tests of plastered infill walls. In the absence these tests Eqs. (15) and (16) can be used to predict the strength and stiffness of the diagonal strut.

$$f_{mc} = \frac{f_{in} t_{in} + f_m t_p}{t_{st}} \tag{15}$$

$$E_{sm} = \frac{E_{in} t_{in} + E_m t_p}{t_{st}} \tag{16}$$

In Eq. (16), E_{in} is the elasticity modulus of the infill material, which generally varies between 500 to 1500 times the compressive strength of the infill material. Strain value at which strength loss initiates has been observed to occur after the failure of FRP tie. Therefore, ε_{so} should be larger than $\varepsilon_{f,eff}$ in the presence of FRPs and should be equal to the cracking strain of mortar (ε_{crs}) in the absence of any strengthening. Following relationship proved to yield satisfactory estimations for the deformation capacity of the strut:

$$\varepsilon_{so} = \begin{cases} \varepsilon_{crs} \text{ without FRP} \\ 2\varepsilon_{f,eff} \text{ with FRP} \end{cases} \tag{17}$$

Eq. (17) implies that no ductility should be expected for the compression strut in the absence of FRP strengthening whereas some ductility is available for the strut when FRPs are used delaying the complete failure. Failure strain of the compression strut, ε_{fs}, was assumed

to occur at a strain of 0.01 by El-Dakhakhni et. al (2003). A similar assumption is made here for the infill walls without any strengthening or failing due to anchorage failure. This strain limit can be taken as 0.02 when failure of the FRP tie occurs beyond a strain level of 0.005.

Researcher	Material	Compressive strength (MPa)	Tensile strength (MPa)	Modulus of Elasticity (MPa)
Erduran (Ozcebe et al, 2003)	FRP	-	3450	230000
	Concrete	15	-	18400
	Plaster	4.3	0.4	9800
	Infill	10 (2)[a]	-	7000 (2000) [1]
Erdem (Ersoy et al, 2003)	FRP	-	3450	230000
	Concrete	9.5	-	14600
	Plaster	5	0.5	9800
	Infill	11.2 (2)	-	7000 (2000) [1]
Akgüzel (2003)	FRP	-	3450	230000
	Concrete	15	-	18400
	Plaster	5	0.5	10600
	Infill	11 (2)	-	7000 (2000)

a) Numbers in parenthesis denote values in the weak direction of infill material.

Table 1. Material properties for analyzed specimens

Researcher	Columns				Beams			Anchors	
	Dimensions (mm x mm)	ρ_l[a] (%)	s[b] (mm)	l_d[c] (mm)	Dimensions (mm x mm)	ρ_l (%)	s (mm)	n[d]	d[e] (mm)
Erduran (Ozcebe et al, 2003)	100 x 150	1.3	90	300	150 x 150	0.9	90	3	60
Erdem (Ersoy et al, 2003)	110 x 110	1.6	100	320	110 x 150	1.4	100	3	70
Akgüzel (2003)	100 x 150	1.3	95	160	150 x 150	1.3	130	3 (5)[f]	50 (80)

a) Longitudinal reinforcement ratio
b) Spacing of transverse reinforcement
c): Lap splice length in the plastic hinge region
d) Number of anchors provided on one face at a corner
e) Depth of anchors
f) Values for the second specimen failing with FRP debonding

Table 2. Member details for analyzed frames

4.4 Experimental verification

Models described above have been validated by comparing the estimated response curves with the results obtained from the experiments conducted by different researchers at different institutions. Material properties of the infill walls used in the analyses are presented in Table 1. Specimen details are presented in Table 2. All the analyses were conducted in a displacement controlled mode with the reference loads applied at given proportions at different storeys. The Opensees analysis platform was used to conduct the analyses. The envelope curves of the quasi-static tests are compared herein with the pushover analyses using the models described above.

Akgüzel (2003) tested four two-storey one bay frames, two of them unstrengthened and two with FRP upgrades. All the columns in the frame members were deficient for confining steel and had lap splices in the plastic hinge regions. Lateral load was applied incrementally and lateral load ratio of the second storey to the first storey was two throughout the tests. One

of the unstrengthened specimens had no infill walls whereas the other one had infill walls in both storeys. Strengthening was achieved through bonding of 200 mm wide FRP sheets on both sides of the frame. Total base shear plotted against roof displacement values are compared for the analytical and experimental results in Figure 22. FRP strain limit was taken as 0.006 for the case when FRP debonding was the failure mode and 0.002 was used when anchor strength was critical. It can be observed that FRP strengthening resulted in an increase of about 100% in base shear capacity when proper anchors were used. Estimations of stiffness and strength of all the test specimens reasonably agree with the measured response.

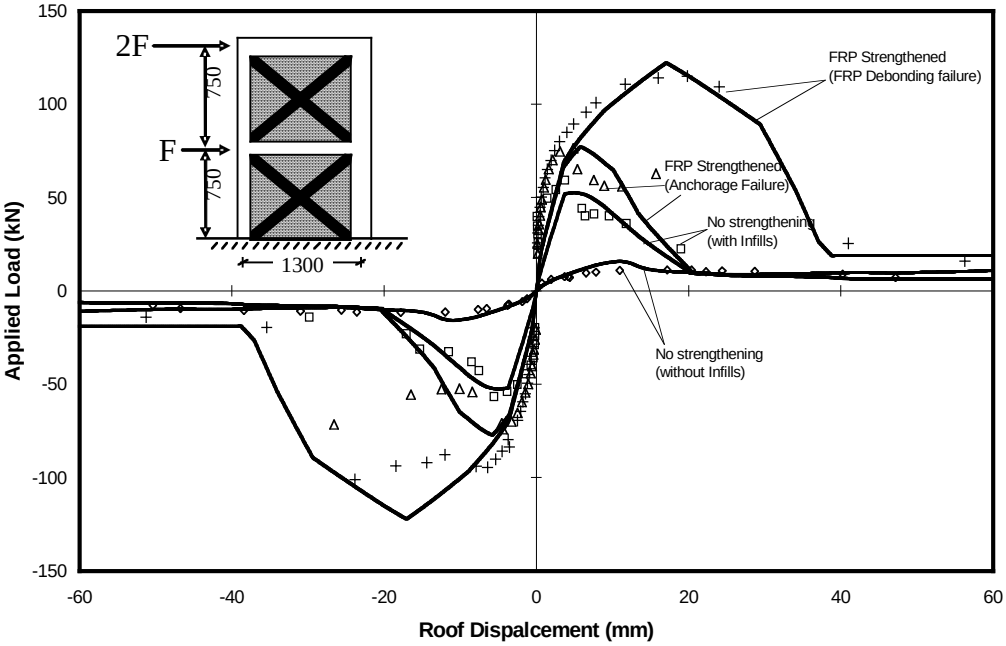

Fig. 22: Comparisons of experiments conducted by Akgüzel(2003) with analysis results (Points are the experimental points, lines are analytical estimations)

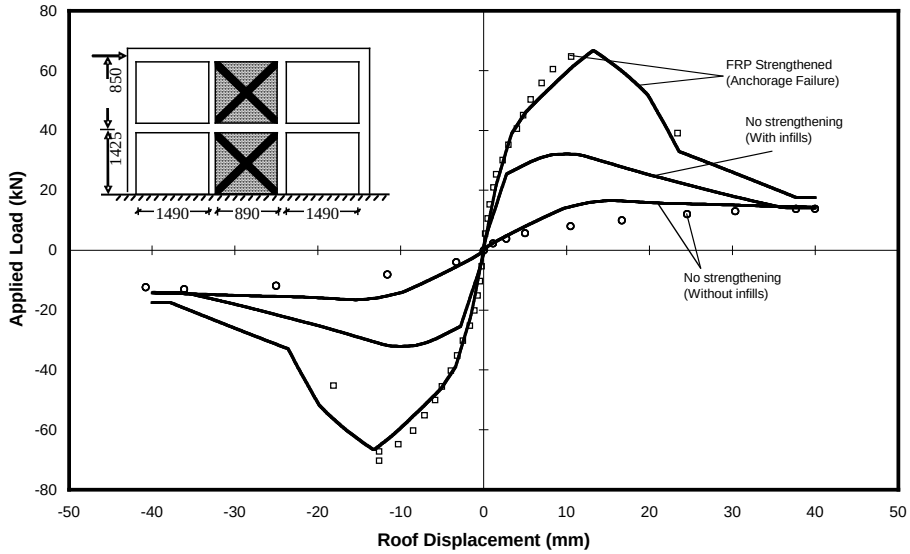

Fig. 23: Comparisons of experiments conducted by Erdem (Ersoy et al, 2003) with analysis results (Points are the experimental points, lines are analytical estimations)

Erdem (Ersoy et al, 2003) tested two three-bay two-storey frames, one bare frame and one infilled frame strengthened with FRPs. Load was applied to the second storey floor level only. Strengthened specimen had infills only in the center bay of the frame. Confining steel deficiencies and lap splices in the plastic hinge region existed in these specimens.

Strengthening was performed by bonding 400 and 200 mm wide FRPs on the infills of the first and second storey infill walls, respectively. Analyses results are shown together with experimental results for total base shear versus roof displacement in Figure 23. A strain limit of 0.002 was used to curves obtained from these tests are compared herein with the pushover tests using the models described above. It can be observed that capacity of the strengthened frame is approximately twice that of the one prior to upgrading. Furthermore, behaviour of the strengthened frame approaches the behaviour of the bare frame at large lateral deformations. Analytical estimations of ultimate strength and corresponding deformations agree well with the measured values.

Tests of Erduran (Ozcebe et al, 2003) with FRP strengthening without any strengthening are compared to the analysis results in Figure 24. Both frames were two-storey one bay frames. 200 mm wide FRPs were used in both storeys of the one bay two storey frames tested by Erduran (Ozcebe et al, 2003). An effective strain limit of 0.003 was chosen for FRP ties to simulate anchorage failure of CFRP anchors.

Strength increase obtained compared to the reference specimen with no strengthening was about 85% with significant increase in deformation capacity. Load deformation trends obtained from analyses agree well with the results from experiments. It can be concluded that comparisons presented above on global load deformation response of the specimens provide confidence on the accuracy of the models proposed in this study.

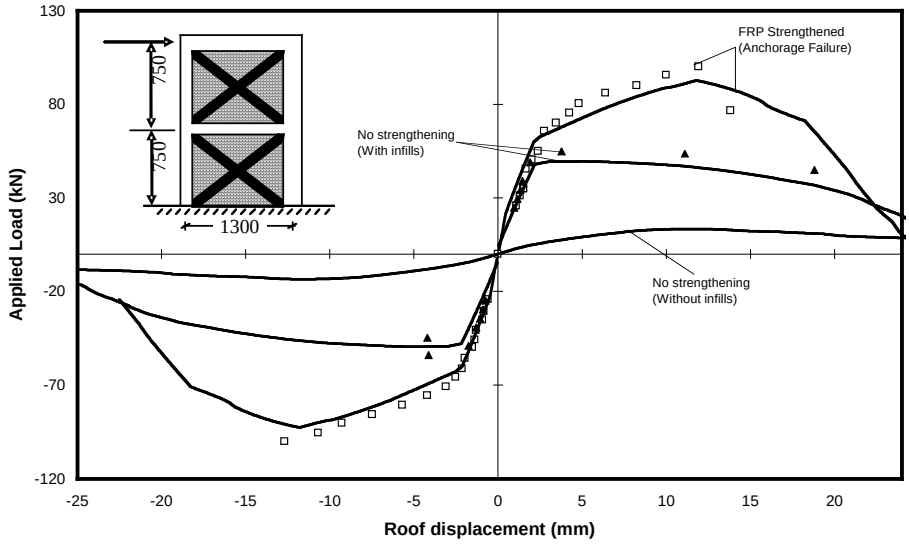

Fig.24: Comparisons of experiments conducted by Erduran (Ozcebe et al, 2003) with analysis results (Points are experimental points, lines are analytical estimations)

4.5 Case study

A typical interior frame of a regular plan building requiring upgrade was analyzed to demonstrate the capacity increases that can be obtained through the use of FRPs. The elevation view of the four-bay, five-storey building frame including the locations of the infill walls is shown in Figure 25. All the columns were 400 mm x 400 mm with a longitudinal reinforcement ratio of 1 % whereas the beams had dimensions of 300 mm x 600 mm with 0.5% longitudinal reinforcement ratio. Stirrup spacing of the columns were approximately equal to the effective depth of the section resulting in insufficient confinement for ductile behaviour. Concrete strength was 10 MPa simulating typical construction quality in Turkey whereas the reinforcement had a yield strength of 420 MPa. The infill walls were composed

of hollow-clay brick with a thickness of 100 mm and a compressive strength of 2 MPa. Additional plaster on the infill walls was 40 mm thick with a compressive strength of about 2 MPa.

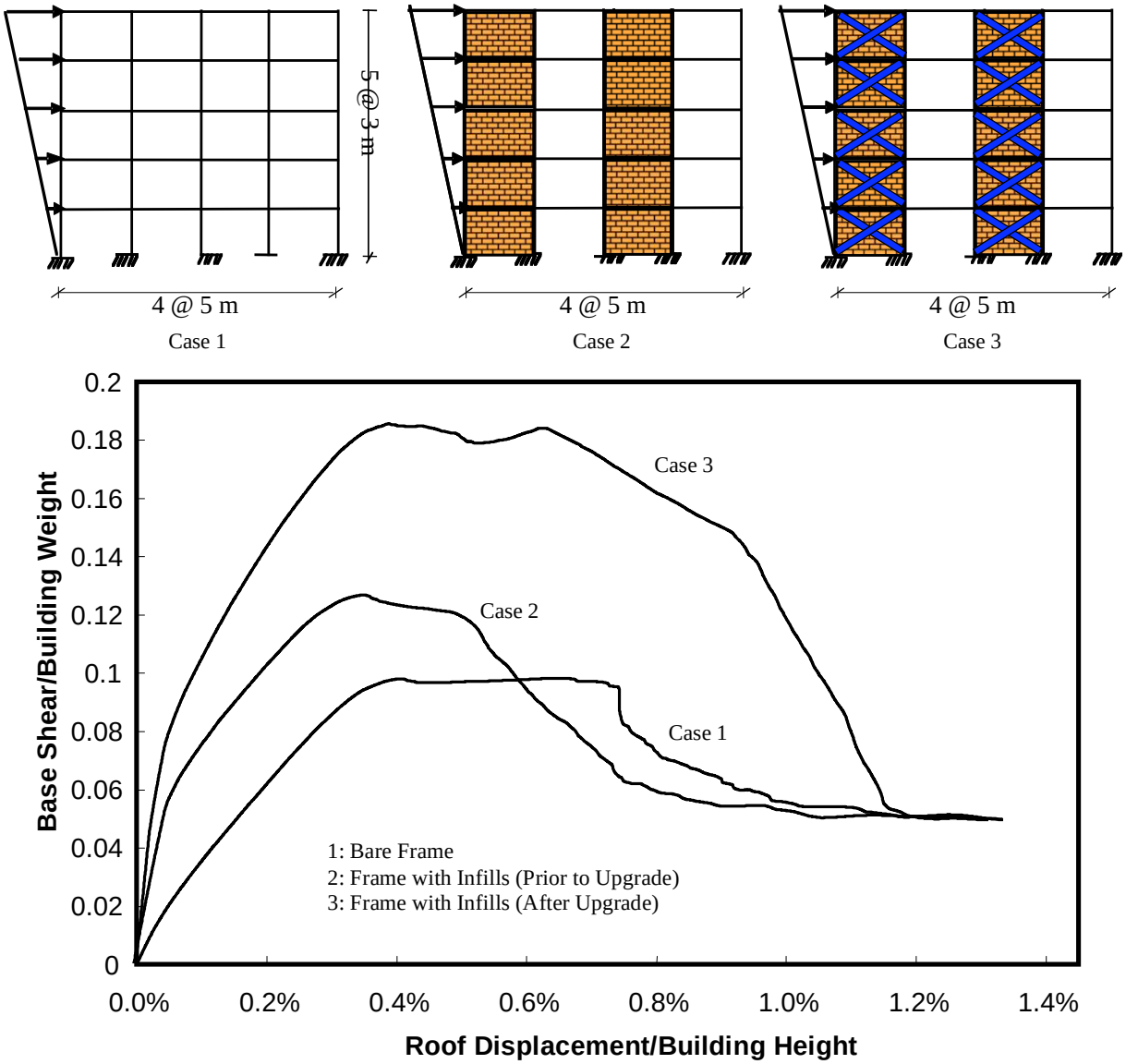

Fig. 25: Analysis results for the building frame analysis

Three cases were analyzed by subjecting the frames to an inverted triangular displacement profile along the building height, Figure 25. First analysis was conducted by neglecting the presence of the infill walls. Second analysis was performed by considering the infill walls with the model previously described in this study. A third analysis was conducted by performing an upgrade of the building with carbon fibre reinforced polymers with material properties given in Table 1. Retrofit design was conducted by considering a CFRP width similar to the width of the estimated compression strut (750 mm). In this way, the compression struts can remain intact and sustain large deformations prior to failure of FRP ties. Sufficient CFRP anchors were provided to eliminate anchorage failures. All the infill walls were retrofitted with CFRPs bonded on two sides of the walls. Normalized base shear ratio was plotted against the normalized roof displacement in Figure 25 to compare the response of different scenarios. It can be observed that presence of the infill walls increases the lateral load carrying capacity by about 30%, whereas the displacement capacity of the

building decreases due to rapid degradation of the infill walls and neighboring frame elements once the base shear capacity is reached. Analysis results show that CFRP retrofit resulted in strength increases of about 90% compared to the bare frame whereas capacity increase was about 50% prior to strengthening with infill walls. For the strengthened frame, some ductility was observed due to progressive failure of the strengthened infill walls. It also can be observed that at large displacements capacity approaches to that of the bare frame. As a result it is possible to say that application of the CFRP retrofit can enhance both the load carrying capacity and deformation capacity of reinforced concrete frames with infill walls.

4.6 Summary and conclusions

A structural model is presented in this study to estimate the behaviour of FRP strengthened reinforced concrete frames with infill walls. The strengthened infill model is composed of a compression strut and a tension tie with trilinear stress strain response. Frame members are modeled with an elastic beam with hinges that are defined by fibres with appropriate stress-strain relations. Static inelastic analyses were conducted to verify the proposed models and comparisons with test results were presented. A good agreement between measured and estimated stiffness, strength and deformation capacity was observed. A case study of typical reinforced concrete frame with infill walls was analyzed with and without upgrades. Substantial strength and deformation capacity increases were observed as a result of the applied retrofit design.

The proposed model for inelastic static analysis of FRP strengthened reinforced concrete frames can be used to in seismic evaluation where pushover analysis is required to obtain a capacity curve. It is believed that the outcome of this research will help the structural engineers in making a decision on the retrofit scheme as the models developed have proven to provide reasonable estimates of strength and deformation capacities.

References

Akgüzel, U. (2003) Seismic Retrofit of Brick Infilled R/C Frames with Lap Splice Problem in Columns. MS thesis, Department of Civil Engineering, Bogaziçi University, Istanbul.

ANSYS 6.1 Documentation, http://www.oulu.fi/atkk/tkpalv/unix/ansys-6.1/content/

Aschheim, M., Gülkan, P., Sezen, H., Bruneau, M., Elnashai, A., Halling, M., Love, J. and Rahnama, M. (2000) Performance of Buildings, *Earthquake Spectra* 16, 237.

Binici, B. and Ozcebe, G. (2005) “Analysis of infilled reinforced concrete frames strengthened with FRPs” Proceedings of the NATO Science for Peace Workshop, Advances in Earthquake Engineering for Urban Risk Reduction, May-June 2005, Istanbul, NATO Science Series, **IV**(66), 455-470, Springer.

Bogazici University Earthquake Master Plan for Istanbul (2003) presented to the Metropolitan Municipality of Istanbul Planning and Construction Directoriat Geotechnical and Earthquake Investigation Department by the Bogazici University, Istanbul Technical University, Middle East Technical University and Yildiz Technical University

El-Dakhakhni, W. W., Elgaaly, M. and Hamid, A. A. (2003) Three-strut model for concrete masonry infilled steel frames, ASCE, Journal of Structural Engineering, 129(2), 177-185.

Ersoy, U., Ozcebe, G., Tankut, T., Akyüz, U., Erduran, E. and Erdem, I. (2003) Strengthening of Infilled Walls with CFRP Sheets”, Proceedings of the NATO Science for Peace

Workshop on Seismic Assessment and Rehabilitation of Existing Buildings, Izmir, NATO Science Series, IV(29), 305-334, Kluwer Academic Publishers.

Flanagan, R. D. and Bennett, R. M. (1999) In-plane behaviour of structural clay tile infilled frames, ASCE, Journal of Structural Engineering, 125(6) 590-599.

Hamoush, S. A., McGinley, M. W., Mlakar, P., Scott, D. and Murray, K. (2001) Out-of-plane strengthening of masonry walls with reinforced composites, ASCE Journal of Composites for Construction, 5(3), 139-145.

Marjani, F. (1997) Behaviour of brick infilled reinforced concrete frames under reversed cyclic loading, Ph.D thesis submitted to Middle East Technical University, Department of Civil Engineering, p. 185, Ankara.

NATO Science for Peace Project SfP977231 (2003) http://www.seru.metu.edu.tr/sfp977231/231_main.html

OpenSees, Open system for earthquake engineering simulation user manual, PEER Center, http://opensees.berkeley.edu/OpenSees/manuals/usermanual/OpenSeesManual.pdf.

Ozcebe, G., Ramirez, J. A., Wasti, S. T. and Yakut, A. (2004) Bingöl earthquake engineering report, TÜBİTAK Structural Engineering Research Unit, Publication No: 2004-01, p. 125.

Ozcebe, G., Ersoy, U., Tankut, T., Erduran, E., Keskin, R. S. and Mertol, H. C. (2003) Strengthening of brick-infilled RC frames with CFRP, TUBITAK Structural Engineering Research Unit Report, No. 2003-01, p. 67.6.

Saneinejad, A. and Hobbs, B. (1995) Inelastic design of infilled frames, ASCE, Journal of Structural Engineering, 121(4), 634-650.

Scott, B. D., Park, R. and Priestley, M. J. N. (1982) Stress-strain behaviour of concrete confined by overlapping hoops at low and high strain rates, ACI Journal, 79(1), 13-27.

Smith, B.S. (1968) "Model Test Results of Vertical and Horizontal Loading of Infilled Frames", ACI Journal, pp.618-624.

Triantafillou, T. C. (1998) Strengthening of masonry structures using epoxy-bonded FRP laminates, ASCE, Journal of Composites for Construction, 2(2), 96-104.

Turkish Ministry of Public Works and Settlement (1998) “Specification for Structures to be Built in Disaster Areas PART III - EARTHQUAKE DISASTER PREVENTION” Government of Republic of Turkey, Ankara

Valluzzi, M. R., Tinazzi, D. and Modena, C. (2002) Shear behaviour of masonry panels strength-ened by FRP laminates, Construction and Building Materials, 16(7), 409-416.

Yuksel, E., Ilki, A., Erol, G., Demir, C. , and Karadogan, F. (2006) “Seismic Retrofit of Infilled Reinforced Concrete Frames with CFRP Composites”, Proceedings of the NATO Science for Peace Workshop, Advances in Earthquake Engineering for Urban Risk Reduction, May-June 2005, Istanbul, NATO Science Series, **IV**(66), 285-300, Springer.

Design rules for seismic retrofitting with FRPs according to Eurocode 8 and their background

Michael N. Fardis
University of Patras, Greece

1. Introduction

1.1 FRP-wrapping for seismic retrofitting of concrete members

The contribution of FRP-wrapping to the improvement of the cyclic deformation capacity of concrete members has been investigated by several researchers: for circular bridge piers, as well as for square or rectangular columns. For buildings, it is the square or rectangular columns that are mainly of interest. In few of these investigations, the original column had lap-splicing of ribbed bars with straight ends in the plastic hinge region.

A European Standard has been recently approved for the seismic assessment and retrofitting of existing buildings (EN 1998-3: 2005, i.e. Part 3 of Eurocode 8, CEN, 2005). This European Standard gives simple rules and expressions for the calculation of the moment capacity, of the effective stiffness at incipient yielding, of the ultimate deflection (or drift) and of the cyclic shear resistance of rectangular or square columns with ribbed (deformed) or smooth (plain) bars, with or without lap splices at floor level, retrofitted through FRP wrapping. These rules are presented here. Their background documentation is presented here for the first time.

1.2 Performance-based criteria for the retrofitting of concrete members according to Eurocode 8

The recently approved European Standard for seismic assessment and retrofitting of existing buildings (i.e. Part 3 of Eurocode 8: EN 1998-3: 2005) adopts a fully performance-based approach. Three performance levels (termed in the European tradition "Limit States") are defined:

- "Near Collapse" (NC). At this Limit State the structure is heavily damaged, may have large permanent drifts, retains little residual lateral strength or stiffness, but vertical elements can still carry the gravity loads. In the verifications, a member may approach its ultimate force or deformation capacity.
- "Significant Damage" (SD), corresponding to the local-collapse prevention performance level to which new buildings are designed according to Part 1 of Eurocode 8 (EN 1998-1:2005). At this Limit State the structure is significantly damaged, may have moderate permanent drifts, but retains some residual lateral strength and stiffness and its full vertical load-bearing capacity. The verifications provide a margin against member ultimate force or deformation capacities.
- "Damage Limitation" (DL). At this Limit State the structure has no permanent drifts; its elements have no permanent deformations, retain fully their strength and stiffness and do not need repair. Members should be verified to remain elastic.

A fully displacement-based approach is applied, in which ductile mechanisms (i.e. concrete members in bending) are checked in terms of deformations. Chord rotations at

member ends are adopted as the main deformation measure for concrete elements. As the analysis aims at capturing the member seismic deformation demands, it should be based on realistic values of the member effective secant-to-yield rigidity. According to Part 3 of Eurocode 8 (CEN, 2005) the secant-to-yield rigidity at each end of a concrete member, EI_{eff}, may be computed from the yield moment, M_y, and the chord rotation at yielding at that end, θ_y, as:

$$EI_{eff}=M_y L_s/3\theta_y \quad (1)$$

where L_s is the shear span (moment-to-shear ratio) at that end.

For the three Limit States mentioned above, Annex A in Part 3 of Eurocode 8 specifies for members of concrete buildings the performance requirements shown in Table 1. Flexure is always considered as a ductile mechanism and checked in terms of deformations - in this case in terms of chord-rotation demands at member ends, compared to the chord rotation at yielding, θ_y, or to conservative estimates of the ultimate chord rotation, θ_u. Shear is considered as a brittle mechanism and checked in terms of forces.

Member	Limited Damage (LD)	Significant Damage (SD)	Near Collapse (NC)
Ductile primary	$\theta_E \le \theta_y$ (1)	$\theta_E \le 0.75\theta_{u,m-\sigma}$ (2)	$\theta_E \le \theta_{u,m-\sigma}$ (2)
Ductile secondary		$\theta_E \le 0.75\theta_{u,m}$ (3)	$\theta_E \le \theta_{u,m}$ (3)
Brittle primary	$V_{E,max} \le V_{Rd,EC2}$ (4), $V_{Rd,EC8}/1.15$ (5)		
Brittle secondary	$V_{E,max} \le V_{Rm,EC2}$ (6), $V_{Rm,EC8}$ (6)		

(1) θ_E: chord-rotation demand from the analysis; θ_y: chord-rotation at yielding, Eqs.(2), (3).

(2) $\theta_{u,m-\sigma}$: mean-minus-stand. deviation chord-rotation supply, equal to $\theta_y+\theta^{pl}_{u,m}/1.8$, with θ_y from Eqs.(2), (3) and $\theta^{pl}_{u,}$ from Eq.(4).

(3) $\theta_{u,m}$: mean chord-rotation supply, $\theta_{u,m}=\theta_y+\theta^{pl}_{u,m}$, with θ_y from Eqs.(2), (3) and $\theta^{pl}_{u,}$ from Eq.(4).

(4) $V_{Rd,EC2}$: shear resistance before flexural yielding, as given for monotonic loading in Eurocode 2, using mean material strengths divided by partial factors of materials and by a "confidence factor" that depends on the amount and reliability of available information.

(5) $V_{Rd,EC8}$: shear resistance for shear failure in cyclic loading after flexural yielding, given by Eqs. (14)-(16) as applicable, with mean material strengths divided by partial factors for materials and the "confidence factor" depending on the available information.

(6) As in (5), (6) above, but using mean material strengths.

Table 1. Compliance criteria for assessment or retrofitting of concrete members in Annex A of Eurocode - Part 3

Annex A in Part 3 of Eurocode 8 (CEN, 2005) gives rules and expressions for the calculation of the mean value of the chord rotation at yielding, θ_y, or at ultimate, $\theta_{u,m}$, as outlined in Section 2.1 below for members with longitudinal reinforcement that is continuous in the plastic hinge region and in Section 2.2 for members with lap-spliced longitudinal bars in the plastic hinge region. The shear resistance under cyclic loading after flexural yielding, $V_{R,EC8}$, is also given Annex A in Part 3 of Eurocode 8, to supplement the relevant rules in Eurocode 2 that address only the shear resistance in monotonic loading, $V_{Rd,EC2}$, and do not reflect the decrease in shear resistance with the cyclic chord-rotation ductility demand.

2. Design rules for the strength, stiffness and deformation capacity of concrete members with FRP-wrapped ends

2.1 Stiffness, flexural strength and deformation capacity of members with no lap splicing in the plastic hinge and without FRP-wrapping

2.1.1 Introduction

The rules for the calculation of the yield moment, the secant stiffness at apparent yielding and the cyclic deformation capacity of FRP-jacketed members with or without lap splicing in the plastic hinge region are based on appropriate modification of the corresponding values of concrete members with longitudinal bars without lap splicing and no FRP wrapping.

2.1.2 Flexural strength and effective stiffness

The yield moment M_y of the end section of a concrete member with longitudinal bars not lap-spliced in the vicinity of the end section may be determined, along with the yield curvature, ϕ_y, from first principles (see Panagiotakos and Fardis, 2001). The effective stiffness to yielding at each end of such a member is determined for the shear span L_s from Eq.(1), where the chord rotation at yielding at that end, θ_y, may be determined as follows (Biskinis, and Fardis, 2004, CEN, 2005):

- in beams or columns:

$$\theta_y = \phi_y (L_s + a_V z)/3 + 0.0013(1 + 1.5h/L_s) + 0.13\phi_y d_{bL} f_{yL}/\sqrt{f_c} \quad (2)$$

- in rectangular, T- or barbelled walls:

$$\theta_y = \phi_y (L_s + a_V z)/3 + 0.002(1 - 0.125L_s/h) + 0.13\phi_y d_{bL} f_{yL}/\sqrt{f_c} \quad (3)$$

where:

- f_{yL}, f_c are in MPa,
- h depth of cross-section,
- $\alpha_V z$ = tension shift of bending moment diagram, with:
  - z = length of internal lever arm (equal to the distance between tension and compression in beams, columns, or walls with barbelled or T-section, or to z=0.8h in walls with rectangular section),
  - α_V = 1 if shear cracking precedes flexural yielding at the end section (i.e. if the value of M_y there exceeds the product of L_s times the shear resistance of the member considered without shear reinforcement, $V_{R,c}$),
  - α_V = 0 otherwise (i.e. if $M_y < L_s V_{R,c}$).

The 3rd term represents the fixed-end rotation due pull-out of the tension reinforcement from its development beyond the member end, and is omitted if such pull-out is not physically possible (f.i., if the end of the longitudinal bars is fixed at the end section). The diameter d_{bL} of the tension reinforcement and the value of f_c along its anchorage beyond the end section of the member should be used in this term.

For about 1500 tested beams or columns and 160 walls, Eqs.(2), (3) give a median of 1.0 for the ratio experimental-to-predicted chord rotation at yielding and a coefficient-of-variation of 33.7% for the beams and the columns and 32.2% for the walls (Biskinis, and Fardis, 2004).

2.1.3 Deformation capacity in flexure

The flexure-controlled deformation capacity of the monolithic or the jacketed member is expressed in terms of the plastic part, θ_u^{pl} of the ultimate chord rotation (total ultimate chord rotation, θ_u, minus value at yielding, θ_y) at the end of the member. For single- or double-cantilever members, the chord rotation at the fixed end is equal to the drift ratio (relative displacement of the two ends, divided by member length). An empirical expression is given for the value of θ_u^{pl} in members with rectangular cross-section, ductile hot-rolled or heat-treated deformed longitudinal bars, possibility for slip of the longitudinal bars from their development beyond the section of maximum moment and detailing for earthquake resistance (including avoidance of lap splices in the plastic hinge region, but not including diagonal bars). With units MN and m (Biskinis, and Fardis, 2004, CEN, 2005):

$$\theta_u^{pl} = 0.0145 \cdot a_{wall} \cdot \left(0.25^{\nu}\right) \cdot \left[\frac{\max\left(0.01,\omega'\right)}{\max\left(0.01,\omega\right)}\right]^{0.3} \left(f_c\right)^{0.2} \left(\frac{L_s}{h}\right)^{0.35} 25^{\left(\alpha\rho_{sx}\frac{f_{yw}}{f_c}\right)} \quad (4)$$

where:

- a_{wall} = 1 for beams or columns,
- a_{wall} = 0.6 for walls,
- ν = N/bhf_c (with b denoting the width of the compression zone and the axial force N being positive for compression),
- ω = $\rho f_{yL}/f_c$, mechanical reinforcement ratio of tension longitudinal reinforcement (including any longitudinal reinforcement between the two flanges),
- ω' = $\rho' f_{yL}/f_c$, mechanical reinforcement ratio of compression, reinforcement,
- ρ_{sx} = $A_s/b_w s_h$, transverse steel ratio parallel to the direction (x) of loading,
- α = $\left(1-s_h/(2b_o)\right)\left(1-s_h/(2h_o)\right)\left[1-\sum_{i=1,n_{restr}} b_i^2/(6h_o b_o)\right]$, confinement effectiveness factor (Sheikh and Uzumeri, 1982), with:
  - b_o, h_o= dimensions of the confined core to the center of the hoop, and
  - b_i = spacing between centers of the n_{restr} longitudinal bars (index i) laterally restrained by a stirrup corner or a cross-tie along the cross-section perimeter.

For monotonic loading, coefficient 0.0145 in Eq.(4) should be replaced by 0.03. If fixed-end rotation due pull-out of the tension reinforcement from its development beyond the member end is not physically possible, then the plastic part of the ultimate chord rotation, θ_u^{pl}, monotonic or cyclic, should be divided by 1.625 (Biskinis, and Fardis, 2004, CEN, 2005).

In 934 cyclic tests of members detailed for earthquake resistance, Eq.(4) gives a median of 1.0 and a coefficient-of-variation - C.o.V. of 38% for the ratio of experimental-to-predicted cyclic chord rotation capacity, θ_u (plastic part, θ_u^{pl}, plus value at yielding, θ_y). The corresponding values for about 300 monotonic tests of members regardless of detailing are 1.0 for the median and 53.5% for the C.o.V. (Biskinis, and Fardis, 2004, CEN, 2005).

The results of the very few available tests on columns with smooth (plain) longitudinal bars and 180^o hooks suggest that Eq.(4) is also applicable in that case.

For members with ribbed (deformed) bars without lap splices in the plastic hinge region, but with details not appropriate for earthquake resistance (e.g., not closed stirrups), the right-hand-side of Eq.(4) should be multiplied by 0.825. In 42 cyclic tests of members not detailed for earthquake resistance, this rule gives a median of 1.005 and a C.o.V. of 33.6% for the ratio of experimental-to-predicted cyclic chord rotation capacity, θ_u, i.e. for the plastic part, θ_u^{pl}, plus the value at yielding, θ_y (Biskinis, and Fardis, 2004, CEN, 2005).

2.2 Stiffness, flexural strength and deformation capacity of members with lap splices in the plastic hinge, but without FRP-wrapping

2.2.1 Members with smooth longitudinal bars and standard 180° hooks

The few test results on columns with smooth bars suggest that the rules in 2.1.2 above for the calculation of M_y and θ_y of members with rectangular section and ribbed longitudinal bars without lapping, can be taken to apply to rectangular columns with smooth longitudinal bars as well, even when these bars are lapped starting at the end section over a lapping $l_o \geq 15d_{bL}$.

In rectangular columns with smooth longitudinal bars lapped starting at the end section over a lapping $l_o \geq 15d_{bL}$, the plastic part of the cyclic chord rotation capacity given by the rules reviewed in 2.1.3 above (cf. Eq.(4)) is reduced via (CEN, 2005):

- multiplication by $0.0035(60+\min(50, l_o/d_{bL}))(1-l_o/L_s)$, and
- subtraction of the lap length l_o from the shear span L_s, as the ultimate condition is controlled by the region right after the end of the lap.

In four available cyclic tests of columns with lap-spliced smooth bars, this rule gives a median of 0.9 for the ratio experimental-to-predicted cyclic chord rotation capacity and a C.o.V. of 30.4%.

2.2.2 Members with lap-spliced ribbed longitudinal bars

The available test results on members with rectangular section and ribbed longitudinal bars with lapped straight ends starting at the end section show that in the calculation of:

- the yield moment M_y,
- the yield curvature ϕ_y (which is used in the determination of the parts of the chord rotation at yielding, θ_y, which is due to flexure or to fixed-end rotation due to slippage of the bars from their anchorage zone beyond the member end), and of
- the plastic part of the cyclic chord rotation capacity, θ_u^{pl},

the compression reinforcement ratio should be doubled over the value applying outside the lap splice. Moreover, if the straight lap length l_o is less than $l_{oy,min}$, given by:

$$l_{oy,min}=0.3d_{bL}f_{yL}/\sqrt{f_c}, \quad (5)$$

with f_{yL} and f_c in MPa, then M_y, ϕ_y, θ_u and θ_u^{pl} should be calculated with the yield stress of the tensile longitudinal reinforcement, f_{yL}, multiplied by $l_o/l_{oy,min}$.

In 81 tested columns with lap splices, this set of rules gives a median of 1.005 for the ratio of experimental-to-predicted yield moment and a C.o.V. of 11.9%. Figures 1(a) and 1(b) show the ratio of experimental-to-predicted M_y before and after the correction according to the above rules, as a function of $l_o/(d_{bL}f_{yL}/\sqrt{f_c})$, while Figure 1(c) compares the experimental value of M_y to the predicted value after the above correction.

The 2nd term in the right-hand-side of Eqs.(2) and (3) for the chord rotation at yielding should be multiplied by the ratio of the yield moment M_y as modified due to the lap splicing, to the yield moment outside the lap splice. This rule gives a median of 0.975 and a C.o.V. of 23.3% for the ratio of experimental-to-predicted effective stiffness at yielding in 61 columns with lap splices. Figures 2(a) and 2(b) show the ratio of experimental-to-predicted θ_y before and after the correction according to these rules, as a function of $l_o/(d_{bL}f_{yL}/\sqrt{f_c})$; Figure 2(c) compares the experimental value of θ_y to the predicted value after the above correction. Figure 3(a) presents the ratio of experimental-to-predicted $EI_{eff}=M_yL_s/3\theta_y$ after the above corrections of M_y and θ_y as a function of $l_o/(d_{bL}f_{yL}/\sqrt{f_c})$ and Figure 3(b) compares the experimental value of EI_{eff} to the predicted one after these corrections.

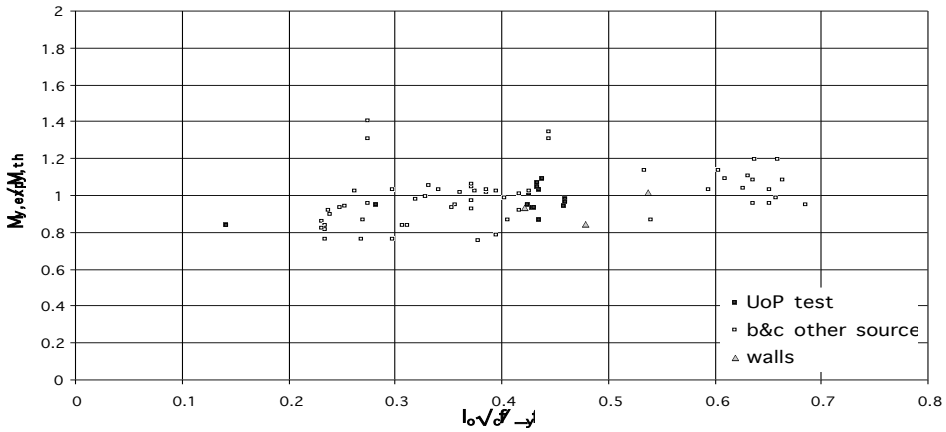

(a)

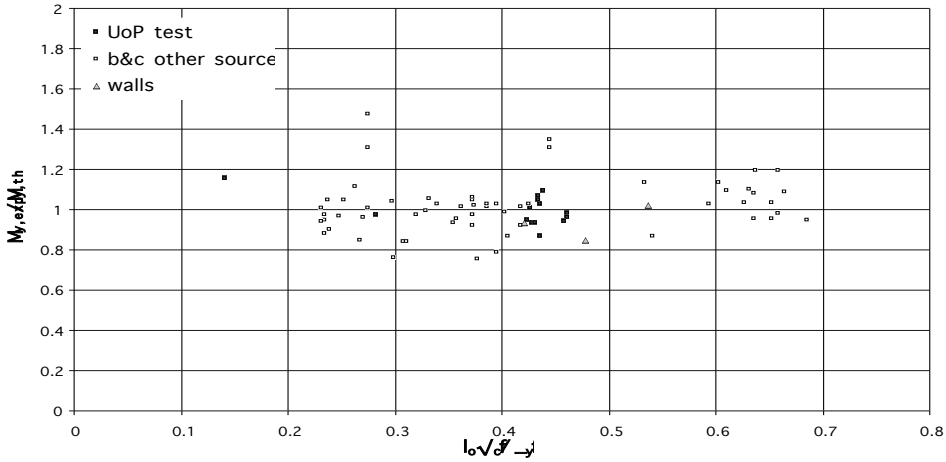

(b)

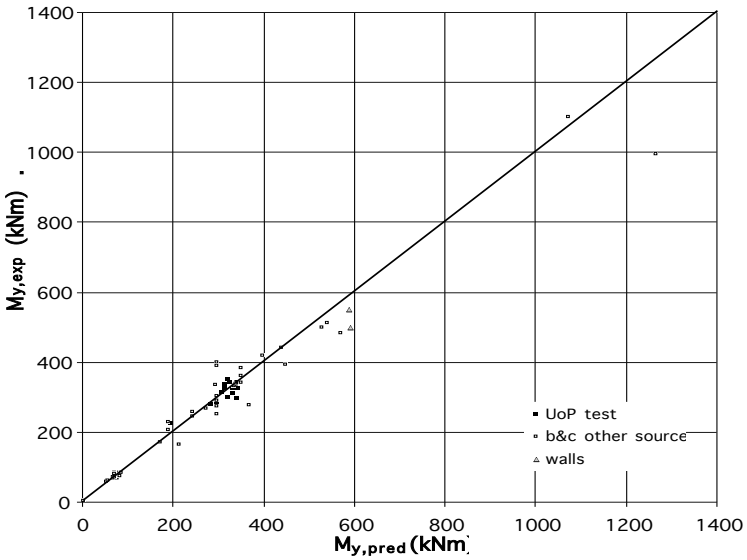

(c)

Fig. 1: Comparison of experimental M_y of members with lap-spliced ribbed bars to value predicted: (a) without, or (b), (c) with the correction according to the rules in 2.2.2.

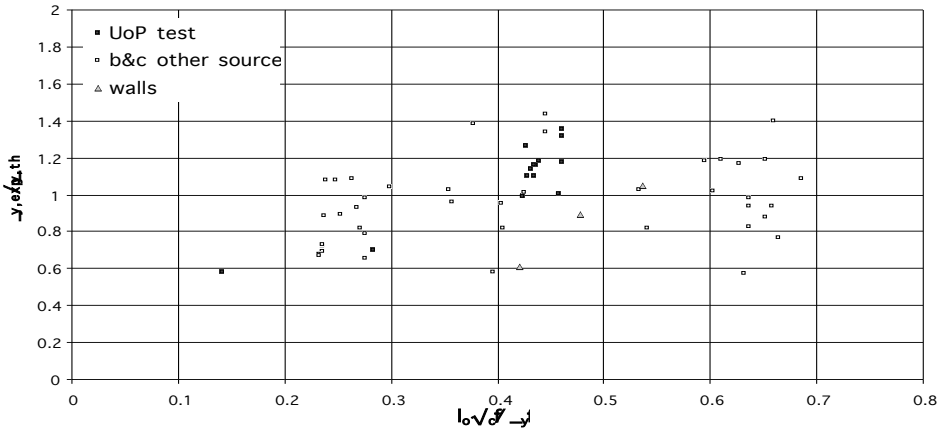

(a)

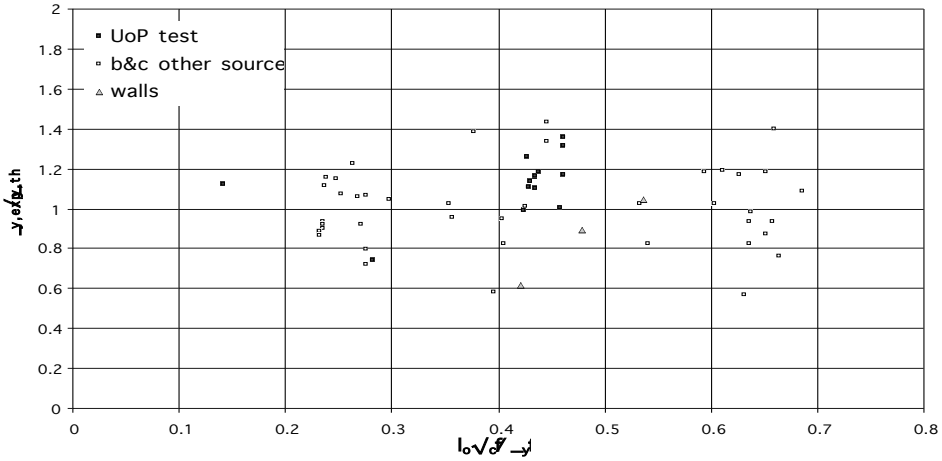

(b)

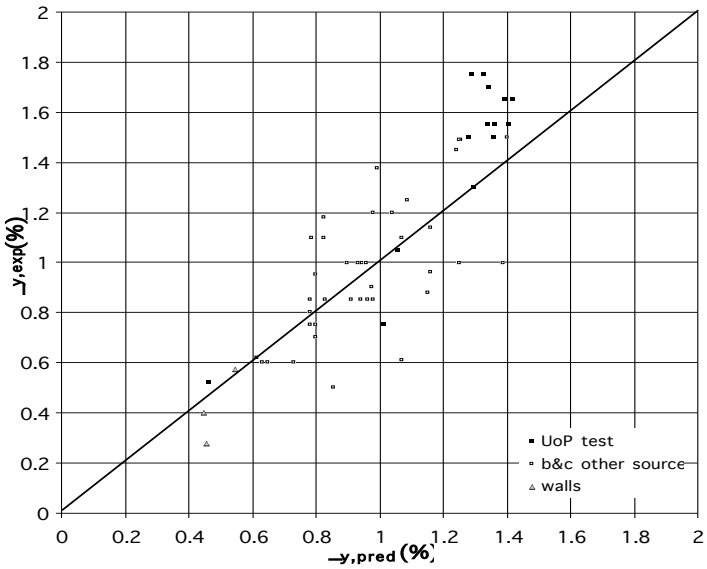

(c)

Fig. 2: Comparison of experimental θ_y of members with lap-spliced ribbed bars to value predicted: (a) without, or (b), (c) with the correction according to the rules in 2.2.2.

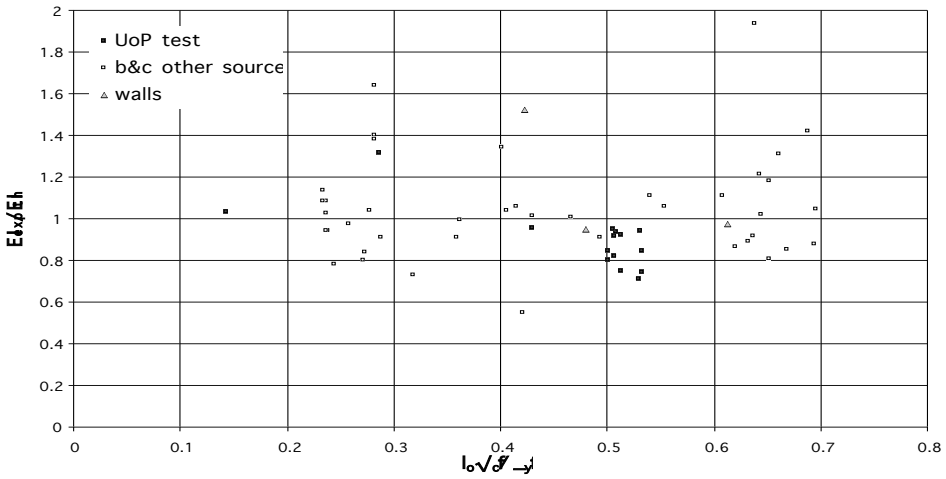

(a)

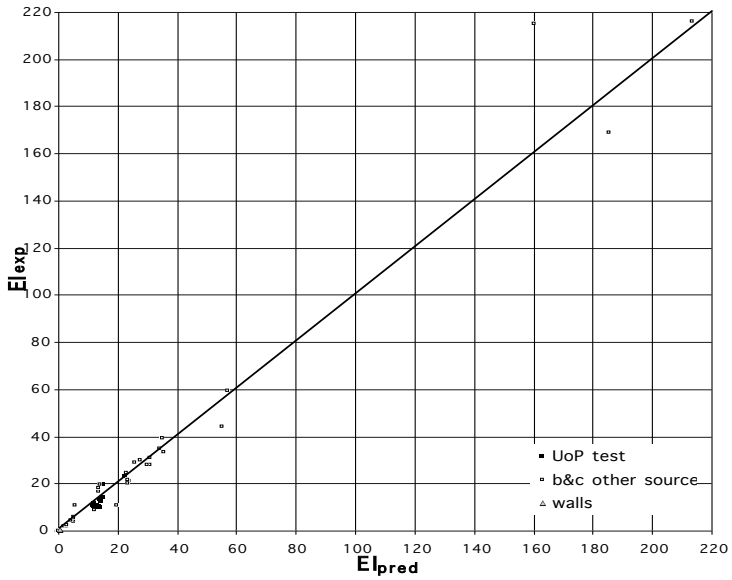

(b)

Fig. 3: Comparison of experimental value of $EI_{eff} = M_y L_s / 3\theta_y$ of members with lap-spliced ribbed bars to value predicted after the corrections of M_y, θ_y according to the rules in 2.2.2.

The tests to failure on members with rectangular section and ribbed longitudinal bars with straight lap-spliced ends show that the plastic part of chord rotation capacity, θ_u^{pl}, decreases with l_o in proportion to $l_o/l_{ou,min}$, if $l_o < l_{ou,min}$, where $l_{ou,min}$ is given by:

$$l_{ou,min} = d_{bL} f_{yL} / [(1.05 + 14.5 \alpha_l \rho_{sx} f_{yw} / f_c) \sqrt{f_c}] \quad (6)$$

where:

- f_{yL}, f_{yw}, f_c (all in MPa), ρ_{sx} and d_{bL} have been defined previously, and
- $\alpha_l = (1-0.5 s_h/b_o)(1-0.5 s_h/h_o) n_{restr}/n_{tot}$, with
  - s_h: stirrup spacing,
  - b_o, h_o: dimensions of the confined core to the hoop centerline,
  - n_{tot}: total number of longitudinal bars along the cross-section perimeter and
  - n_{restr}: number of these bars laterally restrained by a stirrup corner or a cross-tie.

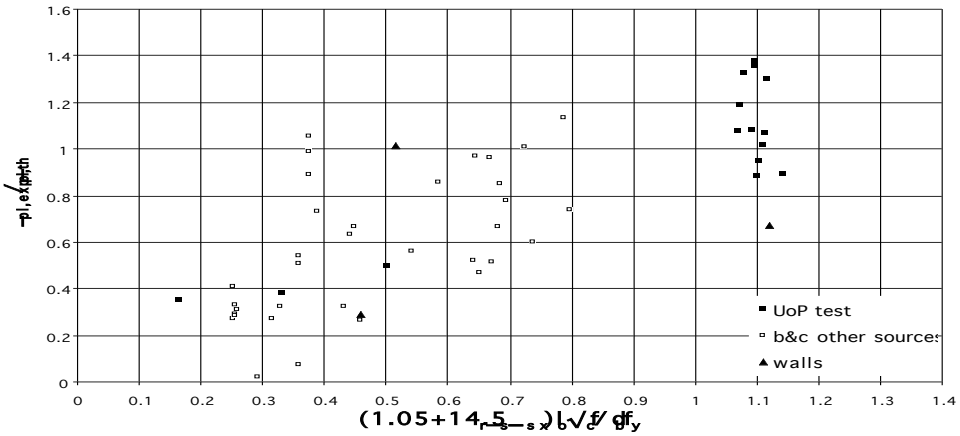

(a)

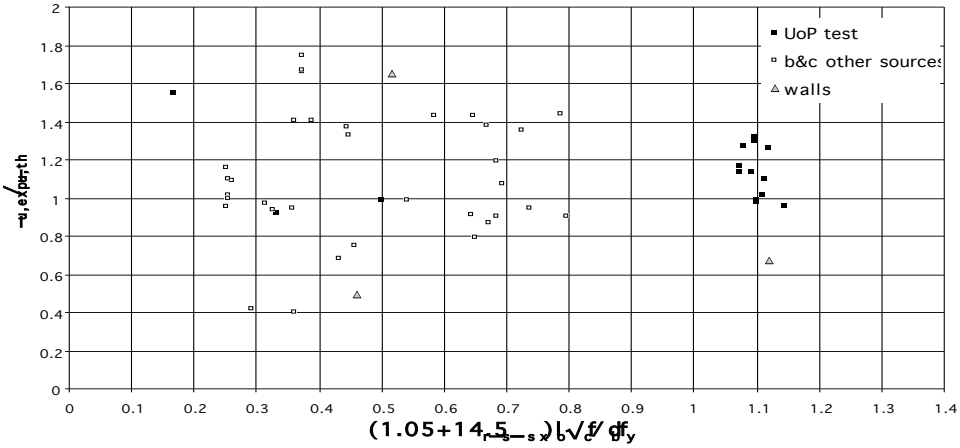

(b)

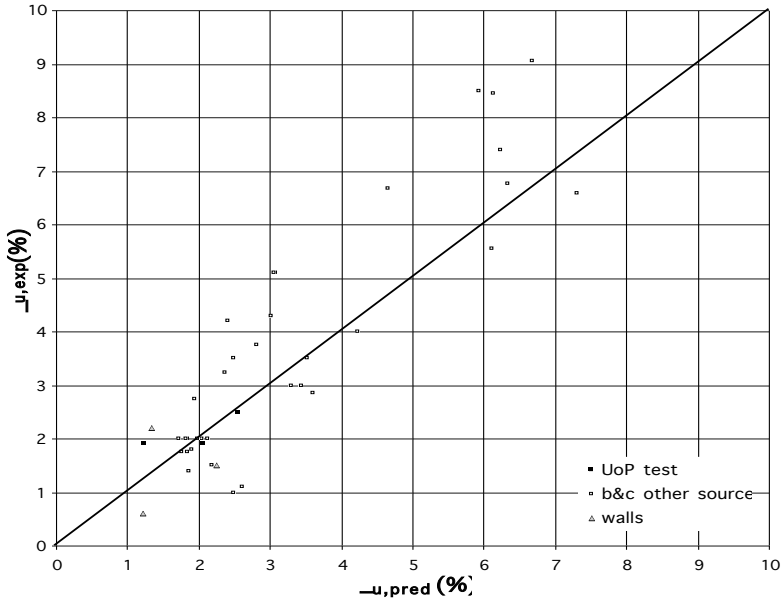

(c)

Fig. 4: Comparison of experimental θ_u of members with lap-spliced ribbed bars to value predicted: (a) without, or (b), (c) with the correction according to the rules in 2.2.2.

The value of the chord rotation at yielding, θ_y, to be added to the so-computed θ_u^{pl} to obtain θ_u, should also account for the effect of lapping if l_o is less than $l_{oy,min}$ given by Eq. (5).

In the 40 available cyclic tests of members with lap length less than $l_{ou,min}$, this rule gives a median of 1.0 for the ratio of experimental-to-predicted to cyclic chord rotation capacity, θ_u^{pl}, and a C.o.V. of this ratio of 31.3%. Figures 4(a) and 4(b) show the ratio of experimental-to-predicted θ_u before and after the correction according to the above rules, as a function of $l_o/(d_{bL} f_{yL}/\sqrt{f_c})$, while Figure 4(c) compares the experimental value of θ_u to the predicted value after these corrections.

2.3 Stiffness, flexural strength and deformation capacity of members with FRP-wrapping

2.3.1 Members without lap splicing in the plastic hinge

According to the available tests on rectangular columns with either ribbed or smooth longitudinal bars and no lapping, in first approximation the values of M_y and θ_y may be assumed to be unaffected by FRP wrapping of the member end. Better agreement with test results may be obtained, though, if the calculation of M_y and θ_y is based on the compressive strength of confined concrete, f_{cc}, instead of the uniaxial strength of unconfined concrete, f_c. If this later assumption is made, the median of the ratio of experimental-to-predicted value of M_y in 116 tests is equal to 1.04 and the C.o.V. of this ratio is equal to 18.8%; the median of the experimental-to-predicted-ratio of effective stiffness at yielding in 109 tests is equal to 0.98 and its C.o.V. is 28%. The experimental results for M_y, θ_y and $EI_{eff} = M_y L_s/3\theta_y$ are compared to the so-predicted values in Figures 5, 6 and 7, respectively.

The enhancement of the deformation capacity of the member, θ_u, and the improvement of any lap splices due to FRP sheets wrapped around the member end with the fibres oriented along the perimeter, may be obtained as described in the following paragraphs.

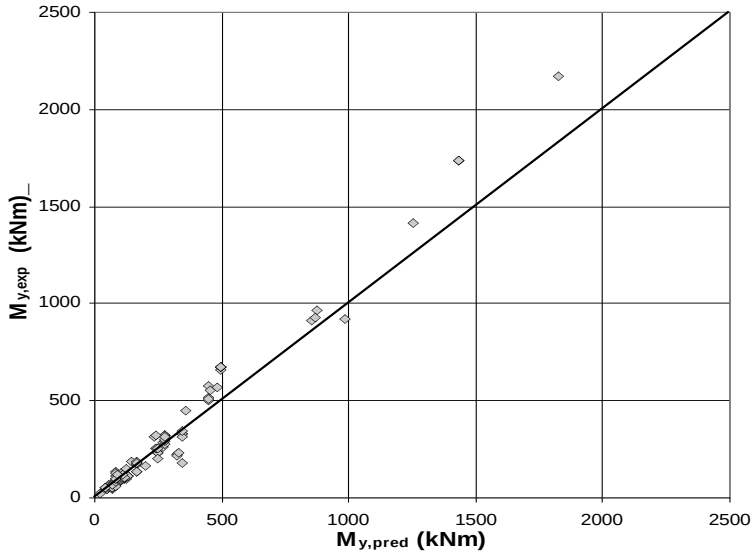

Fig. 5: Comparison of experimental M_y of members with continuous (not lap-spliced) ribbed bars and with FRP wrapping to value predicted on the basis of first principles and of the effect of confinement by the FRP on concrete compressive strength.

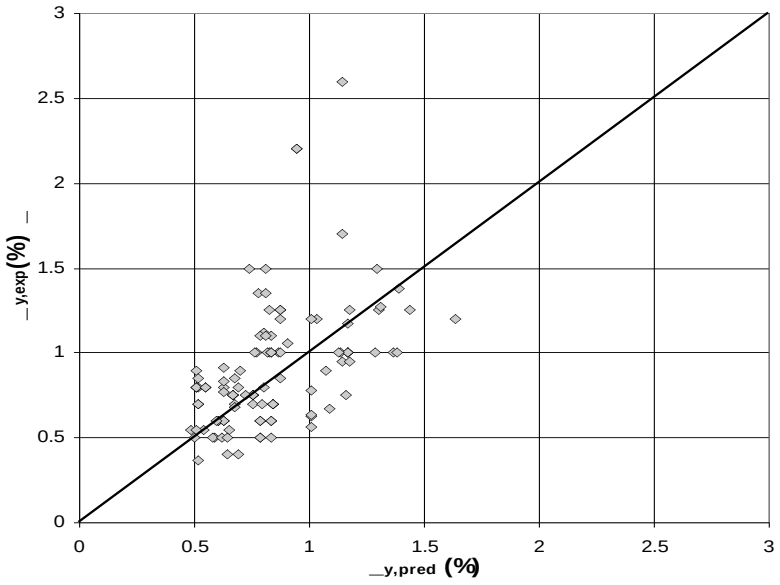

Fig. 6: Comparison of experimental θ_y of members with continuous (not lap-spliced) ribbed bars and with FRP wrapping to value predicted from Eqs.(2) or (3), considering the effect of confinement by the FRP on concrete compressive strength.

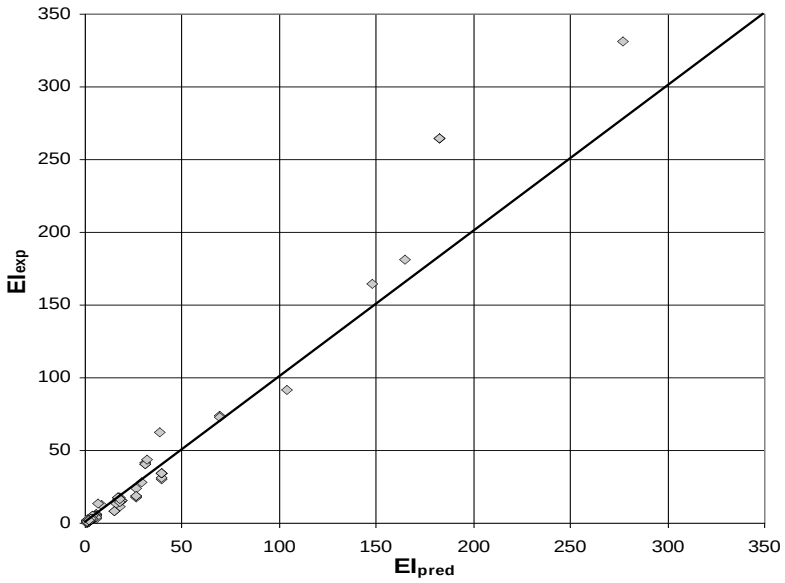

Fig. 7: Comparison of experimental $EI_{eff} = M_y L_s / 3\theta_y$ of members with continuous ribbed bars and FRP wraps to the value predicted from first principles and Eqs. (2) or (3), considering the effect of confinement by the FRP on concrete compressive strength.

The member deformation capacity will profit from confinement by the FRP wrapping of its end, provided that such wrapping extends up to a distance to the end section which is sufficient to ensure that the yield moment M_y in the unwrapped part is not exceeded before the end section reaches its flexural strength, as this increases due to confinement by the FRP. If this condition is met, the increase of the plastic part of the chord rotation capacity, θ_u^{pl}, may

be determined by adding a term due to the FRP to the term describing confinement by the transverse reinforcement, $\alpha \rho_{sx} f_{yw}/f_c$, where $\rho_{sx} = A_{sx}/b_w s_h$, f_{yw}, f_c and α were defined previously in connection with Eq. (3). The term describing confinement by the FRP is $\alpha_f f_{f,e} \rho_f / f_c$ where:

- $\rho_f = 2t_f/b_w$ is the transverse FRP ratio in the loading direction, x,
- $f_{f,e} = \min(f_{u,f}; \varepsilon_{u,f} E_f)[1-0.7\min(f_{u,f}; \varepsilon_{u,f} E_f)\rho_f/f_c]$ is an effective FRP strength, with:
  - $f_{u,f}$, E_f: FRP strength and Modulus, and
  - $\varepsilon_{u,f}$: limit strain, equal to 0.015 for Carbon- or Aramid-FRP, to 0.02 for Glass-FRP

  and,
- $\alpha_f = 1-[(b-2R)^2+(h-2R)^2]/(3bh)$, is the FRP confinement effectiveness factor, with:
  - b, h: full dimensions of the section, and
  - R rounding radius at the corner.

This rule gives a median experimental-to-predicted chord rotation capacity in 90 cyclic tests with Carbon- Aramid- or Glass-FRP equal to 1.005 and a C.o.V. of 31%. The experimental results for θ_u are compared to the so-predicted values in Figure 8.

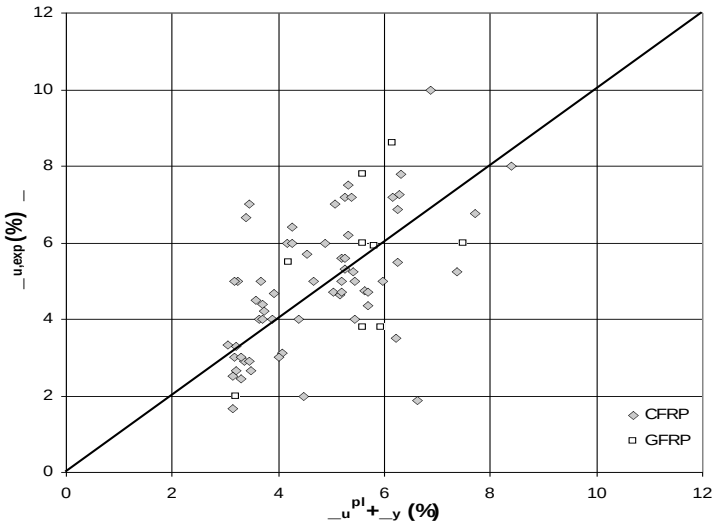

Fig. 8: Comparison of experimental θ_u of members with continuous ribbed bars and FRP wraps to value from Eq.(4) modified according to the rules in 2.3.2 for the effect of the FRP.

2.3.2 Members with lap splicing in the plastic hinge region

The rules given in this section apply to members with:

- rectangular section,
- longitudinal bars lap-spliced over a length $l_o \geq 15 d_{bL}$, starting at the end section, and
- FRP-wrapping of the end region over a length at least equal to $2l_o/3$.

For <u>smooth</u> longitudinal bars with standard 180^o hooks, the available tests suggest that M_y, θ_y and θ_u may be computed taking into account the FRP according to 2.3.1 above, neglecting the lap splicing.

For <u>ribbed</u> longitudinal bars with straight ends, M_y, ϕ_y, θ_y can be calculated according to the first paragraph of 2.2.2, except that $l_{oy,min}$ is now reduced to two-thirds of the value given by Eq.(5) (i.e. to*:* $l_{oy,min} = 0.2 d_{bL} f_{yL}/\sqrt{f_c}$). In 20 tests of columns with such lap splice regions wrapped with FRP, this rule gives a median of 1.065 and a C.o.V. of 9.2% for the ratio of experimental-to-predicted M_y and a median of 1.01 and a C.o.V. of 22% for the ratio of experimental-to-predicted effective stiffness at yielding.

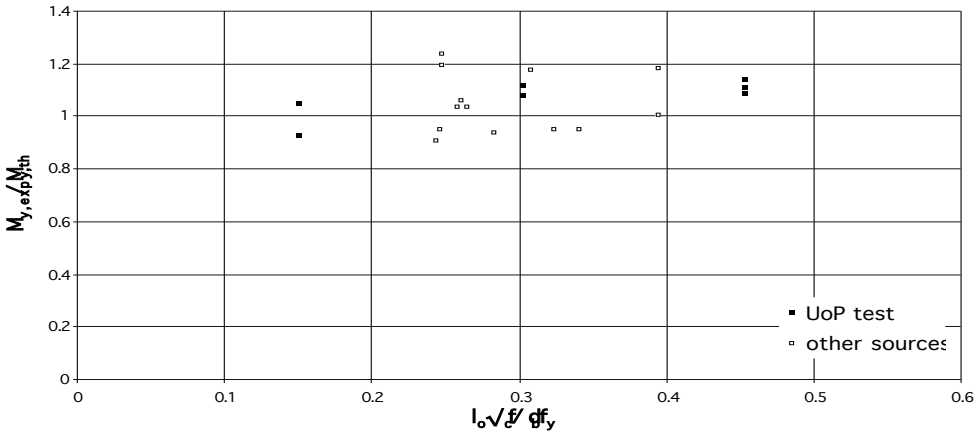

(a)

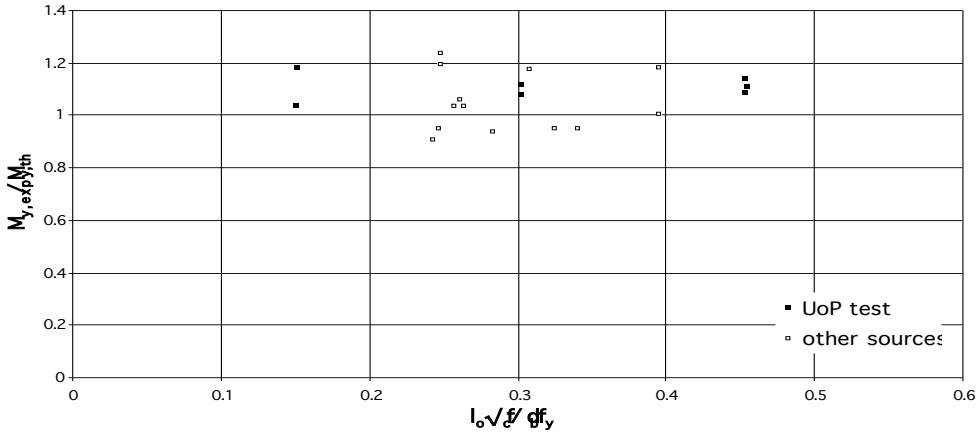

(b)

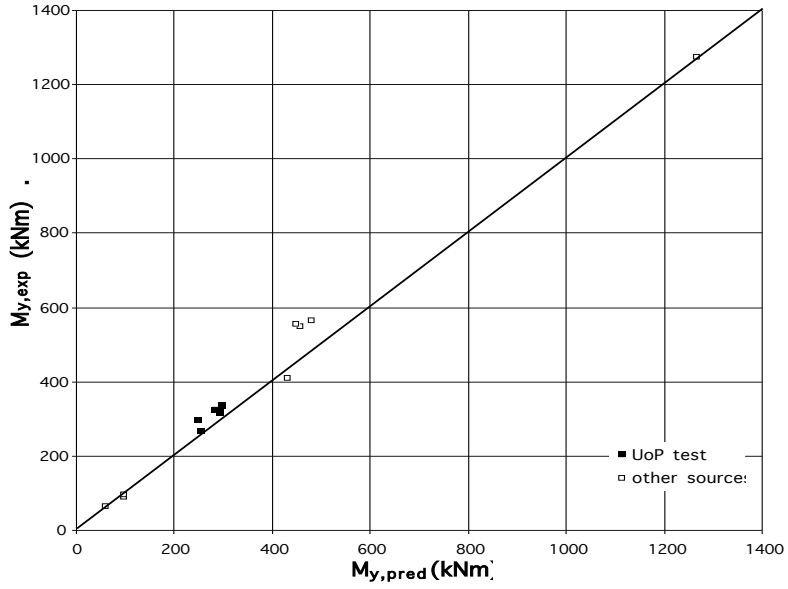

(c)

Fig. 9: Comparison of experimental M_y of members with lap-spliced ribbed bars and FRP wrapping to value predicted: (a) without, or (b), (c) with the correction for the effect of lap splicing.

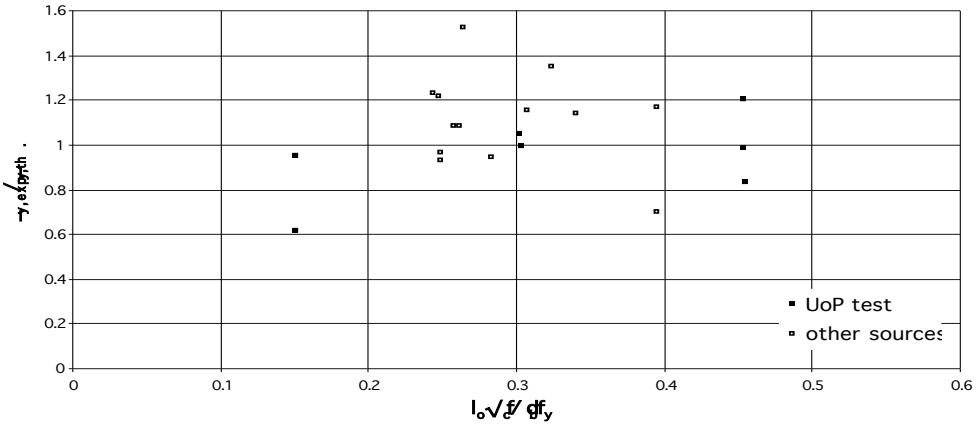

(a)

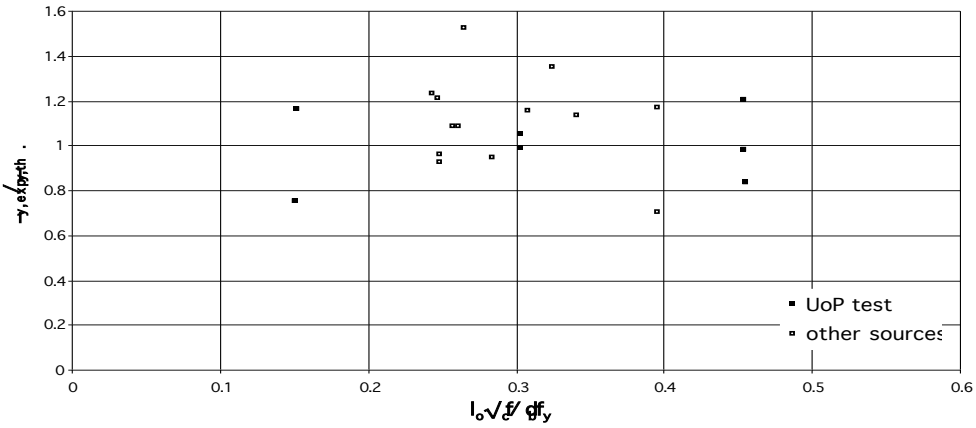

(b)

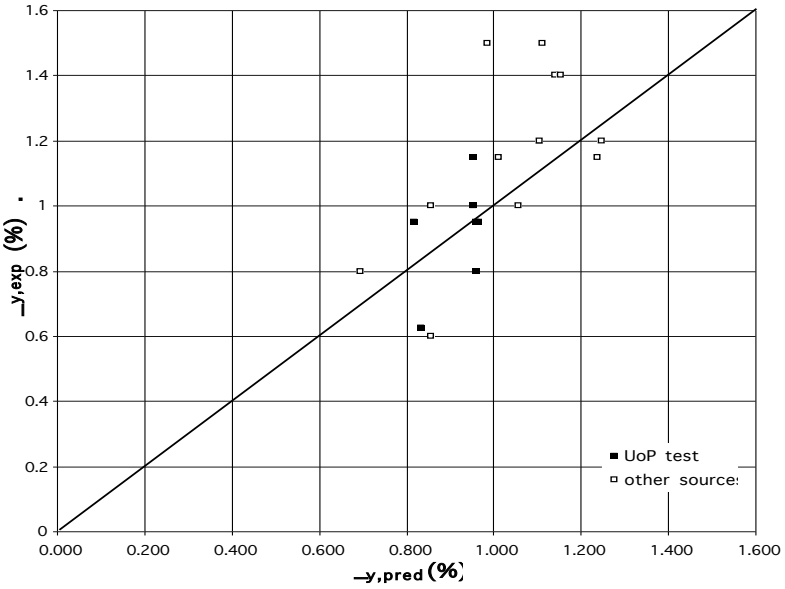

(c)

Fig. 10: Comparison of experimental θ_y of members with lap-spliced ribbed bars and FRP wrapping to value predicted: (a) without, or (b), (c) with the correction for the effect of lap splicing.

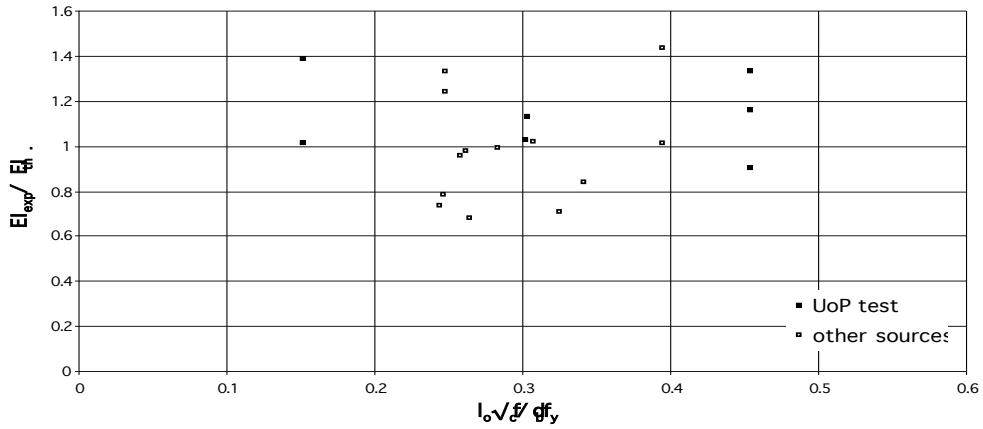

(a)

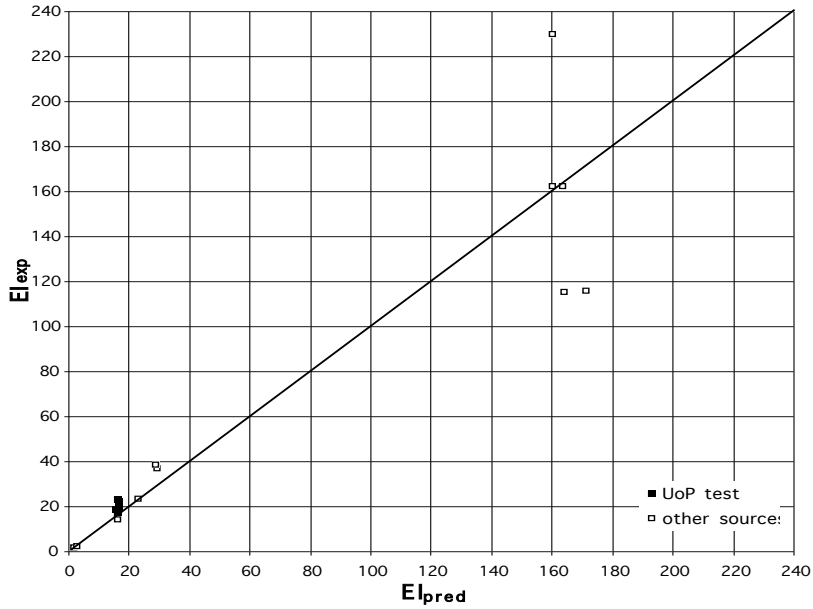

(b)

Fig. 11: Comparison of experimental $EI_{eff} = M_y L_s / 3\theta_y$ of members with lap-spliced ribbed bars to value predicted after correction of M_y, θ_y for the effect of lap splicing according to the rules in 2.3.2.

Figures 9(a) and 9(b) show the ratio of experimental-to-predicted M_y before and after the correction according to the above rules, as a function of $l_o/(d_{bL} f_{yL}/\sqrt{f_c})$, while Figure 9(c) compares the experimental value of M_y to the predicted value after the above correction. Similarly, Figures 10(a) and 10(b) present the ratio of the experimental-to-predicted θ_y before and after the correction according to these rules, as a function of $l_o/(d_{bL} f_{yL}/\sqrt{f_c})$, and Figure 10(c) compares the experimental value of θ_y to the predicted value after the above correction. Finally, Figure 11(a) presents the ratio of experimental-to-predicted $EI_{eff} = M_y L_s/3\theta_y$ after the above corrections of M_y and θ_y as a function of $l_o/(d_{bL} f_{yL}/\sqrt{f_c})$ and Figure 11(b) compares the experimental value of EI_{eff} to the predicted one after these corrections.

The rules of 2.2.2 apply for the calculation of the plastic part of the cyclic chord rotation capacity, θ_u^{pl}, as well, except that it is not possible to profit for the same purpose from the benefits of confinement by the transverse bars and the FRP. More specifically, θ_u^{pl} may be estimated as:

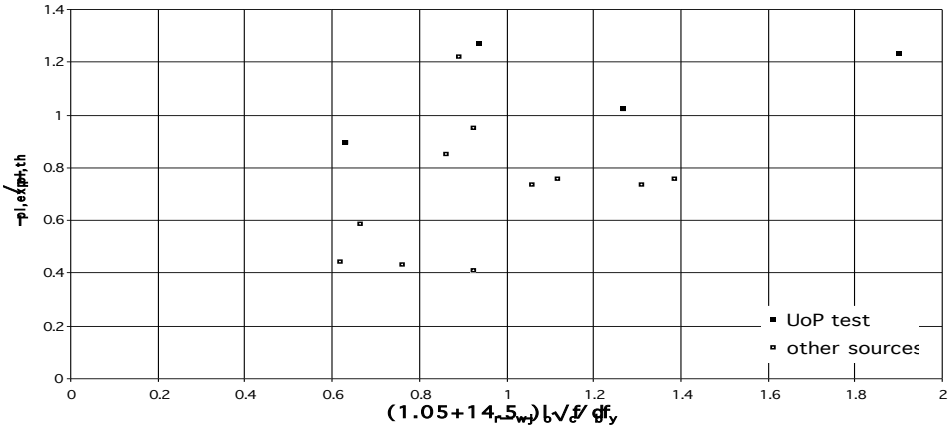

(a)

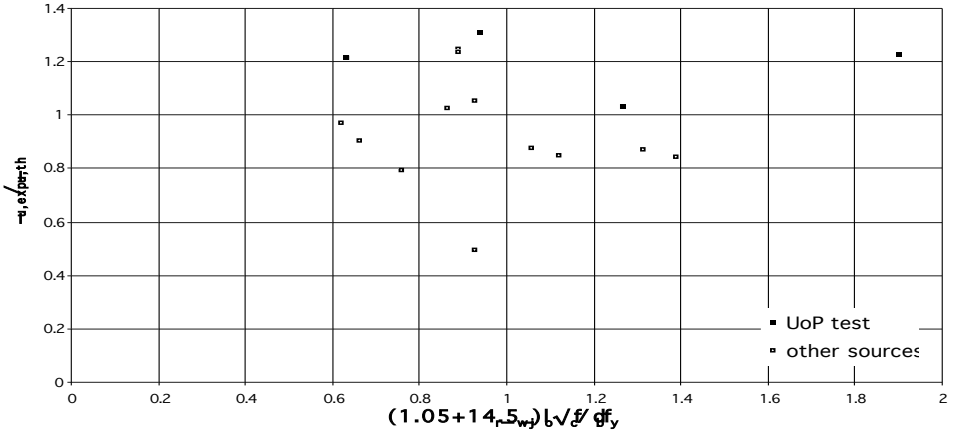

(b)

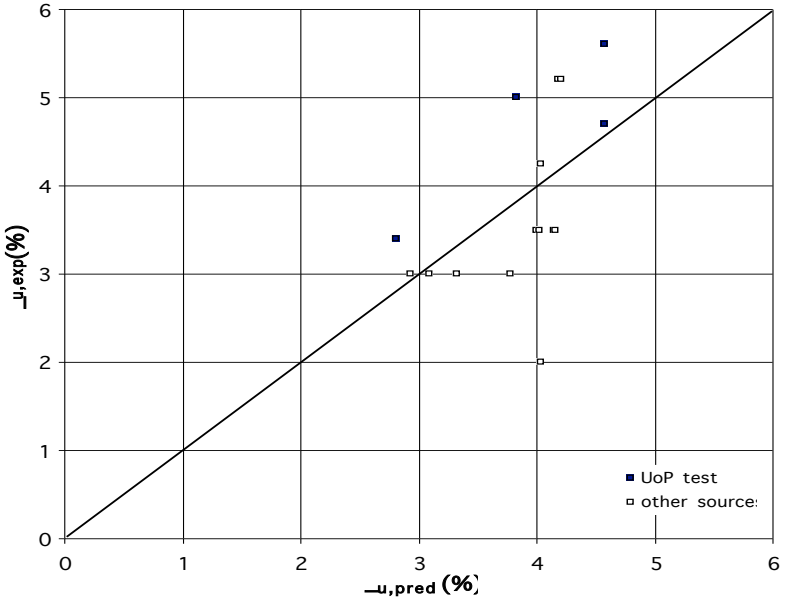

(c)

Fig. 12: Comparison of experimental θ_u of members with lap-spliced ribbed bars and FRP wraps to the value predicted: (a) without, or (b), (c) with the correction for the effect of lap splicing.

- the value obtained according to 2.1.3 above for members with rectangular section and ribbed bars without lapping, for confinement only by the transverse bars ($\alpha\rho_{sx}f_{yw}/f_c>0$, $\alpha_f f_{f,e}\rho_f=0$), times
- $l_o/l_{ou,min}$, with $l_{ou,min}$ estimated on the basis of the FRP alone through a modification of Eq. (5) as follows, with only the corner bars considered as restrained by the FRP, i.e $\alpha_{l,f}=4/n_{tot}$:

$$l_{ou,min}= d_{bL} f_{yL} /[(1.05+14.5\alpha_{l,f} \rho_f f_{f,e} /f_c)\sqrt{f_c}] \quad (7)$$

If this rule is followed, the median of the ratio of experimental-to-predicted θ_u in 16 tests with lap-spliced ribbed longitudinal bars and FRP wraps is 0.995 and its C.o.V. is 21.6% (see Figure 12).

2.4 Shear strength of members with FRP wrapping under cyclic deformations beyond flexural yielding

The results of 10 cyclic tests from the literature, in which concrete members with FRP-wrapped ends ultimately failed in shear after experiencing flexural yielding, show that the semi-empirical expression proposed by Biskinis et al (2004) for the degradation of shear resistance, V_R, with post-yield cyclic displacements applies also in the presence of FRP-wrapping, after addition of the contribution of the FRP to the shear resistance of the plastic hinge zone:

$$V_R = \frac{h-x}{2L_s}\min(N, 0.55A_c f_c)+\left(1-0.05\min\left(5, \mu_\theta^{pl}\right)\right)\left[0.16\max(0.5, 100\rho_{tot})\left(1-0.16\min\left(5, \frac{L_s}{h}\right)\right)\sqrt{f_c}A_c + V_w\right]+V_f \quad (8)$$

where units are MN and m and:

- f_c, h and L_s $= M/V$ have been defined previously, in connection with Eqs.(2) and (3),
- $\mu_\theta^{pl} = \mu_\theta - 1$: plastic part of ductility demand in terms of the ductility factor of the chord rotation at the member end, $\mu_\theta = \theta/\theta_y$,
- x: compression zone depth,
- N: compressive axial force (positive, taken as zero for tension),
- A_c: cross-section area, equal to $b_w d$ for a section with a rectangular web of width b_w and structural depth d,
- ρ_{tot} total longitudinal reinforcement ratio,
- V_w contribution of transverse reinforcement to shear resistance in accordance with a 45-deg truss:

  $$V_w = \rho_{sx} b_w z f_{yw} \quad (9)$$

  with z defined previously in connection with Eqs. (2), (3) and ρ_{sx}, f_{yw} in connection with Eq. (3),
- V_f contribution of FRP to the shear resistance of the plastic hinge for a 45-deg truss:

  $$V_f = 0.5\rho_f b_w z f_{u,f} \quad (10)$$

  with the transverse FRP ratio, ρ_f , and the ultimate strength of the FRP, $f_{u,f}$, defined in 2.3.1.

The factor of 0.5 in Eq.(10) is due to the linear reduction of the FRP stress over the internal lever arm z, from the maximum value $f_{u,f}$, at the extreme tension fibres to zero at the neutral axis.

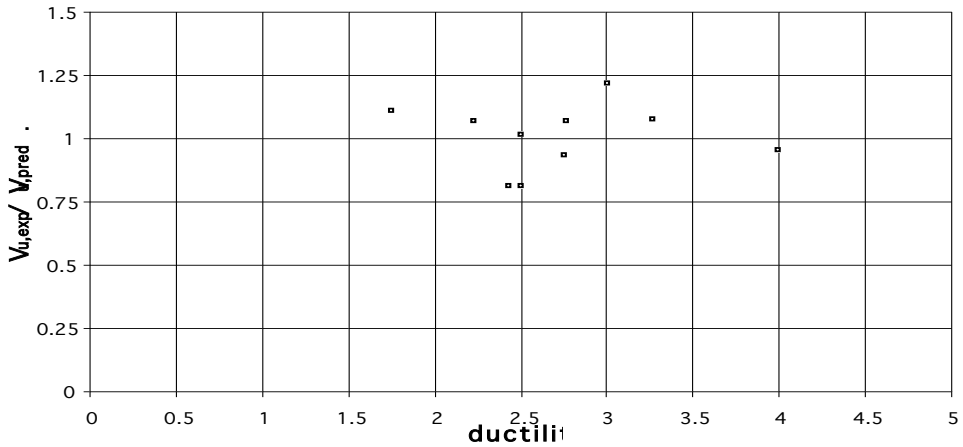

Fig. 13: Ratio of experimental shear resistance V_R to Eq. (7) prediction for FRP-wrapped members

In the 10 tests of columns wrapped with FRP and failing in shear after flexural yielding, this rule gives a median of 1.04 and a C.o.V. of 12.9% for the ratio of experimental-to-predicted shear resistance V_R. Figure 13 shows the ratio of experimental-to-predicted V_R, as a function of the chord rotation ductility factor, $\mu_\theta = \theta / \theta_y$.

The shear resistance given by Eq.(10) refers to failure by diagonal tension, as controlled by the stirrups and the FRP. The value of shear resistance at which diagonal compression failure ("web crushing") takes place is not affected by the FRP. So, regardless of the enhancement of the resistance to diagonal tension failure by the last term of Eq.(10), the final value of shear resistance cannot exceed the following maximum value, controlled by diagonal compression in the web:

- for walls with rectangular web (for 45° compression in the web):

$$V_R = 0.85\left(1 - 0.06 \min\left(5, \mu_\theta^{pl}\right)\right)\left(1 + 1.8 \min\left(0.15, \frac{N}{A_c f_c}\right)\right)\left(1 + 0.25 \max\left(1.75, 100\rho_{tot}\right)\right)\left(1 - 0.2 \min\left(2, \frac{L_s}{h}\right)\right)\sqrt{\min\left(f_c, 100\right)}\, b_w z \quad (11)$$

- for squat columns, with $L_s/h \leq 2$ (crushing along the diagonal of the column in elevation):

$$V_R = \frac{4}{7}\left(1 - 0.02 \min\left(5, \mu_\theta^{pl}\right)\right)\left(1 + 1.35 \frac{N}{A_c f_c}\right)\left(1 + 0.45 \cdot 100\rho_{tot}\right)\sqrt{\min\left(f_c, 40\right)}\, b_w z \sin 2\delta \quad (12)$$

where δ is the angle between the diagonal of the column in elevation and its axis:

$$\tan\delta = h/2L_s \quad (13)$$

These empirical expressions, Eqs.(11) and (12), were developed by Biskinis et al on the basis of the results of cyclic tests on wall or squat columns without FRP retrofitting in shear, that led to failure by diagonal compression, after flexural yielding in the case of squat columns, or before or after flexural yielding in the case of walls.

References

Biskinis, D.E. and Fardis, M.N. (2004). Cyclic strength and deformation capacity of RC members, including members retrofitted for earthquake resistance, *Proceedings 5th International Ph.D Symposium in Civil Engineering*, Delft, Balkema, pp. 1125-1133.

Biskinis, D.E., Roupakias, G. and Fardis, M.N. (2004). Degradation of shear strength of RC members with inelastic cyclic displacements, *ACI Structural Journal*, Vol. 101, No. 6, Nov.-Dec., pp.773-783.

Bousias, S.N., Fardis, M.N. and Biskinis, D. (2005) Retrofitting of RC Columns with Deficient Lap-Splices, *fib* Symposium "Keep Concrete Attractive", Budapest.

CEN (2005). European Standard EN 1998-3:2005. Eurocode 8: Design of structures for earthquake resistance. Part 3: Assessment and retrofitting of buildings, *Comite Europeen de Normalisation*, Brussels,.

Panagiotakos, T.B. and Fardis, M.N. (2001). Deformations of reinforced concrete members at yielding and ultimate, *ACI Structural J.*, Vol. 98, No 2, pp. 135-148.

Sheikh, S.A. and S.M. Uzumeri (1982). Analytical model for concrete confinement in tied columns, *Journal of Structural Division*, ASCE, Vol .108, No. ST12, pp.2703-2722.

fib Bulletins published since 1998

N°	Title
1	Structural Concrete Textbook on Behaviour, Design and Performance; Vol. 1: Introduction - Design Process – Materials Manual - textbook (244 pages, ISBN 978-2-88394-041-3, July 1999)
2	Structural Concrete Textbook on Behaviour, Design and Performance Vol. 2: Basis of Design Manual - textbook (324 pages, ISBN 978-2-88394-042-0, July 1999)
3	Structural Concrete Textbook on Behaviour, Design and Performance Vol. 3: Durability - Design for Fire Resistance - Member Design - Maintenance, Assessment and Repair - Practical aspects Manual - textbook (292 pages, ISBN 978-2-88394-043-7, December 1999)
4	Lightweight aggregate concrete: Extracts from codes and standards State-of-the-art report (46 pages, ISBN 978-2-88394-044-4, August 1999) Original edition out-of-print; available as photocopy only
5	Protective systems against hazards: Nature and extent of the problem Technical report (64 pages, ISBN 978-2-88394-045-1, October 1999)
6	Special design considerations for precast prestressed hollow core floors Guide to good practice (180 pages, ISBN 978-2-88394-046-8, January 2000)
7	Corrugated plastic ducts for internal bonded post-tensioning Technical report (50 pages, ISBN 978-2-88394-047-5, January 2000)
8	Lightweight aggregate concrete Part 1 – Recommended extensions to Model Code 90; Part 2 – Identification of research needs; Part 3 – Application of lightweight aggregate concrete Guide (part 1), technical report (part 2) and state-of-the-art report (part 3) (118 pages, ISBN 978-2-88394-048-2, May 2000)
9	Guidance for good bridge design: Part 1 – Introduction, Part 2 – Design and construction aspects Guide to good practice (190 pages, ISBN 978-2-88394-049-9, July 2000)
10	Bond of reinforcement in concrete State-of-art report (434 pages, ISBN 978-2-88394-050-5, August 2000)
11	Factory applied corrosion protection of prestressing steel State-of-art report (20 pages, ISBN 978-2-88394-051-2, January 2001)
12	Punching of structural concrete slabs Technical report (314 pages, ISBN 978-2-88394-052-9, August 2001)
13	Nuclear containments State-of-art report (130 pages, 1 CD, ISBN 978-2-88394-053-6, September 2001)
14	Externally bonded FRP reinforcement for RC structures Technical report (138 pages, ISBN 978-2-88394-054-3, October 2001)
15	Durability of post-tensioning tendons Technical report (284 pages, ISBN 978-2-88394-055-0, November 2001)
16	Design Examples for the 1996 FIP recommendations *Practical design of structural concrete* Technical report (198 pages, ISBN 978-2-88394-056-7, January 2002)

N°	Title
17	Management, maintenance and strengthening of concrete structures Technical report (180 pages, ISBN 978-2-88394-057-4, April 2002)
18	Recycling of offshore concrete structures State-of-art report (33 pages, ISBN 978-2-88394-058-1, April 2002)
19	Precast concrete in mixed construction State-of-art report (68 pages, ISBN 978-2-88394-059-8, April 2002)
20	Grouting of tendons in prestressed concrete Guide to good practice (52 pages, ISBN 978-2-88394-060-4, July 2002)
21	Environmental issues in prefabrication State-of-art report (56 pages, ISBN 978-2-88394-061-1, March 2003)
22	Monitoring and safety evaluation of existing concrete structures State-of-art report (304 pages, ISBN 978-2-88394-062-8, May 2003)
23	Environmental effects of concrete State-of-art report (68 pages, ISBN 978-2-88394-063-5, June 2003)
24	Seismic assessment and retrofit of reinforced concrete buildings State-of-art report (312 pages, ISBN 978-2-88394-064-2, August 2003)
25	Displacement-based seismic design of reinforced concrete buildings State-of-art report (196 pages, ISBN 978-2-88394-065-9, August 2003)
26	Influence of material and processing on stress corrosion cracking of prestressing steel - case studies Technical report (44 pages, ISBN 978-2-88394-066-6, October 2003)
27	Seismic design of precast concrete building structures State-of-art report (262 pages, ISBN 978-2-88394-067-3, January 2004)
28	Environmental design State-of-art report (86 pages, ISBN 978-2-88394-068-0, February 2004)
	Directory 2004 (132 pages, July 2004)
29	Precast concrete bridges State-of-art report (83 pages, ISBN 978-2-88394-069-7, November 2004)
30	Acceptance of stay cable systems using prestressing steels Recommendation (80 pages, ISBN 978-2-88394-070-3, January 2005)
31	Post-tensioning in buildings Technical report (116 pages, ISBN 978-2-88394-071-0, February 2005)
32	Guidelines for the design of footbridges Guide to good practice (160 pages, ISBN 978-2-88394-072-7, November 2005)
33	Durability of post-tensioning tendons Recommendation (74 pages, ISBN 978-2-88394-073-4, December 2005)
34	Model Code for Service Life Design Model Code (116 pages, ISBN 978-2-88394-074-1, February 2006)
35	Retrofitting of concrete structures by externally bonded FRPs. Technical Report (224 pages, ISBN 978-2-88394-075-8, April 2006)

Abstracts for *fib* Bulletins, lists of available CEB Bulletins and FIP Reports, and a publications order form are given on the *fib* website at www.fib-international.org/publications.